DOCTOR OF PHILOSOPHY

The synthesis of phosphine-based ligands and their application in Pd-catalysed processes in the production of polymethylmethacrylate

Morris, Kevin

Award date:
2008

Awarding institution:
Bangor University

The Synthesis of Phosphine-based Ligands and their Application in Pd-catalysed Processes in the Production of Polymethylmethacrylate.

A Thesis submitted to the
University of Wales
in candidature for the

Degree of
Philosophiae Doctor

in the

School of Chemistry

by

Kevin Morris

Prifysgol Cymru • University of Wales
Bangor

Yn nheyrnas diniweidrwydd-
Gwae hwnnw, wrth y pyrth;
Rhy hen i brofi'r syndod,
Rhy gall i weld y wyrth.

Rwyf yn cyflwyno'r gwaith yma i fy nheulu,
Diolch yn fawr
Kevin Morris
2008

Acknowledgements

I would like to thank Dr Ian Butler, my project supervisor, for his guidance in this most interesting of areas of research in organometallic chemistry. His knowledge and constant new ideas always gave me new insights and interest in an already highly applicable field. My thanks also go to Lucite International for funding this work; in particular Dr Graham Eastham, my industrial supervisor, for his advice and encouragement. Catalyst testing was carried out on site and my thanks go to Dr Mark Waugh and Mr Marc Bardsley for their implementation.

I thank also my research committee Dr Mike Beckett and Dr Paddy Murphy for overseeing my work. I also would like to acknowledge the technical staff, Mr Glyn Connolly, Mr Dennis Williams, Mr John Charles and Mr Gwynfor Davies for their contribution and help in running NMR and GCMS samples, borrowing chemicals etc. Some mass spectral analysis and crystal structural elucidation were carried out by the EPSRC National Service at the University of Wales, Swansea and X-ray crystallography department at the University of Southampton respectively whom I gratefully thank.

My thanks also go to the research group in which I've been happy to be involved in; Dr Dafydd Thomas, Dr Jennifer Amey, Mr Arthur Connell and Miss Sarah Barnes. Dr Thomas was a great help in laboratory matters and some starting materials which had been prepared by other members of the group was gratefully accepted. It was a pleasure to work with all of them.

I am truly grateful for the help and support of my friends and colleagues within the department over my time spent at the university in particular Miss Enlli Haf Huws, Dr Mark Dennis, Dr Gareth Evans, Dr Andy Clayton, Dr Ben Thomas, Mr John Turner, Dr Mark Foley, Miss Erica Roberts, Dr Catherine Bland, Dr Rebecca Dean, Mr Iestyn Jones, Mr Deiniol Davies and Dr Alison Jones. I wish them all the very best.

Lastly I would like to thank my parents and family whose continuing support in my academic studies has been of great value. *Diolch yn fawr.*

Abstract

The research describes the synthesis, characterisation and use of metallocene-based ligands. Examples of these include those bearing a C_4-bridged diphosphine moiety. In researching this topic, routes towards bis-1,2-disubstituted ferrocenes and ruthenocenes were developed. The catalyst ligands as their palladium complexes were tested in the palladium catalysed reaction of carbon monoxide, methanol and ethene to obtain methyl propanoate, a key intermediate in the industrial preparation of methyl methacrylate. The catalytic results were highly favourable in terms of initial rate and turnover when compared to the performance of the existing ligand of choice for this function.

Abbreviations and Acronyms

AcOH	acetic acid
Ac_2O	acetic anhydride
Ad	adamantyl
Ar	aryl
b.p.	boiling point
^{t}Bu	tertiary-butyl
BuLi	butyllithium
cat	catalyst
$CDCl_3$	deuterated chloroform
CH_2Cl_2	dichloromethane
CIP	Cahn-Ingold-Prelog
COD	cycloocta-1,5-diene
Cp	η^5-cyclopentadienyl
δ	chemical shift (ppm)
d	doublet
dba	*trans*,*trans*-dibenzylideneacetone
dppp	bis(diphenylphosphino)propane
e.e.	enantiomeric excess
EI	electron impact
Eschenmoser's salt	*N*,*N*-dimethylmethylene ammonium iodide
Et	ethyl
Fc	ferrocenyl
FGI	functional group interconversion
g	grams
GCMS	gas chromatograph – mass spectrometer
h	hour

HPLC	high performance liquid chromatography
IR	infra-red
J	scalar coupling constants
LDA	lithium *N*,*N*-diisopropylamide
m	multiplet
Me	methyl
MeP	methyl propanoate
MHz	megahertz
ml	10^{-3} litres
MMA	methyl methacrylate
mmol	10^{-3} moles
mol	moles
m.p.	melting point
MS	mass spectrometry
NMR	nuclear magnetic resonance
o-	*ortho-*
p-	*para-*
Ph	phenyl
PMMA	polymethylmethacrylate
ppm	parts per million
^{i}Pr	iso-propyl
q	quartet
R	as defined, otherwise an alkyl or an aryl group
RT	room temperature
s	singlet
t	triplet
THF	tetrahydrofuran
TLC	thin layer chromatography
TMEDA	*N*,*N*,*N*',*N*'-tetramethylethylene-1,2-diamine
TMMDA	*N*,*N*,*N*',*N*'-tetramethylmethylenediamine

Ferrocene: Structure and Nomenclature

In 1951 the discovery of ferrocene, the first of the metallocenes, was reported by Pauson and Kealy.[1] It was prepared by the reaction of cyclopentadienylmagnesium bromide with iron trichloride to give an air-stable and orange crystalline solid (the compound was also reported simultaneously by Miller, Trebboth and Tremaine).[2] It was subsequently shown that ferrocene has a 'sandwich' structure (as proposed by Wilkinson, Rosenblum, Whiting and Woodward).[3, 4] in which the two cyclopentadiene rings lie parallel, with the iron atom positioned in the π electron cloud between them. The iron atom is present in the Fe^{2+} oxidation state, but is capable of undergoing oxidation at the iron centre to give a ferrocenium species with the iron at oxidation state of Fe^{3+}. An early X-ray structural analysis initially indicated that in the crystalline form ferrocene adopts a staggered (or antiprismatic) conformation (**I**), as opposed to the eclipsed (or prismatic) form (**II**), as this would minimise the non-bonding interactions between the heteronuclear carbon atoms. However, in solution the rings are free to rotate (except where tied together by a bridge), since the barrier to rotation of the rings is negligible.[5]

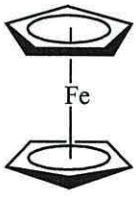

(I)

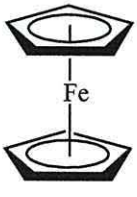

(II)

Where reference is made herein to substituted ferrocenes, the substituents R and R' are named in order of their CIP (Cahn-Ingold-Prelog) priority rather than alphabetically as is often the convention, e.g. 1-bromo-1'-aminoferrocene, R > R'.[6] The CIP priority rules also apply in those cases where there is more than one substituent on the same Cp ring, e.g. 1-(hydroxyl-methyl)-2-dimethylaminomethyl ferrocene. The stereochemistry of such compounds is defined according to the convention of Schlögl.[7]

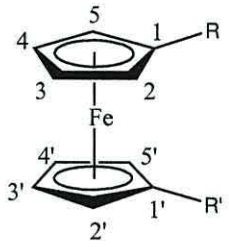

For NMR interpretation, the carbon and hydrogen atoms at the 2-, 2'-, 5-, and 5'-positions are identified as *alpha*, while those at the 3-, 3'-, 4-, and 4'- positions are *beta*.

Contents

Chapter 1

Introduction

Introduction

1.1 Chapter 1: Overview.

This chapter gives some background and an outline to the work described in the remainder of the thesis. Chapter 1 is separated into four sections;

In sections 1.2 and 1.3 the worldwide importance of methyl methacrylate and some of its production methods are reviewed. The discussion covers the managerial issues associated with current production methods, and moves on to describe an alternative preparation of the monomeric precursor to this important material. It is here that the importance of a C_4-diphosphine bridge to this alternative method is introduced.

Section 1.4 fits into this context by describing some general ferrocene chemistry with emphasis on ferrocenyl phosphines and substitution patterns of substituted ferrocenes. It finishes with a report on initial catalytic testing which indicates great potential for the use of these ferrocenyl phosphine ligands in industry. Section 1.5 ends the chapter with a listing of the project's objectives and targets.

1.2 Focus on Perspex.

1.2.1 Introduction to polymethylmethacrylate.

Polymethylmethacrylate (PMMA) **1** or polymethyl-2-methylpropanoate is the synthetic polymer of the monomer methyl methacrylate (MMA) **2** (figure 1). This amorphous, transparent and colourless thermoplastic is sold under the names Perspex, Plexiglas, Acrylite, Acrylplast and Lucite and is commonly called Acrylic glass or simply "Acrylic" – though this really describes a large family of chemically related polymers.

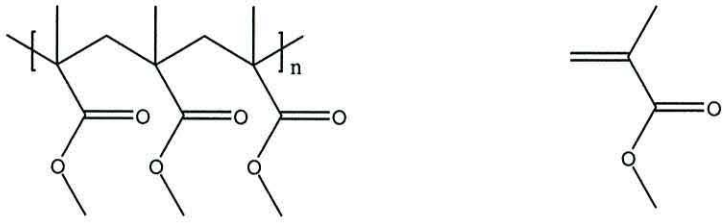

1 2

Figure 1: Structures of PMMA: $(C_5H_8O_2)_n$ and MMA: $C_5H_8O_2$.

This material was developed in 1928 in several laboratories concurrently and was eventually brought to market in 1933. From a commercial standpoint, vinyl polymers such as PMMA are the most important of all polymer types. For this reason, more research has been accomplished in the area of vinyl polymerization than with most other polymerization types. For convenience, it is useful to classify all polymers prepared by addition reactions of carbon-carbon double bonds as vinyl polymers.

Vinyl polymerization reactions are chain-reaction processes, which is the case with most (but certainly not all) addition polymerizations, and they require an initiator to begin the reaction. Polymerization occurs only at the reactive end of a growing chain; hence high molecular weights are reached rapidly at relatively low percentages of conversion, and monomer is always present in significant quantities during the process.

1.2.2 Mechanism of polymerisation.

Initiation of free radical polymerization involves two reactions: formation of the initiator radical, and addition of the initiator radical to monomer.[8] Certain monomers however, most notably methyl methacrylate (MMA) (and styrene and some strained-ring cycloalkenes) undergo polymerization on heating in the absence of any free radical initiator. Evidence for the incorporation of initiator radicals arises from spectroscopic and chemical analysis of end groups. Addition of monomer radical to another monomer molecule, followed by successive addition of polymer radicals to available monomer, comprises the propagation reactions (scheme 1).

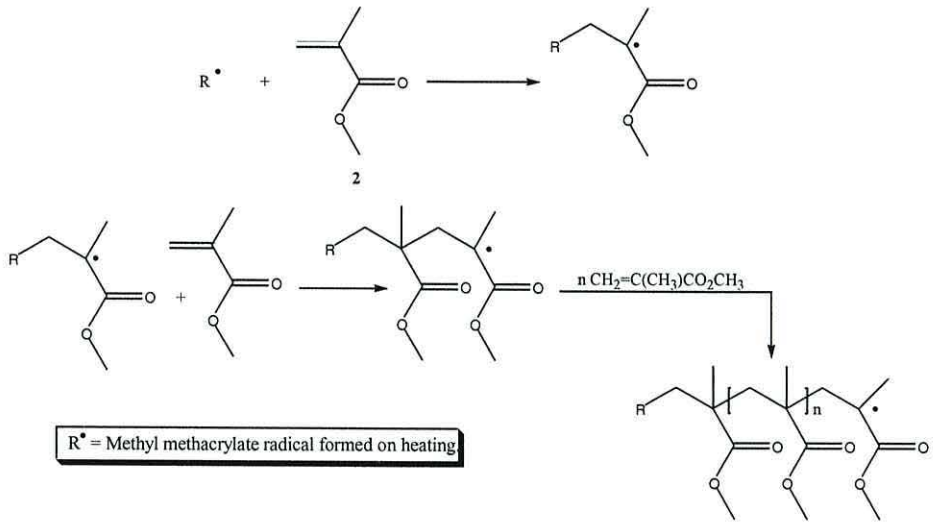

Scheme 1: Free radical polymerization of MMA.

Each addition step follows the predominant *head-to-tail* orientation due to a combination of steric and electronic effects. Steric repulsion favours attack by the radical at the least hindered carbon of the double bond and resonance stabilisation favours formation of the more stable free radical.

Propagation continues until some reaction occurs to terminate the chain propagation. Polymethylmethacrylate radicals undergo mainly disproportionation, which

involves the transfer of hydrogen from one chain end to another; this is diffusion controlled and requires pairing of electron spins (scheme 2).

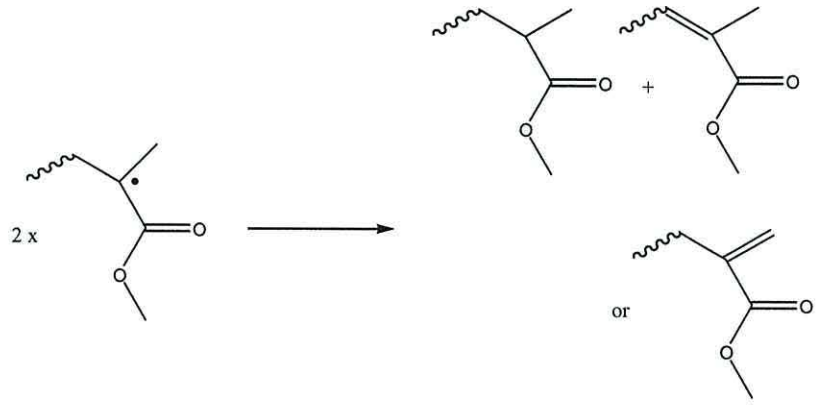

Scheme 2: Termination reaction in the formation of PMMA.

This termination step is favoured due to steric repulsion. Unfavourable coupling of polymethylmethacrylate radicals would lead to four bulky groups on adjacent carbons. Electrostatic repulsion of polar groups (such as ester) may also raise the activation energy for coupling. Availability of alpha hydrogens for hydrogen transfer is a third factor: polymethylmethacrylate radicals have five, compared to two for example with polystyryl radicals.

1.2.3 Stereochemistry of polymerisation.

For monosubstituted and 1,1-di-unsymmetrically substituted monomers, two stereoregular arrangements are possible in a head-to-tail polymer: *isotactic*, with like substituents all on the same side, and *syndiotactic*, with like substituents of alternate repeating units on the same side. A random arrangement is referred to as *atactic*. In 1958 it was reported that free radical polymerization of methyl methacrylate at temperatures below 0°C gave a crystalline polymer,[9] and this was subsequently shown to be syndiotactic using high resolution NMR as a characterisation technique.[10]

There are two factors to consider in describing the stereochemistry of addition of a monomer molecule to a radical chain end: (1) interaction between the terminal chain carbon and the approaching monomer molecule, and (2) the configuration of the penultimate repeating unit in the polymer chain.

Considering firstly the approach of the monomer: the terminal carbon atom presumably has sp^2 hybridization and is planar. For polymerization of the monomer $CH_2 = CXY$, there are two ways that a monomer molecule can approach the terminal carbon: the mirror approach, with like substituents on the same side (figure 2 **A**), or the non-mirror approach, with like substituents on opposite sides (figure 2 **B**). As long as stereochemistry is maintained - that is, free rotation does not occur before the next monomer molecule adds – then the mirror approach will always lead to isotactic polymer and the non-mirror approach to syndiotactic polymer.

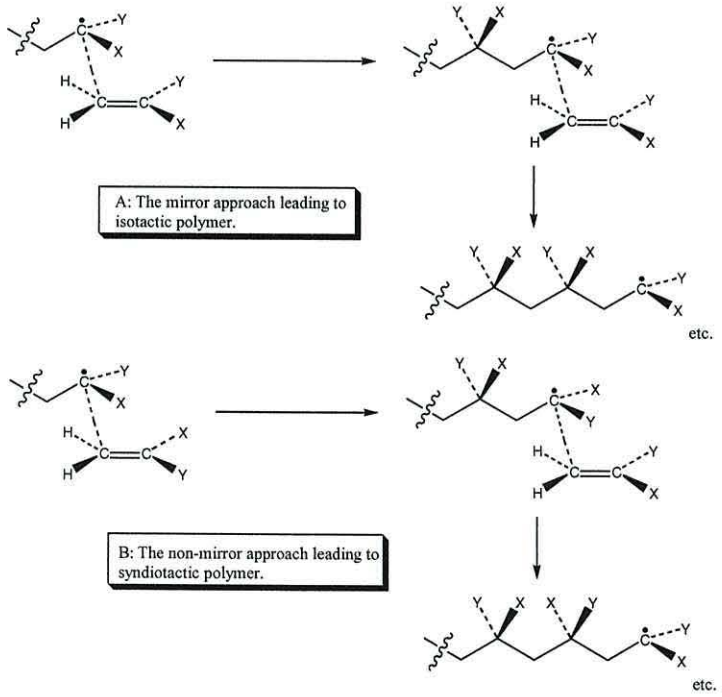

Figure 2: Addition of radicals to monomers leading to two stereoregular arrangements.

If, on the other hand, interactions between the substituents of the penultimate repeating unit and the terminal carbon atom are significant, then conformational factors could also have an influence and the mode of addition could be governed by the conformation that allows the least steric or electrostatic interaction.

One model described in a paper by Cram and Kopecky for the methyl methacrylate polymerization that takes into account penultimate unit interactions and that allows for the least steric hindrance between substituent groups during reaction is shown in scheme 3 (the polymer chain, P, is the bulkiest group).[11]

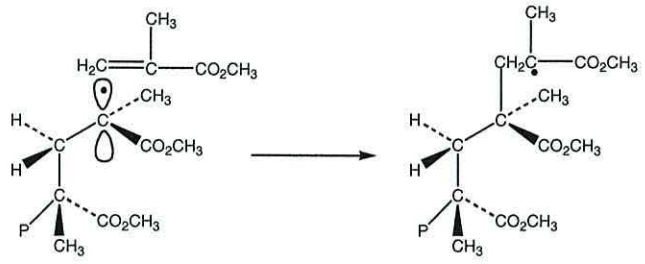

Scheme 3.

In such an arrangement the radical receives optimum exposure for reaction with monomer. The newly formed radical then assumes the preferred conformation with another monomer molecule, and so the process repeats itself to give the syndiotactic structure. This model assumes an energy barrier to rotation that is considerably higher than that of propagation; otherwise a random distribution would result. This would be temperature dependent, and as expected, the degree of stereoregularity decreases at higher temperatures.

While the above model satisfactorily explains the formation of syndiotactic polymethylmethacrylate, it does not take into account possible interaction between chain-end radical and monomer. Using calculations of interaction energies that take into account such factors as distance of separation, angle of approach, and point of radical

addition (at the carbon atom or at the π orbital of the double bond), it has been concluded that interaction between monomer and terminal unit is the predominant factor resulting in syndiotactic placement as long as the terminal carbon has the sp^2 planar structure.[12] This is the non-mirror arrangement, shown in figure 2 **B**. If, however, the terminal radical assumes a substantial amount of sp^3 hybridization, which it might do as it enters the transition state, then the resultant change in configuration could cause interactions with the penultimate unit to be of greater significance. Whichever is the case, syndiotactic placement is favoured.

1.2.4 Applications of polymethylmethacrylate (PMMA).

Commercially important vinyl polymers prepared by free radical polymerization are found in many areas in modern life such as food packaging, cable and wire insulation, foam insulation, tires and many more. Perspex is used as a shatterproof replacement for glass. A familiar example would be the barrier which protects the audience from hockey pucks at ice rinks which is made of PMMA. The material is also more transparent than glass; this is demonstrated most spectacularly at the Monterrey Bay Aquarium, California. Here exists the world's largest single observation window at 16.6m long, 5.5m high, and 33cm thick (54ft x 18ft x 13 inches) to hold back the enormous pressure of millions of gallons of water in the aquarium. At this thickness, glass would be difficult to see through. PMMA has an advantage over other polymers (such as polycarbonates **3**) which are also used as glass substitutes in that they are cheaper.

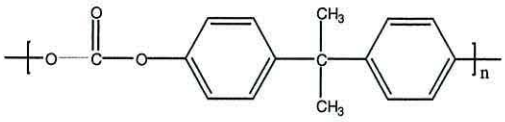

3

Figure 3: Polycarbonate of bisphenol A: the more expensive material also used to make shatterproof windows.

All methacrylates co-polymerise with a range of other monomers, and this ability enhances the monomers versatility, as product properties can be tailored to fit specific applications. For example, MABS (Methacrylate-Acrylonitrile-Butadiene-Styrene) polymers have similar physical properties to ABS (Acrylonitrile-Butadiene-Styrene) polymers, except that methacrylate confers transparency. This is the primary function of MMA in the copolymer.

Other applications for polymethylmethacrylate are in automotive parts, moulding where hardness is to be retained at high temperatures, compositions, decorative panels, skylights and glazing. PMMA also forms 'polymer concrete', a resin used in the construction industry, offering high strength and chemical resistance.

PMMA is also found in paints. Acrylic 'latex' paints often contain PMMA suspended in water. PMMA doesn't dissolve in water, so dispersing PMMA in water requires the use of another polymer to make PMMA and water compatible with each other. Low molecular weight PMMA also prevents lubricating oils and hydraulic fluids from becoming viscous at low temperatures allowing machinery to be operated at temperatures as low as -100°C.

1.2.5 Summary of PMMA.

In conclusion Perspex is ubiquitous. It is the medium through which some of the world's most prestigious brands choose to reflect their corporate identity using signage and point of purchase. Household names such as Shell, Boots, McDonalds, Audi, American Express, Nissan, BP and Mercedes choose Perspex because they can rely on its inherent performance characteristics and exact colour matching ability to portray their identity around the globe with consistent flair and durability. Therefore synthetic studies of its monomer: methyl methacrylate (MMA) is very important with any optimisation being highly advantageous to its producers on an industrial scale.

1.3 Methyl methacrylate (MMA)

1.3.1 Industrial synthesis of MMA: acetone cyanohydrin process.

Until relatively recently (1978), the commercial manufacture of methacrylates, and particularly methyl methacrylate (MMA) **2**, was limited to formation from cyanohydrin. This is a 'dirty' process involving treatment of acetone with hydrogen cyanide and sulphuric acid (scheme 4).[13]

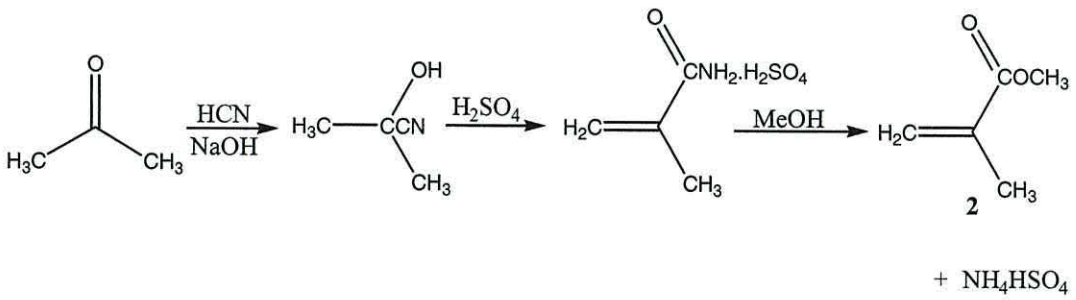

Scheme 4: acetone cyanohdrin process.[13]

In this process, cyanohydrin is first formed by reaction of hydrogen cyanide with acetone using a base such a sodium hydroxide. The reaction is exothermic, and cooling

the reaction shifts equilibrium towards formation of cyanohydrin. Neutralization of the crude cyanohydrin with sulphuric acid precipitates the sodium sulphate by-product. The product mixture then passes through a filter and is separated from the un-reacted hydrogen cyanide and acetone. The concentrated acetone cyanohydrin is dried under vacuum and used at once in methacrylate synthesis. Conversion of the cyanohydrin into methyl methacrylate is effected by equimolar treatment with sulphuric acid to yield methacrylamide sulphate. Addition of methanol esterifies the methacrylamide sulphate to give methyl methacrylate and ammonium bisulphate. Overall yields are high (>95%), and the only significant by-products are the sodium salts formed by neutralization of the NaOH catalyst and ammonium bisulphate.

Ammonium bisulphate is of little commercial value and its management necessitates the provision of a recycling plant. The waste acid ammonium bisulphate residues may be treated with ammonia to yield fertilizer grade ammonium sulphate. Alternatively, they are combusted to form sulphur dioxide, then oxidised to form sulphur trioxide and then converted to sulphuric acid, to be used again in the MMA process. The cost of these additional processes adds significantly to the overall cost of the production of methacrylates, in particular for methyl methacrylate, which does not co-produce ammonium bisulphate.

1.3.2 Environmental considerations and costs.

Production of this material is dependent on narrow margins of profit. Worldwide production levels are immense, and account for around 30% of acetone usage. Many variables will enter the business equation. In addition to land and labour costs, costs of

reaction materials, catalyst lifetimes and so on, operating on such a large scale of production as for that of MMA accentuates the problems of using highly toxic materials like cyanide and acetone cyanohydrin. The process must be operated in a safe and principled manner, however dealing with such noxious substances, and on such scale, meeting legal and moral requirements whilst satisfying the wishes of company shareholders is always going to be difficult.

Despite the problems associated with the existing industrial process for the production of MMA, replacement of this approach is a slow and costly affair. Selection and development of an alternative catalytic system is only part of the investment.

1.3.3 A proposed alternative industrial synthesis of MMA.

Over the last few decades, the production of perfectly alternating polyketones using transition metal catalysts has attracted much interest with highly regarded contributions by Drent,[14,15] Sen,[16-19] and Keim.[20] These polymeric materials are synthesized using the readily available and inexpensive monomers, ethene and carbon monoxide. The properties of these highly crystalline perfectly alternating ethene-CO copolymers are more desired than random copolymers which resulted from the free radical initiated[21] or γ-radiation induced methods[22] previously used. Some of these qualities include good solvent resistance and barrier properties as well as high stiffness, strength and melting point, which make the polymer suitable for a wide range of applications.

The production of short chain ethene-CO co-oligomers however are less well covered.[23] These materials belong to a class of compounds called oxygenates, which can

be employed as solvents for a variety of purposes. Many oxygenates that are readily available from simple processes are volatile and hence potentially polluting. There is a demand for the production of less volatile oxygenates for use as environmentally friendly solvents and their cheap starting materials would be especially appealing. Ethene-CO co-oligomers with up to 11 or more atoms in their backbone such as 3,6-octanedione are low volatility compounds with high solvating ability and so meet these current demands. An examination of catalytic systems which show selectivity to the co-oligomers or to the first members of the series, 3-pentanone or alkyl propanoates (n = 1) (scheme 5) was reported in a review by Cole-Hamilton.[24]

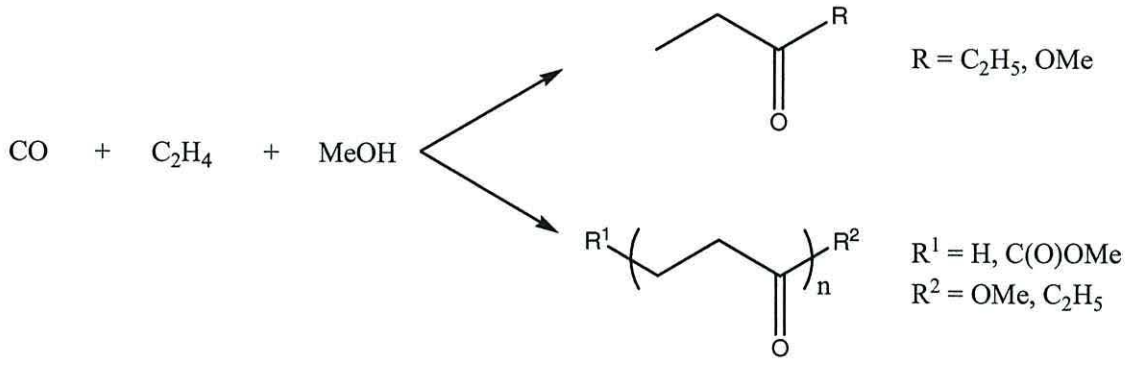

Scheme 5: Possible reaction products of ethene and carbon monoxide in methanol using transition metal catalysts.

The synthesis of esters such as methyl propanoate from hydroesterification processes have been described extensively.[14,15,24] Methyl propanoate **4** is a key intermediate in the production of methyl methacrylate, which is an important monomer in the plastics industry and is produced annually on a multi-million tonne scale.

A primary research objectives for a cheaper, cleaner alternative method of production are the preparation of key intermediates such as methyl propanoate in the industrial preparation of methyl methacrylate **2** (the monomer unit of its synthetic

polymer PMMA, whose applications are numerous), which require palladium catalysed synthesis (scheme 6).

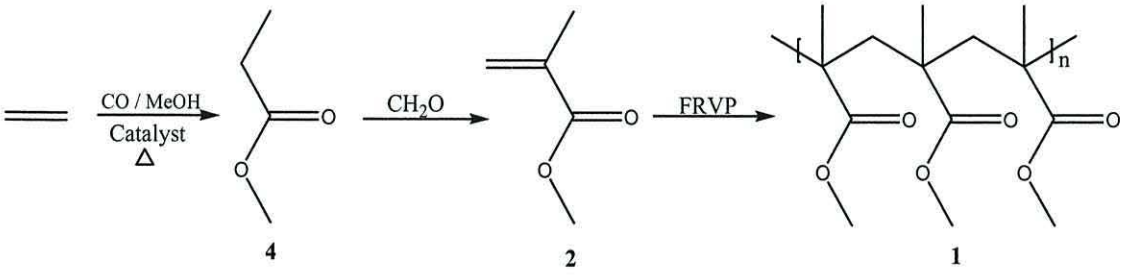

Scheme 6: A novel route towards PMMA from a C_2 precursor.
FRVP: Free radical vinyl polymerization.

1.3.4 Catalyst development and testing.

Standard carbonylation catalysts such as $[Co_2(CO)_8]$ and $[Ni(CO)_4]$ have been largely superseded by Pd, Pt, Rh and Ru catalysts due to improved performance under milder reaction conditions. For example, palladium catalysts have been found to operate successfully at temperatures in the range of 70 – 120 °C and pressures between 1 and 200 bar whereas higher temperatures and pressures (150 – 200 bar) were required for cobalt catalysed systems.[24]

A catalytic system based on coordination of bidentate phosphine ligands to the $PdCl_2$ scaffold has been shown to be highly active in the copolymerization of ethylene and carbon monoxide.[25] Different ligands **5a-c** were evaluated in terms of the length of the bidentate bridge on activity/g of poly ketone **6** (mol of cat)$^{-1}$h^{-1} and molecular weight (scheme 7).

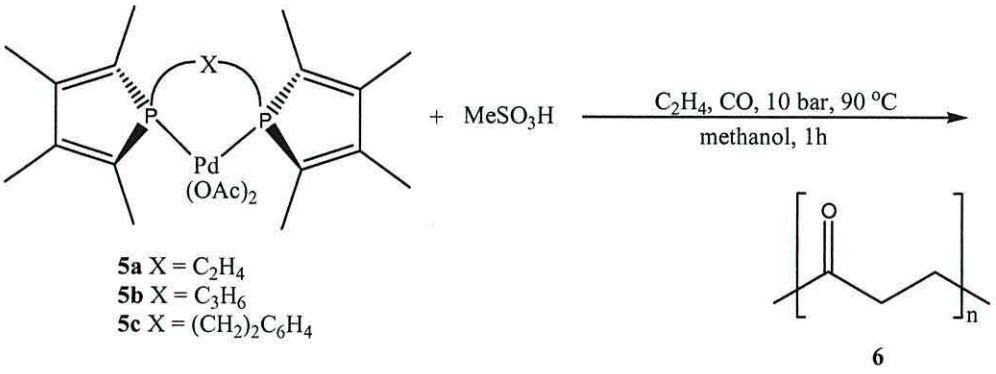

5a X = C_2H_4
5b X = C_3H_6
5c X = $(CH_2)_2C_6H_4$

6

Scheme 7: Ethylene/CO copolymerization using ligands **5a-c**.[25]

The bidentate phosphine ligands with just a C_2-bridge **5a** showed no activity, a C_3 diphosphine bridged system **5b** showed moderate activity (5,100g per mol. catalyst per hour), whilst a C_4 bridged di-phosphine **5c** showed an activity of 46,300g per mol. catalyst per hour. In comparison to the activity of bis(diphenylphosphino)propane (dppp) (activity = 33,100g per mol. catalyst per hour) and that of **5b** the effect of the C_4 bridged ligand is dramatic, and may be attributed to the ligand's wide cone angle imposing a restriction on the L^M^L angle formed by the coordinated olefin and carbonyl groups, thus bringing them closer together to facilitate the reaction.

In a another publication,[26,27] a highly active and selective catalyst for the production of methyl propanoate **4** (the key precursor to methyl methacrylate) in the methoxycarbonylation of ethene has been described (scheme 8), based on a zero valent palladium complex $L_2Pd(dba)$ **7** [where L_2 = 1,2-bis(di-*tert*-butylphosphinomethyl)benzene and dba = *trans,trans*-dibenzylideneacetone].

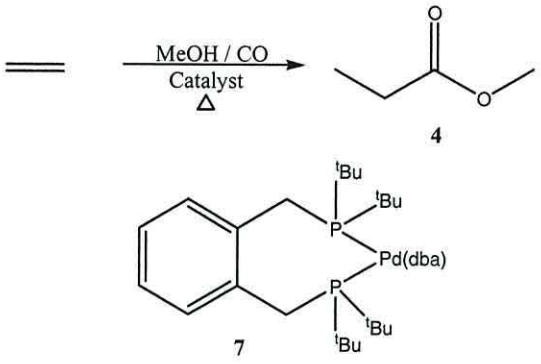

Scheme 8: Highly selective formation of methyl propanoate **4** using a palladium complex of 1,2-bis(di-tert-butylphosphinomethyl)benzene under mild conditions.[26]

In this work the key is the bidentate phosphine ligand 1,2-bis(di-*tert*-butylphosphinomethyl)benzene (another C_4-bridged diphosphine) which offers exceptional activity, selectivity and stability. This ligand has been previously described by Shaw[28] and some of its chemistry had been explored by Spencer,[29] however, prior to the work by Tooze *et al* [26] little structural characterisation and no catalytic studies had been reported using it.

Treatment of complex **7** with a sulfonic acid (e.g. methanesulfonic acid) in MeOH generates the active complex capable of converting ethene, CO and MeOH to methyl propanoate **4** at a rate of 50,000 mol of product per mol of catalyst per hour with a selectivity of 99.98%. The reaction conditions are very mild (80°C and 10 atm combined pressure of ethene and CO). The alkoxycarbonylation of alkenes is of growing importance as this method can be modified so that a range of products is accessible, from high molecular weight 'polyketones', which have useful properties as engineering thermoplastics,[30] to methyl propanoate **4**, an intermediate in the manufacture of methyl methacrylate as described previously.

The study of the complexes shown in figure 4 under the reaction conditions referred to above revealed the expected η^2-binding of one of the alkene groups of the dba

ligand in addition to the chelate ring structure formed by the bidentate ligand. The geometry around the palladium centre was found to be trigonal planar and the diphosphine ligand ligand bite angle of 104° was consistent across the range (**7, 7a-e**).[26]

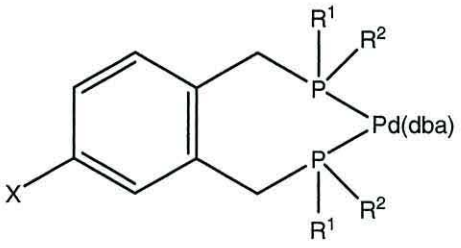

7 $R^1 = R^2 = {}^t$Bu, X = H
7a $R^1 = R^2 = {}^t$Bu, X = NO_2
7b $R^1 = R^2 = {}^t$Bu, X = OMe
7c $R^1 = R^2 = {}^i$Pr, X = H
7d $R^1 = R^2$ = Cy, X = H
7e $R^1 = R^2$ = Ph, X = H

Figure 4: Structure of various catalyst precursors tested for selectivity in formation of methyl propanoate.

The presence of electron donating and withdrawing groups such as OMe and NO_2 on the aryl group (compounds **7a** and **7b** in Fig. 4) does not cause any substantial effect on the catalyst performance, presumably due to the remote location of these functional groups from the palladium centre.

A more dramatic effect than that observed when substituents were present on the ring of ligand **7** in Fig. 4 occurred when the substituents on the phosphorus atoms were changed. The isopropyl analogue was found to be less active by a factor of 60. Not only was the activity reduced by replacement of the *tert*-butyl groups with other substituents, but also the selectivity towards methyl propanoate also decreased. In another example, the complex from the phenyl analogue of the ligand produced a mixture of oligomers and polymers with only 20% selectivity towards methyl propanoate. This effect was thought to be related to the steric environment created by the substituents on phosphorus, which control the possibility of single or multiple monomer insertions prior to termination.[24]

In addition the active complex must contain the ligand bound in a bidentate manner through both P atoms as it is reported in the literature of an example of a similar compound to **7b** (Fig. 4) but containing a Br atom also on the ring. The major species

from the reaction with $[Pd_2(dba)_3]$ was a dimer containing the ligand bound through 1 P atom and an *ortho*-metallated C atom (**8a** in scheme 9).[24, 31] The complex itself was an active catalyst, however related complexes such as **8b** and **8c** in scheme 9, which do not contain the pendant P^tBu_2 functionality were not selective.

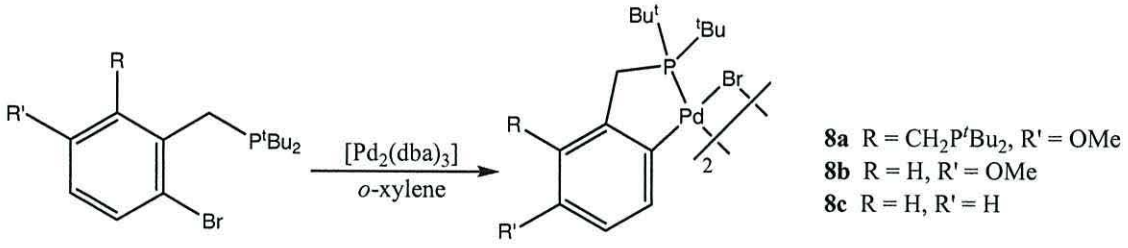

Scheme 9: Metallation of ligands containing Br *ortho* to a $CH_2P^tBu_2$ group.[24]

In a later publication,[32] the effect of phosphine substitution on selectivity of monomer unit versus the polymer production of methyl propanoate was examined. Performance and selectivity of a different C_4 catalyst (scheme 10) showed high sensitivity to steric bulk and ring strain imposed on the catalyst/reagent chelate ring by different stereoisomers of the C_4 bridged diphosphine ligands in the formation of methyl propanoate **4** versus production of the CO-ethylene copolymer **9** (with n ranging from 14 to 20) (scheme 10).

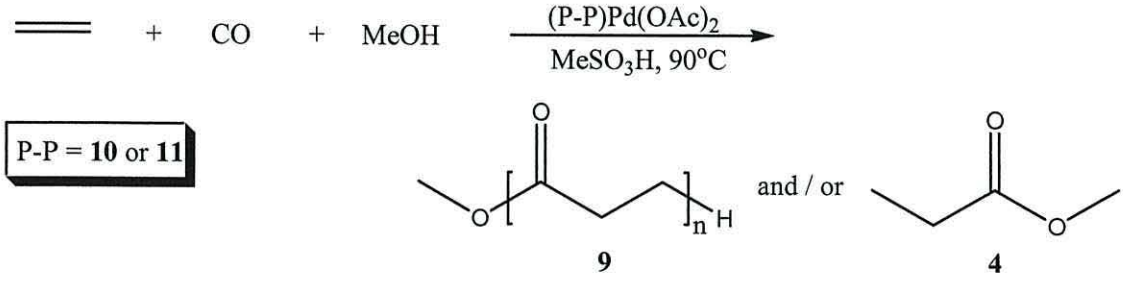

Scheme 10:

For example; *exo,endo*-2,3-bis(diphenylphosphinomethyl) norbornane **10** was highly selective for the production of methyl propanoate (>90%), while *endo,endo*-2,3-

bis(diphenylphosphinomethyl) norbornane **11** showed low activity for the copolymer, and no production of methyl propanoate (figure 5) (catalyst tests were undertaken by using their corresponding palladium complexes [(P-P)Pd(OAc)$_2$] where (P-P) = **10** or **11**).

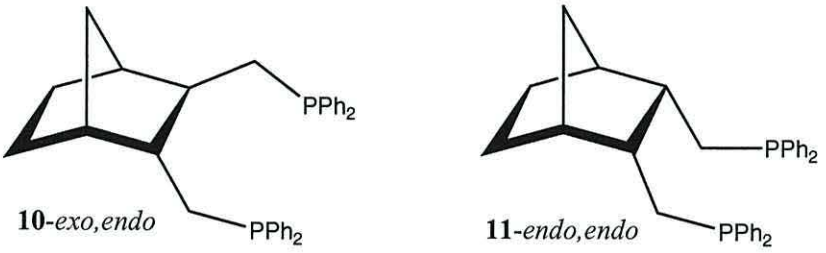

Figure 5: Different stereoisomers of the C_4-bridged ligands.

Such a difference in selectivity for diphenylphosphino-substituted catalysts is unexpected and may be due to the large natural bite angle enforced by the *exo,endo* arrangement of the diphenylphosphinomethyl substituents. If selectivity, for a single site catalyst, is determined by the relative rates of termination after a single turnover, either via methanolysis or protonolysis, versus chain propagation, be it migratory insertion of CO or ethylene, it is difficult to understand how such a subtle change could have such a dramatic effect on product distribution. In particular, if the selectivity of catalysts based on **10** is the result of a large change in the rate of chain transfer relative to propagation upon a change in ligand structure, one would expect largely a single turnover (i.e. formation of methyl propanoate) with rapidly diminishing amounts of dimer and higher oligomers. If this were the case, the average degree of polymerization would be significantly less than 14.

A few other diphosphine ligands have been employed in conjunction with Pd(II) salts to catalyze the copolymerization of CO and ethene.[33] In all cases however, low productivity was observed. These examples include reactions catalyzed by phosphinite-modified palladium catalyst **12-15** (figure 6).[34]

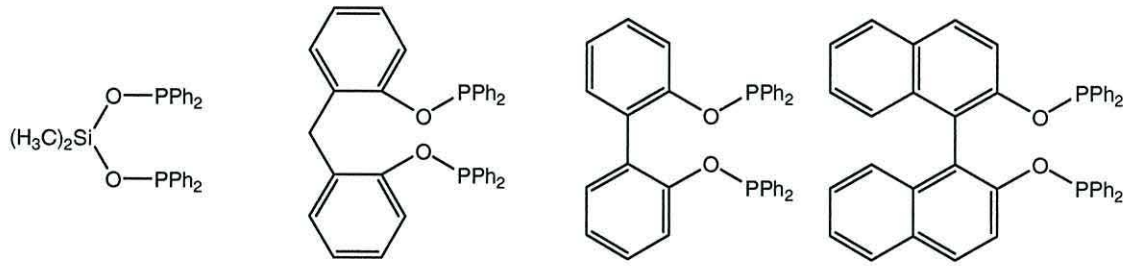

12 **13** **14** **15**

Figure 6: Miscellaneous diphosphine ligands employed in CO/ethene copolymerization.

Examples of complexes containing bidentate phosphine ligands, which promote the Pd catalysed formation of methyl propanoate rather than co-oligomerisation are rare. However, the catalytic system reported by Tooze *et al.*[26] containing 1,2-bis(di-tert-butylphosphinomethyl)benzene **7**, which was capable of producing methyl propanoate with up to 99.98 % selectivity under mild conditions is to date the best known example reported in the literature. Any subsequent catalyst design must therefore be based and compared with this template in mind and of considerable importance is the understanding of its reaction mechanism.

1.3.5 Methoxycarbonylation – mechanistic investigation.

As with the formation of polyketones (see section **1.3.3**) two possible mechanisms for the hydroesterification reaction are typically described.[35] The hydride mechanism involves formation of a metal hydride bond presumably by reaction with a proton source or the alcohol solvent. Alkene insertion into this bond to form a coordinated alkyl group, followed by alkyl migration onto coordinated CO then forms a labile acyl intermediate, which readily undergoes alcoholysis, yielding the ester. The carbomethoxy mechanism stems from formation of a metal alkoxide by reaction with the alcohol. Insertion of CO

and migration of the carbomethoxy ligand formed onto a bound alkene molecule occurs before cleavage of the ester by a proton source.

A detailed spectroscopic investigation of all the possible intermediates in this system has been carried out and the results unambiguously confirmed the sole operation of the hydride cycle in the formation of methyl propanoate (scheme 11).[36]

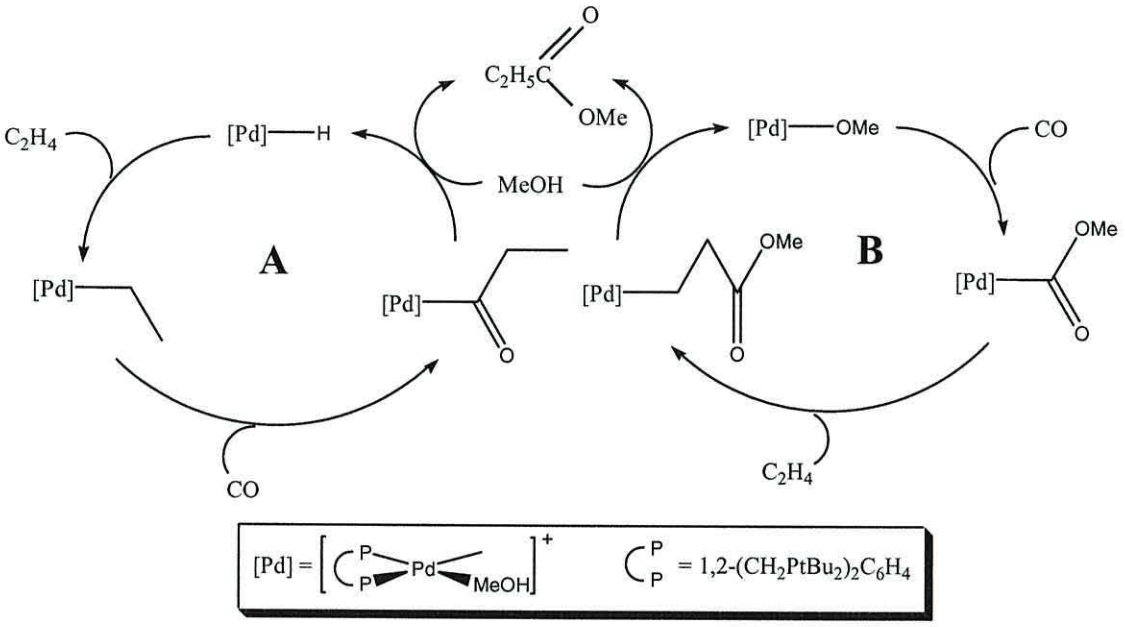

Scheme 11: Alternative functional groups in the methoxycarbonylation of ethene (**A** – hydride cycle; **B** – carbomethoxy cycle).

In scheme 12 all reaction intermediates which have been identified by ^{31}P-, ^{1}H- and ^{13}C-NMR spectroscopy at various stages during the model studies are shown. The addition of HBF_4 or CF_3SO_3H to the catalyst precursor [**a**], in the presence of oxygen or benzoquione, was found to produce a solvento-cation species [**b**], containing a Pd – H bond. The anion was present only as a non-coordinating counter ion. Bubbling of ethene gas through the methanolic solution of [**b**] produced the ethyl complex [**c**] by insertion of ethene into the Pd – H bond. Passing carbon monoxide through the resulting solution immediately produced methyl propanoate and regenerated [**b**] without the observation of

the acyl intermediate from the insertion of CO. However, presence of the acyl intermediate was confirmed by repeating the process in THF instead of methanol. Production of methyl propanoate and regeneration of [**b**] once again ensued upon addition of trace amounts of methanol to a solution of [**e**].

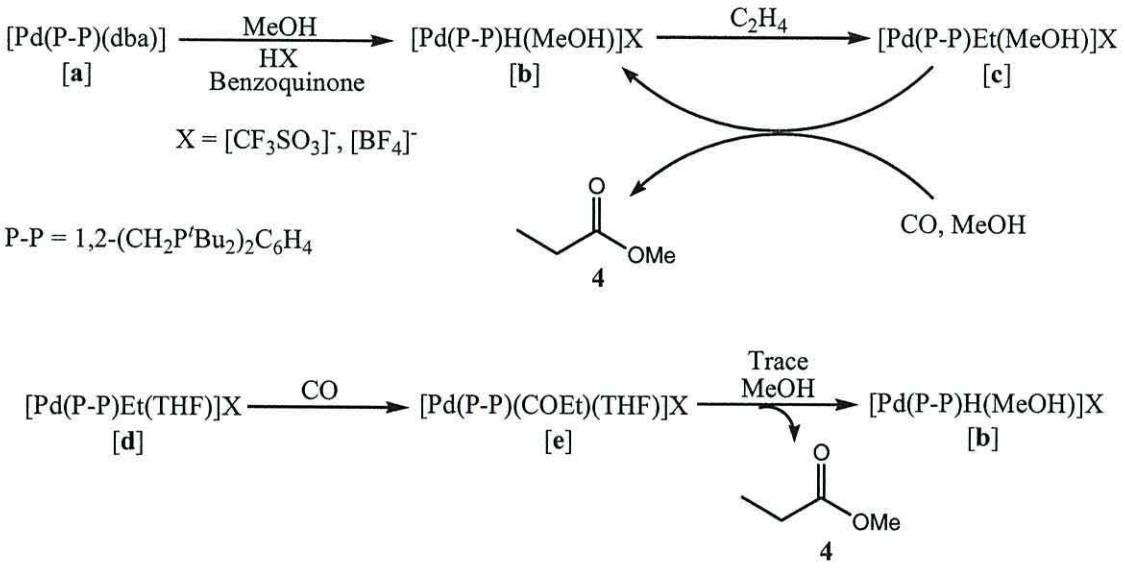

Scheme 12: Intermediates in the hydride cycle for the production of methyl propanoate catalysed by a palladium complex of 1,2-bis(di-*tert*-butylphsphinomethyl)benzene.[24, 36]

Drent, who described the production of polyketones from similar bidentate phosphine systems, provided evidence for the operation of the carbomethoxy cycle (through the observation of diesters) and even suggested that this cycle was dominant over the hydride cycle in the presence of oxidants.[15, 37] An increase in selectivity to the diester products, which can only be generated from the carbomethoxy cycle, in the presence of benzoquinone suggested that oxidation of the palladium hydride into a palladium carbomethoxy species had occurred (scheme 13).[14] An increase in rate was

also noted and possibly indicated a faster rate of the carbomethoxy cycle over the hydride cycle.

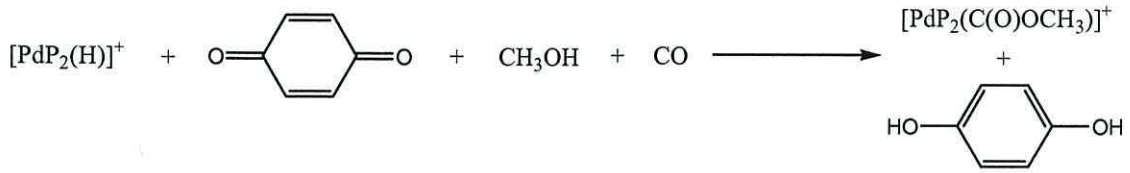

Scheme 13: Oxidation of $[PdP_2(H)]^+$ to $[PdP_2(C(O)OCH_3)]^+$ in the presence of benzoquinone, methanol and carbon monoxide.[14]

However complex [**b**] (scheme 12) was stable in the presence of benzoquinone and upon bubbling of oxygen for 30 min at 80 °C.[36] No evidence for the formation of the methoxy species was found. As a result, the catalytic mechanism for the production of methyl propanoate from these systems was proposed to arise from the hydride cycle only.

Final confirmation that the hydride mechanism is operating in these reactions comes from the labeling pattern of the products obtained from the reactions carried out in CH_3OD using palladium complexes of ligand **7** in Fig. 4. This depended on the rate of mixing during the reaction.[38, 24] Under fast stirring conditions (not mass transport limited) only two products, $CH_2DCH_2CO_2Me$ and CH_3CHDCO_2Me were detected. These show that the hydride mechanism is operating and that the migration of H/D onto the coordinated ethene molecule is fast and reversible. Exchange of the free and bound ethene does not occur to any extent and migration of the ethyl group onto CO is rate determining (scheme 14).

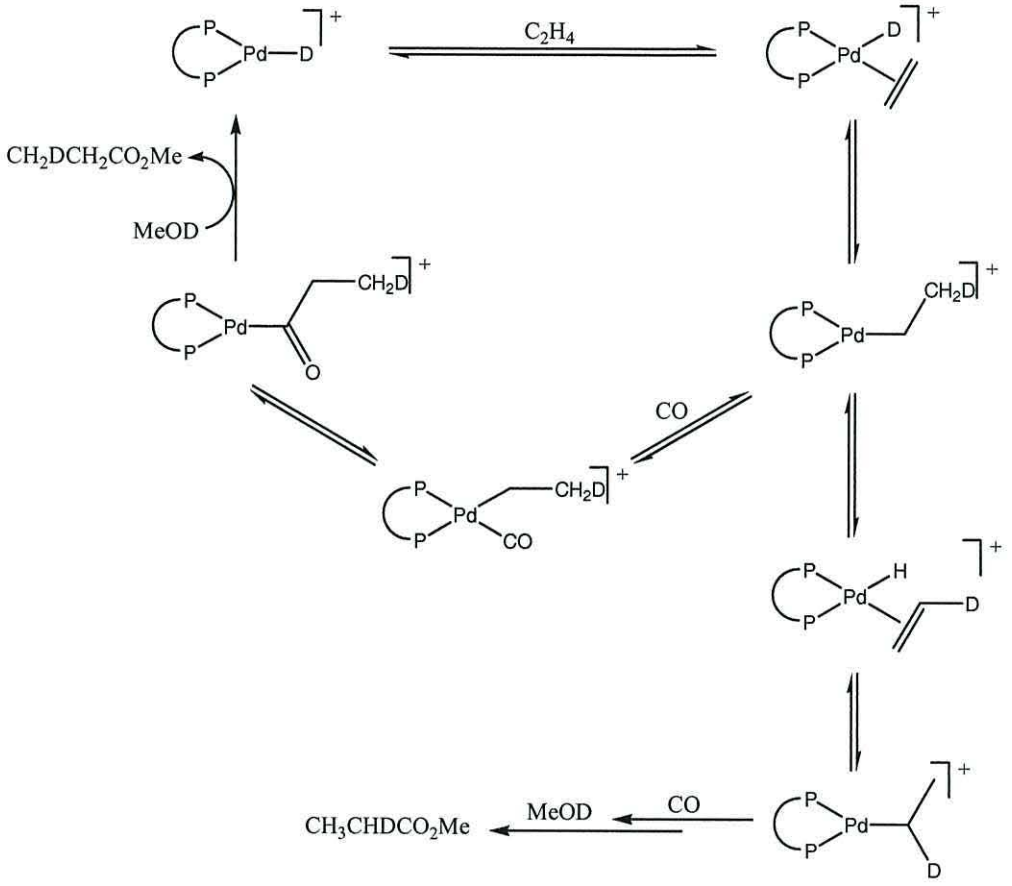

Scheme 14: Formation of monodeuterio products from ethene and CO in CH_3OD under efficient gas transport conditions.[38]

Under conditions of poor mixing, much more extensive scrambling occurs and a significant proportion of the ethyl groups do not contain D. This is interpreted as meaning that CO mass transport is rate limiting and that exchange of free and bound ethene becomes significant. Analysis of the unreacted ethene during the reaction showed incorporation of up to three D atoms.[38, 24] There is no way that the carbomethoxy mechanism can account for the production of undeuterated methyl propanoate, since termination must proceed via protonolysis with CH_3OD and there is little or no exchange of D for H in the solvent.

In summary, for the overall production of methyl methacrylate, the mixing of olefin, carbon monoxide and methanol with a catalyst [$Pd(OAc)_2$] or [$Pd(dba)_2$] with (P-P) (P-P = C_4-bridged diphosphine) is carried out under nitrogen at 90°C. The olefin and CO are required in equimolar quantities, and methanol in around 50:1 excess together with 10 % mol of the catalytic species. A polar aprotic solvent is required, and methyl propanoate or the ester product can be successfully used for this purpose. Under these conditions, coordination of ethene and carbon monoxide to palladium, and attack by methoxy anion at the coordinated carbonyl carbon atom prompts 2 + 2 cyclisation, forming a new bond between CO and the olefin, followed by reductive elimination of the methyl propanoate product from palladium (scheme 15). Subsequent oxidation with formaldehyde in a later process generates methyl methacrylate.

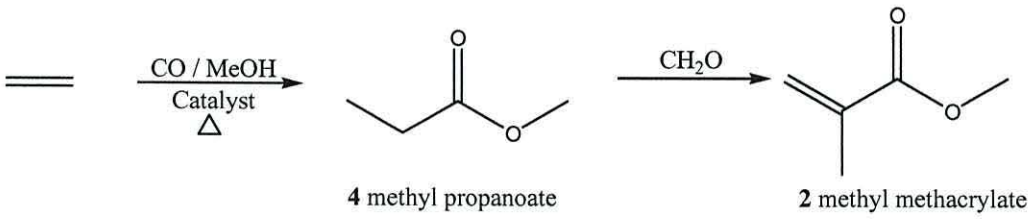

Scheme 15: Route towards MMA from a C_2 precursor.

The proposed catalytic system, involving ligation of a di-phosphine ligand to palladium incurs high costs in maintenance. One of the problems identified early on in catalytic testing is deactivation of the catalyst by demetallation of one of the phosphorus atoms. Thus, for the system to remain productive, it must be maintained by addition of more catalyst, or if possible by regeneration of the catalyst. The design of the ligand is considered as crucial to reduce the rate of deactivation, in addition to optimising selectivity and maintaining high turnover.

1.4 Ferrocenyl Catalysis.

1.4.1 Bidentate ferrocenyl phosphine ligands.

Since the discovery of ferrocene over 50 years ago in 1951,[1] a large body of literature relating to the compound, its derivatives and its complexes has evolved. Thus there are numerous derivatives of ferrocene; among these are the bidentate ferrocenyl amines and ferrocenyl phosphines connecting to a metal centre via the nitrogen or phosphorus heteroatom, which have proven to be effective in many homogeneous catalytic applications.

Bidentate phosphine ligands such as 1,1'-bis(diphenylphosphino)ferrocene (dppf) have a large volume of literature describing their transition metal complexes.[39,40] More recently, there have been reports of 1,2-substituted ferrocenes bearing phosphine moieties coupled directly on the Cp ring.[41-43] If the homoannular ring substituents are non-equivalent, the compound will posses planar chirality. Much less common are reports of ferrocenyl ligands with the phosphine ligand separated by a methine link with an adjacent phosphine directly to the Cp ring. Such a bidentate ligand allows much more flexibility in bite angle onto a transition metal centre. This flexibility may enhance catalytic activity, as a phosphine moiety may disconnect from the metal centre as part of the catalytic mechanism. Such a dissociation of a phosphine atom has been suggested as being part of the mechanism for Grubbs catalyst.[44]

A bidentate ligand has an advantage over a monodentate ligand in that reattachment of the partially dissociated ligand is more likely than complete ligand loss which would occur with a monodentate ligand. This 'rechelation' step may be a limiting factor in the catalytic mechanism of the carbonylation of olefins.

1.4.2 Examples of ferrocenyl based ligand catalysis in industry.

Probably the most important class of planar-chiral ferrocenes is that of chelating ligands for transition metal catalyzed asymmetric reactions. Progress in this area is characterized, among others, by ligands of type **16**,[45] **17**,[46] and **18** [47] (figure 7).

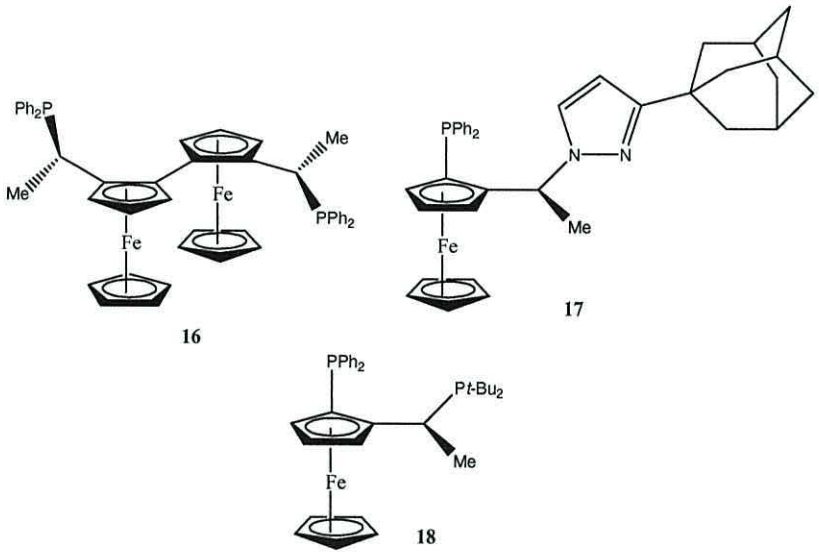

Figure 7: Planar chiral ferrocenes used in transition metal catalyzed asymmetric reactions.

The C_2-symmetric biferrocene **16** has been reported by Ito and co-workers to behave as a *trans*-spanning chelating ligand. The combination of C_2-symmetry and *trans* coordination geometry is conceptually new in the field and is promising for future development. TRAP (the abbreviation for this kind of compounds) affords high enantioselectivities in the Rh-catalyzed asymmetric Michael reaction of 2-cyanopropionates, the hydrosilylation of simple ketones, and the hydrogenation of β,β-disubstituted *N*-acetylaminoacrylic acid derivatives.

The P, N ligand **17** represents a class of chiral auxiliaries that are amenable to easy steric and electronic tuning, an aspect that is anticipated to play an important role in the further development of asymmetric catalysis. Thus, ligands of this type have been

shown to afford the highest enantioselectivities reported so far for the Rh-catalyzed hydroboration of styrenes with catecholborane (up to 98.5 % *ee*) and for the Pd-catalyzed substitution of allylic acetates and carbonates with benzylamine (up to > 99 % *ee*). The advantage offered by these ligands is the ease of their synthetic modification, which relies upon the simple idea of a construction kit.

The same types of considerations apply to diphosphanes of the Josiphos type such as **18**.[47] This specific compound, containing the bulky $^{t}Bu_2P$ group, has been found to be the only ligand that affords a very high diastereoface selectivity in the hydrogenation of compound **19** to give **20**, an intermediate in a new synthesis of (+)-biotin (scheme 16).[48,49] The analogous achiral starting material containing a benzyl protecting group, instead of a stereogenic phenethyl group, affords under the same reaction conditions 90 % *ee*. This quite remarkable process, which involves the hydrogenation of a fully substituted C==C bond, is currently being applied on a commercial scale by Lonza AG.

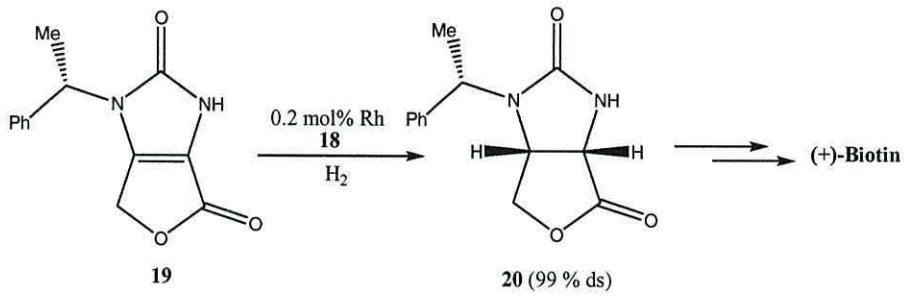

19 **20** (99 % ds)

Scheme16: Assymetric hydrogenation of **19** to give **20**, which is used in the preparation of (+)-biotin.[48]

A second and probably more important technical application of this type of ligands has recently been disclosed by Ciba-Geigy. Derivative **21** constitutes the chiral component of the exceptionally active iridium catalyst used for enantioselective hydrogenation of imine **22**, an intermediate in the synthesis of the herbicide (S)-Metolachlor **24** (scheme 17).[48,50]

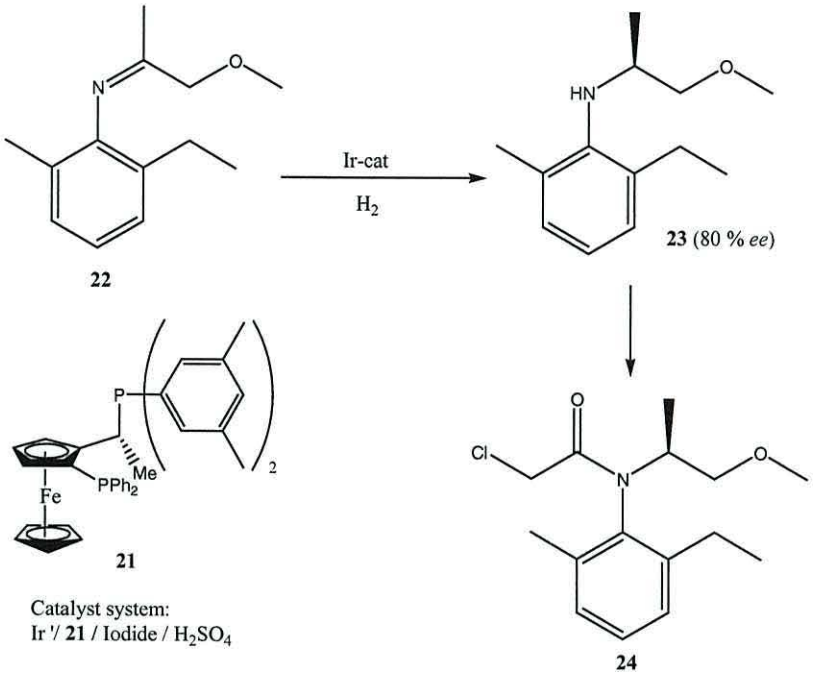

Scheme 17: Asymmetric imine hydrogenation in the process of the herbicide (S)-Metolachlor **24**.[48]

The relatively low selectivity obtained in this catalytic reaction (80 % *ee*) is tolerable for an agrochemical product. Much more important in this specific case are the activity and productivity of the catalyst. Besides the decisive co-catalytic effect of the added acids (the exact role of the added iodide salt and of the acid are still unclear), one of the key features of this large industrial process is the use of ferrocenyl ligand **21**, which turns out to be superior to all commercially available chiral chelating diphosphanes with respect to a combination of several important aspects.

The latter two examples constitute the first industrial applications of chiral ferrocenyl ligands and are a clear demonstration of the potential of this class of compounds. Any improvement of their synthetic versatility will mirror not only their fundamental interest, but shall be welcome also by the practitioner in the fine-chemical industry who is willing to extend the scope of homogeneous catalysis as a powerful synthetic method.

1.4.3 The development of 1,2-ferrocenyl phosphine ligands.

There have been many reports of 1,2-substituted ferrocenyl phosphines, including those which are enantiomerically pure. High enantiomer purity is obtained by diastereoselective *ortho*-lithiation of a ferrocenyl derivative containing a tertiary amine as an ortho directing moiety.[51]

An early report into the synthesis of 1,2-disubstituted ferrocenes by Hadlington[52] by nucleophilic displacement of 2-(hydroxydiphenylmethyl)ferrocenyl-1-methyltrimethylammonium iodide, itself obtained by quaternisation of the neutral 1-(hydroxydiphenyl)-2-dimethylaminomethyl ferrocene by various nucleophilic reagents. These included EtOH-NaOH to give R = OEt, and Ph_2NH to give R = NPh_2 **25** (figure 8).

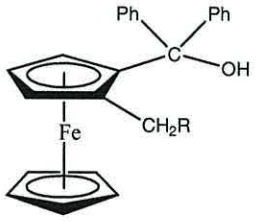

25

Figure 8: Hadlington's 1,2-disubstituted ferrocene.[52]

The paper did not report the preparation of any phosphine compounds; however these ferrocenes did contain two important features: 1) they were 1,2-disubstitued though not by bis-substitution and 2) they contained a methylene 'linker' group.

A 1,2-disubstituted phosphino ferrocene **26** active in the copolymerization of carbon monoxide and propene to produce a polyketone product was prepared from sterically crowded Josiphos type ligands bearing trifluoromethyl substituents.[53] Productivity for the series of ligands ranged from a disappointing 50 g $(Pd)^{-1}h^{-1}$ for the

methoxy substituted phenyl ring type ligand to 1,797 g $(Pd)^{-1}h^{-1}$ with greater than 99 % selectivity for the bis-trifluormethyl substituted ligand (figure 9).

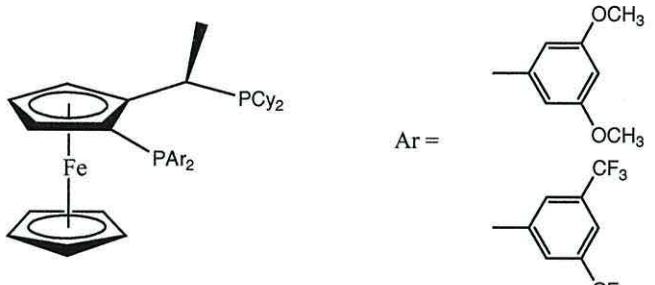

26

Figure 9: Gambs 1,2-disubstituted Josiphos type ferrocene, with the two discussed aryl substituents.[53]

The bis-1,2-disubstituted phosphino compound is different from the 1,2-disusbstitued ferrocene, in that the two phosphine substituents are identical. The ligand is further distinct from the more common bis-1,1'-disubstituted ferrocene in that the substitution is only on one ring. An example of which has been reported that 1,1'-bis(diphenylphosphino) ferrocene catalysts are scarcely selective in the formation of methyl propanoate producing substantial amounts of cooligomers **27** (figure 10).[33, 54]

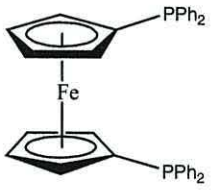

27

Figure 10: 1,1'-bis(diphenylphosphino) ferrocene (dppf).[39, 40]

The first report of a bis-1,2-disubstitued ferrocene **30** by Kagan was made as recently as 1998.[41] This involved the treatment of a chiral ferrocenyl sulphoxide **28** with LDA, and quench with the chlorinated substituent of choice, for example $ClPCy_2$. This was followed by metallation of the sulphoxide position with *t*-butyllithium, and subsequent quench with a second aliquot of the halogenated substituent (scheme 18).

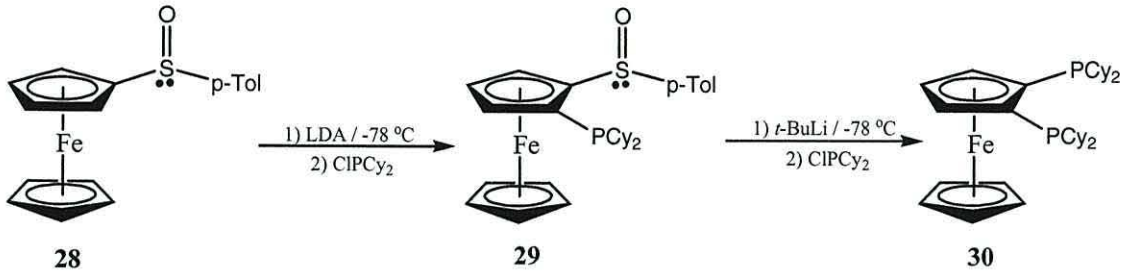

28 **29** **30**

Scheme 18: Kagan's route towards bis-1,2-disubstituted phosphino ferrocene.[41]

Another approach towards bis-1,2-substituted ferrocenes, and indeed also towards bis-1,1' and bis-1,3 disubstituted ferrocenes was reported by Broussier.[43] Broussier's approach was to first prepare the corresponding substituted cyclopentadienes, and then react them with $FeCl_2$ to produce the product ferrocenes in various mixtures which could be separated and isolated by column chromatography.

Other examples of 1,2-disubstituted ferrocenes are recent studies reported by Meunier *et al* which include the synthesis,[55-58] coordination chemistry[59] and catalytic properties[60] of the conformationally blocked ferrocenyl tetraphosphine (1,1',2,2'-tetrakis(diphenylposphino)-4,4'-di-*tert*-butylferrocene **31** (figure 11). These studies highlighted the efficiency of this triarylphosphine ligand in conjunction with palladium in Suzuki and Heck cross coupling reactions.[60]

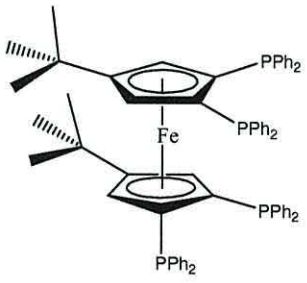

31

Figure 11: (1,1',2,2'-tetrakis(diphenylposphino)-4,4'-di-*tert*-butylferrocene **31**.[58]

Of considerable interest in our studies however are bis-1,2-ferrocenyl phosphine ligands which contain a methylene (-CH_2-) linker group as a potential catalyst precursor similar in design to that of the template **7** (see **section 1.3.4**).

1.4.4 Ferrocenyl phosphine ligands containing a methylene linker.

In 1963 a route towards a ferrocenyl phosphine: diphenylphosphinomethyl ferrocene **36,** incorporating a methylene linker group between the ferrocene and the phosphorus atom was reported by Pauson.[61] The route involved first quaternisation of the amine in dimethylaminomethyl ferrocene **32**, and substitution of trimethylamine by triphenylphosphine. Deprotonation of the CH_2 unit by phenyllithium to form the phosphorane and finally reduction with lithium aluminium hydride resulted in the ferrocenyl phosphine **36** (scheme 19).

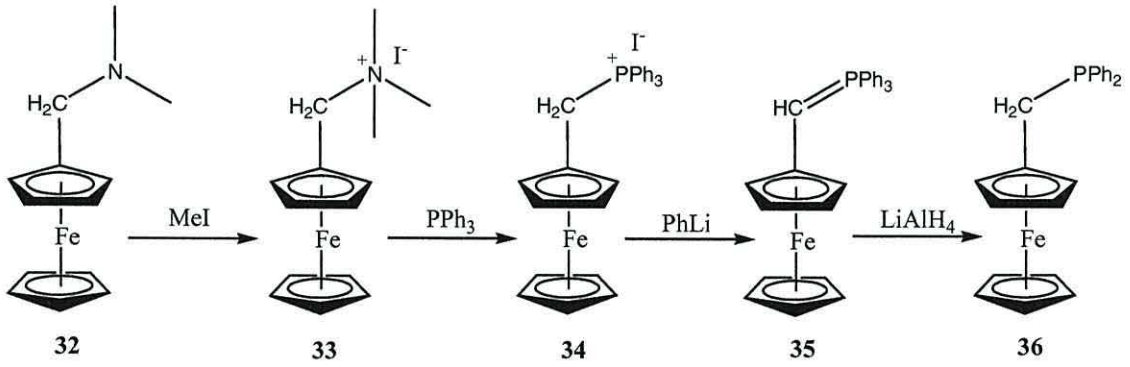

Scheme 19: Pauson & Watts 1963 preparation of diphenylphosphino ferrocene **36**.[61]

Generally phosphines are quite air sensitive, and readily form oxides. The reaction can be energetic, and phosphines are sometimes pyrophoric. It is common to see an oxide signal in the ^{31}P NMR spectrum of phosphines e.g. bis(diphenylphosphino) propane phosphine signal appears at a chemical shift of -17.50 ppm while its oxide has a chemical shift of 32.47 ppm.

Several mono-substituted ferrocenes containing a methylene linker to produce a range of derivatives has been developed by Goodwin *et al.*[62-65] These derivatives include the air stable phosphine bis-hydroxymethylaminomethyl ferrocene **37** and the air stable primary alkyl phosphine: phosphanylmethyl ferrocene **38** (figure 12). The presence of the CH_2 is attributed for the air stability of these compounds although Goodwin was uncertain as to how this was accomplished.[62] However, later electrochemical studies[66] have shown $FcCH_2^+$ to be a relatively stable cleavage species, supporting Goodwins earlier speculation that positive charge on the phosphine might migrate to the adjacent CH_2 linker group, thus avoiding electrophilic attack by oxygen.

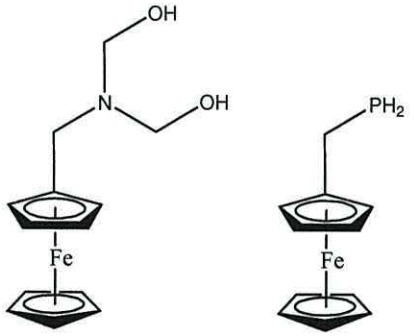

37 **38**

Figure 12: bis-hydroxymethylaminomethyl ferrocene **37** and phosphanylmethyl ferrocene **38**.

1.4.5 Bis-1,2-ferrocenyl phosphine ligands containing methylene linker groups.

This class of ligand posseses a C_4 bridge between two phosphorus atoms. It is a 1,2-disubstituted ferrocene reported by Butler *et al* in which the two phosphorus atoms are bridged by a butyl backbone in which the 2 and 3 positions are derivatised.[67] The species is present in the bis-1,2-disubstituted phosphino ferrocene with CH_2 linkers between the phosphorus atoms and the ferrocenes Cp rings **39** (a relatively new class of ligand as reports are rare in the literature). Further modifications at the phosphorus R

groups are possible, with phenyl- and alkyl-substitution achievable. The *tris*-1,2,3-trisubstituted phosphine **40** developed by Butler *et al* can also be described under this category when chelated to a metal centre in bidentate fashion (figure 13).[67] In effect, there are two C_4 bridges, each sharing the central substituents.

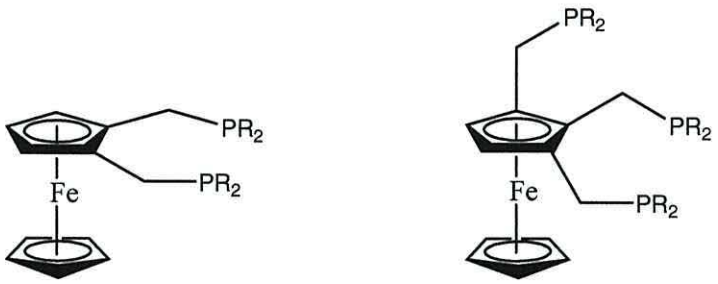

39 **40**

Figure 13: Bis-1,2-disubstituted and tris-1,2,3-trisubstituted phosphino ferrocenes.[67]

They both contain the structural component implicated as important in the carbonylation of carbon monoxide and ethene in the production of methyl propanoate.[25,32] The phenyl compound 1,2-di-*tert*-butylphosphinomethyl benzene **7** (section **1.3.4**) has been used as a ligand as a successful catalyst for carbonylation of CO and ethene. It is partly because of the potential in improvement in performance of already well-established catalyst templates that the chemistry of phosphine ligands containing ferrocenyl substituents has become so widely investigated.[39]

The presence of the C_4 bridge when coordinated to a metal centre forms a 7-membered ring, with a large P^M^P bite angle and it may be the case that this angle is instrumental in the high activity and selectivity of the resultant complex in the catalysis of carbonylation of olefins, as in a square planar complex for a large P^M^P angle, geometry requires that ligands *trans*- to the two phosphorus atoms must move closer

together. There have been very few reports of this type of compound being prepared[43] and, preparation has been reported as problematic.[68]

However recent work by Butler *et al*,[69] covers the development of these types of ferrocenyl phosphine ligands for the palladium mediated carbonylation of olefins, especially of ethene in the presence of carbon monoxide and methanol, to produce methyl propanoate as a precursor to methyl methacrylate.

1.4.6 Routes towards 1,2- and 1,2,3-substituted ferrocenyl derivatives bearing C_4-bridged diphosphines.

A desire to produce a ferrocenyl analogue of the already established and successful catalyst ligand bis-1,2-(di-*tert*-butylphosphinomethyl)benzene **7** (section **1.3.4**), led to the preparation of the first example of a bis-1,2-disubstituted aminomethyl ferrocene **41**.[67] This was synthesised by treatment of the commercially available dimethylaminomethyl ferrocene **32** (Ugi's amine)[51] with 1 molar equivalent of n-butyllithium in diethyl ether giving the ortho metallated product 1-lithium-2-dimethylaminomethyl ferrocene. Subsequent quench under chilled conditions with Eschenmoser's salt ($[CH_2=NMe_2]I$)[70] gives the product 1,2-bis-dimethylaminomethyl ferrocene **41**. Conversion of the bis amino ferrocene into the C_4-bridged diphosphine was achieved by a modification of Togni's literature method of refluxing the phosphine together with the ferrocenyl amine in acetic acid under nitrogen.[71] Togni's example was for a mono-substituted ferrocene, and was much less sterically hindered than the target compound 1,2-bis-di-*tert*-butylphosphinomethyl ferrocene **42** and so the required reaction

time was found to be at least 24 hours. The analytically pure product was obtained in 83% yield as yellow crystals (scheme 20).[67]

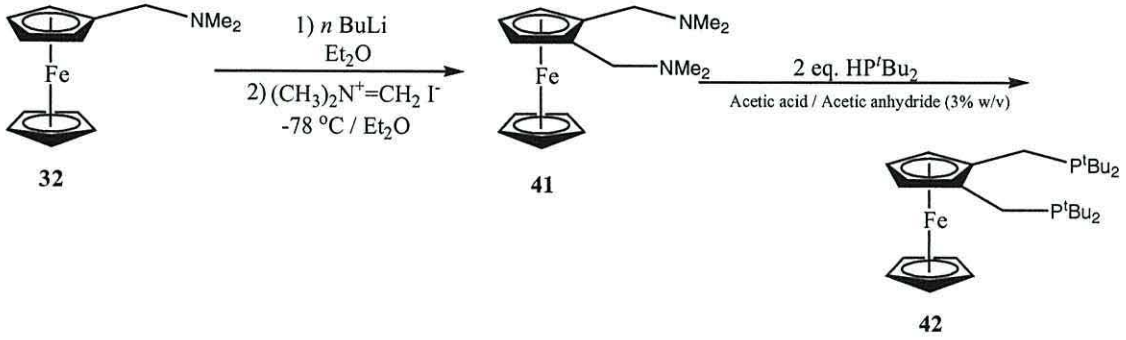

32 41 42

Scheme 20: Synthetic route to 1,2-bis-di-*tert*-butylphosphinomethyl ferrocene **42**.[67]

After an attempt to find a synthesis of tris-1,2,3-substituted ferrocenes had not been forthcoming despite tridentate ferrocenylphosphines being known with such examples as tris-1,2,1'-diphenylphosphino ferrocene **43** and tris-1,3,1'-diphenylphosphino ferrocene **44** (figure 14)[68] it was decided to attempt the synthesis of the 1,2,3-di-methylaminomethyl ferrocene precursor towards 1,2,3-trisubstituted phosphine following an adapted methodology to that used for the bis compound **42**. None of the tris-product was ever isolated.

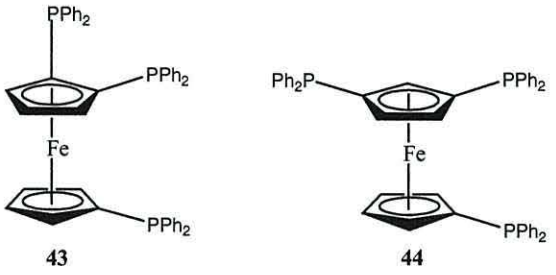

43 44

Figure 14: Tridentate ferrocenyl phosphines.[68]

It was originally thought that Eschenmoser's salt was insufficiently electrophilic to substitute the 3-position of the largely deactivated bis-substituted ferrocene. An alternative approach was to try formaldehyde, as the electrophile, thereby installing a

hydroxymethyl group. Reactions of **41** with *para*-formaldehyde were unsuccessful, giving only a small amount of product. Formaldehyde in its polymeric form was insufficiently electrophilic due to the energy cost of breaking the bonds of the polymer precursor to formaldehyde, thus it was decided to attempt the thermal de-polymerization of *para*-formaldehyde and subsequent reaction of molecular formaldehyde with the lithiated bis-substituted ferrocene. Pfeffer *et al* reported the thermal decomposition of CH_2O and its subsequent reaction with substrates in solution, by heating to 180°C and carrying the molecular formaldehyde into a reaction vessel via an inert gas.[72] Employing this methodology an attempt was made to prepare 1-hydroxymethyl-2,3-dimethylaminomethyl ferrocene **45** (figure 15).

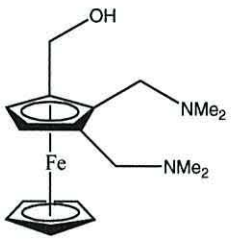

45

Figure 15: 1-hydroxymethyl-2,3-dimethylaminomethyl ferrocene **45**.

Evidence from ^1H NMR analysis showed the target compound **45** to be produced in good yield however there were other unidentifiable products also present, presumably resulting from the reaction of the amine lone pair and the highly reactive formaldehyde. Molecular formaldehyde was therefore deemed too reactive for a process intended for industrial application. It was realised however that residual *p*.CH_2O in the heating vessel had become quite thoroughly calcined; a realisation that came from the fact that initially water was driven off first from the formaldehyde polymer during thermal decomposition.

It was also found that the presence of water had been the reason for poor yields and high percentage recovery of ferrocenyl starting materials.

Thus, calcined formaldehyde instead of Eschenmoser's salt was used to react with the monosubstitued ferrocene **32** as a test which gave the disubstitued product **46** in 18 % yield as an orange oil. Once prepared it was further reacted with di-*tert*-butyl phosphine to ensure that the phosphine would substitute both the amine and the hydroxyl functionality and furnish the desired target compound 1,2-bis-di-*tert*-butylphosphinomethyl ferrocene **42**. Reaction of 1-hydroxymethyl-2-dimethylaminomethyl ferrocene **46** with excess di-*tert*-butyl phosphine in refluxing acetic acid, and in the presence of acetic anhydride gave the bis-phosphine **42** in 53% yield (scheme 21).[67] This success meant that there were now two synthetic approaches to the bis-1,2-phosphinomethyl ferrocene, the original method however was quite costly in using the expensive Eschenmoser's salt as a quench. It is advantageous to use the cheaper formaldehyde; as such any optimisation of this route would be of some significance.

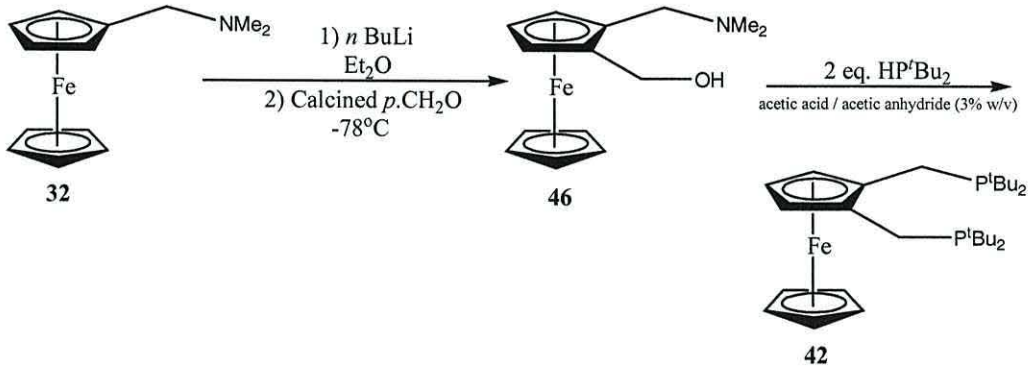

Scheme 21: Alternative route to **42**.[67]

Following the successful attempts of synthetic routes towards ligand **42** it was clear that it was possible to further extend the route to obtain 1,2,3-trisubstituted ferrocene 1-hydroxymethyl-bis-2,3-dimethylaminomethyl ferrocene **45**, and then proceed

with substitution of the two amines and hydroxyl functionality with three equivalents of phosphine to obtain tris-1,2,3-*tert*-butylphosphino ferrocene (tris-P) **47** (scheme 22).[67]

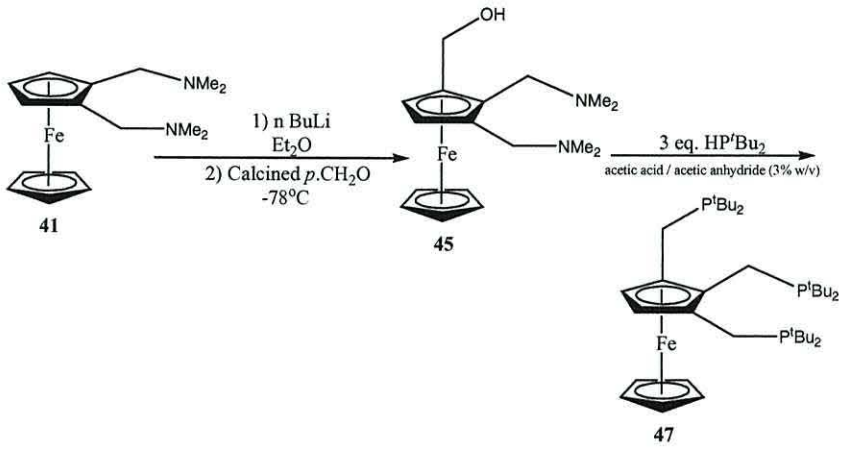

Scheme 22: Route towards tris-1,2,3-*tris*-butylphosphino ferrocene **47**.[67]

Thus *ortho*-lithiation of 1,2-bis-dimethylaminomethyl ferrocene **41** and subsequent treatment with calcined *para*-formaldehyde and subsequent reaction with the phosphine with workup, ether extraction, filtration and evaporation resulted **47** as orange oil in 91 % yield.

1.4.7 Substitution effect on π-acidity.

Varying the substitution of the phosphorus atoms will alter both the ligands steric and electronic properties.

With electronegative substituents, like Ph or halogen, trivalent phosphines are endowed with strong π-acid properties, and notwithstanding steric factors, their π-bonding characteristics will vary with electronegativity of the substituents.

An ordering of decreasing π-bonding ability or increasing lewis basicity, based on IR-data and ^{13}C NMR spectral data of carbonyl bonds in the complex $[L(Ni(CO)_5]$ [73] is as follows:

$$PF_3 > PCl_3 > P(Oar)_3 > P(OR)_3 > P(Ar)_3 > PR(Ar)_2 > PR_2Ar > PR_3$$

It can be seen from this order that a ligand such as 1,1'-diphenylphosphino ferrocene (dppf) **27** would fall under the category of $P(Ar)_3$ or $PR(Ar)_2$, where R = ferrocene. Whereas phosphines with alkyl substituents such as bis-1,2-di-*tert*-butylphosphinomethyl benzene **7**, or bis-1,2-di-*tert*-butylphosphinomethyl ferrocene **42**, where in each case the phosphorus is directly bonded to three alkyl moieties for which π-acceptor characteristics is poor, falls to the far right, under PR_3. Using a di-alkyl phosphine in place of diphenyl phosphine produced a ligand with more basic properties, with much less π-acceptor character.

1.4.8 Phosphine steric effect on the geometry of complex.

The steric influence of a ligand is most usually expressed in terms of Tolman's cone angle, θ (figure 16).[74]

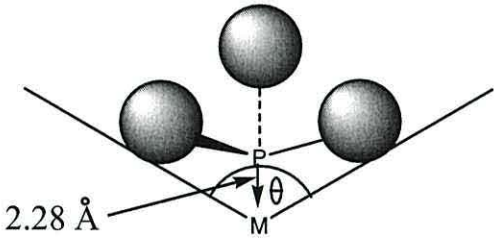

Figure 16: Illustration of Tolmans cone angle, θ.[74]

The cone angle is the angle that just encompasses the Van der Waal's radii of all the ligands constituent atoms, throughout all possible orientations and conformations about the metal-phosphorus bond. As an example the cone angle for triphenyl phosphine is 145°, and P^tBu_3 is approximately 182°.

A phosphorus atom with branched chain substituents, for example a *tert*-butyl group causes the cone angle to become very large. The σ-donor ability, or lewis-basicity

of the ligand will also increase due to increased electron induction. This impacts the geometry of any metal complex prepared using the ligand, particulary in the case of a bidentate ligand. An increase of the bite angle as of a bidentate ligand will reduce the associated L^M^L angle (L = ligand, M = metal centre) of species *trans* to the two phosphorus atoms. In a square planar complex, with four identical ligands, the L^M^L angle will be 90°, an increase in this angle will therefore result in either a decrease in the analogous angle on the opposite side, or distortion towards a more tetrahedral geometry.

This will produce a distortion in a square planar Pd complex in giving it a more tetrahedral character. In an octahedral complex, distortion from the plane has a higher energy than for a 4-coordinate structure, and so increased bite angle is likely to be compensated more by a decrease in the *trans* L^M^L bond angle.

This 'compression' of the ligands *trans* to the phosphine atoms in a metal complex used in a catalytic application will favour a dissociative mechanism, whereby the rate limiting step requires the prior disconnection of an existing ligand from the metal centre. Complexes with lower coordination numbers will also be favoured by sterically demanding ligands.

In the case of a catalytic complex, a change in electron-donor / π-acceptor ability and geometry can increase or decrease the energies of other bonds in the complex, particularly those bonds that are *trans*- to the ferrocenyl ligand. Weakening of a bond involved in a catalytic mechanism will lower the activation energy for the catalytic reaction, and provide an exponential increase in the rate of the catalysed reaction.

1.4.9 Initial catalytic testing.

Some catalytic testing of carbonylation of ethene using these ferrocenyl ligands have been carried out by Ineos Acrylics plc.[13] Coordination of the ferrocenyl phosphine ligands to palladium to form the active catalyst was carried out as the method reported for $[(dppp)Pd(OAc)_2]$.[75] In a typical run, $[Cl_2Pd(OAc)_2]$ (0.014mmol) was added to an autoclave, together with the bis-phosphine **42** (0.076 x 10^{-3}mmol) and 70% $_{w/w}$ methyl propanoate / methanol (300ml). The autoclave was heated to 100°C, and held at this operating temperature for the duration of each experiment.

The experiment was duplicated for each ligand: Bis-P **42**, Tris-P **47** and also the previously known ligand; bis-1,2-di-*tert*-butylphosphinomethyl benzene **7** (Benz-P) (section **1.3.4**). The results from these tests are presented in figure 17.[13]

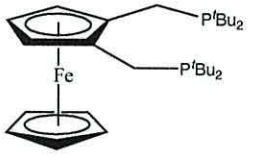

42 Bis-P

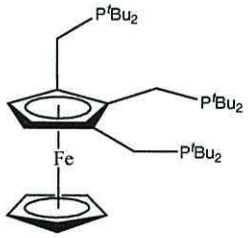

47 Tris-P

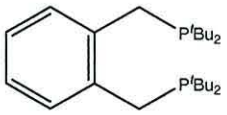

7 Benz-P

	Run	Initial Rate	Turnover number
		Moles catalyst / moles product / hr	moles catalyst / moles product
Bis-P	1	31,810	59,941
	2	30,322	63,941
Tris-P	1	24,506	50,751
	2	32,884	50,751
Benz-P	1	29,106	44,775
	2	30,335	51,997

Figure 17: Turnover and rate data for catalytic carbonylation of ethene.[13]

It can be seen that the initial rates of reaction for all three ligands are similar however the turnover numbers for Bis-P **42** and Tris-P **47** each show significant improvement over the performance of the existing ligand Benz-P **7**. The increase in

turnover number for the ferrocenyl ligated catalyst may be attributed to the greater basicity of the ferrocenyl ligand, and to its greater bite angle imposing steric restrictions on the coordinated substrates.

Both the Bis-P **42** and Tris-P **47** had been shown to outperform the previously known catalyst for the production of methyl propanoate (the precursor to MMA).

1.5 Project objectives and targets.

1.5.1 Aims of the project.

A catalytic system based on coordination of bidentate phosphine ligands to palladium (II) has been shown to be highly active in the copolymerisation of ethylene and carbon monoxide.[25] A number of ligands have been evaluated in terms of the effect of the length of the bidentate bridge in the ligand on activity (g mol cat^{-1} h^{-1}), and molecular weight of product. It has been found that the catalyst bearing a C_4 diphosphine bridge showed the highest activity of 46,300 g per mol per hour activity and Mw of 14,400. This may be attributed to the ligands wide cone angle L^M^L formed by the coordination of the olefin and carbonyl groups, thus bringing them closer to facilitate the reaction. Different stereoisomers of the C_4 bridged diphosphine ligands in the catalyst differ in performance and selectivity as the reactions show high sensitivity to steric bulk and ring strain imposed on the catalyst/reagent chelate ring.

The overall aim of the work is to investigate the use of ferrocenyl phosphine ligands for the palladium mediated carbonylation of olefins, especially of ethene in the presence of carbon monoxide and methanol, to produce methyl propanoate **4** as a precursor to methyl methacrylate **2**. There are two possible products in these

carbonylation reactions, the monomer methyl propanoate or a polymer in which the olefin and CO functions are incorporated subsequently. The key to a good catalyst is to have 100 % selectivity for the monomer precursor and a high turnover number. It is observed that the ferrocene-ligand based catalysts fulfil both these objectives.

This research project was directed at the synthesis and characterisation of a series of phosphine-based ligands which will be used in an industrial catalytic process. These ligands will be incorporated into metal complexes which will act as pre-catalysts. The primary objectives are the preparation of key intermediates such as methyl propanoate in the industrial preparation of methyl methacrylate, which require palladium catalysed synthesis. The work program involved optimising the established synthesis of ferrocene-based ligands such as the ferrocenyldiphosphine target compounds and the synthesis of a range of new ligands and metal complexes.

Initial targets involved the optimisation of current synthetic methodology towards the ferrocenyldiphosphine ligands by optimising key precursors such as 1,2-bis-dimethylaminomethyl ferrocene **41** and 1-hydroxymethyl-2-dimethylaminomethyl ferrocene **46**. Alternative synthetic routes to these ligands can also be explored. Such synthetic strategies could involve addition of substituted dicyclopentadiene to iron chloride to produce the corresponding ferrocene compound.

Another target is the structural modification of the ligands to either enhance the catalytic rate or selectivity or to obtain functionalised ligands that may be attached to inorganic supports. A series of chiral ligands can be prepared which may be used in associated catalytic reactions.

The functionalisation of the lower (unsubstituted ring) of ferrocene-based ligands with bulky groups can also be carried out in an effort to functionalise the ligands. An example of which is pentaphenylferrocenyl di-*tert*-butylphosphine **48** which has been prepared in a high yield from a two-step process, and the scope of various cross-coupling reactions catalysed by complexes baring this ligand has been reported by Hartwig and co-workers.[76] Another example would be to use anthracene as the support (compound **49**) (figure 18).

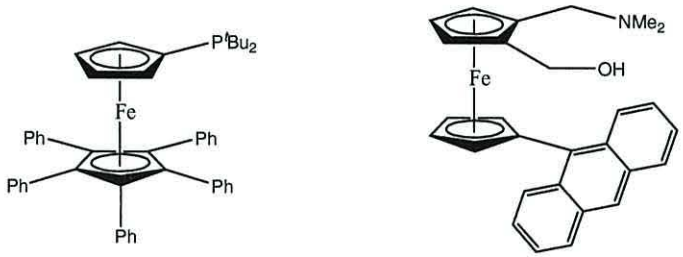

48 **49**

Figure 18: Functionalisation of the lower ring of ferrocene-based ligands.[76]

The synthesis of a range of ligands which are not ferrocene based can also be investigated. These will have important features require in that they will be 1,2-disubstituted species held with a rigid confirmation.

Chapter 2

Synthetic Results & Discussion

Synthetic Results and Discussion

2.1 Chapter 2: Overview.

In order to clarify the contents this chapter is divided into five sections:

Section 2.2 – describes the work done on optimising already existing routes towards four carbon backbone diphosphine ferrocene derivatives. This includes the investigation of the formation of bis-1,2-di-*tert*-butylphosphinomethyl ferrocene (**42**) by ^{31}P NMR spectroscopy and reports on the development of two unreported palladium complexes of C_4 bridged diphosphine ligands $[PdCl_2(P\text{-}P)]$ **52** and $[Pd(dba)(P\text{-}P)]$ **53**: where (P-P) = bis-1,2-di-*tert*-butylphosphinomethyl ferrocene and (dba) = *trans,trans*-bis(dibenzylideneacetone).

Section 2.3 – describes the synthesis of ruthenium analogues of the catalytic phosphine precursor in which steps were undertaken to prepare the unreported precursor ligand bis-1,2-dimethylaminomethyl ruthenocene **58**.

Section 2.4 – describes the functionalisation of ferrocene-based ligands with bulky groups in an effort to increase the steric bulk which improves catalytic activity in the methoxycarbonylation of ethene.

Section 2.5 – describes the synthetic studies on alternative ferrocenylphosphine ligands which may be used for catalytic applications.

Section 2.6 – describes the work on the synthesis and use of non-ferrocenyl compounds which may be used for catalytic applications i.e. xylyl derivatives.

2.2 Optimisation of current synthetic routes.

2.2.1 Introduction.

The aim of the work described in this section was to prepare ligands for application in the palladium catalysed methoxycarbonylation of ethene. The first target was to optimise the synthetic route of the ferrocenyl analogue of the already established and successful catalyst ligand bis-1,2-di-*tert*-butylphosphinomethyl benzene. This requires the preparation of a di-1,2-disubstituted aminomethyl ferrocene, bearing methylene linkers between the Cp ring and the amino groups. The FGI of the amino groups to phosphine substituents gives the bis-phosphine target compound and catalytic testing of this compound in the carbonylation of ethylene gave very encouraging turnover numbers when compared to its benzene analogue. The key to the success of this ligand was thought to be the presence of a four-carbon bridge between the two phosphines. This section describes the work on four carbon backbone diphosphine ferrocene derivatives carried out within the current research group. New routes have been developed to synthesise 1,2-disubstituted and 1,2,3-trisubstituted ferrocenes as described in section **1.4.5**.

As precursors to the target compounds 1,2-bis-di-*tert*-butylphosphinomethyl ferrocene **42**, bis-1,2-dimethylaminomethyl ferrocene **41** and 1-hydroxymethyl-2-dimethylaminomethyl ferrocene **46** were required. Synthesis of the phosphine could then proceed following the well known method published by Togni of refluxing the aminomethyl ferrocene together with the desired secondary phosphine in acetic acid.[71, 39] The overall scheme from ferrocene **50**, through to bis-1,2-di-*tert*-butylphosphinomethyl

ferrocene **42** is shown in scheme 23. This short synthetic methodology is considered suitable for a large scale industrial ligand synthesis.

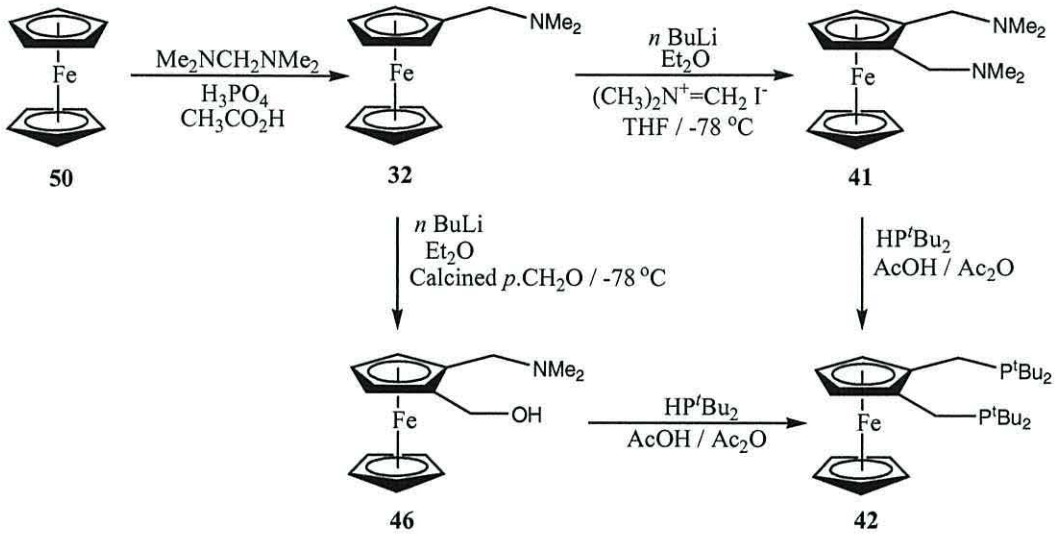

Scheme 23: Synthetic route to 1,2-di-*tert*-butylphosphinomethyl ferrocene **42**.

This section describes the attempt to optimise this existing methodology in order to maximise the benefits for an industrial process and also reports on the preparation of novel palladium complexes of **42** which may be tested in the described catalytic process.

2.2.2 Preparation of dimethylaminomethyl ferrocene (32).

Although commercially available, the cost of purchasing sufficient quantities of dimethylaminomethyl ferrocene **32** (the starting material in existing routes towards both the 1,2 and 1,2,3-substituted ferrocenes) was deemed too great and so steps were taken to prepare it in bulk using a method based on the work by Ledmicer *et al.*[77] This not only described a bulk preparation of dimethylaminomethyl ferrocene **32** but also a route to its main precursor N,N,N',N',-tetramethylmethylenediamine **51**.

Treatment of 37% aqueous formaldehyde solution with 25% aqueous solution of dimethylamine under cooled conditions and later addition of potassium hydroxide pellets

yielded (after distillation) very pure N,N,N',N'-TMMDA (**51**) (figure 19) in 77 % yield, as a clear colourless liquid. This material was produced in bulk quantities (>50g) and characterised by boiling point determination, ^{1}H NMR and ^{13}C NMR spectroscopy.

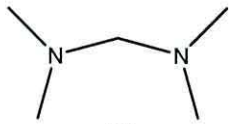

51

Figure 19: N,N,N',N'-tetramethylmethylenediamine **51**.

The product had a boiling point in a range 84-86°C which is consistent with the reported literature boiling point of 83-84°C.[77] Proton NMR showed two resonances, the four N-methyl groups were shown to be present as a singlet at δ 2.16 ppm and the N-methylene singlet was also present at δ 2.64 ppm. The integral ratio of 6:2 respectively confirms the correct number of hydrogen environments as the molecule is symmetric. The ^{13}C NMR spectrum also showed two resonances reflecting the two unique carbon environments; at δ 43.12 (s; NCH_3) and δ 80.16 ppm (s; NCH_2N).

With sufficient and cost effective quantities of the amine reagent **51** the preparation of **32** in bulk was also carried out as reported in the same literature report (scheme 24).[77]

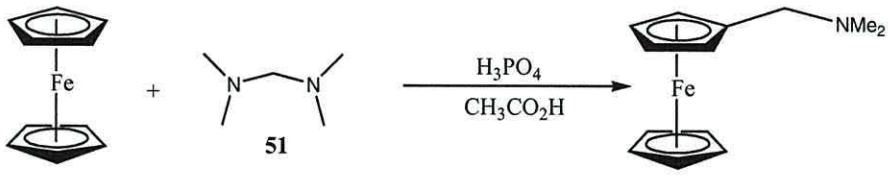

50 **51** **32**

Scheme 24: Synthetic preparation of dimethylaminomethyl ferrocene **32**.[77]

A well stirred mixture of bis-dimethylaminomethane **51**, phosphoric acid and acetic acid was treated with ferrocene **50** and subsequently heated on a steam bath for five hours under a slow stream of nitrogen. After water quench, and extraction with

diethyl ether the aqueous layer was cooled and made alkaline by addition of sodium hydroxide pellets. The tertiary amine separated from the alkaline solution and the mixture was extracted again with ether. The organic phase was then washed with water, dried over magnesium sulphate and filtered. Subsequent evaporation of the solvent gave dimethylaminomethyl ferrocene **32** in bulk (30.77g) as a dark red mobile liquid in 51 % yield.

The product (**32**) was subsequently characterised by ^{1}H and ^{13}C NMR spectroscopy. Proton NMR showed five resonances; the two N-methyl groups were present as a singlet at δ 2.15 ppm and the N-methylene was also present as a singlet at δ 3.26 ppm. These had an integral of 6:2 respectively. The un-substituted Cp ring appeared as a singlet at δ 4.09 ppm with an integral of five, and the four protons on the substituted ring appeared as overlapped resonances at δ 4.12 ppm and δ 4.18 ppm from which no coupling constants can be obtained. The ^{13}C NMR spectrum shows six resonances reflecting six unique carbon environments at δ 44.76 (s; NCH_3), δ 59.15 ($CpCH_2N$), δ 67.97 (Cpα-C), δ 68.45 (Cp5), δ 70.05 (Cpβ-C), and δ 83.32 (Cp *ipso*-C).

Dimethylaminomethyl ferrocene **32** was subsequently used in further reactions without further purification as the purity of the compound was verified by NMR spectroscopy; as no visible impurities were apparent. This material was prepared throughout this work but was also used in conjunction with commercial samples from Aldrich from time to time due to time constraints in preparing the compound, at times where the company required derivatised samples urgently.

2.2.3 Preparation of bis-1,2-dimethylaminomethyl ferrocene (41).

Treatment of dimethylaminomethyl ferrocene **32** with 1.2 molar equivalent of *n*-butyllithium in diethyl ether gave the *ortho* metallated product 1-lithium-2-dimethylaminomethyl ferrocene due to the *ortho* directing nature of the amine.[51,78-80] Subsequent addition of THF (to dissolve the quench reagent) and quench under cooled conditions with Eschenmoser's salt, followed later by work up with hydroxide solution, extraction with ether, drying, filtering and removal of volatiles gives the product bis-1,2-dimethylaminomethyl ferrocene **41** together with un-reacted starting material (scheme 25). Separation of the ferrocene was effected by re-crystallisation of **41** from petrol at -17°C. The product was isolated as orange/brown crystals in 36 % yield.

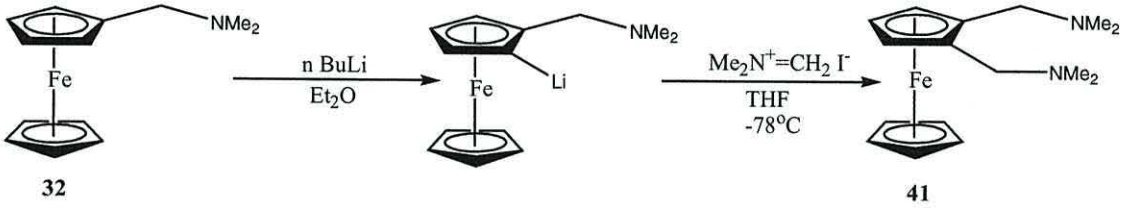

32 **41**

Scheme 25: Preparation of 1,2-bis-dimethylaminomethyl ferrocene **41**.

The product (**41**) was air stable, though hydroscopic, and was characterised by elemental analysis, melting point determination, X-ray crystallography, ^{1}H and ^{13}C NMR spectroscopy. Elemental analysis of **41** gave good match to the calculated values with C %: 63.3 (64.0), H %: 7.9 (8.1), N %: 9.4 (9.3); (calculated values in parenthesis). The compound showed a melting point of 69-73 °C in air with no apparent decomposition (lit. 74 °C).[13] The proton NMR spectrum of the product showed the four N-methyl groups to be present as a singlet at δ 2.19 ppm. The NCH_2Cp quartet was seen as a doublet at δ 3.19 ppm, with ^{2}J coupling of 13.12 Hz, and a second doublet at δ 3.31 ppm and a coupling constant of 12.82 Hz. The un-substituted Cp ring appeared as a singlet at δ 4.11 ppm, and

the three protons on the substituted ring appeared as a triplet (1H, inefficient calibration of the triplet peak) at δ 4.16 ppm, and as a doublet (2H, 2.44Hz) at δ 4.21 ppm, thus confirming the 1,2-bis substitution pattern of the ferrocenyl derivative. The ^{13}C NMR spectrum showed six resonances reflecting the six different carbon environments at δ 45.33 (s; N**C**H_3), δ 57.19 (s; N**C**H_2), δ 66.74 (Cpα-C), δ 69.04 (Cp5), δ 70.07 (Cpβ-C) and δ 84.04 (Cp *ipso*-C).

The crystal structure has previously been determined by X-ray analysis and the structure is shown in figure 20. When ultra pure samples are required this compound can be vacuumed sublimed as reported by Fortune.[13] Note how alignment of the two N-methyl groups 'upwards' and away from the ferrocene body results in the methylene protons being directed downwards, and being an 'inner' or an 'outer' hydrogen atom. Since rotation of the N-methyl groups is sterically hindered by the ferrocene body, this is the cause of the splitting observed in the ^{1}H NMR spectrum. Note also that packing of the amino constituents is such that the lone pairs on nitrogen are directed in the same sense, anticlockwise around the Cp ring when viewed from above the substituted ring.

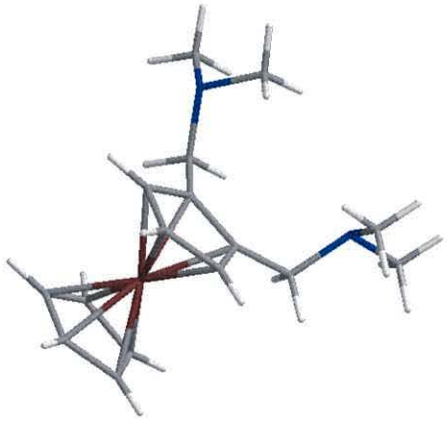

Figure 20: X-ray crystal structure of **41**.[13]

The quench reagent Eschenmoser's salt was used as received and the low initial yields are attributed to variations in purity of the commercial supplies. Earlier work in the synthetic procedure for this compound reported a yield of around 50 %.[13] Therefore it was decided to concentrate on the alternative route towards 1,2-diphosphino ferrocenyl ligands mainly because the product was hydroscopic and this could impact on subsequent reactions. Another reason was the use of expensive reagents such as Eschenmoser's salt was a disadvantage it was decided that research into optimising the much cheaper formaldehyde route was favourable.

2.2.4 Preparation of 1-(hydroxyl-methyl)-2-(dimethylaminomethyl) ferrocene (46).

As was explained earlier (section 1.4.6) when used as a quench molecular formaldehyde gave undesired products. When using *para*-formaldehyde as quench gave low yield it had us consider that the problems experienced were due to water present within the polymer, it was therefore decided to calcine the *para*-formaldehyde for a period of two hours at 180°C before using as a quench. Ortho lithiation of **32** with *n*-butyllithium in 2:1 excess and quench with dried formaldehyde in substantial excess of 4:1 and overnight stirring under N_2 resulted in a bright yellow suspension which had not been previously reported. Subsequent water quench, extraction with ether, drying and evaporation of the solvent furnished the crude product. Trace quantities of the starting material **32** was removed by column chromatography and the desired planar chiral product **46** was obtained in bulk quantity (> 30 g) as an oil and crystal mixture in a yield of 96 % (scheme 26). This result greatly improves on previous attempts which gave at best only 18 % yield. In earlier work calcined formaldehyde was only used in a 2:1 excess therefore a substantial increase in the quench material greatly improved the result.

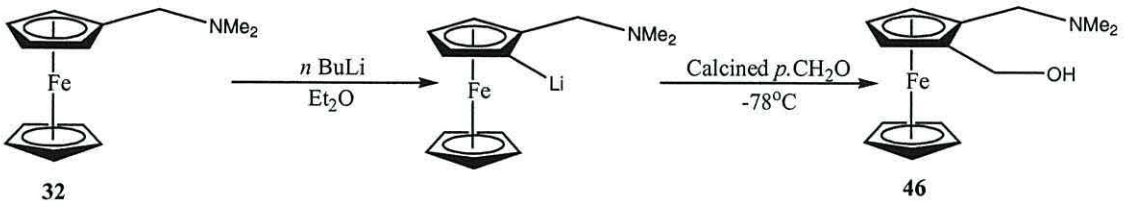

32 46

Scheme 26: Preparation of 1-(hydroxyl-methyl)-2-(dimethylaminomethyl) ferrocene **46**.

The product (**46**) was characterised by elemental analysis, infrared spectroscopic analysis, ^{1}H and ^{13}C NMR spectroscopy. Elemental analysis verified the purity: observed values for carbon, hydrogen and nitrogen and the calculated values (in parenthesis) were C %: 61.5 (61.6), H %: 7.4 (7.0), N %: 4.6 (5.1). The infrared spectrum showed hydrogen bonding associated with the hydroxyl group at 3350 cm^{-1}, also strong vibrations due to C-O stretching and O-H bending at a primary alcohol group were seen at 1352 cm^{-1} and 1036 cm^{-1} respectively. The ^{1}H NMR spectrum of the product **46** showed the presence of dimethylaminomethyl group as a singlet at δ 2.13 ppm and a spin system quartet at δ 2.78 ppm (with ^{2}J coupling of 12.36 Hz) and δ 3.90 ppm (with a coupling constant of 12.36 Hz). The two pairs of doublets are separated to a greater extent than in bis-1,2-dimethylaminomethyl ferrocene **41** which showed the doublets at δ 3.19 ppm and δ 3.31 ppm, a separation of 0.12 ppm. The hydroxyl compound **46** shows a separation of 1.12 ppm and since the hydroxyl group is less bulky than the dimethylamine, it is reasoned that the increased difference between the two CH_2N signals was due to the proximity of more electronegative oxygen atom. The hydroxyl arm CH_2 protons were also seen as two doublets at higher frequencies at δ 4.07 ppm (1H) and δ 4.74 ppm (1H, 11.91 Hz) also due to the high electronegativity of the oxygen atom. The doublet at 4.07 ppm was partially overlapped by the un-substituted Cp ring singlet at δ 4.05 ppm. The substituted Cp protons all lie in different environments due to the chiral nature of the product. These

are situated at δ 4.00 ppm (1H), δ 4.10 ppm (1H) and δ 4.15 ppm (1H) and seem to be multiplets being partially overlapped by other resonances making it difficult to determine their coupling constants.

In the ^{13}C NMR spectrum, the methyl carbon atoms were present at δ 44.56 ppm, and the associated CH_2 group as a resonance at δ 58.21 ppm. The CH_2O-carbon atom was seen at a slightly higher frequency at δ 60.19 ppm. The substituted Cp ring gave the expected five discreet resonances due to five non-equivalent carbon atoms, and the un-substituted Cp ring was seen as a sharp singlet at δ 68.65 ppm. These results corresponds to the data first reported by Fortune.[13]

In conclusion; substantial improvements in yield in the successful preparation of 1-(hydroxyl-methyl)-2-(dimethylaminomethyl) ferrocene (**46**) has been achieved and steps have been undertaken to prepare the 1,2-diphosphinomethyl ferrocenyl ligands by subsequent reaction of **46** with di-*tert*-butyl phosphine.

2.2.5 Preparation of 1,2-di-*tert*-butylphosphinomethyl ferrocene (42).

The reaction of 1-(hydroxyl-methyl)-2-(dimethylaminomethyl) ferrocene (**46**) with excess di-*tert*-butyl phosphine in refluxing acetic acid, and in the presence of acetic anhydride under argon gave 1,2-di-*tert*-butylphosphinomethyl ferrocene **42** isolated in 53% yield as orange crystals (scheme 27).

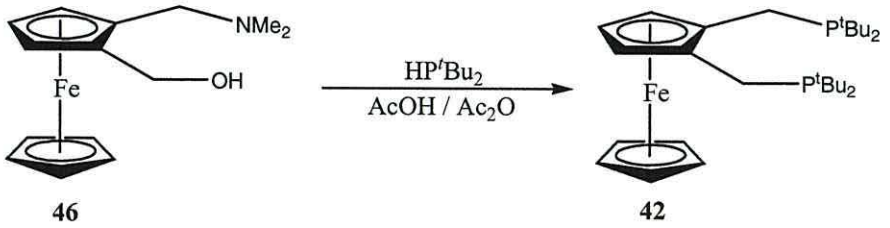

46 **42**

Scheme 27: Preparation of 1,2-di-*tert*-butylphosphinomethyl ferrocene **42**.

The product (**42**) was characterised by melting point determination, elemental analysis, mass spectroscopy, ^{1}H, ^{13}C and ^{31}P NMR spectroscopy. The compound showed a melting point of 79-83 °C in air with no apparent decomposition. Elemental analysis gave a satisfactory match between the observed values for carbon and hydrogen and the calculated values (in parenthesis) with C %: 66.4 (66.9), H %: 11.9 (9.6). The proton spectrum shows the 36 methyl protons as two pairs of doublets each with an integration of 18. One doublet at δ 1.13 ppm showed a $^{3}J_{PH}$ as 10.40 Hz, the other at δ 1.16 ppm with a $^{3}J_{PH}$ coupling constant of 10.72 Hz. The CH_2 spacers between the Cp ring and the phosphorus were seen as a spin system at δ 2.70 and δ 2.87 ppm with a $^{2}J_{PH}$ coupling constant of 15.45 Hz and 14.50 Hz respectively. The substituted Cp ring system was seen as a triplet (2H) at δ 3.74 ppm (α-H's) and a doublet at δ 3.03 ppm (β-H). The non-substituted Cp ring was seen as a singlet δ 4.04 ppm (5H). This pattern indicates that the $CH_2P^tBu_2$ groups were at position 1 and 2 of the substituted Cp ring. The ^{13}C NMR spectrum shows that the methyl groups were visible as two pairs of overlapping doublets, one at δ 29.92 ppm with ^{2}J phosphorus-carbon coupling of 12.83 Hz, and the other at δ 29.82 ppm with a coupling of 11.00 Hz. This difference in shifts is attributed to the 'inner' *tert*-butyl arm, positioned between the two phosphorus atoms would be most shielded from applied magnetic field and so would be observed at a lower frequency than the 'outer' *tert*-butyl arm. Likewise, the tertiary carbon atoms of the *t*-butyl groups were also seen as two separate shifts at δ 31.46 ppm (20.16 Hz) and δ 32.03 ppm (22.00 Hz). The CH_2 linker groups were seen as a pair of doublets at δ 21.08 ppm (24.47 Hz). The non-substituted Cp ring was seen as a large resonance representing five carbon atoms at δ 69.50 ppm. The substituted Cp ring showed a singlet for the unique carbon atom at δ

63.82 ppm, and the two CH carbon atoms were seen as a pair of doublets at δ 70.08 ppm split by ^{3}J coupling to phosphorus. The two substituted carbon atoms were observed as a very weak resonance at around δ 86.00 ppm (these should also be a pair of doublets however the spectrum wasn't very clear). This resonance pattern also indicates a 1,2-disubstituted product however there were other resonances present indicating that the product was not pure, possibly due to partial oxidation in the NMR tube. It is observed therefore that this compound is highly oxygen sensitive. The ^{31}P NMR spectrum of the compound showed only one resonance at δ 22.97 ppm indicating that the two phosphorus atoms were equivalent. The spectrum also showed trace signal at δ 66.74 ppm indicating possible oxidation which again may attribute for the impurity. This is in the expected area for an oxidised product. The mass spectrum of the product also showed a clean parent ion at m/z 502.

The preparation of compound **42** indicated successful conversion of a tertiary amine and a primary alcohol to two highly sterically hindered tertiary phosphines via reflux in acetic acid from its 1-(hydroxyl-methyl)-2-(dimethylaminomethyl) ferrocene **46** precursor. The one step conversion of the amine into the phosphine by this method greatly improves on an alternative route described in a recent publication by Stepnicka *et al* who reports on a three step conversion of a tertiary amine into a sterically hindered tertiary phosphine.[81]

2.2.6 The investigation of the formation of bis-1,2-di-*tert*-butylphosphinomethyl ferrocene (42) by ^{31}P NMR spectroscopy.

It was a priority to optimise the synthesis of the bidentate phosphine ligand **42** from 1-(hydroxyl-methyl)-2-(dimethylaminomethyl) ferrocene **46** as a precursor (figure

21). To study this it was decided to carry out an NMR investigation and find out the optimum conditions on a Bruker Avance 500 spectrometer operating at 202 MHz for ^{31}P.

Two ^{31}P NMR experiments were undertaken by using a specialized NMR tube which contained a 5mm tube inside a 10mm tube. The outer tube contained the reaction mixture as stated in scheme 27 and the inner tube contained deuterated water (D_2O) as lock (chosen due to its higher boiling point than $CDCl_3$)(figure 21).

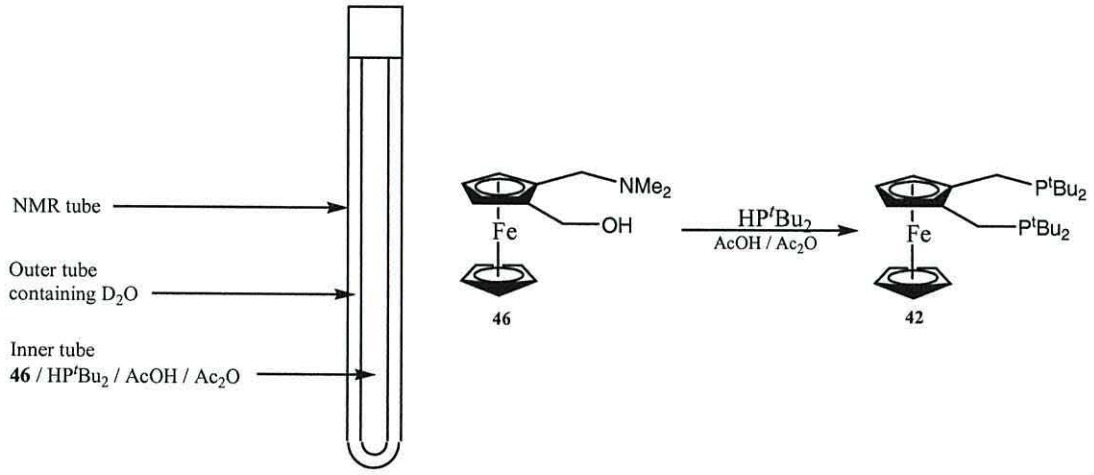

Figure 21: A schematic of the NMR tube used in finding optimum conditions of the formation of **46** from **42** (scheme 27).

It was decided to monitor the formation of the product **42** by ^{31}P NMR spectroscopy by comparing its spectrum (δ 22.97 ppm) to that of the starting phosphine reagent di-*tert*-butylphosphine (HP^tBu_2) which had a single resonance at δ 20.89 ppm. Two factors were considered to find the optimum conditions: the temperature needed for optimum conversion and the time taken for reaction completion. Both needed to be limited to acceptable industrial conditions for any viable potential use in ligand synthesis on an industrial scale.

Experiment 1 – Temperature.

The first experiment involved the reaction taking place on increasing temperature with ^{31}P spectra recorded at room temperature, 40, 60, 80 and 90°C respectively (figure 22). Unfortunately the temperature scale could not be set higher as the deuterated solvent would boil at 100°C. A trend is seen as new resonances are identified slightly downfield on increasing the temperature, from the original δ 20.89 ppm (starting phosphine) to δ 22.97 ppm (product **42**). Interestingly, the spectrum also shows the appearance and disappearance of phosphorus resonances further downfield at around δ 25, 40 and 60 ppm (intermediate and oxide formation). These resonances may be explained by the formation of one phosphine function (replacing the alcohol group) first with a subsequent exchange of the amine with the second phosphine forming the desired bis-phosphine product **42**.

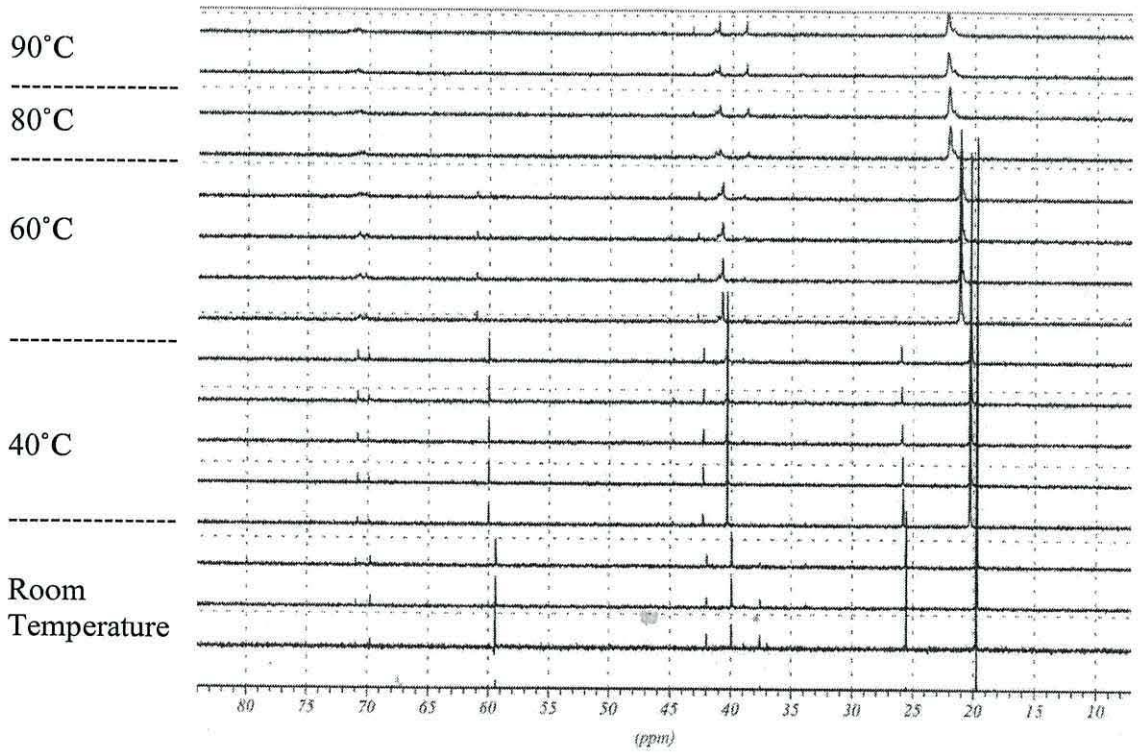

Figure 22: ^{31}P NMR spectra of product formation **42** on increasing temperature.

Figure 23 shows the close up on the area around the reagent and product resonances showing clearly the new resonance shift downfield with increasing temperature. As the reaction is being monitored on increasing temperature it can only be indicated from this result; that a temperature of 80°C is all that is required for full conversion and product formation since at this temperature the main ^{31}P resonance seen is that of the desired product 1,2-bis-di-*tert*-butylphosphinomethyl ferrocene **42**.

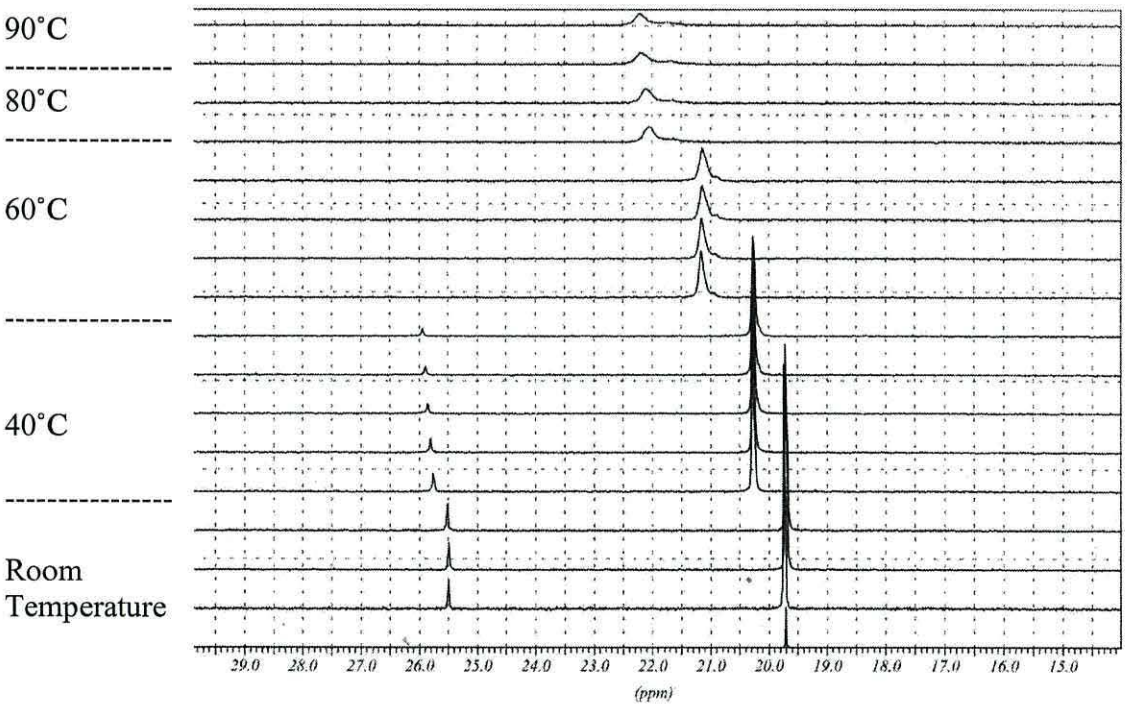

Figure 23: ^{31}P NMR spectra indicating phosphine reagent disappearance and product formation with increasing temperature.

Experiment 2 – To determine the amount of time needed for completion.

The second experiment involved the reaction being undertaken at a constant temperature of 80°C and obtaining ^{31}P NMR spectra at set times (figure 24). At time 0 h the spectrum showed the expected single resonance of the starting material (HP^tBu_2) at δ 20.89 ppm. After 23 min a new resonance appears immediately downfield to around δ 22

ppm indicating partial reaction. The product resonance is at δ 22.97 ppm (taken from a pure sample of 1,2-di-*tert*-butylphosphinomethyl ferrocene **42**). Spectra were recorded at 0 h, 0.23 h, 1.23 h, 2.23 h, 2.53 h and 3.23 h after initial insertion. The spectra also show the formation of extra resonances downfield (δ 41 ppm) which indicate the formation of the oxide or an intermediate. Over time these resonances show decreasing intensity after its initial formation at 0.23 h which indicates the conversion into the product. The reaction is quite rapid at a temperature of 80°C with satisfactory conversion within the first 30 min. It is clear that the product formed within the first 23 min and may be found even earlier.

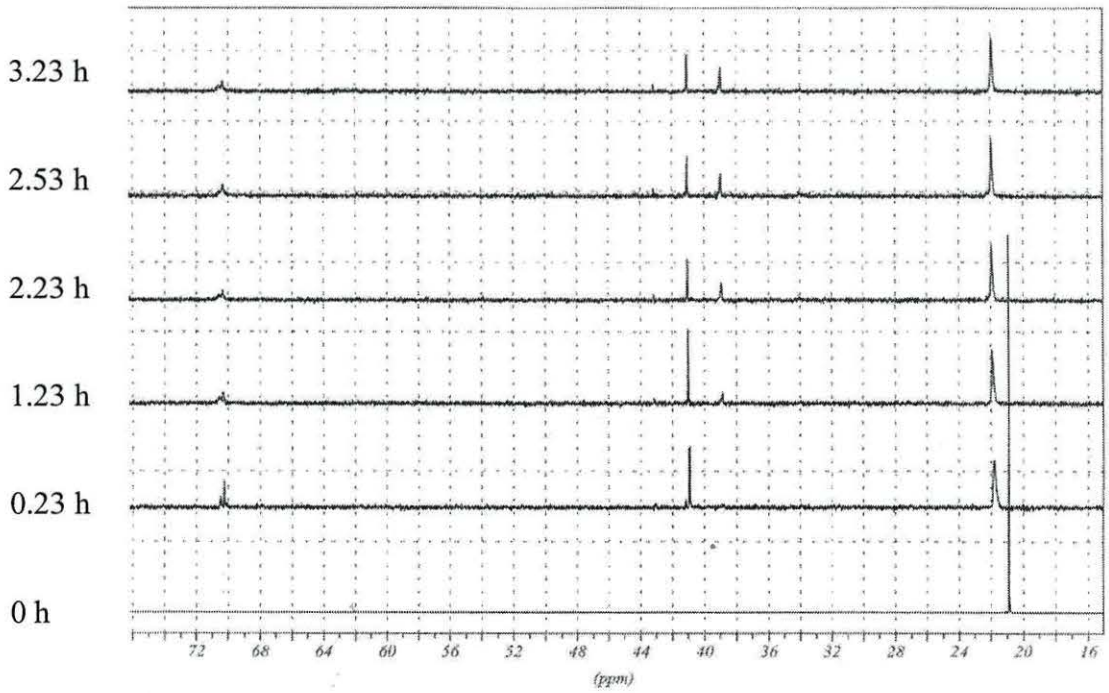

Figure 24: ^{31}P NMR spectra of product formation at set times (constant temperature of 80°C).

In conclusion from the initial results it seems that the optimum conditions for the reaction is a temperature around 80°C and for practical purposes it is sufficient to know that the reaction requires less than 30 minutes.

2.2.7 Complexes of palladium synthesized from 1,2-di-*tert*-butylphosphinomethyl ferrocene 42.

The immediate treatment of 1,2-di-*tert*-butylphosphinomethyl ferrocene **42** with 1 molar equivalent of $Pd[COD]Cl_2$ in dichloromethane was then undertaken on a very small scale and was left to stir (scheme 28). Subsequent evaporation to dryness left a residue which was washed with petrol. Very small amounts of the hitherto unreported orange/red crystalline palladium complex **52** formed in 83 % yield and samples of these crystals were sent for single crystal X-ray analysis.

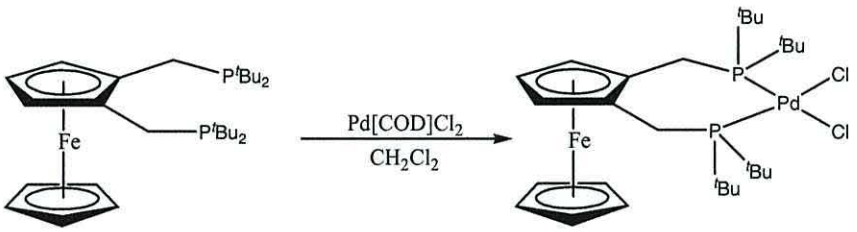

42 **52**

Scheme 28: Complex of palladium **52** synthesized from **42**.

The product (**52**) was characterised by melting point determination, elemental analysis, mass spectroscopy, X-ray analysis, ^1H, ^{13}C and ^{31}P NMR spectroscopy. The compound showed a melting point of 138-142 °C in air with indication of partial decomposition and the mass spectrum showed the major ion was found at m/z 608 $[M-2Cl]^+$. This appears to be common for palladium complexes of this type. Elemental analysis gave a less than satisfactory match between the observed values for carbon and hydrogen and the calculated values (in parenthesis) with C %: 43.1 (49.5), H %: 7.9 (7.1). The proton spectrum shows the 36 methyl protons as two pairs of doublets each with an integration of 18. One doublet at δ 1.45 ppm showed a $^3J_{PH}$ as 7.57 Hz, the other at δ 1.58 ppm with a $^3J_{PH}$ coupling constant of 7.57 Hz. The CH_2 spacers between the Cp ring and the phosphorus were seen at δ 3.09 and δ 3.37 ppm (2H). The substituted Cp ring

system was seen as a triplet (2H) at δ 4.41 ppm (α-H's) and a doublet at δ 3.68 ppm (β-H). The non-substituted Cp ring was seen as a singlet δ 4.03 ppm (5H). This pattern verifies that the $CH_2P^tBu_2$ groups were at position 1 and 2 of the substituted Cp ring. The ^{13}C NMR spectrum shows that the C-methyl groups were visible as two pairs of resonances, one at δ 28.04 ppm and the other at δ 28.92 ppm. The tertiary carbon atoms of the *t*-butyl groups were also seen as two separate shifts at δ 31.68 ppm and δ 32.37 ppm. The methylene spacer groups were seen at δ 22.65 ppm. The non-substituted Cp ring was seen as a large resonance representing five carbon atoms at δ 70.53 ppm. The substituted Cp ring showed a singlet for the unique carbon atom at δ 71.15 ppm, and CH carbon atoms were seen at δ 78.60 ppm. The two substituted carbon atoms were observed as a very weak resonance at around δ 81.99 ppm. This peak pattern also indicates a 1,2-disubstituted product however there were other resonances present indicating that the product was not pure. The ^{31}P NMR spectrum showed a single resonance at δ 42.67 ppm indicating that the two Pd bound phosphorus atoms were equivalent.

The crystal structure was determined by X-ray diffraction and the structure is shown in figure 25.

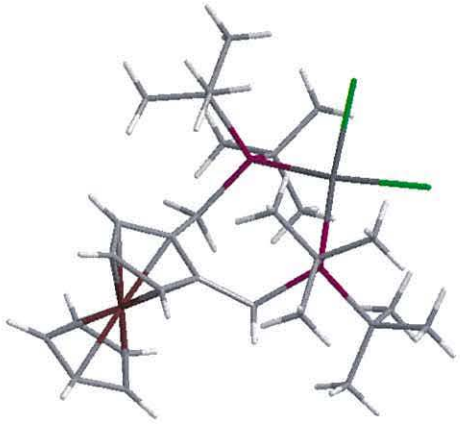

Figure 25: X-ray crystal structure of **52**.

Note how alignment of the two phosphine groups 'upwards' and away from the ferrocene body results in the methylene protons being directed downwards, and there being an 'inner' or an 'outer' hydrogen atom. The Pd metal centre is also positioned away from the ferrocene body and lies in between two highly steric environments of the ^{t}Bu groups restricting the pathway of substrate to the active metal centre.

The compound **52** is an example of the complex which could be tested as a new catalyst for the production of methyl propanoate (MeP) by the palladium catalysed methoxycarbonylation of ethene as explained in chapter 1. However according to the current literature the compound of choice used to form the metal complex in industrial catalytic testing is Pd (0) bis(dibenzylideneacetone) [$Pd(dba)_2$].[36] The arene-ligand based catalyst, generated *in situ via* the reaction of [Pd(L-L)(dba)] [L-L = 1,2-$(CH_2P^tBu_2)_2C_6H_4$; dba = *trans,trans*-$(PhCH{=}CH)_2CO$] with methanesulfonic acid, gives methyl propanoate with a selectivity of 99.98 % at a production rate of 50,000 mol product $(mol\ Pd)^{-1}h^{-1}$ under very mild conditions (353 K and 10 atm pressure of CO-C_2H_4). Therefore steps were undertaken to prepare and isolate an unreported sample of this catalyst's more efficient ferrocenyl analogue [Pd(L'-L')(dba)] [L'-L' = 1,2-$(CH_2P^tBu_2)_2Fc$; dba = *trans,trans*-$(PhCH{=}CH)_2CO$] **53** (scheme 29).

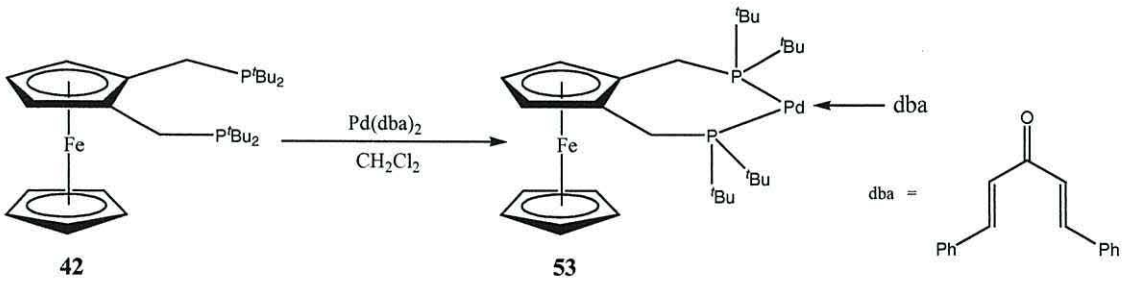

42 **53**

Scheme 29: Preparation of the ferrocenyl analogue complex of the catalyst **53**.

Treatment of 1,2-(di-*tert*-butylphosphinomethyl) ferrocene **42** with 1 molar equivalent of $Pd(dba)_2$ in dichloromethane was undertaken on a very small scale and the mixture left to stir for 30 min (scheme 29). Subsequent evaporation to dryness left a residue which was washed with petrol. Very small amounts of the hitherto unreported palladium complex **53** formed in 39 % yield as an orange/yellow crystalline solid after drying under vacuum.

The sample **53** was characterised by melting point analysis, elemental analysis, mass spectroscopy, infrared spectrometry, ^{1}H, ^{13}C and ^{31}P NMR spectroscopy. Crystallography was attempted however the product was extremely sensitive and it was found to be too difficult to obtain the structure. The compound showed a melting point of 105-109 °C in air with indication of partial decomposition and the mass spectrum showed the major ion was found at m/z 608 $[M–dba]^{+}$ and the dba fragment was present at m/z 235. Elemental analysis did not give a satisfactory match between the observed values for carbon and hydrogen and the calculated values (in parenthesis) with C %: 71.0 (64.1), H %: 8.6 (7.4) but this may be explained by the decomposition of the compound over a limited amount of time or perhaps the presence of a mixture of compounds. The infrared spectrum showed an intense signal associated with the carbonyl group at 1670 cm^{-1}, also strong vibrations due to alkene and aromatic C=C stretching were seen at 1621 cm^{-1} and 1560 cm^{-1} respectively. A medium signal at 3063 cm^{-1} indicates alkene C-H bonding. The proton spectrum shows the 36 methyl protons as two pairs of doublets each with an integration of 18. One doublet at δ 1.57 ppm showed a $^{3}J_{PH}$ as 13.55 Hz, the other at δ 1.43 ppm with a $^{3}J_{PH}$ coupling constant of 14.19 Hz. The CH_2 spacers between the Cp ring and the phosphorus were seen as a spin system at δ 3.11 and δ 3.38 ppm both with a

$^{2}J_{PH}$ coupling constant of 14.50 Hz. The substituted Cp ring system was seen as a triplet (2H) at δ 4.39 ppm (α-H's) and a doublet at δ 3.88 ppm (β-H). The non-substituted Cp ring was seen as a singlet δ 3.99 ppm (5H). This pattern indicates that the $CH_2P^tBu_2$ groups were at position 1 and 2 of the substituted Cp ring. The dba alkene protons were represented as four singlets: the two protons next to the carbonyl were seen at δ 7.01 and δ 7.04 ppm (1H) while the protons next to the aromatic ring was seen further downfield at δ 7.66 and δ 7.69 ppm (1H). The aromatic protons on the terminal phenyl groups are present as triplet resonances at δ 7.34 ppm (4H, 2.20 Hz), 7.36 ppm (2H, 1.58 Hz) and 7.55 (4H, 2.20 Hz). The ^{13}C NMR spectrum shows that the methyl groups were visible as two pairs of resonances, one at δ 27.14 ppm and the other at δ 28.92 ppm. The tertiary carbon atoms of the *t*-butyl groups were also seen at a shift of δ 30.94 ppm. The CH_2 linker groups were seen at δ 19.44 ppm. The non-substituted Cp ring was seen as a large resonance representing five carbon atoms at δ 70.18 ppm. The substituted Cp ring showed a singlet for the unique carbon atom at δ 70.07 ppm, and the two CH carbon atoms were seen at δ 73.18 ppm. The two substituted carbon atoms were observed as a very weak resonance at around δ 80.51 ppm. This peak pattern also indicates a 1,2-disubstituted product. The dba alkene carbon atoms were present at δ 125.44 and δ 143.34 ppm with the latter indicating the carbon next to the aromatic ring. The phenyl dba carbon atoms were present as four resonances at δ 134.82 (C-*ipso*), 130.51 (*para*-CH), 128.41 (*meta*-CH) and 128.98 ppm (*ortho*-CH). The carbonyl carbon was present at δ 188.95 ppm. The ^{31}P NMR spectrum showed a single resonance at δ 42.53 ppm indicating that the two Pd bound phosphorus atoms were equivalent.

Given the successful preparation of the complex the sample was prepared at the industrial site at Lucite International and tested in the methoxycarbonylation of ethene against the standard xylyl analogue of the ligand **7** of which details are presented in chapter 3. It is noted at this point however that additional variations of the ligand have also been prepared from the bis-amine and hydroxyl-amine precursors **41** and **46**, namely adamantyl phosphine substituted complexes. These compounds were prepared using the same methodology used here using a number of different secondary phosphines. This work was carried out in collaboration with Dr. Graham Eastham and Dr. Mark Waugh while the writer was on industrial placement at Lucite International. This will be explained more fully in chapter 3. It should be noted at this juncture that these complexes were not isolated as they were prepared *in situ* during catalytic testing as was the standard industrial procedure.

2.3 The study of alternative metallocenes.

2.3.1 Ruthenocene analogues.

The work described so far in the development of phosphine-based ligands has used benzene and ferrocenyl backbones. Cleary these have been shown to be effective when complexed with palladium as active catalysts in the carbonylation of ethene.

It was felt that a comparison with other metallocenes should be carried out in order to obtain additional data about other ligand scaffolds on the reactivity of the catalytic process. Ruthenocene **54** and cobaltocene **55** are examples of a stable π-bonded organometallic compounds which undergoes substitution reactions similar to those displayed by ferrocene **50** (figure 26).[82, 83]

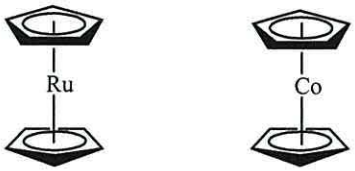

54 55

Figure 26: ruthenocene **54** and cobaltocene **55**.

Cobaltocene **55** is readily oxidized in air and therefore wasn't a viable alternative to work with although the oxidized form cobaltcenium may be an option. Ruthenocene on the other hand is of course directly related to ferrocene and would be an ideal alternative. Structural modification of ruthenocene using the methodology developed for ferrocene is not necessarily easy because there are many examples in the literature where ferrocene **50** and ruthenocene **54** exhibit similar chemistry but very different reactivity. Ferrocene is more susceptible to electrophilic addition than ruthenocene[84] and the ferrocenyl Cp protons are less acidic than the corresponding ruthenocenyl protons; hence it is difficult to generate mono-lithioruthenocene without significant quantities of di-lithioruthenocene.[84,85] In contrast both mono- and di-lithioferrocene can be readily prepared.[85-88]

It would be interesting to compare the results of catalytic trials of ruthenium and ferrocenyl analogues of the phosphine ligands and steps were undertaken to prepare the hitherto unreported precursor ligand bis-1,2-dimethylaminomethyl ruthenocene **58**. It is recognized however that the commercial starting reagent ruthenium trichloride is relatively expensive and therefore ruthenocene derivatives as creditable catalysts may be deemed unfavourable.

As a starting point the synthesis of ruthenocene **54** was undertaken (figure 27). Treatment of ruthenium trichloride with freshly distilled cyclopentadiene[89] and the

addition of zinc dust resulted in the product **54** as pale yellow crystals in 49 % yield on purification by sublimation.

$$2\,RuCl_3 + 6\,C_5H_6 + 3\,Zn \longrightarrow \underset{\mathbf{54}}{2\,[Ru(C_5H_5)_2]} + 3\,ZnCl_2 + 2\,C_5H_8$$

Figure 27: Preparation of ruthenocene **54**.

The total amount of ruthenocene obtained from a 10g batch of $RuCl_3$ was 4.37g and the product was characterised by melting point determination, ^1H and ^{13}C NMR spectroscopy. All data agreed with the literature indicating successful preparation of the product.[83] The low yield is a direct consequence from trying to sublime the product away from the residue left behind after workup.

The synthesis of dimethylaminomethyl ruthenocene **56** was carried out following a procedure described by *Moss et al* from reaction of mono-lithioruthenocene with Eschenmoser's salt (scheme 30).[90] This reaction yielded a mixture of the monosubstituted product **56** (1.71g) as a white crystalline material and the 1,1'-bis substituted product **57** (0.39g) in 35 % and 5 % yields respectively. These compounds were isolated by column chromatography where hexane was used to elute the unreacted ruthenocene first, followed by hexane-diethyl ether (70:30) to elute **56** and finally diethyl ether-methanol 97:3 was used to elute **57**.

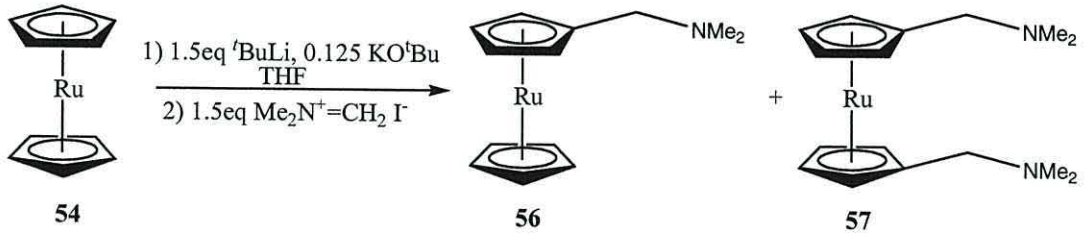

54 **56** **57**

Scheme 30: Prepartion of dimethylaminomethyl ruthenocene **56**.[90]

The product (**56**) was air stable and was characterised by elemental analysis, melting point determination, mass spectrometry, ^{1}H and ^{13}C NMR spectroscopy. Elemental analysis gave a good match between the observed values for carbon, hydrogen and nitrogen and the calculated values (in parenthesis) with C %: 53.5 (54.2), H %: 5.7 (5.9), N %: 4.5 (4.8). The compound had a melting point of 38-40 °C in air with no apparent decomposition (lit. 39-42 °C)[90] and the mass spectrum showed a parent ion was observed at m/z 290. All spectroscopic data agreed with the literature indicating successful preparation of the product.[90]

Treatment of dimethylaminomethyl ruthenocene **56** with 1.4 molar equivalent of *t*-butyllithium in diethyl ether gave the *ortho* metallated product 1-lithium-2-dimethylaminomethyl ruthenocene due to the *ortho* directing nature of the amine. Subsequent quench under cooled conditions with Eschenmoser's salt, followed later by addition of hydroxide solution, extraction with ether, drying, filtering and removal of volatiles gives the previously unreported product bis-1,2-dimethylaminomethyl ruthenocene **58** together with un-reacted starting material (scheme 31). Separation of the ruthenocene was effected by re-crystallisation of **58** from petrol at -17°C. The product was isolated as white crystals in 92 % yield. In this manner, a crystal suitable for X-ray crystallography was obtained.

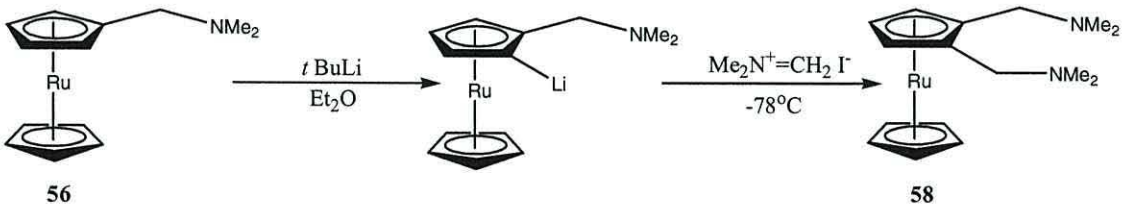

56 **58**

Scheme 31: Preparation of bis-1,2-dimethylaminomethyl ruthenocene **58**.

The product (**58**) was air stable, though hydroscopic, and was characterised by melting point determination, mass spectrometry, X-ray crystallography, ^{1}H and ^{13}C NMR spectroscopy. The compound had a melting point of 47-50 °C in air with no apparent decomposition. The proton NMR spectrum of the product showed the four N-methyl groups to be present as a singlet at δ 2.24 ppm. The NCH_2Cp resonances were observed as a doublet at δ 3.05 ppm, with ^{2}J coupling of 13.13 Hz, and a second doublet at δ 3.26 ppm with the same coupling constant of 13.13 Hz. The un-substituted Cp ring appeared as a singlet at δ 4.45 ppm, and the three protons on the substituted ring appeared as a triplet (1H, 1.99 Hz) at δ 4.48 ppm, and as a doublet (2H, 1.99 Hz) at δ 4.64 ppm, thus confirming the 1,2-bis substitution pattern of the ruthenocenyl derivative. The ^{13}C NMR spectrum showed six resonances reflecting the six different carbon environments at δ 45.50 (s; NCH_3), δ 57.28 (s; NCH_2), δ 70.53 (Cpα-C), δ 71.32 (Cp5), δ 72.57 (Cpβ-C) and δ 88.21 (Cp *ipso*-C). The mass spectrum of the product also shows a clean parent ion to be found at m/z 346.

The crystal structure was determined by X-ray analysis and the structure is shown in figure 28. Note how (like the ferrocenyl analogue) the alignment of the two N-methyl groups 'upwards' and away from the ruthenocene body results in the methylene protons being directed downwards, and being an 'inner' or an 'outer' hydrogen atom. Since rotation of the N-methyl groups is sterically hindered by the ruthenocene body, this is the cause of the splitting observed in the ^{1}H NMR spectrum. Note also that packing of the amino constituents is such that the lone pairs on nitrogen are directed in the same sense around the Cp ring when viewed from above the substituted ring.

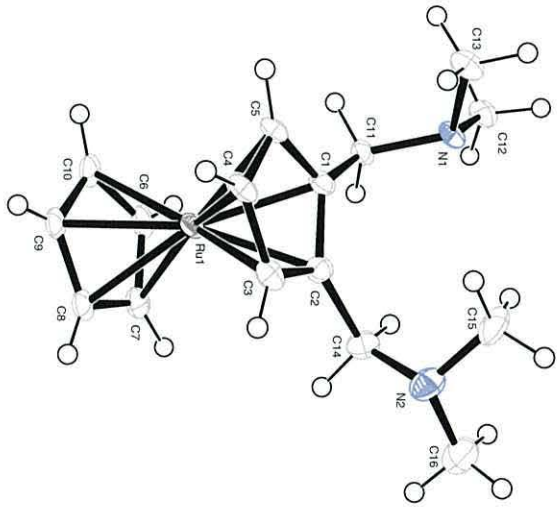

Figure 28: X-ray crystal structure of **58**.

As only a small amount of bis-1,2-dimethylaminomethyl ruthenocene **58** was obtained the sample was sent to Lucite International UK Ltd. based at Wilton for further elaboration into the Pd complex of 1,2-di-*tert*-butylphosphinomethyl ruthenocene **59** (figure 29) using the discussed procedures and therefore for catalytic testing (as requested by Lucite). Comparison with its ferrocenyl analogue was investigated and a more detailed report of these results is given in chapter 3.

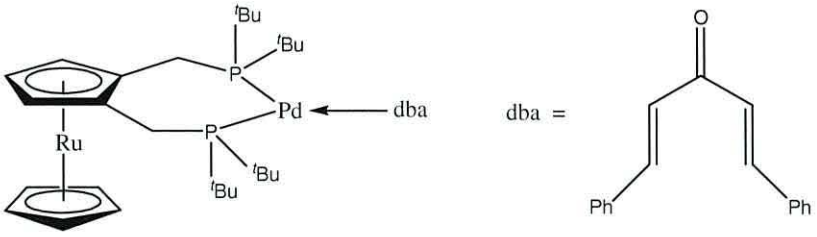

59

Figure 29: The Pd complex of 1,2-di-tert-butylphosphinomethyl ruthenocene **59** used in testing.

The overall low yield and cost of expensive reagents may be the limiting factor for further study of ruthenocene derivatives as potential industrial catalysts used in the

carbonylation of ethene. Clearly, in order to attempt the three step reaction towards the phosphine-based precatalyst the quantity of starting materials must be available in bulk and so the synthetic methodology at present seems unfavourable.

Therefore attention was refocused at trying to further improve catalyst activity by developing substituted derivatives of the already existing bis-1,2-di-*tert*-butylphosphinomethyl ferrocene **42** as bulk quantities can be obtained as ferrocenyl reagents are less expensive than ruthenocenyl ones. At the time of writing therefore ruthenocenyl-based compounds as catalyst (although efficient) are deemed too expensive for the proposed industrial scale catalytic process.

2.4 The investigation of increasing steric bulk.

2.4.1 Introduction.

The functionalisation of the lower (unsubstituted ring) of ferrocene-based ligands with bulky groups was carried out in an effort to increase the steric bulk which should improve catalytic activity in the carbonylation of ethene. This is because the addition of bulky groups to the unsubstituted ring should ensure that the conformation believed to be important for the methoxycarbonylation is favoured. This should increase the bite angle of the ligands on the upper ring and stabilise the active conformation. An example of a functionalised system is pentaphenylferrocenyl di-*tert*-butylphosphine **48** which has been prepared in a high yield from a two-step process, and the scope of various cross-coupling catalysed by complexes baring this ligand have been reported by Hartwig and co-workers (section 1.5.1).[76] An early attempt using a similar methodology to synthesise 1-

(hydroxyl-methyl)-2-(dimethylaminomethyl)-1',2',3',4',5'-[pentaphenyl] ferrocene **60** failed (scheme 32).

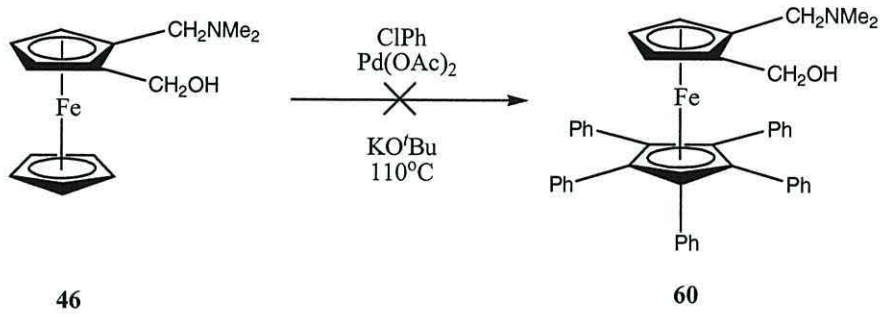

46 **60**

Scheme 32: Attempted preparation of **60**.

NMR analysis of the reaction mixture showed that it was mostly recovered starting material **46**. Therefore another route was devised. Large scale preparations of bis-1,1'-dibromoferrocene **61** was undertaken by bis-lithiation of ferrocene **50** with TMEDA and subsequent addition of THF and quench with two equivalents of 1,1,2,2-tetrabromoethane at -78°C. After workup and purification procedures the product was isolated in 62 % yield as dark orange crystals (scheme 33).

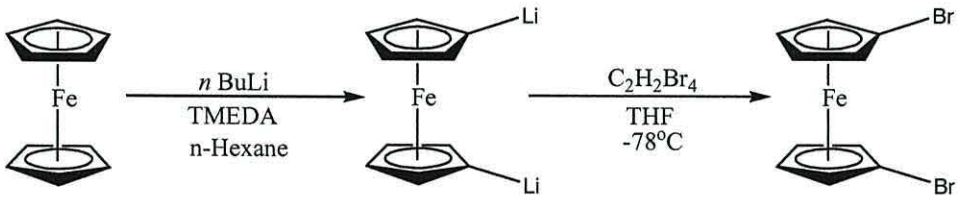

50 **61**

Scheme 33: Preparation of bis-1,1'-dibromoferrocene **61**.

The product **61** was characterised by ^{1}H and ^{13}C NMR spectroscopy. The proton NMR spectrum showed two singlet resonances at δ 4.11 and 4.44 ppm with an equal integral ratio (4H) corresponding with the two different proton environments on the Cp rings. The ^{13}C NMR spectrum showed the three different carbon environments as three

resonances at δ 69.80 (the β-carbon atoms), 72.54 (the α-carbon atoms) and 78.15 ppm (the *ipso*-carbon).

The strategy of using an *ortho*-directing group is a key process in producing variety of ferrocenyl systems.[39,51,91,92] The halides (chloride[93] and bromide[94,95]) however are *ortho*-directing *and* removable as well as sulfinyl and sulfonyl groups.[41,96,97] Bis-1,1'-dibromoferrocene **61** was therefore used as the key precursor in the synthesis of the discussed bulky ligands as it is the bromide that was best suited for our purpose.

It was intended at first to substitute the bromine on the top Cp ring with a dimethylaminomethyl group and the bottom with any relevant bulky substituent. Further reaction with calcined *p*-formaldehyde would then hopefully result in the 1,2,1'-trisubstituted ferrocenyl precursor.

In order to test the proposed method a small scale reaction was set up involving compound **62** which was already available in the laboratory. It was intended to substitute the bromine with a dimethylaminomethyl group by lithiation in THF and quench with Eschenmoser's salt to yield compound **63** (scheme 34). The bulky steric group in this example was anthracene substituted at the 9 position.

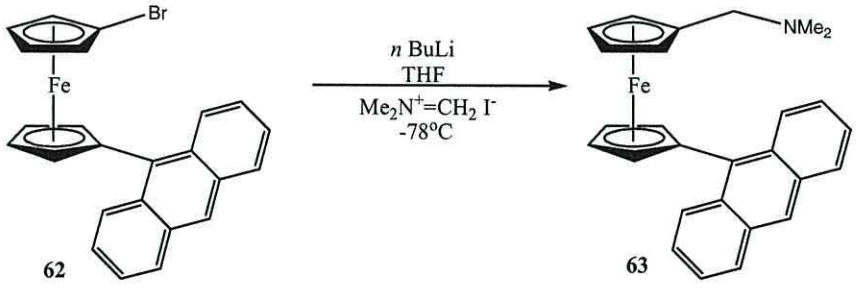

Scheme 34.

During the course of the reaction however it became clear that the reaction wasn't progressing as expected as the addition of Eschenmoser's salt did not cause a significant change in the mixture despite additional stirring with heating. In order to test if the lithium was still active one equivalent of DMF was added. The expectation was that if an aldehyde signal was present in the proton NMR spectrum of the product then the lithium was still active. However no observable changes occurred after addition of DMF, and after subsequent workup and purification of the sample NMR analysis showed that the product was ferrocenylanthracene **64** (figure 30) indicating that the lithium had become deactivated explaining why the Eschenmoser's salt did not react.

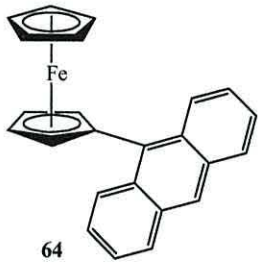

64

Figure 30: Ferrocenylanthracene **64**.

This is almost certainly because of a secondary intermolecular attack by the lithiated intermediate on the anthracene which essentially removes the lithium from the ferrocene ring producing a weak anion which is only quenched with water. Despite early setbacks desired products were prepared in a three step synthesis from 1,1'-dibromoferrocene.

2.4.2 Routes towards triphenylsilyl and trimethylsilyl 'anchored' bis-1,2-dimethylaminomethyl ferrocenes.

At this juncture it was decided to examine a range of compounds which should be relatively easy to prepare in a cost effective manner. After consideration of a number of

ideas it was decided to examine the preparation of silyl substituted groups on the free Cp ring because the chemistry of such groups in ferrocenes has been studied widely. In the search for alternative methods, the investigation of the reaction sequence as depicted in scheme 35 was carried out starting from ferrocene **50**. Two novel compounds; bis-1,2-dimethylaminomethyl-1'-trimethylsilyl ferrocene **64** and bis-1,2-dimethylaminomethyl-1'-triphenylsilyl ferrocene **67** which are precursors to the desired phosphine ligands were successfully prepared.

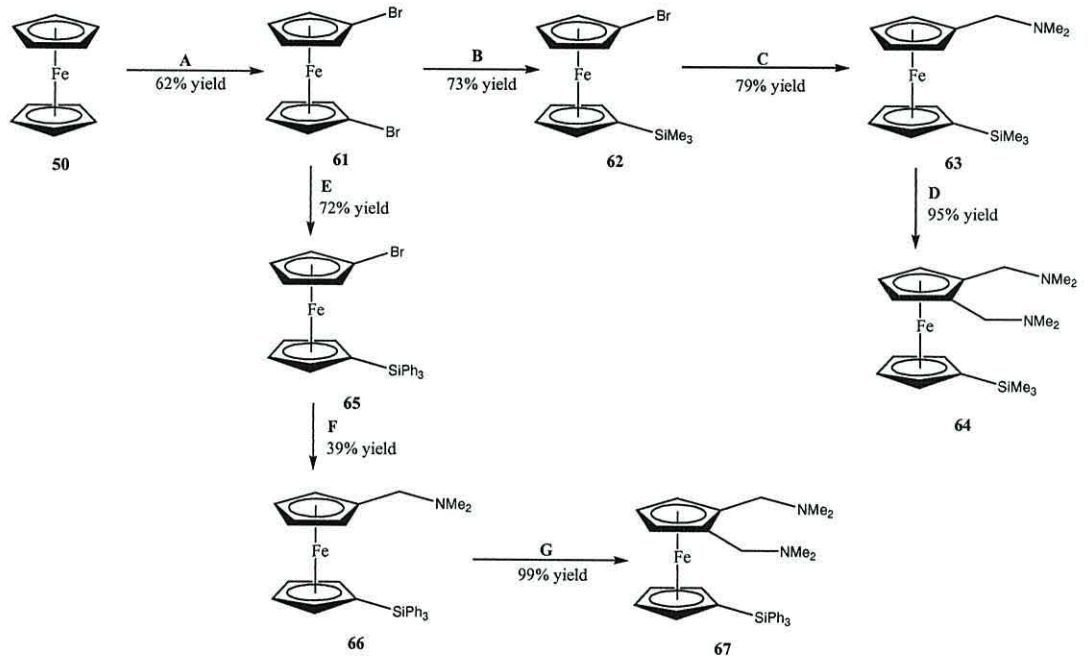

Scheme 35: A: 1) *n* BuLi, TMEDA, n-hexane. 2) $C_2H_2Br_4$, THF. **B:** 1) *n* BuLi, THF. 2) $ClSiMe_3$. **C:** 1) *n* BuLi, Et_2O. 2) $Me_2N^+CH_2I^-$, THF. **D:** 1) *n* BuLi, Et_2O. 2) $Me_2N^+CH_2I^-$, THF. **E:** 1) *n* BuLi, THF. 2) $ClSiPh_3$. **F:** 1) *n* BuLi, Et_2O. 2) $Me_2N^+CH_2I^-$, THF. **G:** 1) *n* BuLi, Et_2O. 2) $Me_2N^+CH_2I^-$, THF.

The precursor ligands **64** and **67** had to be obtained in sufficient quantity so that batch testing of the subsequent catalyst could be undertaken. These samples would then sent to Lucite International for amine conversion into their corresponding tertiary phosphines and subsequent reaction with $Pd(dba)_2$ to form the active catalyst and tested in the carbonylation of ethene (chapter 3).

Therefore large scale formation of bis-1,1'-dibromoferrocene **50** was undertaken as stated earlier to prepare the starting material for both routes.

2.4.3 Preparation of bis-1,2-dimethylaminomethyl-1'-trimethylsilyl ferrocene (64).

Treatment of bis-1,1'-dibromoferrocene **61** at -78°C with 0.95 molar equivalent of *n*-butyllithium in THF results in the removal of a bromide and formation of the metallated product 1-bromo-1'-lithio ferrocene due to the facile exchange of the bromine. Subsequent quench with one equivalent of chlorotrimethylsilane followed later by addition of water, extraction with ether, drying, filtering and removal of volatiles gives the product 1-bromo-1'-trimethylsilyl ferrocene **62** together with mono-bromo by-products (scheme 36). The product was purified by column chromatography and isolated as red oil in 73 % yield.

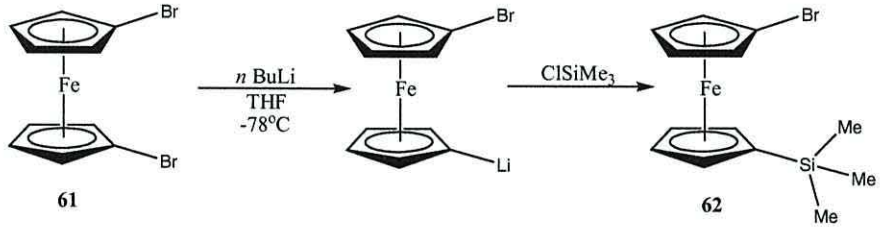

Scheme 36: Preparation of 1-bromo-1'-trimethylsilyl ferrocene **62**.

The product (**62**) was characterised by ^{1}H and ^{13}C NMR spectroscopy. Proton NMR showed five resonances; the three Si-methyl groups were present as a singlet at δ 0.05 ppm with an integral of nine. The α-positioned protons on the substituted Cp appeared as triplets at δ 4.16 and 4.19 ppm (1.89 Hz) (2 x CH) respectively, and the four protons on the β-position of the substituted ring appeared as triplet resonances at δ 3.85 ppm and δ 3.96 ppm (1.89 Hz) (2 x CH). The ^{13}C NMR spectrum shows the terminal carbon of the methyl groups as a singlet at δ 0.00 ppm. The ferrocenyl carbon

environments are observed as six intense resonances. The (C-Br) and (C-Si) *ipso*-carbon atoms are seen at δ 78.45 and 77.91 ppm respectively. The α-carbons on the bromide and trimethylsilyl substituted Cp rings are seen at δ 76.95 and 74.16 ppm respectively while the β-carbons are to be found at δ 70.12 and 67.27 ppm.

From NMR analysis it was decided that 1-bromo-1'-trimethylsilyl ferrocene **62** had been successfully prepared and the product was used immediately in further reactions. Treatment of compound **62** with 1.1 molar equivalent of *n*-butyllithium in diethyl ether at room temperature removed the second bromide. Subsequent addition of THF and quench with Eschenmoser's salt under cooled conditions followed later by quenching with water, extraction with ether, drying, filtering and removal of volatiles gives the product 1-dimethylaminomethyl-1'-trimethylsilyl ferrocene **63** together with by-products (scheme 37). The product was purified by column chromatography by eluting first the starting material with 9:1 petrol/ether, and then the product with 1:1 petrol/ether (5% triethylamine) and isolated as red oil in 79 % yield.

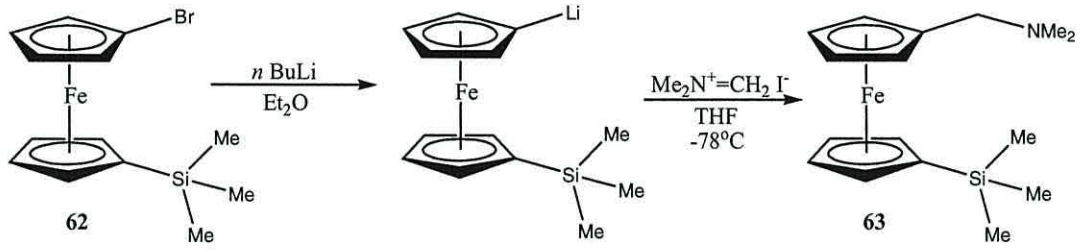

Scheme 37: Preparation of 1-dimethylaminomethyl-1'-trimethylsilyl ferrocene **63**.

The product (**63**) was characterized by mass spectrometry, ^{1}H and ^{13}C NMR spectroscopy. The mass spectrum of the sample gave the parent ion at m/z 316 $(M + H)^{+}$. Proton NMR showed seven resonances; the three Si-methyl groups were present as a singlet at δ 0.00 ppm with an integral of nine. The two N-methyl groups were present as a singlet at δ 1.94 ppm and the N-methylene was also present as a singlet at δ 3.04 ppm.

These had an integral of 6:2 respectively. The α-positioned protons on the substituted Cp appeared as apparent triplets at δ 4.04 and 3.91 ppm (1.89 Hz and 1.90 Hz) (2 x CH) respectively, and the four protons on the β-position of the substituted ring appeared as pseudo triplet resonances at δ 3.84 ppm and δ 3.79 ppm (1.89 Hz and 2.00 Hz) (2 x CH). The ^{13}C NMR spectrum shows the terminal methyl groups as a singlet at δ 0.00 ppm. Two resonances are present showing the carbon environments at δ 44.94 (s; NCH_3) and δ 59.38 ppm ($CpCH_2N$). The ferrocenyl carbon environments are seen as six intense resonances. The ferrocenyl (C-methylene) and (C-Si) *ipso*-carbon atoms are shown at δ 83.43 and 73.49 ppm respectively. The α-carbons on the dimethylaminomethyl and trimethylsilyl substituted Cp rings are seen at δ 72.43 and 71.59 ppm respectively while the β-carbons are to be found at δ 70.39 and 68.42 ppm.

The success of preparing 1-dimethylaminomethyl-1'-trimethylsilyl ferrocene **63** meant that further reaction to form the desired phosphine precursor ligand was implemented. Treatment of 1-dimethylaminomethyl-1'-trimethylsilyl ferrocene **63** with 1.2 molar equivalent of *n*-butyllithium in ether gave the *ortho* metallated product 1-lithium-2-dimethylaminomethyl-1'-trimethylsilyl ferrocene again due to the *ortho* directing nature of the amine.[51,78-80] Subsequent addition of THF and quench under cooled conditions with Eschenmoser's salt, followed later by quenching with water, extraction with ether, drying, filtering and removal of volatiles gives the product bis-1,2-dimethylaminomethyl-1'-trimethylsilyl ferrocene **64** together with un-reacted starting material (scheme 38). The product was purified by column chromatography by eluting the product with 1:1 petrol/ether (5% triethylamine) and isolated as red oil in 95 % yield.

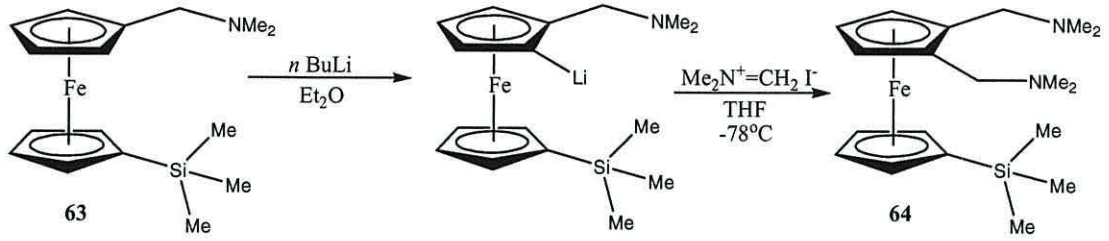

Scheme 38: Preparation of bis-1,2-dimethylaminomethyl-1'-trimethylsilyl ferrocene **64**.

The product (**64**) was characterised by mass spectrometry, elemental analysis, ^{1}H and ^{13}C NMR spectroscopy. The mass spectrum shows a clean parent ion was found to be at m/z 373. Elemental analysis of **64** gave good match to the calculated values with C %: 59.8 (61.1), H %: 8.7 (8.9), N %: 7.4 (7.5); (calculated values in parenthesis). The proton NMR spectrum of the product showed the three Si-methyl groups were present as a singlet at δ 0.00 ppm with an integral of nine. The four N-methyl groups were present as a singlet at δ 1.97 ppm (12H). The NCH_2Cp quartet was seen as a doublet at δ 2.99 ppm, with ^{2}J coupling of 12.92 Hz, and a second doublet at δ 3.13 ppm and a coupling constant of 12.93 Hz. The three protons on the dimethylaminomethyl substituted ring appeared as a triplet (2.84 Hz, 1H) at δ 3.81 ppm, and as a doublet (2H, 2.21Hz) at δ 3.97 ppm, thus confirming the 1,2-bis substitution pattern of the ferrocenyl derivative. The trimethylsilyl substituted Cp protons were seen at δ 3.76 (2H, β-position) and δ 3.87 ppm (2H, α-position). There was insufficient resolution of the resonance to obtain coupling constants. The ^{13}C NMR spectrum shows the terminal methyl groups as a singlet at δ 0.00 ppm. Two resonances are present showing the carbon environments at δ 45.33 (s; NCH_3) and δ 57.49 ppm ($CpCH_2N$). The ferrocenyl carbon environments are shown as six intense resonances. The (C-methylene) and (C-Si) *ipso*-carbon atoms are shown at δ 83.92 and 73.91 ppm respectively. The α-carbons on the dimethylaminomethyl and trimethylsilyl substituted Cp rings are seen at δ 73.15 and 70.78 ppm respectively while the β-carbons

are to be found at δ 68.37 and 67.32 ppm. This compound should serve as a universal precursor to a series of 'clean' bis phosphines. It should be possible to also obtain the tri-amine compound by further lithiation and quench if this is required in the future.

Given the successful preparation of this novel compound the sample was sent to Lucite International UK Ltd. based at Wilton for the preparation of the Pd complex of 1,2-bis-di-(3,5-dimethyl)-1-adamantylphosphinomethyl-1'-trimethylsilyl ferrocene **68** (figure 31) using the discussed procedures (with an dimethyladamantyl phosphine reagent) and catalytic testing (as requested by Lucite). The use of the alternative reagents such as this also considerably increases the steric bulk on the phosphine surrounding the active site. Comparison with its triphenylsilyl substituted ferrocenyl analogue was investigated and a more detailed report of these results is given in chapter 3.

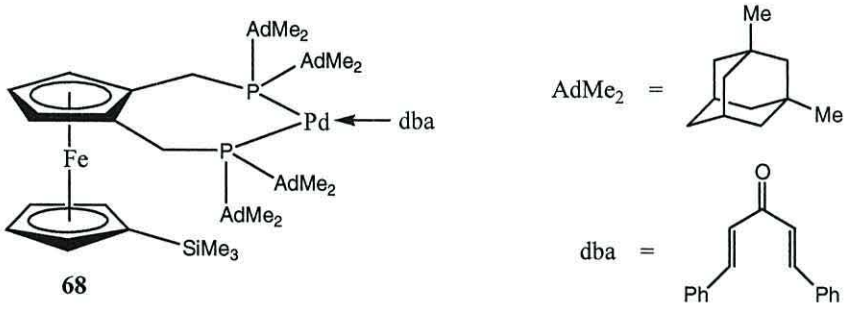

Figure 31: Pd complex of 1,2-bis-di-(3,5-dimethyl)-1-adamantylphosphinomethyl-1'-trimethylsilyl ferrocene **68**.

This new route towards the desired ligands produces relatively good yields which can be produced in bulk quantities from readily available materials. The derived catalyst itself is more efficient than the established ferrocenyl analogue **53** in the carbonylation of ethene due to the presence of the bulky trimethylsilyl group increasing steric repulsion and directing the active site of the complex further away from the main ferrocenyl 'body'. This means that the geometry around the Pd centre can be controlled more effectively so

that the active site is more accessible to the substrates (ethylene and CO) and as a consequence catalytic activity improves. Therefore the bulkier the 'anchoring' group is; the greater the steric repulsion within the system which results in improvements in the catalytic activity. This led to the steps undertaken to produce the triphenyl derivative of the of the catalyst precursor, bis-1-dimethylaminomethyl-1'-triphenylsilyl ferrocene **67** by using the same methodology.

2.4.4 Preparation of bis-1,2-dimethylaminomethyl-1'-triphenylsilyl ferrocene (67).

Treatment of bis-1,1'-dibromoferrocene **61** at -78°C with 0.95 molar equivalent of *n*-butyllithium in THF results in the removal of a bromide and formation of the metallated product 1-bromo-1'-lithio ferrocene. Subsequent quench with one equivalent of chlorotriphenylsilane (dissolved in the minimum amount of THF) followed later by quenching with water, extraction with ether, drying, filtering and removal of volatiles gives the product 1-bromo-1'-triphenylsilyl ferrocene **65** together with mono-bromo by-products (scheme 39). The product was purified by column chromatography and isolated as orange crystals in 72 % yield.

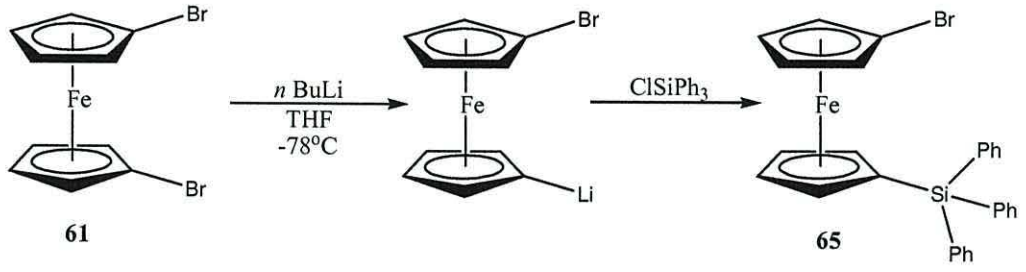

Scheme 39: Preparation of 1-bromo-1'-triphenylsilyl ferrocene **65**.

The product (**65**) was characterised by elemental analysis, mass spectrometry, ^{1}H and ^{13}C NMR spectrometry. Elemental analysis of **65** gave good match to the calculated values with C %: 64.2 (64.3), H %: 4.4 (4.4); (calculated values in parenthesis). The mass

spectrum shows that the parent ion was found to be at m/z 524 and 522 - (1:1, Br isotope). The proton NMR spectrum shows the α-positioned protons on the substituted Cp appeared as triplets at δ 4.41 and 4.28 ppm (2 x CH) respectively, and the four protons on the β-position of the substituted ring appeared as triplet resonances at δ 3.79 ppm and δ 4.23ppm (1.57 and 1.58 Hz respectively) (2 x CH). The aromatic protons on the terminal phenyl group are present as triplet resonances at δ 7.41 ppm (6H, 6.94 Hz), 7.45 ppm (3H, 6.94 Hz) and 7.62 ppm (6H, 5.36 Hz). The ^{13}C NMR spectrum shows the ferrocenyl carbon environments as six intense resonances. The (C-Br) and (C-Si) *ipso*-carbon atoms are shown at δ 81.20 and 77.36 ppm respectively. The α-carbons on the bromide and trimethylsilyl substituted Cp rings are seen at δ 75.02 and 73.03 ppm respectively while the β-carbons are to be found at δ 70.61 and 68.15 ppm. The aromatic carbon environments are present as four resonances at δ 135.96 (*ipso*-C), 135.34, 129.55 and 127.79 ppm.

The successful preparation of 1-bromo-1'-triphenylsilyl ferrocene **65** resulted in its immediate use in further reaction. Treatment of compound **65** with 1.1 molar equivalent of *n*-butyllithium in diethyl ether at room temperature removed the second bromide. Subsequent addition of THF and quench with Eschenmoser's salt under cooled conditions followed later by quenching with water, extraction with ether, drying, filtering and removal of volatiles gives the product 1-dimethylaminomethyl-1'-triphenylsilyl ferrocene **66** together with by-products (scheme 40). The product was purified by column chromatography by eluting first the starting material with 9:1 petrol/ether, and then the product with 1:1 petrol/ether (5% triethylamine) and isolated as red/orange crystals in 39 % yield.

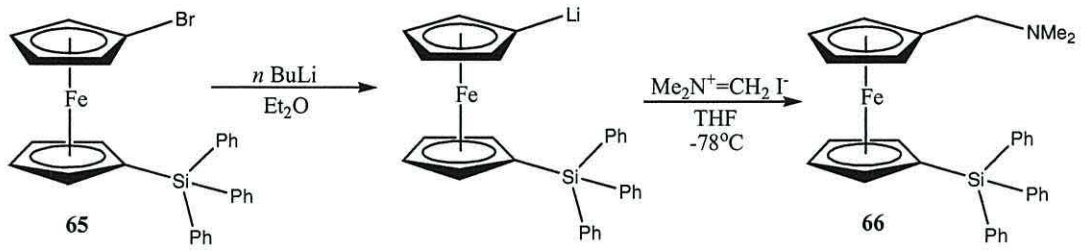

Scheme 40: Preparation of 1-dimethylaminomethyl-1'-triphenylsilyl ferrocene **66**.

The product (**66**) was again characterised by melting point determination, mass spectrometry, ^{1}H and ^{13}C NMR spectroscopy. The compound showed a melting point of 102-106 °C in air with no apparent decomposition and the mass spectrum shows that the parent ion was found to be at m/z 502. Proton NMR showed the two N-methyl groups were present as a singlet at δ 1.97 ppm and the N-methylene was also present as a singlet at δ 2.84 ppm. These had an integral of 6:2 respectively. The α-positioned protons on the substituted Cp appeared as pseudo triplets at δ 4.31 and 4.05 ppm (1.26 Hz and 1.26 Hz) (2 x CH) respectively, and the four protons on the β-position of the substituted ring appeared as triplet resonances at δ 3.93 ppm and δ 3.83 ppm (1.26 Hz and 1.26 Hz) (2 x CH). The aromatic protons on the terminal phenyl group are present as triplet resonances at δ 7.33 ppm (6H, 1.26 Hz), 7.52 ppm (3H, 1.26 Hz) and 7.54 ppm (6H, 1.26 Hz). The ^{13}C NMR spectrum shows resonances indicating the carbon environments at δ 44.57 (s; NCH_3) and δ 58.52 ppm ($CpCH_2N$). The ferrocenyl carbon environments are observed as six intense resonances. The (C-methylene) and (C-Si) *ipso*-carbon atoms are seen at δ 83.47 and 76.77 ppm respectively. The α-carbons on the dimethylaminomethyl and triphenylsilyl substituted Cp rings resonate at δ 72.02 and 70.68 ppm respectively while the β-carbons are to be found at δ 69.31 and 66.50 ppm. The aromatic carbon environments are present as four resonances at δ 136.00 (*ipso*-C), 135.63, 129.46 and 127.75 ppm.

The successful preparation of 1-dimethylaminomethyl-1'-triphenylsilyl ferrocene **66** meant that it was possible to progress in the next step in the synthesis towards the desired phosphine precursor ligand. Treatment of bis-1-dimethylaminomethyl-1'-triphenylsilyl ferrocene **66** with 1.2 molar equivalent of *n*-butyllithium in ether gave the *ortho* metallated product 1-lithium-2-dimethylaminomethyl-1'-triphenylsilyl ferrocene again due to the *ortho* directing nature of the amine.[51,78-80] Subsequent addition of THF and quenching at -70°C with Eschenmoser's salt, followed later by addition of water, extraction with ether, drying, filtering and removal of volatiles gives the product bis-1,2-dimethylaminomethyl-1'-triphenylsilyl ferrocene **67** together with un-reacted starting material (scheme 41). The product was purified by column chromatography by eluting the product with 1:1 petrol/ether (5% triethylamine) which was isolated as viscous red oil in 99 % yield.

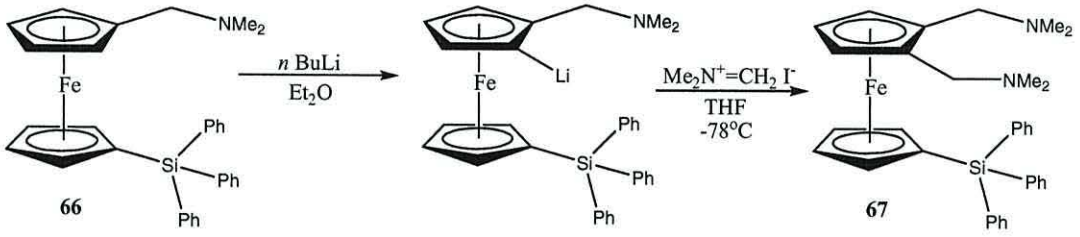

Scheme 41: Preparation of bis-1,2-dimethylaminomethyl-1'-triphenylsilyl ferrocene **67**.

The product (**67**) was characterised by elemental analysis, mass spectroscopy, ^{1}H and ^{13}C NMR spectrometry. The mass spectrum shows that the parent ion was found to be at m/z 559. Elemental analysis of **67** gave good match to the calculated values with C %: 72.8 (73.1), H %: 6.9 (6.9), N %: 4.8 (5.0); (calculated values in parenthesis). The proton NMR spectrum of the product again showed all the characteristic resonances: the four N-methyl groups were present as a singlet at δ 2.00 ppm (12H). The NCH_2Cp quartet was seen as a doublet at δ 2.87 ppm, with ^{2}J coupling of 12.46 Hz, and a second

doublet at δ 3.13 ppm and a coupling constant of 12.46 Hz. The three protons on the dimethylaminomethyl substituted ring appeared as a triplet (2.05 Hz, 1H) at δ 4.25 ppm, and as a doublet (2H, 2.05 Hz) at δ 3.93 ppm, thus confirming the 1,2-bis substitution pattern of the ferrocenyl derivative. The triphenylsilyl substituted Cp protons were seen as triplet resonances at δ 3.88 (2H, 1.57 Hz, β-position) and δ 4.01 ppm (2H, 1.57 Hz, α-position).). The aromatic protons on the terminal phenyl group are present as triplet resonances at δ 7.29 ppm (6H, 1.26 Hz), 7.32 ppm (3H, 2.21 Hz) and 7.47 ppm (6H, 1.26 Hz). The ^{13}C NMR spectrum shows two resonances which correspond to the carbon environments at δ 44.58 (s; $N\mathbf{C}H_3$) and δ 56.94 ppm ($Cp\mathbf{C}H_2N$). The ferrocenyl carbon environments are again observed as six intense resonances. The (C-methylene) and (C-Si) *ipso*-carbon atoms are shown at δ 75.55 and 73.92 ppm respectively. The α-carbons on the dimethylaminomethyl and triphenylsilyl substituted Cp rings are seen at δ 72.02 and 70.67 ppm respectively while the β-carbons are to be found at δ 69.04 and 67.98 ppm. The aromatic carbon environments are present as four resonances at δ 136.00 (*ipso*-C), 135.57, 129.46 and 127.74 ppm.

Given the successful preparation of compound **67** the sample was sent to Lucite International UK Ltd. based at Wilton for the rapid preparation of the complex of 1,2-bis-di-(3,5-dimethyl)-1-adamantylphosphinomethyl-1'-triphenylsilyl ferrocene **69** (figure 32) using the discussed procedures and standard catalytic testing (as requested by Lucite). Comparison with its trimethylsilyl ferrocenyl analogue was investigated and a more detailed report of these results is given in chapter 3.

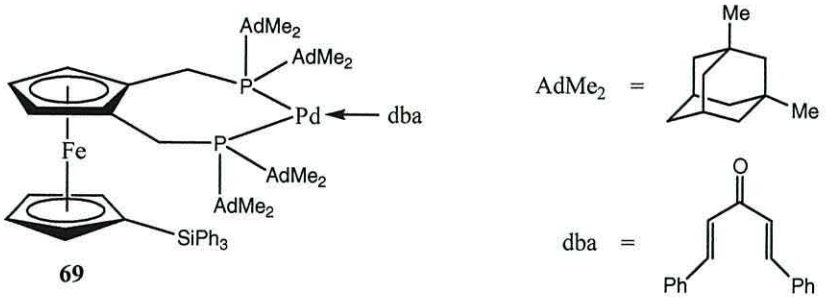

Figure 32: Pd complex of 1,2-bis-di-(3,5-dimethyl)-1-adamantylphosphinomethyl-1'-triphenylsilyl ferrocene **69**.

This new route towards the desired ligands enables the production of bulk quantities from readily available materials however a yield of 39 % in the preparation of the mono-amine precursor **66** may be limiting. To date this is the best yield achieved during numerous repeat reactions of this procedure. It may be simply that the steric bulk of the triphenylsilyl group inhibits clean exchange. The derived palladium catalyst itself is more efficient than the unsubstituted ferrocenyl analogue **53** and its trimethyl derivative **68** in the carbonylation of ethene due to the presence of the bulky triphenylsilyl group increasing steric repulsion and maintaining the correct geometry of the metal centre for efficient catalysis i.e. the geometry of the complex can be controlled so that the active site is more accessible to the substrates (ethylene and CO) and as a consequence catalytic activity improves. Therefore the bulkier the 'anchoring' group is; the greater the steric repulsion within the system which results in improvements in the catalytic activity (see chapter 3).

2.4.5 An alternative route towards steric ligands.

An alternate route towards these ligands from 1,1'-dibromoferrocene **61** was also considered by the initial substitution of a bromine atom with Eschenmoser's salt to prepare 1-bromo-1'-dimethylaminomethylferrocene **70**. Treatment of bis-1,1'-

dibromoferrocene **61** at -78°C with 0.95 molar equivalent of *n*-butyllithium in THF results in the removal of a bromide and formation of the metallated product 1-bromo-1'-lithio ferrocene. Subsequent quench with 1.2 equivalent of Eschenmoser's salt followed later by quenching with water, acid-base extraction with ether, drying, filtering and removal of volatiles gives the product 1-bromo-1'-dimethylaminomethylferrocene **70** as an orange oil in 21 % yield (scheme 42). The low yield may be a direct result from extraction which consequently limits the use of this route towards the desired precursors.

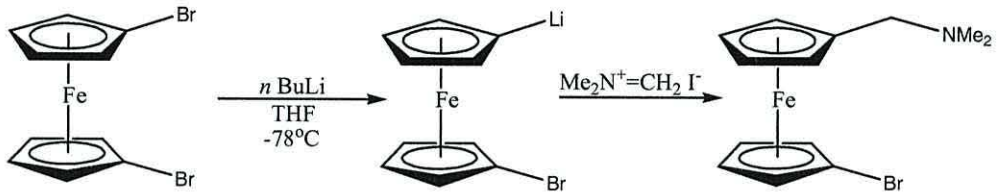

61 **70**

Scheme 42: The preparation of 1-bromo-1'-dimethylaminomethylferrocene **70**.

The product **70** was characterised by elemental analysis, ^{1}H and ^{13}C NMR spectrometry. Elemental analysis of **70** gave good match to the calculated values with C %: 47.2 (48.5), H %: 4.8 (5.0), N %: 4.1 (4.3); (calculated values in parenthesis). Proton NMR showed that the two N-methyl groups were present in the spectrum as a singlet at δ 2.11 ppm and the N-methylene was also present as a singlet at δ 3.23 ppm. These had an integral of 3:1 respectively. The α-positioned protons on the substituted Cp appeared as pseudo triplets at δ 4.25 and 4.09 ppm (1.89 Hz and 1.89 Hz) (2 x CH) respectively, and the four protons on the β-position of the substituted ring appeared as triplet resonances at δ 4.04 ppm and δ 3.98 ppm (1.89 Hz and 1.89 Hz) (2 x CH). The ^{13}C NMR spectrum shows two aliphatic resonances indicating the carbon environments at δ 30.84 (s; NCH_3) and δ 45.58 ppm ($CpCH_2N$). The ferrocenyl carbon environments are shown as six intense resonances. The (C-methylene) and (C-Br) *ipso*-carbon atoms are shown at δ

69.32 and 70.52 ppm respectively. The α-carbons on the dimethylaminomethyl and bromine substituted Cp rings are seen at δ 67.73 and 68.24 ppm respectively while the β-carbons are to be found at δ 65.61 and 67.35 ppm. Despite successful preparation of the compound the low yield meant that this route would be unfavourable given the higher yielding reactions of the initial route. The next step of the reaction would have been bromine substitution to produce silyl compounds **63** and **65**. The low yield of this initial step however limits the probability of using this route towards ligand development and consequently other ferrocenyl ligands were studied.

2.4.6 Further studies into increasing steric bulk.

Further studies for suitable methods of increasing steric bulk included the investigation of the reaction sequence as depicted in scheme 43. Starting from dimethylaminomethyl ferrocene **32**, two novel compounds; 1,2-bis-dimethylaminomethyl-5,1'-bis-trimethylsilyl ferrocene **72** and 1,2-bis-dimethylaminomethyl-5,1'-bis-triphenylsilyl ferrocene **74** which were two alternative precursors to some new phosphine ligands were successfully prepared. In addition by further reaction the highly steric compound; 1,2-bis-dimethylaminomethyl-3,5,1'-tris-triphenylsilylferrocene **75** was isolated. These compounds were again prepared as precursors for elaboration into phosphines which would be compared with the earlier ligands and therefore the samples were sent to Lucite International for amine conversion into their corresponding tertiary phosphines and subsequent reaction with $Pd(dba)_2$ to form the active catalyst and tested in the carbonylation of ethene. Again it was important

therefore to work on a large scale so that there was sufficient quantities of ligand can be isolated and tested for their catalytic activity.

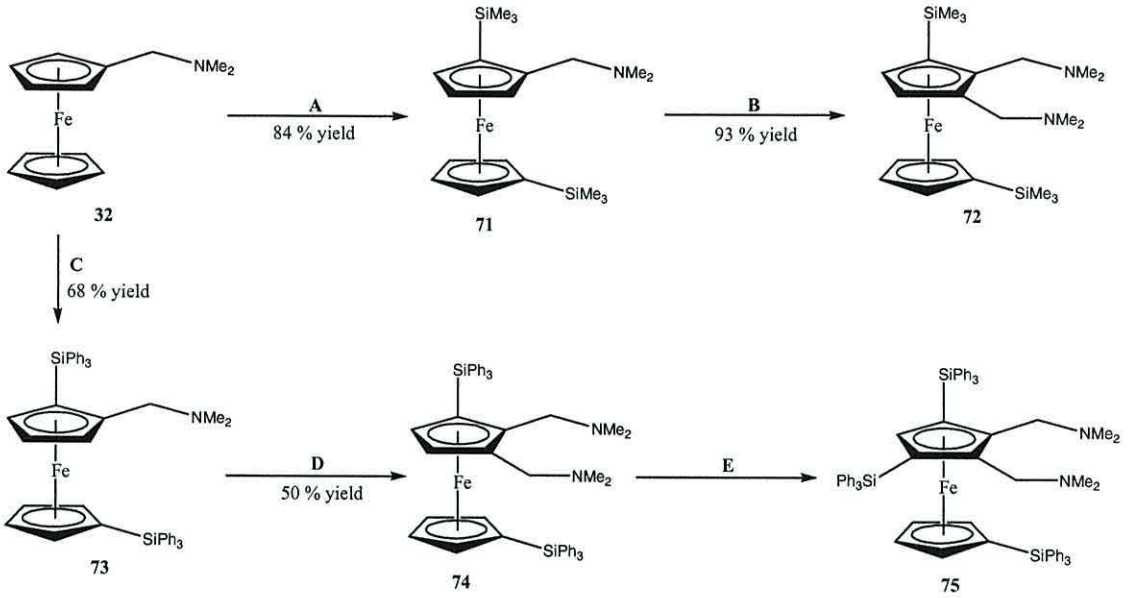

Scheme 43: A: 1) *n* BuLi, TMEDA, Et_2O. 2) $ClSiMe_3$. **B:** 1) *n* BuLi, Et_2O. 2) $Me_2N^+CH_2I^-$, THF. **C:** 1) *n* BuLi, TMEDA, Et_2O. 2) $ClSiPh_3$, THF. **D:** 1) *n* BuLi, Et_2O. 2) $Me_2N^+CH_2I^-$, THF. **E:** 1) *n* BuLi, Et_2O. 2) $ClSiPh_3$.

2.4.7 Preparation of 1,2-bis-dimethylaminomethyl-5,1'-bis-trimethylsilyl ferrocene (72).

Treatment of dimethylaminomethyl ferrocene **32** with 2.5 molar equivalent of *n*-butyllithium in Et_2O and 1 molar equivalent of TMEDA at room temperature results in the formation of the metallated product 1-dimethylaminomethyl-5,1'-di-lithio ferrocene. Subsequent cooling to -78°C and quench with 2.2 equivalent of chlorotrimethylsilane followed later by addition of water, extraction with ether, drying, filtering and removal of volatiles gives the product 1-dimethylaminomethyl-5,1'-bis-trimethylsilyl ferrocene **71** together with starting material (scheme 44). The product was purified by column chromatography and isolated as red oil in 84 % yield.

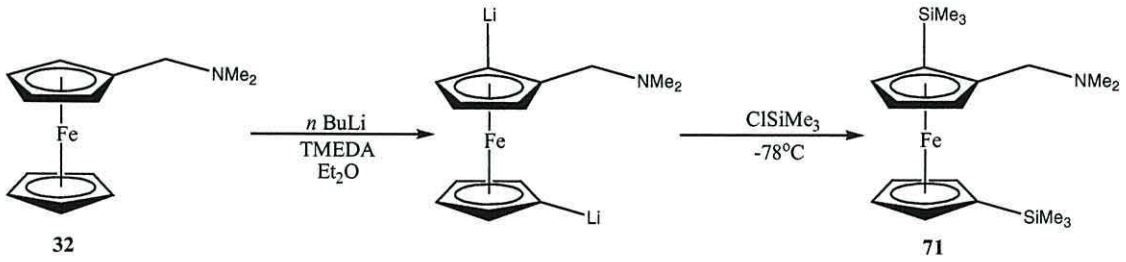

Scheme 44: Preparation of 1-dimethylaminomethyl-5,1'-bis-trimethylsilyl ferrocene **71**.

The product (**71**) was characterised by elemental analysis, ^{1}H and ^{13}C NMR spectroscopy. Elemental analysis of **71** gave good match to the calculated values with C %: 58.6 (58.9), H %: 8.4 (8.6), N %: 3.6 (3.6); (calculated values in parenthesis). The proton NMR spectrum of the product showed the two Si-methyl groups were present as two singlets at δ 0.25 and 0.30 ppm with a relative integral value of nine. The N-methyl group was present as a singlet at δ 2.11 ppm (6H). The NCH_2Cp was seen as a doublet of doublet; one doublet at δ 3.00 ppm, with ^{2}J coupling of 12.45 Hz, and a second doublet at δ 3.45 ppm and a coupling constant of 12.45 Hz. The three protons on the dimethylaminomethyl substituted ring appeared as a pseudo triplet (1.74 Hz, 1H) at δ 4.19 ppm, and as two doublets (1.74 Hz, 1H) at δ 4.27 ppm and (1.74 Hz, 1H) at δ 4.29 ppm, thus confirming the 1,2-bis substitution pattern of the ferrocenyl derivative. The trimethylsilyl substituted Cp protons were seen as triplet resonances at δ 3.98 (2H, 1.26 Hz, β-position) and δ 4.06 ppm (2H, 1.26 Hz, α-position). The ^{13}C NMR spectrum shows the silyl terminal methyl groups as two singlet resonances at δ 0.00 and 0.41 ppm. Two resonances is present showing the carbon environments at δ 45.03 (s; NCH_3) and δ 59.72 ppm ($CpCH_2N$). The ferrocenyl carbon environments are shown as eight intense resonances. The (C-methylene) and the two (C-Si) *ipso*-carbon atoms are shown at δ 89.97, 74.25 and 74.00 ppm respectively. The α-carbons on the dimethylaminomethyl substituted Cp ring are seen at δ 72.88 and 72.68 ppm respectively while the β-carbon is

to be found at δ 71.77 ppm. The α-carbons on the trimethylsilyl substituted Cp ring are seen at δ 72.01 ppm while the β-carbon was to be found at δ 70.03 ppm.

The success of preparing 1-dimethylaminomethyl-5,1'-bis-trimethylsilyl ferrocene **71** meant that further reaction towards the desired phosphine precursor ligand was implemented. Treatment of 1-dimethylaminomethyl-5,1'-bis-trimethylsilyl ferrocene **71** with 1.2 molar equivalent of *n*-butyllithium in ether gave the *ortho* metallated product 2-lithium-1-dimethylaminomethyl-5,1'-trimethylsilyl ferrocene again due to the *ortho* directing nature of the amine.[51,78-80] Subsequent addition of THF and quench under cooled conditions with Eschenmoser's salt, followed later by addition of water, extraction with ether, drying, filtering and removal of volatiles gives the product 1,2-bis-dimethylaminomethyl-5,1'-bis-trimethylsilyl ferrocene **72** together with un-reacted starting material (scheme 45). The product was purified by column chromatography by eluting the product with 1:1 petrol/ether (5% triethylamine) and isolated as viscous red oil in 93 % yield.

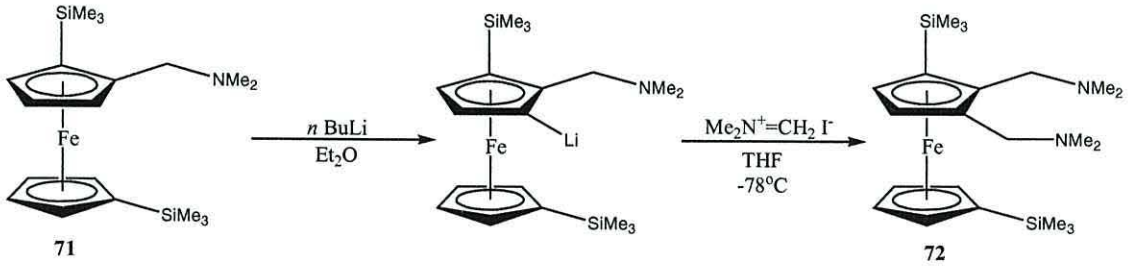

Scheme 45: Preparation of 1,2-bis-dimethylaminomethyl-5,1'-trimethylsilyl ferrocene **72**.

The product (**72**) was characterised by elemental analysis, ^{1}H and ^{13}C NMR spectroscopy. Elemental analysis of **72** gave a reasonable match to the calculated values with C %: 57.2 (59.4), H %: 8.6 (9.1), N %: 6.0 (6.3); (calculated values in parenthesis). The proton NMR spectrum of the product showed the two Si-methyl groups were present

as two singlets at δ 0.00 and 0.03 ppm with an integral of nine. The four N-methyl groups were present as two singlets at δ 1.86 and 1.93 ppm (6H each). The NCH_2Cp quartet was seen as a doublet at δ 2.97 ppm, with ^2J coupling of 12.77 Hz, and a second doublet at δ 3.24 ppm and a coupling constant of 12.77 Hz. The two protons on the dimethylaminomethyl substituted ring appeared as two doublets (2.37 Hz, 1H) at δ 3.95 ppm, and (1H, 2.37 Hz) at δ 4.08 ppm, thus confirming the 1,2-bis substitution pattern of the ferrocenyl derivative. The trimethylsilyl substituted Cp protons were seen as triplet resonances at δ 3.74 (2H, 1.26 Hz, β-position) and δ 3.81 ppm (2H, 1.26 Hz, α-position). The ^{13}C NMR spectrum shows the silyl terminal methyl groups as two singlet resonances at δ 0.00 and 0.09 ppm. Two resonances are present showing the carbon environments at δ 44.53 (s; NCH_3) and δ 57.31 ppm ($CpCH_2N$). The ferrocenyl carbon environments are shown as eight intense resonances. The (C-methylene) and (C-Si) *ipso*-carbon atoms are observed at δ 83.92, 87.25, 74.94 and 73.68 ppm respectively. The α-carbons on the dimethylaminomethyl substituted Cp ring are seen at δ 72.83 and 72.62 ppm. The α-carbons on the trimethylsilyl substituted Cp ring are seen at δ 71.45 ppm while the β-carbon was to be found at δ 69.73 ppm.

The NMR spectra of this compound however showed extra resonances which indicate the presence of starting material which accounts for the poor analytical data. Sample purification was found to be difficult due to the similar polarities and solubility of the two materials and therefore a sample of the compound **72** was sent for catalytic testing as the mixture. At the time the work was carried out it was felt it was more important to focus on the preparation of compound **74** than dwell on the purification of compound **72** so the work was moved on towards obtaining compound **74**. In addition

compound **74** should be able to be purified more easily. Therefore it was deemed more important to concentrate on the work undertaken to produce and purify in bulk quantities the novel precursor ligand 1,2-bis-dimethylaminomethyl-5,1'-bis-triphenylsilyl ferrocene **74**.

2.4.8 Preparation of 1,2-bis-dimethylaminomethyl-5,1'-bis-triphenysilyl ferrocene (74).

Treatment of dimethylaminomethyl ferrocene **32** with 2.5 molar equivalent of *n*-butyllithium in Et_2O and 1 molar equivalent of TMEDA at room temperature again results in the formation of the metallated product 1-dimethylaminomethyl-5,1'-di-lithio ferrocene. Subsequent cooling to -78°C and quench with 2.1 equivalent of chlorotriphenylsilane dissolved in the minimum amount of THF followed later by quenching with water, extraction with ether, drying, filtering and removal of volatiles gives the product 1-dimethylaminomethyl-5,1'-bis-triphenylsilyl ferrocene **73** together with starting material (scheme 46). The product was purified by crystallisation and isolated as orange/red crystals in 68 % yield.

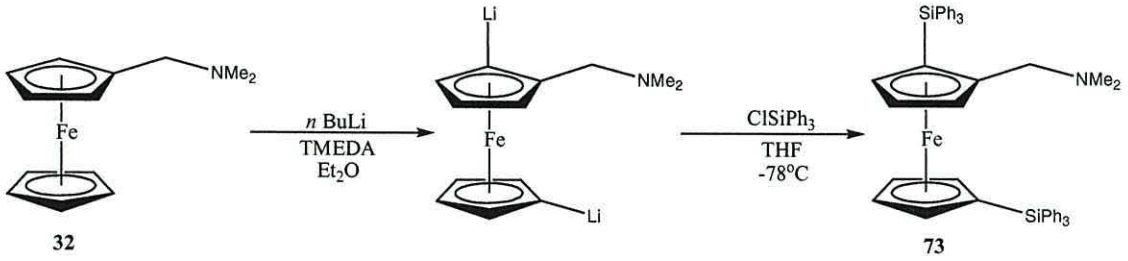

Scheme 46: Preparation of 1-dimethylaminomethyl-5,1'-bis-triphenylsilyl ferrocene **73**.

The product (**73**) was characterised by melting point determination, elemental analysis, mass spectroscopy, X-ray analysis, ^1H and ^{13}C NMR spectroscopy. The compound had a melting point of 154-157 °C in air with no apparent decomposition and

the mass spectrum showed that the parent ion was found at m/z 759. Elemental analysis gave a satisfactory match between the observed values for carbon, nitrogen and hydrogen and the calculated values (in parenthesis) with C %: 77.6 (77.5), H %: 6.0 (6.0), N %: 1.8 (1.8). The proton NMR spectrum of the product shows the N-methyl group present as a singlet at δ 1.71 ppm (6H). The NCH_2Cp was seen as a doublet at δ 2.59 ppm, with ^2J coupling of 12.46 Hz, and a second doublet at δ 2.93 ppm and a coupling constant of 12.46 Hz. The three protons on the dimethylaminomethyl substituted ring appeared as a triplet (1.74 Hz, 1H) at δ 3.99 ppm, and as two doublets (1H) at δ 4.21 ppm and (1.74 Hz, 1H) at δ 4.28 ppm, thus confirming the 1,2-bis substitution pattern of the ferrocenyl derivative. The triphenylsilyl substituted Cp protons were seen as triplet resonances at δ 4.01 (2H, 1.10 Hz, β-position) and δ 4.05 ppm (2H, 1.10 Hz, α-position). The aromatic protons on the terminal phenyl groups were present as triplet resonances at δ 7.38 ppm (6H, 1.58 Hz), 7.39 ppm (3H, 1.26 Hz), 7.42 ppm (6H, 1.57 Hz), 7.47 ppm (3H, 1.26 Hz), 7.60 ppm (6H, 1.57 Hz), and 7.68 ppm (6H, 1.26 Hz). The ^{13}C NMR spectrum showed two resonances indicating the carbon environments at δ 44.61 (s; NCH_3) and δ 58.43 ppm ($CpCH_2N$). The ferrocenyl carbon environments are shown as eight intense resonances. The (C-methylene substituted carbon) and the two (C-Si) *ipso*-carbon atoms are shown at δ 91.09, 75.75 and 75.66 ppm respectively. The α-carbons on the dimethylaminomethyl substituted Cp ring are seen at δ 74.77 and 74.67 ppm respectively while the β-carbon is to be found at δ 72.36 ppm. The α-carbons on the triphenylsilyl substituted Cp ring are seen at δ 73.34 ppm while the β-carbon was to be found at δ 66.86 ppm. The aromatic carbon environments indicate the two non-equivalent triphenylsilyl groups as two sets of four resonances at δ 136.46 (*ipso*-C), 135.69, 129.51 and 127.79

ppm and also at δ 135.98 (*ipso*-C), 135.52, 129.24 and 127.52 ppm. This is due to one of the triphenyl environments being *ortho* to a dimethylaminomethyl group while the other is on an otherwise unsubstituted Cp ring.

This is clearly shown in the crystal structure as determined by X-ray analysis as seen in figure 33.

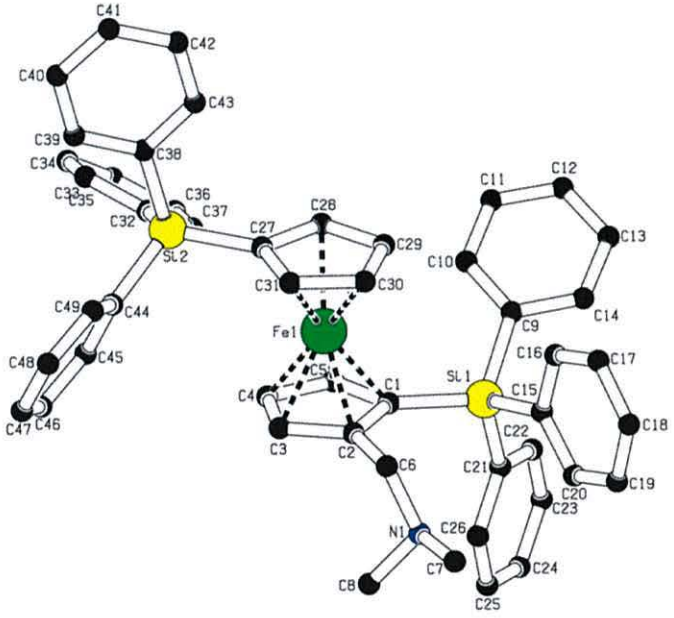

Figure 33: X-ray crystal structure of **73**.

The successful preparation of 1-dimethylaminomethyl-5,1'-bis-triphenylsilyl ferrocene **73** meant that the next reaction in the sequence could be initiated. Treatment of 1-dimethylaminomethyl-5,1'-bis-triphenylsilyl ferrocene **73** with 1.2 molar equivalent of *n*-butyllithium in ether gave the *ortho* metallated product 2-lithium-1-dimethylaminomethyl-5,1'-triphenylsilyl ferrocene. Subsequent addition of THF and quench under cooled conditions with Eschenmoser's salt, followed later by addition of water, extraction with ether, drying, filtering and removal of volatiles gives the product

1,2-bis-dimethylaminomethyl-5,1'-bis-triphenylsilyl ferrocene **74** (scheme 47). The product was purified by crystallisation and isolated a red crystalline solid in 50 % yield.

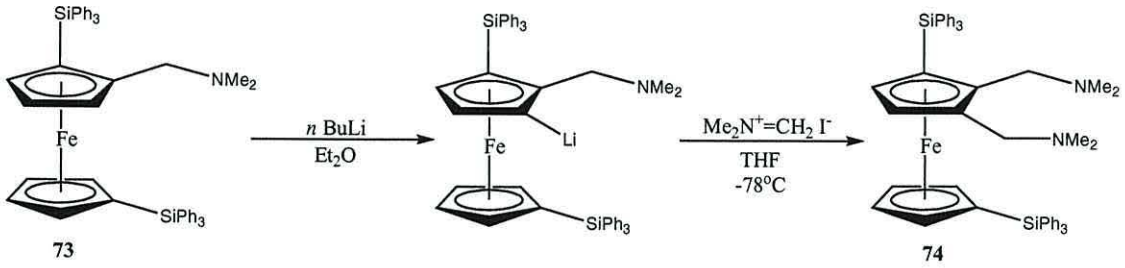

Scheme 47: Preparation of 1,2-bis-dimethylaminomethyl-5,1'-triphenylsilyl ferrocene **74**.

The product (**74**) was characterised by melting point determination, elemental analysis, mass spectroscopy, X-ray analysis, ^{1}H and ^{13}C NMR spectroscopy. The compound had a melting point of 150-154 °C in air with no apparent decomposition and the mass spectrum showed that the parent ion was found at m/z 817. Elemental analysis gave a satisfactory match between the observed values for carbon, nitrogen and hydrogen and the calculated values (in parenthesis) with C %: 74.6 (76.5), H %: 6.2 (6.4), N %: 3.1 (3.4). The proton NMR spectrum shows the four N-methyl groups were present as two singlets at δ 1.69 and 2.08 ppm (6H each). The NCH_2Cp methylene groups were observed as a doublet at δ 2.81 ppm, with ^{2}J coupling of 12.30 Hz, and a second doublet at δ 3.40 ppm and a coupling constant of 12.30 Hz. The two protons on the dimethylaminomethyl substituted ring appeared as two doublets (2.40 Hz, 1H) at δ 4.27 ppm, and (1H, 2.40 Hz) at δ 4.38 ppm, thus confirming the 1,2-bis substitution pattern of the ferrocenyl derivative. The triphenylsilyl substituted Cp protons were seen as triplet resonances at δ 4.05 (2H, 1.42 Hz, β-position) and δ 4.08 ppm (2H, 1.42 Hz, α-position). The aromatic protons on the terminal phenyl groups were present as triplet resonances at δ 7.83 ppm (6H, 1.57 Hz), 7.71 ppm (3H, 1.57 Hz), 7.47 ppm (6H, 1.57 Hz), 7.81 ppm

(3H, 1.26 Hz), 7.70 ppm (6H, 1.26 Hz), and 7.45 ppm (6H, 1.26 Hz). The ^{13}C NMR spectrum shows two resonances indicating the carbon environments at δ 45.22 (s; $N\mathbf{C}H_3$) and δ 56.67 ppm ($Cp\mathbf{C}H_2N$). The ferrocenyl carbon environments are shown as eight intense resonances. The (C-methylene) and (C-Si) *ipso*-carbon atoms are shown at δ 90.73, 88.31, 77.95 and 76.21 ppm respectively. The α-carbons on the dimethylaminomethyl substituted Cp ring are seen at δ 75.07 and 74.02 ppm. The α-carbons on the triphenylsilyl substituted Cp ring are seen at δ 68.63 ppm while the β-carbon was to be found at δ 67.43 ppm. The aromatic carbon environments indicate the two non-equivalent triphenylsilyl groups as two sets of four resonances at δ 136.55 (*ipso*-C), 136.07, 129.61 and 127.94 ppm and also at δ 136.17 (*ipso*-C), 135.53, 129.07 and 127.45 ppm. This is again due to one of the triphenyl environments being *ortho* to a dimethylaminomethyl group while the other was isolated.

This is clearly shown in the crystal structure as determined by X-ray analysis as seen in figure 34.

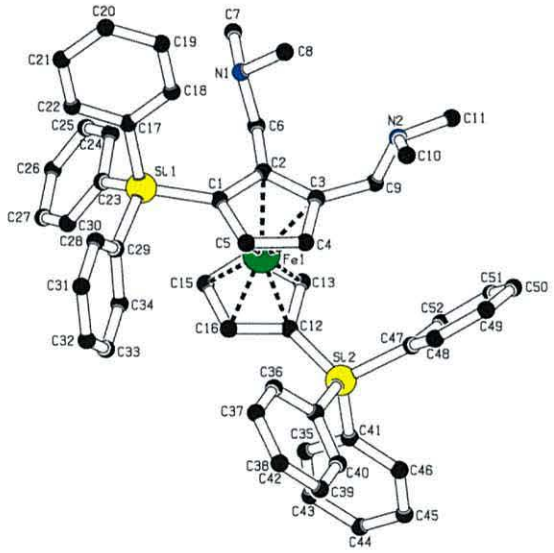

Figure 34: X-ray crystal structure of **74**.

An attempt to further increase steric bulk was also carried out. Treatment of 1,2-bis-dimethylaminomethyl-5,1'-bis-triphenylsilyl ferrocene **74** with 1.2 molar equivalent of *n*-butyllithium and subsequent quench at -78 °C with chlorotriphenylsilane dissolved in dry ether, followed later by addition of water, extraction with ether, drying, filtering and removal of volatiles gives the product 1,2-bis-dimethylaminomethyl-3,5,1'-tris-triphenylsilylferrocene **75** as a red crystalline material (scheme 48). However product could not be purified by crystallisation as NMR and mass spectrometry of the crystallized sample indicated that the sample was a mixture of starting material and the expected bulky product **75**.

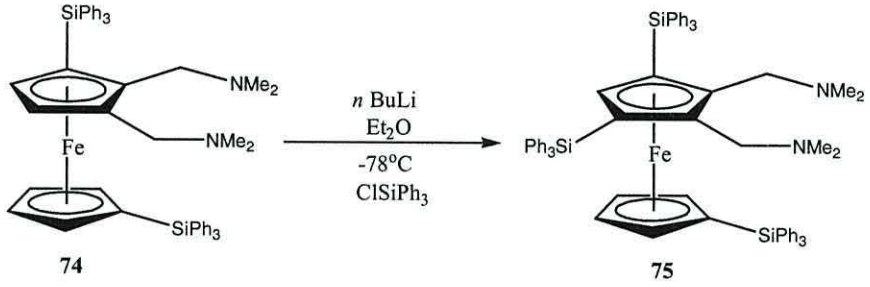

Scheme 48: Attempted preparation of **75**.

The mass spectrum of the sample showed the parent ion to be that of the expected product with m/z 1075 however a signal with m/z 817 which corresponds to the molecular weight of the starting material was also present. ^{1}H and ^{13}C NMR spectroscopy also confirmed a mixture of two compounds were apparent. No catalytic tests were undertaken for this sample due to the lack of purity.

2.4.9 Dimeric dinuclear ferrocenes.

The synthesis of dinuclear ferrocenes containing the dimethylaminomethyl ligand (which again should be able to be substituted to produce phosphine ligands) was thought to be possible. An attempt was made to prepare a ligand with two metal binding sites which should in theory at least extend the longevity of the derived catalyst. To do this it was felt that diferrocenes would be preferred to monoferrocenes because of possible problems with the formation of high complex products where monoferrocenes are used (scheme 49).

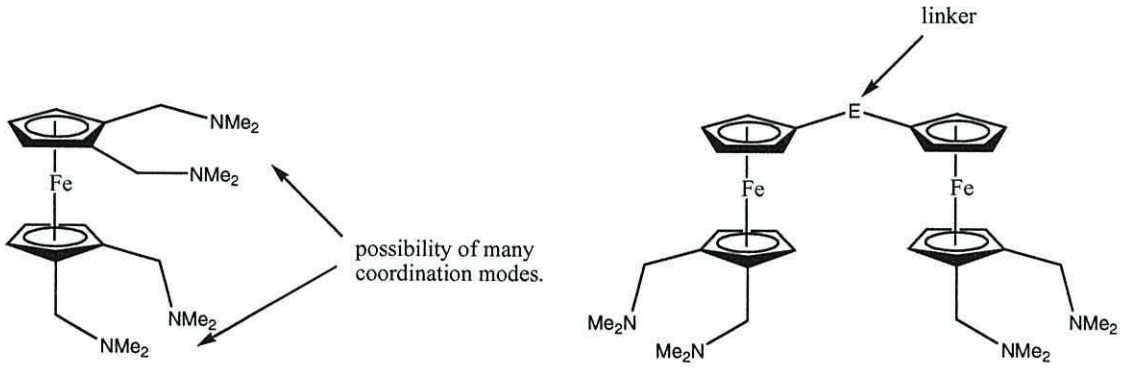

Scheme 49.

The structure of these dinuclear ferrocenes would in theory seem to be advantageous to the catalytic process. They are significantly steric and also contain two active sites to receive the substrates during the methoxycarbonylation of ethene. The initial stages in the preparation route were achieved in moderate yields (scheme 50) and were intended (if possible) to produce similar catalyst precursors for testing as previously discussed. Compound **76** was prepared by the treatment of 1,1'-dibromoferrocene **61** with 0.95 equivalent of *n* butyllithium in THF at -78°C, and subsequent quench with 0.48 equivalent of dichlorodimethylsilane. After warming to room temperature, followed later by addition of water, extraction with ether, drying, filtering and removal of volatiles gives

the compound **76** together with mono-bromo by-products. The product was purified by column chromatography and isolated as orange solid in 61 % yield. The product (**76**) was characterised by melting point determination, elemental analysis, ^{1}H and ^{13}C NMR spectroscopy. The compound had a melting point of 37-39 °C in air with no apparent decomposition. Elemental analysis gave a satisfactory match between the observed values for carbon and hydrogen and the calculated values (in parenthesis) with C %: 44.8 (45.1), H %: 3.6 (3.8). Proton NMR showed five resonances; the two Si-methyl groups were present as a singlet at δ 0.33 ppm with an integral of six. The α-positioned protons on the substituted Cp appeared as doublets at δ 4.20 and 4.13 ppm (1.57 Hz and 1.58 Hz) (4 x CH) respectively, and the four protons on the β-position of the substituted ring appeared as doublet resonances at δ 3.92 ppm and δ 3.79 ppm (1.58 Hz and 1.57 Hz) (4 x CH). The ^{13}C NMR spectrum shows the silyl terminal methyl groups as a singlet resonance at δ 0.67 ppm. The ferrocenyl carbon environments are shown as six intense resonances. The (C-Br) and the (C-Si) *ipso*-carbon atoms are shown at δ 77.71 and 75.64 ppm respectively. The α-carbons on the bromine substituted Cp ring are seen at δ 74.05 ppm respectively while the β-carbons were to be found at δ 70.51 ppm. The α-carbons on the dimethylsilyl substituted Cp rings are seen at δ 72.32 ppm while the β-carbons were to be found at δ 67.41 ppm.

From NMR analysis it was decided that bis-1-bromo-1'-dimethylsilyl bridged ferrocene **76** had been successfully prepared and the product was used immediately in further reactions. Treatment of compound **76** with 2.1 molar equivalent of *n*-butyllithium in diethyl ether at room temperature removed the two bromine atoms. Subsequent addition of THF and quench with 2.2 molar equivalent of Eschenmoser's salt under

cooled conditions followed later by quenching with water, extraction with ether, drying, filtering and removal of volatiles gives the product bis-1-dimethylaminomethyl-1'-dimethylsilyl bridged ferrocene **77** together with by-products (scheme 50). The product was purified by column chromatography by eluting first the starting material with petrol, and then the product with 1:1 petrol/ether (5% triethylamine) and isolated as red oil in 76 % yield.

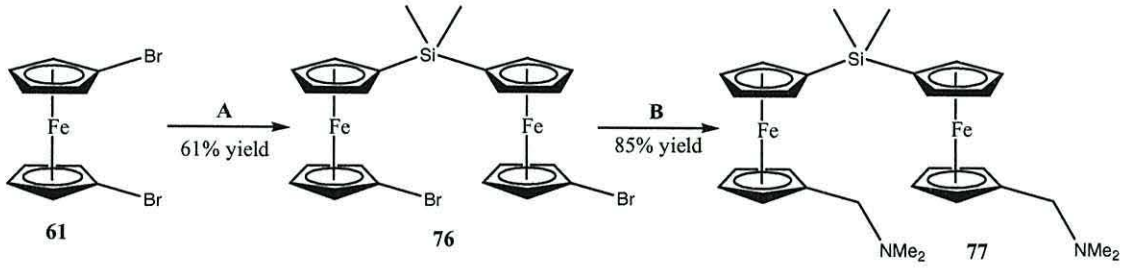

Scheme 50: Preparation of bis-1-dimethylaminomethyl-1'-dimethylsilyl bridged ferrocene **77**. **A:** 1) n BuLi, THF. 2) Cl_2SiMe_2. **B:** 1) *n* BuLi, Et_2O. 2) $Me_2N^+{=}CH_2I^-$, THF.

The product (**77**) was characterised by ^1H and ^{13}C NMR spectroscopy. Proton NMR showed eight intense resonances; the two Si-methyl groups were present as a singlet at δ 0.28 ppm with an integral of six. The two N-methyl groups were present as two singlet resonances at δ 0.69 and 1.32 ppm and the N-methylene groups was also present as a triplet at δ 2.05 ppm (4H, 7.91 Hz). These had an integral of 6:6:4 respectively. The α-positioned protons on the substituted Cp appeared as triplets at δ 4.03 and 3.81 ppm (1.26 Hz and 1.27 Hz) (4 x CH) respectively, and the protons on the β-position of the substituted rings appeared as triplet resonances at δ 3.78 ppm and δ 3.74 ppm (1.89 Hz and 1.57 Hz) (4 x CH). The ^{13}C NMR spectrum shows the terminal methyl groups as a singlet at δ 0.00 ppm. Three resonances is present showing the carbon environments at δ 29.97, 34.14 (s; NCH_3) and δ 42.11 ppm ($CpCH_2N$). The ferrocenyl carbon environments are shown as six intense resonances. The (C-methylene substituted

carbon) and (C-Si) *ipso*-carbon atoms are shown at δ 90.16 and 74.33 ppm respectively. The α-carbons on the dimethylaminomethyl and dimethylsilyl substituted Cp rings are seen at δ 72.29 and 69.06 ppm respectively while the β-carbons are to be found at δ 68.93 and 68.10 ppm.

An attempt in the synthesis of bis-1,2-dimethylaminomethyl-1'-dimethylsilyl bridged ferrocene **78** was also carried out. Treatment of bis-1-dimethylaminomethyl-1'-dimethylsilyl bridged ferrocene **77** with 2.1 molar equivalent of *n*-butyllithium and subsequent quench at -78 °C with Eschenmoser's salt dissolved in THF, followed later by addition of water, extraction with ether, drying, filtering and removal of volatiles did not give the desired product in a pure form (scheme 51).

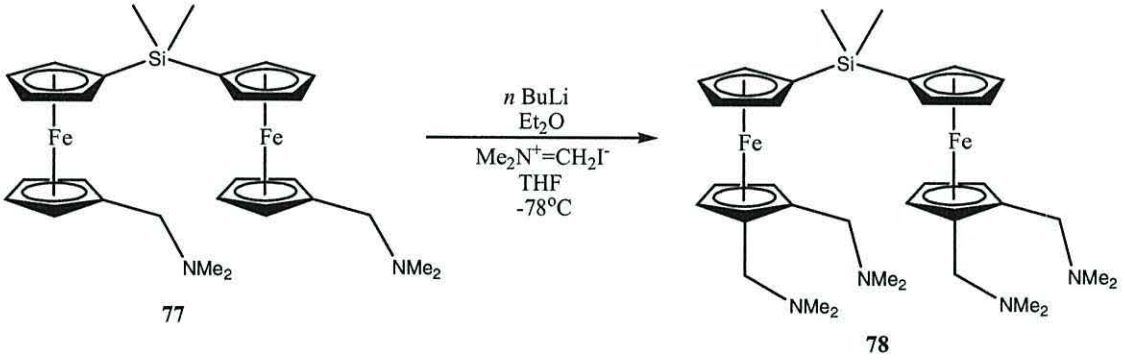

Scheme 51: Attempted preparation of **78**.

The ^{1}H and ^{13}C NMR spectrum of the product confirmed a mixture was present. This was due to the ability of the dimethylaminomethyl groups to *ortho*-lithiate on both sides in one of the Cp rings thus forming a mixture of the required compound **78** and undesired 1,2,3-trisubstiuted products which could not be separated by column chromatography. This synthetic route was therefore abandoned as it was deemed to be impractical for any industrial scale synthesis.

2.5 Synthetic studies on alternative ferrocenylphosphine ligands.

2.5.1 Introduction.

Since its discovery in the early 1970s,[98] the metallophosphine 1,1'-bis(diphenylphosphino)ferrocene (dppf) **27** has been widely used in organometallic chemistry and homogeneous catalysis.[99] Palladium (II) complexes are relatively numerous and have also proved to be effective catalysts in a variety of homogeneous processes.[100] A relatively recent article by Gusev *et al* describes the preparation and characterization of several mononuclear and binuclear Pd(II) complexes stabilized by the analogue of **27**, 1,1'-bis(diphenylphosphino)octamethyl ferrocene (dppomf) **79** (figure 35).[54]

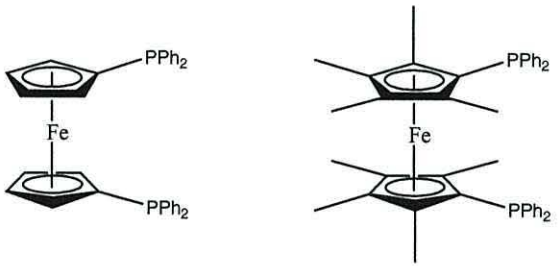

dppf **27** dppomf **79**

Figure 35: dppf and dppomf.

Selected dppf and dppomf Pd (II) complexes have been scrutinized for the first time as catalyst precursors for the methoxycarbonylation of ethene, which is the industrially relevant reaction efficiently catalyzed in the homogeneous phase by palladium (II) bis-phosphine complexes. Minor changes in these latter species and/or in the experimental conditions can remarkably affect the selectivity of the alkoxycarbonylation reaction, leading to the formation of a range of products from alternating polyketones to methyl propanoate **4**. It was stated in the paper by Gusev and co-workers that dppomf **79** generates a selective catalyst for methyl propanoate, while

dppf **27** leads to a mix of low molecular-weight oxygenates spanning from methyl propanoate to alternating oligoketones.

The work in this section reports the preparation of octamethyl ferrocene precursors containing different phosphine ligands which may be complexed to palladium, tested and compared to existing ligands in catalysts in methyl propanoate production. The general synthetic route towards these ferrocenyl precursors is shown in scheme 52. It should be possible to carry this out on the bulk scale starting from cheap commercially available starting materials diethyl ketone **80** and acetaldehyde.

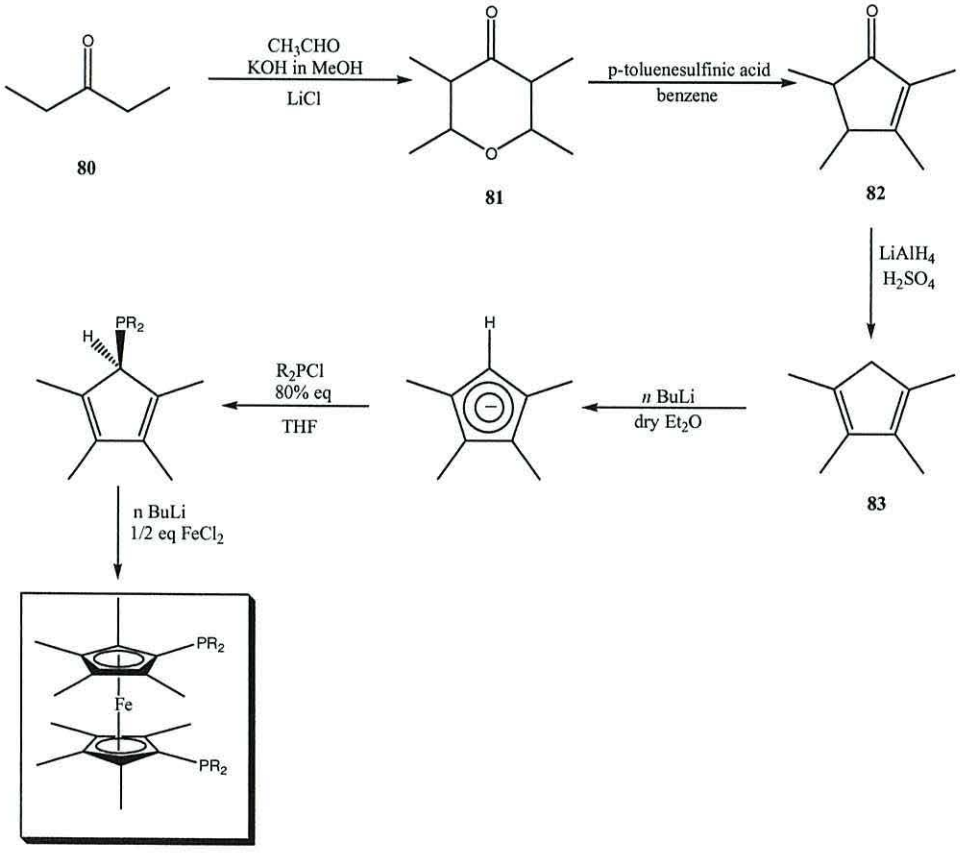

Scheme 52: Route towards octamethylferrocenyl phosphines.

The following sections document the synthesis of octamethylferrocenes from basic precursors.

2.5.2 Preparation of 2,3,5,6-tetrahydro-2,3,5,6-tetramethyl-γ-pyrone (81).

According to early literature reports it was thought that the formation of pyrone-derivative **81** was obtained by a double Aldol addition however subsequent work by Kohl *et al* found that the reaction can be carried out in one step (scheme 53).[101]

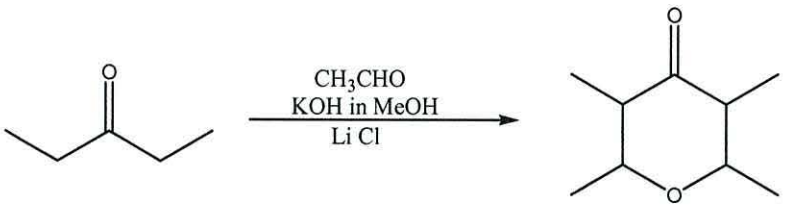

80 **81**

Scheme 53: Preparation of 2,3,5,6-tetrahydro-2,3,5,6-tetramethyl-γ-pyrone **81**.

Diethyl ketone **80** in methanol and potassium hydroxide was treated with a small amount of lithium chloride with gentle warming. The Li^+-cation formed complexes with the carbonyl compounds, whose geometries favour conversion to the pyrone derivative **81**. After 12 hours, the mixture was neutralized with hydrochloric acid. The product was washed, and simple distillation under reduced pressure produced the crude product. Re-distillation through a 20cm Vigreux-column under reduced pressure yielded 42 % of **81** in bulk scale (> 350g) as a clear colourless liquid.

The product (**81**) was characterised by ^1H NMR spectroscopy, ^{13}C NMR spectroscopy and infrared spectroscopy. Proton NMR showed the four methyl groups as two doublets (3H) at δ 0.93 ppm with a coupling constant of 6.40 Hz and the other slightly downfield due to the ether at δ 1.29 ppm with a similar coupling of 6.11 Hz. Two multiplets (1H) were seen indicating the two protons on the ring are coupled with the methyl groups and with each other, one resonance at δ 2.24 ppm (3.36 Hz) and the other being next to the ether at δ 3.28 ppm (3.36 Hz). The ^{13}C NMR spectrum showed five resonances indicating the five different carbon environments. The four methyl carbons

were seen as two singlet resonances at δ 9.46 and δ 20.41 ppm. The quaternary carbon next to the carbonyl group was seen at δ 51.25 ppm and the one adjacent to the ether was seen at δ 78.98 ppm. The carbonyl was present with a resonance at δ 209.61 ppm. The infrared spectrum showed strong vibrations due to carbonyl and C-O stretching at 1714 cm^{-1} and 1379 cm^{-1} respectively. This data is in agreement with the literature.[101]

The preparation of **81** had been successful on a bulk scale and steps were taken to proceed onto the second step of the synthesis.

2.5.3 Preparation of 2,3,4,5-tetramethylcyclopent-2-enone (82).

In this second step it was known that refluxing of the pyrone derivative **81** in benzene with 10 mol% of *p*-toluenesulfinic acid leads to the formation of the pentenone derivative **82** in satisfactory yields (65%) in bulk (> 200g) as a clear colourless liquid (scheme 54). As a by-product, the α,β-unsaturated ketone is obtained (≈ 10% yield), which can be used as an additional starting material in the Aldol addition step.

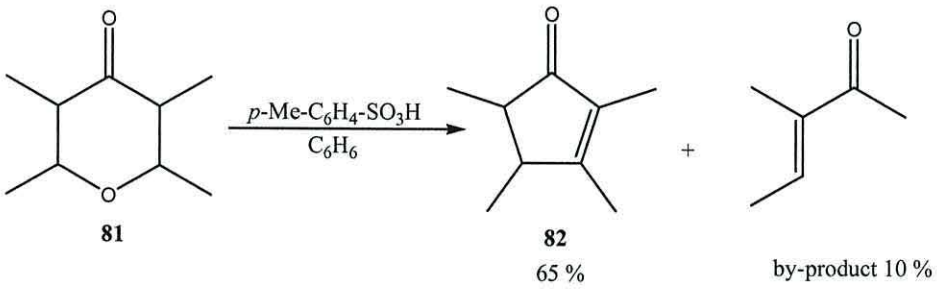

81 **82** 65 % by-product 10 %

Scheme 54: Preparation of 2,3,4,5-tetramethylcyclopent-2-enone **82**.

The product **82** was purified by distillation under reduced pressure and was again characterized by ^{1}H and ^{13}C NMR spectroscopy, infrared spectroscopy and by low resolution EI mass spectrometry. The proton NMR spectrum shows two methyl groups as two doublets (3H) at δ 1.07 ppm with a coupling constant of 7.62 Hz and at δ 1.13 ppm

with a coupling constant of 7.02 Hz. The two olefinic methyl groups are observed as singlet resonances (3H) one at δ 1.61 ppm and the other slightly downfield due to it's proximity to the carbonyl at δ 1.92 ppm. Two multiplets (1H) were observed indicating the two protons on the ring being coupled with the methyl groups and with each other, one resonance at δ 2.20 ppm (7.02 Hz) and the other being next to the carbonyl at δ 2.62 ppm (7.32 Hz). The ^{13}C NMR spectrum shows nine major resonances with the four terminal methyl groups present at δ 8.05, 14.52, 14.98 and 17.63 ppm. The two between 14 and 15 ppm are the olefinic terminal methyl groups while the resonance at δ 17.63 is due to the terminal methyl which is nearest to the carbonyl. The non-olefinic carbon atoms in the ring are observed at δ 46.27 and 48.34 ppm while the olefinic carbon atoms are more downfield at δ 134.43 and 136.58 ppm. The carbonyl group is also present at δ 210.93 ppm. The infrared spectrum showed strong vibrations due carbonyl and C=C stretching at 1699 cm^{-1} and 1648 cm^{-1} respectively. In addition to NMR and IR spectroscopic evidence for **82** a low resolution mass spectrum was obtained. In the mass spectrum, a molecular ion with m/z 138.1 was found, comparing to 138.2 g mol^{-1} calculated for **82**.

The preparation of **82** had been successful on a bulk scale and steps were taken to proceed onto the third step of the synthesis.

2.5.4 Preparation of 1,2,3,4-tetramethylcyclopentadiene (83).

The reduction of the pentenone derivative **82** was undertaken following a methodology described in a paper by Fendrick *et al* (scheme 55).[102] Slow addition of **82** to $LiAlH_4$ in diethyl ether and subsequent stirring over eight hours produced an alcohol

intermediate. The dehydration of the alcohol by addition of repeated aliquots of 33% H_2SO_4 was monitored via GC by monitoring the disappearance of the alcohol peak until no alcohol could be detected by GC. Operations after the addition of H_2SO_4 were carried out as rapidly as possible to avoid loss of product from undesirable side reactions. When no alcohol was present, a saturated aqueous solution of potassium carbonate was added until the aqueous layer was strongly alkaline. Anhydrous potassium carbonate was added to the organic layer and after subsequent filtration and evaporation a small amount of sodium metal was added and the product **83** purified by trap-to-trap distillation. This gave the product as a clear colourless liquid with a yield of 37 % (64g).

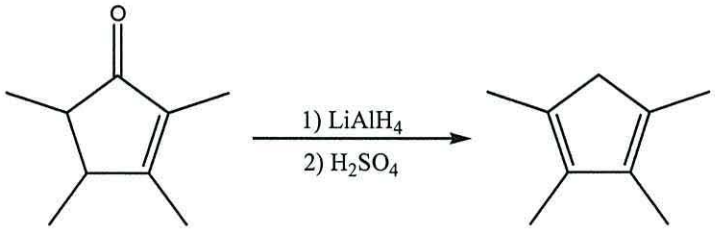

82 **83**

Scheme 55: Preparation of 1,2,3,4-tetramethylcyclopentadiene **83**.

The product **83** was characterised by ^1H NMR spectroscopy, infrared spectroscopy and by low resolution EI mass spectrometry. The proton NMR spectrum showed three singlet resonances with two olefinic methyl group resonances (6H) at δ 1.84 ppm and δ 1.93 ppm. The olefinic methylene (2H) was seen at δ 2.74 ppm. The infrared spectrum showed no strong vibrations due carbonyl or OH stretching. Further to NMR and IR spectroscopic evidence for **83** a low resolution mass spectrum was obtained. The mass spectrum, showed a molecular ion with m/z 122 for the product **83**.

In conclusion the reduction of **82** to **83** was successful however the quantity of the material had greatly reduced. The loss of product to side reactions after addition of H_2SO_4

accounts for this, and although the yield compared reasonably favourably to the yield reported in the paper which was 45 %. For further reactions a 5g sample was used in the preparation of octamethylferrocenes containing different phosphine ligands.

2.5.5 Preparation of 1,1'-bis(diphenylphosphino)octamethyl ferrocene (86).

A paper by Szymoniak *et al* describes the deprotonation of 1,2,3,4-tetramethylcyclopentadiene **83** to give an anion which is highly air and moisture sensitive.[103] In a modification of the literature method a solution of *n*-BuLi was added to an ethereal solution of **83** at 0°C. The mixture was left to stir overnight to give a white precipitate of the anion **84**, which was filtered, washed with dry ether and left to dry under vacuum. A solution of fresh chlorodiphenylphosphine in THF was then added to a stirred suspension of the anion in THF to yield 1-(diphenylphosphino)-2,3,4,5-tetramethylcyclopentadiene **85**. This was then re-lithiated under cold conditions and after warming to room temperature, quenched with 0.5 equivalent iron chloride to form the ferrocenyl derivative **86**. Purification via column chromatography and subsequent evaporation of solvent yielded the product as an orange solid in 33 % yield (scheme 56).

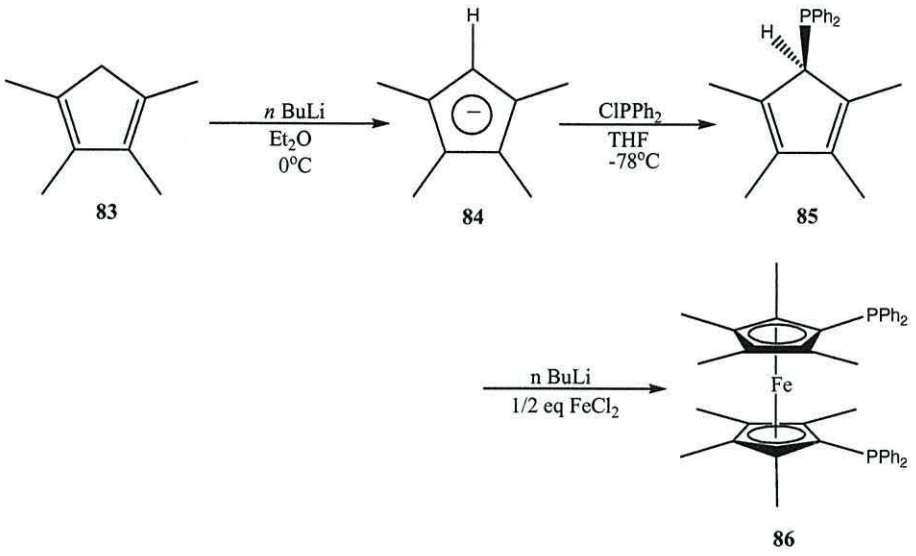

Scheme 56: Preparation of 1,1'-bis(diphenylphosphino)octamethyl ferrocene **86**.

The product **86** was characterised by ^{1}H, ^{13}C and ^{31}P NMR spectroscopy and a low resolution fast-atom bombardment mass spectrum was obtained. The proton NMR spectrum shows the eight methyl groups as two singlet resonances at δ 1.23 ppm (12H) and δ 1.69 ppm (12H); the latter being the methyl groups on the α-carbon atoms of the Cp ring. The methyl groups on the α-carbon atoms on the Cp ring are further downfield due to their closer proximity to the phosphorus atom. No resonances were present in the normal ferrocenyl region between δ 4–5 ppm indicating full substitution of both Cp rings. The aromatic region of the spectrum showed three main triplet resonances at δ 7.08 ppm (8H, coupling constant of 6.94 Hz), the *ortho*-protons; δ 7.16 ppm (8H, 1.58 Hz), the *meta*-protons and δ 7.29 (4H, resonance was partially overlapped) being most likely the *para*-protons. The ^{13}C NMR spectrum shows the methyl groups as two weak resonances at δ 9.94 and δ 11.51 ppm. It also includes four singlet resonances corresponding to four different aromatic carbon environments at δ 127.86, 128.18, 132.80 and 134.97 ppm. The ^{31}P NMR spectrum shows a single resonance at δ -22.27 ppm indicating that the phosphorus atoms lie in the same environment. A low resolution mass spectrum was also

obtained. In the mass spectrum, a molecular ion with m/z 666 was found with an observed isotope model [M^+] m/z (rel. int) of 666 (100), 667 (60), 668 (15), comparing to 666 g mol^{-1} calculated for **86** and a theoretical isotope model [M^+] m/z (rel. int) as 666 (100), 667 (50), 668 (10).

The preparation of dppomf **86** was successful leading onto the preparation of other phosphine ligands by use of the same methodology using different phosphine quench reagents.

2.5.6 Preparation of 1,1'-bis(diisopropylphosphino)octamethyl ferrocene (88).

Preparation of compound **88** was carried out using a similar procedure to that of **86** but this time the quench reagent used was chlorodiisopropylphosphine leading to the formation of 1-(diisopropylphosphino)-2,3,4,5-tetramethylcyclopentadiene **87** in the intermediate step (scheme 57). Relithiation followed by addition of $FeCl_2$ yielded the target compound, purification via column chromatography and subsequent evaporation of solvent under high vacuum isolated the product as red crystals in 50 % yield.

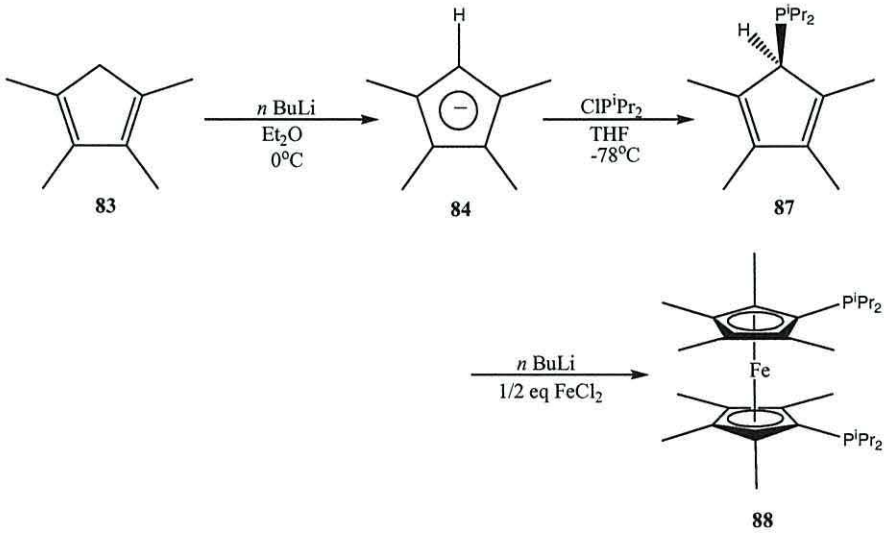

Scheme 57: Preparation of 1,1'-bis(diisopropylphosphino)octamethyl ferrocene **88**.

The product **88** was characterised by elemental analysis, ^{1}H, ^{13}C and ^{31}P NMR spectroscopy and a low resolution fast-atom bombardment mass spectrum was obtained. Elemental analysis of **88** gave good match to the calculated values with C %: 67.7 (67.9), H %: 9.7 (9.9), N %: 0.0 (0.0); (calculated values in parenthesis). The proton NMR shows the *iso*-propyl methyl groups as four doublets each with the same coupling constant of 6.94 Hz at δ 1.04, 1.07, 1.16 and 1.18 ppm (6H). The methyl groups on the substituted Cp ring are shown as two singlet resonances at δ 1.75 and 1.84 ppm (12H); the latter being the methyl groups on the α-carbon atoms of the Cp ring. A quartet resonance is also present downfield indicating the presence of the proton on the *ipso*-carbon of the *iso*-propyl at δ 2.23 ppm with a coupling constant of 2.93 Hz (4H). Once again ferrocenyl proton resonances are not present indicating full substitution on both Cp rings. The ^{13}C NMR spectrum shows that the Cp methyl groups are present with the methyl groups on the β-carbon atoms of the Cp ring as a singlet at δ 10.33 ppm. The methyl groups on the α-carbon atoms of the Cp ring are shown as a doublet due to ^{3}J coupling to the phosphorus atom at δ 12.86 ppm (8.25 Hz). The *iso*-propyl methyl groups were visible as two pairs of overlapping doublets, one at δ 20.88 ppm with ^{2}J phosphorus-carbon coupling of 10.99 Hz, and the other at δ 22.48 ppm with a coupling of 11.92 Hz. This difference in shifts is attributed to the 'inner' *iso*-propyl arm, positioned between the two phosphorus atoms on the two Cp rings would be most shielded from applied magnetic field and so would be observed at a lower frequency than the 'outer' *iso*-propyl arm. Likewise, the inner carbon atoms of the *iso*-propyl groups were also seen as a doublet at δ 30.46 ppm (18.32 Hz). The substituted Cp ring showed a singlet for the two β-carbon atoms at δ 75.44 ppm, and a resonance for the two α-carbon atoms were seen at δ 82.57.

The substituted *ipso*-carbon atom was observed as doublet resonance at around δ 83.47 ppm split by ^{1}J coupling to phosphorus of 10.99 Hz. The ^{31}P NMR spectrum showed a main resonance at δ 1.04 ppm indicating that the two phosphorus atoms were equivalent. The spectrum also showed a weak signal at δ 4.04 ppm indicating possible trace phosphine impurity. A low resolution mass spectrum was also obtained, which showed a molecular ion with m/z 530 with an observed isotope model [M^{+}] m/z (rel. int) of 530 (100), 531 (40), 532 (10), comparing to 531 g mol^{-1} calculated for **88** and a theoretical isotope model [M^{+}] m/z (rel. int) as 530 (100), 531 (40), 532 (7).

This hitherto unpublished compound was thus successfully prepared in satisfactory yield and provides another example of a compound that can be coordinated to Pd and the product tested in catalytic reactions. Another unpublished analogue was then targeted.

2.5.7 Attempted synthesis of 1,1'-bis(di-*tert*-butylphosphino)octamethylferrocene(90)

Preparation of compound **90** was carried out in a similar procedure but this time the quench reagent was chloro di-*tert*-butylphosphine leading to the formation of 1-(di-*tert*-butylphosphino)-2,3,4,5-tetramethylcyclopentadiene **89** in the intermediate step (scheme 58). This was then relithiated and 0.5eq $FeCl_2$ added.

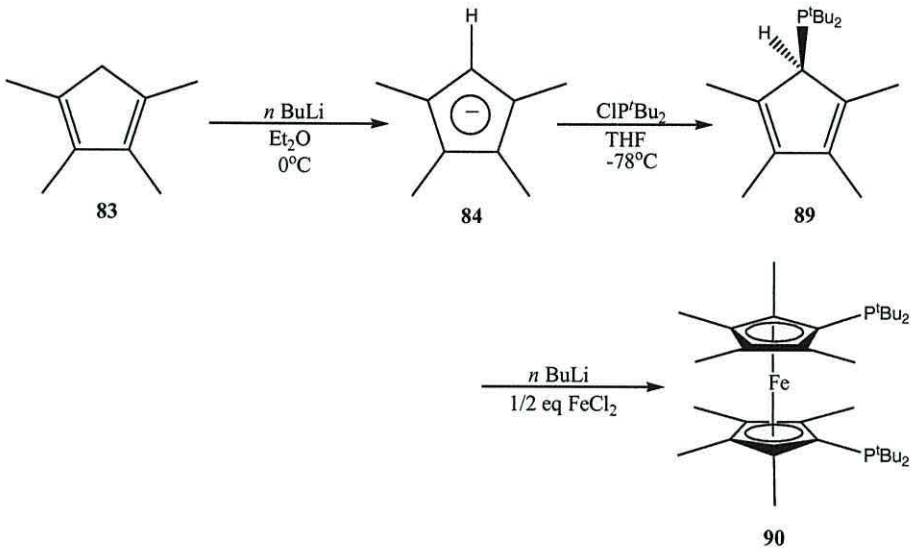

Scheme 58: Attempted synthesis of 1,1'-bis(di-*tert*-butylphosphino)octamethylferrocene **90**.

After subsequent workup and purification procedures a small quantity of orange crystals were obtained however following NMR analysis and a obtaining a low resolution fast-atom bombardment mass spectrum of the sample it was deduced that the reaction had failed. The NMR data gathered was consistent with octamethylferrocene **91** ($C_{18}H_{26}Fe$, F.W. 298.25 g mol^{-1}) (figure 36) and the mass spectrum showed an M^+ of m/z (rel. int.) 298 (100) 297 (30) 296 (15). It was deduced that the *t*-butyl groups were too 'bulky' and that the compound would be too stericly hindered. It was thought that the lithiated tetramethylcyclopentadiene must have hydrolysed with addition of water following the addition of iron chloride to result in the sample gathered.

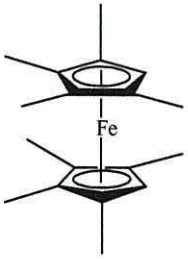

Figure 36: Octamethylferrocene **91**.

Despite this setback a useful route of preparing octamethylferrocenyl phosphine derivatives has been tested and it would be interesting to see how their Pd-complexes would compare to existing ligands in the catalytic reactions of ethene methoxycarbonylation.

2.6 Synthetic studies on non-ferrocenyl ligands.

2.6.1 Introduction.

A highly active and selective catalyst for the production of methyl propanoate **4** (a key precursor to methyl methacrylate) *via* the methoxycarbonylation of ethene has been described in section **1.3.4**, based on a zero valent palladium complex $L_2Pd(dba)$ **7** [where L_2 = 1,2-bis(di-*tert*-butylphosphinomethyl)benzene and dba = *trans,trans*-dibenzylideneacetone].[26]

This short section describes some work carried out on benzene based ligands on the based on modification of work described in a paper by Hauser *et al.*[104] In this paper they investigated the metallation of *N*, *N*-dimethyl benzylamine **92** with a number of strong bases. When treating the amine with BuLi.*t*-BuOK in a mixture of THF and hexane an α-metallated product **93** was obtained. The dark-red solution of **93** reacts very well with alkyl halides even at very low temperatures (scheme 59).

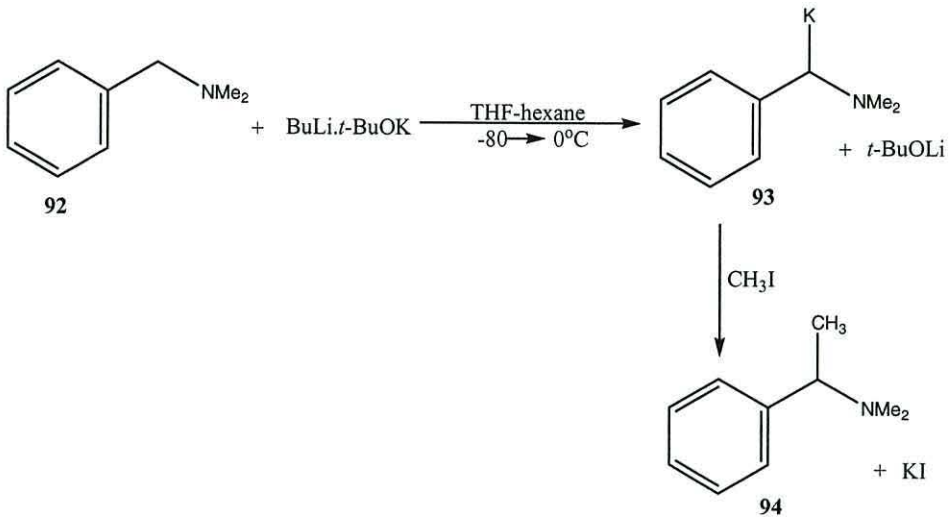

Scheme 59: The work on benzene based ligands described by Hauser *et al.*[104]

Work was carried along this general scheme but interest mainly lay in whether the α-metallated product **93** would react with Eschenmoser's salt. With this in mind a test scale experiment was carried out.

2.6.2 Preparation of mono-(α-dimethylaminomethyl-dimethylaminomethyl)benzene (95).

Treatment of *N,N*-dimethyl benzylamine **92** in THF with *n*-butyllithum in hexane and then *t*-BuOK in THF in cool conditions resulted in the α-metallated intermediate **93** as a dark-red solution. This solution was then quenched with Eschenmoser's salt, hydrolysed with water and extracted with ether. After subsequent drying with potassium carbonate, filtering and concentrating on the rotary evaporator to give yellow oil. The literature product **95**[105,106] was isolated from the starting material by distillation under reduced pressure as a clear colourless liquid in a yield of 34 % (scheme 60).

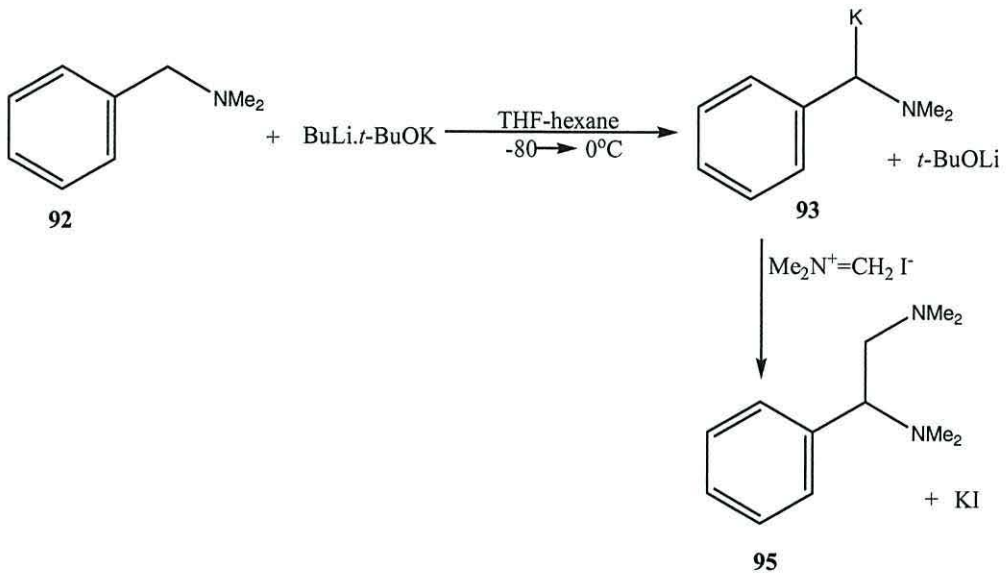

Scheme 60: Preparation of mono-(α-dimethylaminomethyl-dimethylaminomethyl) benzene 95.[105]

The product **95** was characterised by elemental analysis, ^{1}H and ^{13}C NMR spectroscopy, and by low resolution EI mass spectrometry. Elemental analysis of **95** gave good match to the calculated values with C %: 74.9 (75.0), H %: 10.2 (10.5), N %: 14.4 (14.6); (calculated values in parenthesis). The proton NMR spectrum shows that the two N-methyl groups as two singlet resonances at δ 2.14 ppm (6H) and δ 2.20 ppm (6H). The N-methylene on the β-carbon was seen as a doublet at δ 3.35 ppm (2H) with a coupling constant of 5.35 Hz. The proton on the α-carbon was shown as a triplet at δ 3.51 ppm (1H) with a coupling constant of 2.52 Hz. The aromatic region of the spectrum showed three main triplet resonances at δ 7.16 ppm (1H, coupling constant of 1.58 Hz), the *para*-proton; δ 7.22 ppm (2H, 3.78 Hz), the *meta*-protons and δ 7.29 (2H, resonance was partially overlapped) being most likely the *ortho*-protons. The ^{13}C NMR spectrum shows eight main resonances. The methyl (NCH_3) groups are present as two signals at δ 41.99 and 46.08 ppm. The β- and α-methylene carbons were seen at δ 62.21 and 67.31 ppm respectively. Aromatic carbons were present as four major resonances at δ 127.14,

127.89, 128.69 ppm with the *ipso*-carbon more downfield at δ 138.08 ppm. Further to NMR spectroscopic evidence for **95** a low resolution mass spectrum was obtained. In the mass spectrum, a molecular ion [M – H^+] with m/z 191.1 was found, comparing to 192.3 g mol^{-1} calculated for **95**.

Following the successful test with Eschenmoser's salt, further reactions were initiated to prepare the bis-1,2 derivative of *N,N*-dimethylaminomethyl benzene **92** so that the bis α-metallation with BuLi.t-BuOK could be investigated.

2.6.3 Preparation of bis-1,2-dimethylaminomethyl benzene (96).

Treatment of *N,N*-dimethylaminomethyl benzene **92** in diethyl ether with 1.2 equivalent of *n*-butyllithium gave the *ortho* metallated product 1-lithium-2-dimethylaminomethyl benzene as the amine is *ortho* directing. Subsequent quench under cooled conditions with Eschenmoser's salt with a small quantity of THF, followed later by further quench with water, extraction with ether, drying, filtering and removal of volatiles gives the product bis-1,2-dimethylaminomethyl benzene **96** together with un-reacted starting material. The sample was purified by fractional distillation under reduced pressure to give the product as clear, yellow liquid in 76 % yield (scheme 61).

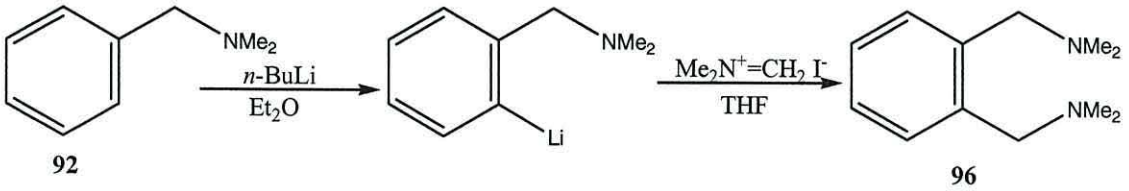

Scheme 61: Preparation of bis-1,2-dimethylaminomethyl benzene **96**.

The product **96** was characterised by elemental analysis, ^1H and ^{13}C NMR spectroscopy, and by low resolution GC mass spectrometry. Elemental analysis of **96** gave good match to the calculated values with C %: 74.8 (75.0), H %: 10.3 (10.5), N %:

14.4 (14.6); (calculated values in parenthesis). The proton NMR spectrum shows the two N-methyl groups as a singlet resonance at δ 2.25 ppm (12H). The N-methylene groups on the α-alkyl chain were seen as a singlet at δ 3.54 ppm (4H). The aromatic region of the spectrum showed two main resonances with a triplet at δ 7.22 ppm (2H, coupling constant of 1.58 Hz); the protons on the β-aromatic carbon atoms and a doublet at δ 7.30 ppm (2H, coupling constant of 1.58 Hz); the protons on the α-aromatic carbon atoms. The ^{13}C NMR spectrum shows five main resonances. The methyl (NCH_3) groups are present a signals at δ 45.61 ppm The α-methylene carbons were seen as a singlet at δ 61.31 ppm. Aromatic carbons were present as three major resonances at δ 126.83 and 130.23 ppm with the *ipso*-carbon more downfield at δ 138.03 ppm. Further to NMR spectroscopic evidence for **96** a low resolution mass spectrum was obtained. In the mass spectrum, a molecular ion [$M^+ + H^+$] with m/z 193.1 was found, comparing to 192.3 g mol^{-1} calculated for **96**.

After the successful production of compound **96**, it was immediately used to investigate whether the bis α-metallation with BuLi.t-BuOK would occur.

2.6.4 Preparation of bis-1,2-(α-dimethylaminomethyl-dimethylaminomethyl) benzene (97).

Treatment of bis-1,2-dimethylaminomethyl benzene **96** in THF with two equivalents *n*-butyllithum in hexane and then with two equivalents of t-BuOK in THF under cooled conditions resulted in the bis-α-metallated intermediate as a dark-red solution. This solution was then quenched with two equivalents of Eschenmoser's salt, hydrolysed with water and extracted with the ether. After subsequent drying with potassium carbonate, filtering and concentrating on rotary evaporator a yellow oil

resulted. The crude product **97** was isolated from the starting material by distilling with a Kugelrohr distillation apparatus under reduced pressure as a clear orange liquid with a potential yield of 36 % (scheme 62).

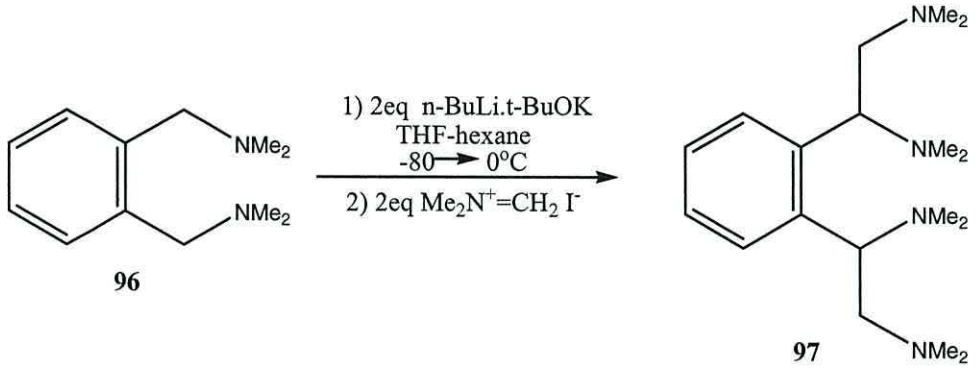

Scheme 62: Preparation of bis-1,2-(α-dimethylaminomethyl-dimethylaminomethyl) benzene **97**.

The sample was characterised by ^{1}H NMR spectroscopy and a low resolution (ESI) mass spectrum was obtained and was found to be a mixture of the product and a by-product. In the mass spectrum, a molecular ion $[M + H^{+}]$ with m/z 307.2 was found, comparing to 306.5 g mol^{-1} calculated for **97** confirming its presence. However the most abundant signal had an $[M^{+} + H^{+}]$ with m/z 250.2. This corresponds with compound **98** ($C_{15}H_{27}N_3$; F.W. 249.39 g mol^{-1}); a result of metallation of only one of the α-CH_2N linker groups and quenching with Eschenmoser's salt (figure 37). The proton NMR spectrum helps confirm the structure of the by-product although more data was needed.

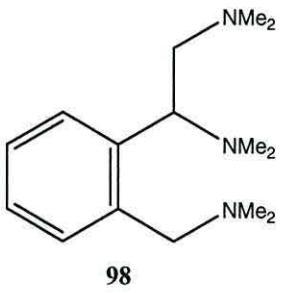

Figure 37: By product formed during reaction.

It would be interesting to convert these α-substituted benzyl amines (**97** and **98**) into phosphines as these structures posses the four carbon backbone which seems significant in their activity as catalyst in the methoxycarbonylation of ethene to produce methyl propanoate **4**, such as the existing example **7** mentioned in section **1.3.4**. Comparison of the activity of the phosphine analogues of **97** and **98** with the ligand **7** could be studied after their subsequent coordination to a Pd-complex.

Chapter 3

Catalytic Testing

Catalytic Testing

3.1 Chapter 3: Overview.

This chapter describes the catalytic testing of the metallocene based catalysts which were prepared using the synthetic methodology described in chapter 2. Reactions were carried out in conjunction with Lucite International UK Ltd and the results presented here are of those carried out during a placement at the industrial site at the Wilton Centre with Dr. Graham Eastham and Dr. Mark Waugh. All data was compared with those from the well known xylyl system, bis-1,2-di-*tert*-butylphosphinomethyl benzene **7** (as discussed in chapter 1) which was considered as the standard.

This chapter also introduces the new ferrocenyl phosphine ligands with adamantyl substituents **99** and **100** (figure 38). These ligands were prepared using the standard methodology from samples of the bis-amine **41** and amine-alcohol **46** precursors as described in chapter 2.

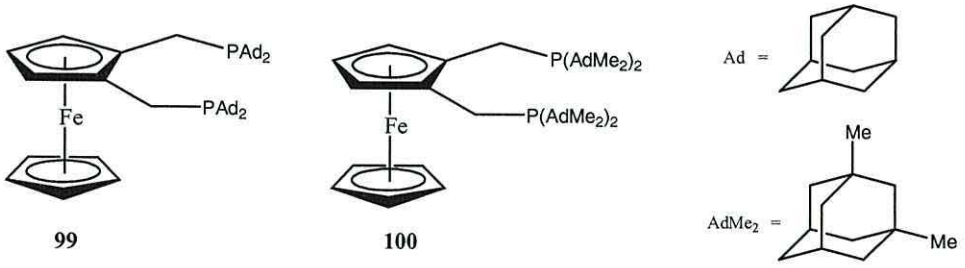

99 **100**

Figure 38: Bis-phosphine ferrocenyl ligands used in catalysis testing.

Several xylyl and metallocene phosphine ligands have been evaluated for their activity in the palladium catalysed methoxycarbonylation of ethene. In addition, ligand

recycling experiments in neat methanol and 70% weight methyl propanote (MeP) has been performed to test catalyst stability within the new process.

3.2 Introduction.

The alkoxycarbonylation of alkenes is of increasing scientific and technological importance. This reaction can give rise to a broad spectrum of products; for ethene, this can range from high melting thermoplastic polymers – the so called polyketones to low boiling liquids such as methyl propanoate **4**. The former materials have attracted more attention in the literature as they have been developed into commercial products.[15, 37] This work however focuses on methyl propanoate, a key intermediate in the manufacture of methyl methacrylate **2**, an important monomer produced annually on a multi-million tonne scale world wide.[107]

A new catalyst for the production of methyl propanoate *via* the palladium catalysed methoxycarbonylation of ethene has been reported.[26] The catalyst which is generated *in situ* by the reaction of [Pd(L-L)(dba)] [L-L = 1,2-$(CH_2P^tBu_2)_2C_6H_4$; dba = *trans,trans*-$(PhCH{=}CH)_2CO$] **7** with methanesulfonic acid, gives methyl propanoate with a selectivity of 99.98 % at a production rate of 50,000 mol product (mol Pd)$^{-1}$ h^{-1} under comparatively mild conditions (353 K and 10 atm pressure of CO-C_2H_4). This compound therefore was regarded as the standard that all subsequent testing using the new ferrocenyl and ruthenocenyl ligands were compared to. A mini-pilot plant has already been commissioned and is currently in operation by Lucite International at the industrial site at Wilton to produce bulk quantities of methyl propanoate; this system is shown in the block line diagram in figure 39.

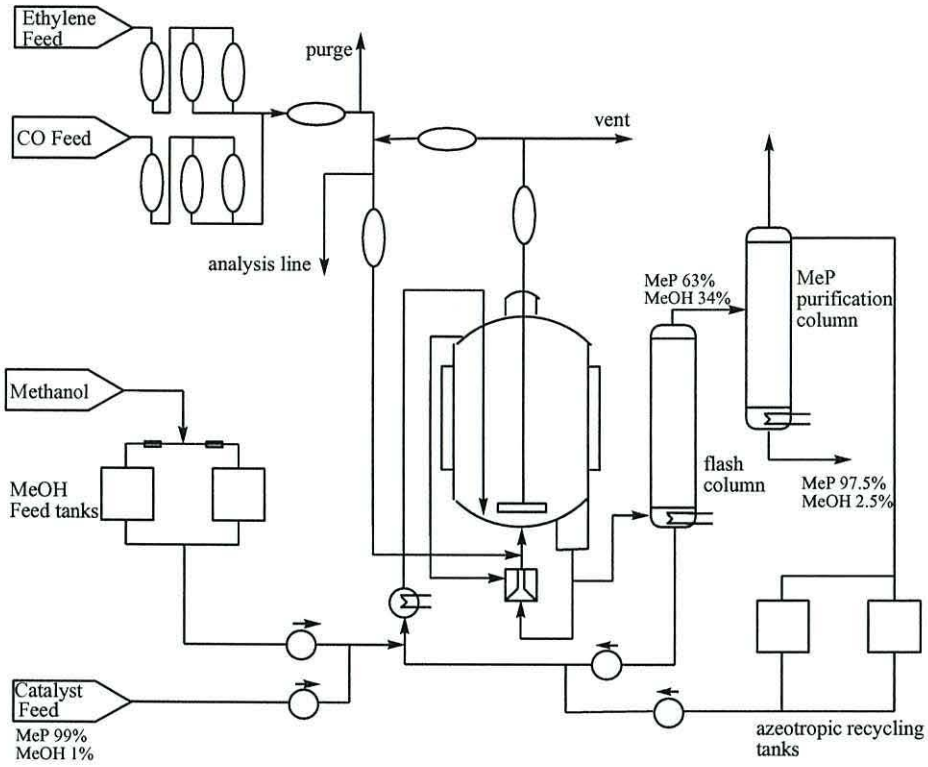

Figure 39: Mini-pilot block flow diagram used in the production of methyl propanoate **4** (MeP).

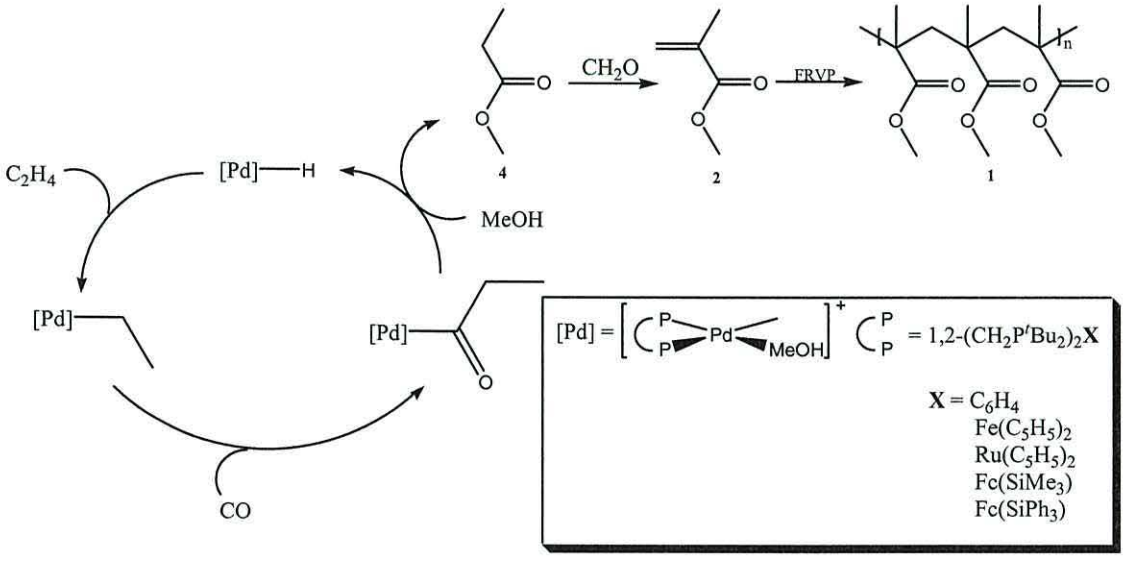

Figure 40: The overall production of polymethymethacrylate **1** from the methoxycarbonylation of ethene using the new ligands.

The methoxycarbonylation reaction has been shown to occur *via* a hydride rather than a methoxycarbonyl catalytic cycle in the presence of acid[36] and the proposed

reaction profile from starting material to the production of polymethylmethacrylate **1** is shown in figure 40. The process of producing polymethylmethacrylate **1** from methyl propanoate **4** has already been discussed in chapter 1. The important goal at the outset was to optimise the methoxycarbonylation cycle and methyl propanoate production on an industrial scale. This was implemented by producing stable substituted metallocene linkers bridging the two phosphorus atoms of a bidentate phosphine ligand. Ferrocene and ruthenocene based phosphine ligands were synthesised from the amine precursors (discussed in chapter 2) and their activity in the palladium phosphine catalysed methoxycarbonylation of ethene were studied. This chapter reports detail of their activity and the results of recycling experiments designed to determine if the new ligands are likely to result in a more stable catalyst system.

3.3 Preliminary catalyst testing data for ferrocenyl derived bis-phosphines.[108]

3.3.1 General Experimental.

The catalytic experiments were undertaken using a Batch Hastelloy autoclave system in the semi-technical building at the Wilton industrial site by Lucite International. The autoclave was pressure tested with nitrogen overnight. Standard reactions were carried out as follows:

The $Pd(OAc)_2$ (22mg, 0.1 mmol) and the respective phosphine ligand (0.5 mmol) were weighed out in an inert atmosphere glove box into a 500ml 3-neck round bottom flask. On removal, 300ml of degassed MeOH was added and the mixture stirred for 1 hour. To this solution methanesulphonic acid (140µl, 2 mmol) was added and the weight of the catalyst solution recorded. The autoclave was charged with the solution and heated

to 100°C with stirring (3.0 bar vapour pressure) at 1000 rpm. The reaction was started by the introduction of CO/ethylene (1:1) gaseous mixture to the autoclave to a total pressure of 13.0 bars. This resulted in a 1:1 ratio of ethylene to CO with a total pressure of gasses of 10 bars above solvent vapour pressure. The temperature and pressure were maintained for 3 hours during which period these values were recorded. At the end of 3 hours the gases were isolated and the unit cooled to room temperature. The depressurized unit was emptied and the final weight of the MeP solution produced was taken.

3.3.2 Results.

Results are presented in table form with the reaction weight gain being used to calculate catalyst turnover number (TON). This is done by calculating the number of moles of MeP produced in each reaction based on the weight gain and dividing this by the number of moles of palladium (0.0001 moles in all cases).

(1). 1,2-Bis-di-*tert*-butylphosphinomethyl benzene (7) (standard).

The table below details the individual and average weight gains obtained for the standard benzyl ligand **7** under these conditions (figure 41). There was no evidence of catalyst decomposition in any of these runs with all solutions coming out of the autoclave being pale green/yellow solutions.

Ligand	Run	Wt Gain (g)	Avg. Wt Gain (g)	TON	Avg. TON
7	1	268.65	257.304	47,973	45,932
7	2	244.47		43,655	
7	3	258.98		46,173	
7	4	252.13		45,023	
7	5	262.29		46,837	

Figure 41: Catalytic results of the standard.

(2). 1,2-Bis-di-*tert*-butylphosphinomethyl ferrocene (42).

The table below details the individual and average weight gains obtained for the ligand 1,2-di-*tert*-butylphosphinomethyl ferrocene **42** under the same conditions.

Ligand	Run	Wt Gain (g)	Avg. Wt Gain (g)	TON	Avg. TON
42	1	302.64	300.90	54,042	53,731
42	2	306.84		54,792	
42	3	293.40		52,392	
42	4	303.09		54,123	
42	5	298.54		53,310	

Figure 42: Catalytic results of the ferrocenyl analogue of the standard **42**.

The graph shown in figure 43 indicating these results show that the ferrocene analogue of the catalyst consistently outperforms the standard in each run.

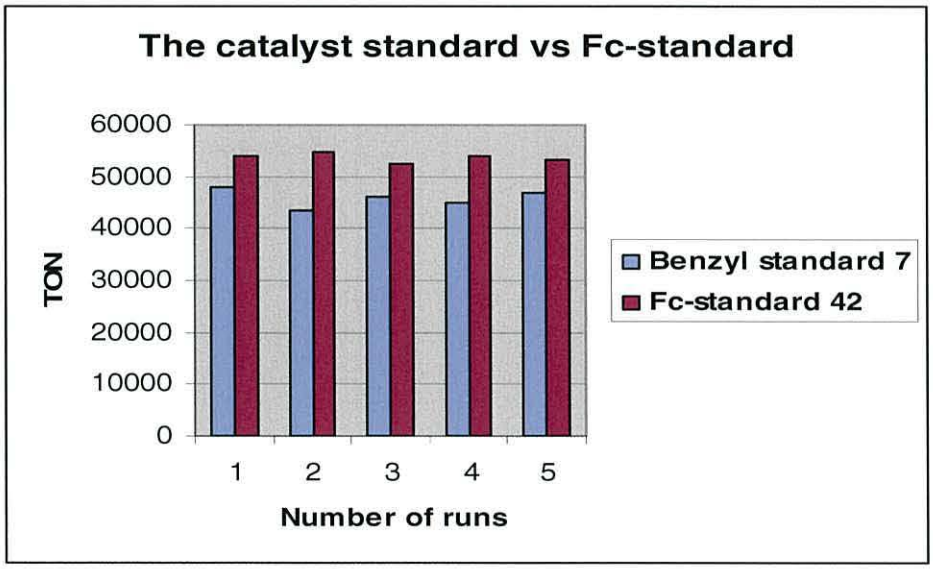

Figure 43: Catalytic activity of the standard and Fc-ligand.

3.3.3 Discussion of xylyl and ferrocenyl catalytic systems.

This set of experiments employed 0.1 mmol of palladium in neat methanol as the solvent. In addition the gas composition used was 50:50 CO/ethene in all experiments.

These conditions are the basis for exemplifying catalytic activity. The use of neat methanol and relatively high palladium concentrations are generally good for high initial rates but under these conditions accelerated catalyst decay ac occur.

The standard benzyl backbone substituent based catalyst (1,2-di-*tert*-butylphosphinomethyl benzene **7**) run under the conditions outlined gives rise to an average productivity after 3 hours of approximately 257.3g or an average TON of 45,932. It is known from research by Lucite International that average productivity can be enhanced when bulky groups such as *tert*-butyl are attached to the 4-position and also by increasing steric bulk of xylyl systems.[108] Current research also shows a possible design disadvantage in xylyl backbone systems as from X-ray analysis it can be seen that the Pd, P and methylene atoms of the ligands lie approximately in the same plane of a square planar palladium (II) complex.[108] The benzene ring then points at a 60-80 degree angle to this plane. This suggests that the benzene ring can flip between three different positions i.e. up, down or one up one down and this ring flipping can in some cases lead to ligand dissociation and hence catalyst decay (figure 44).

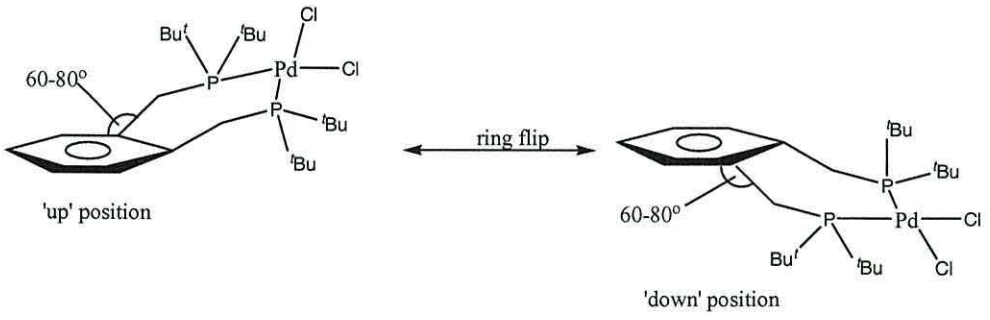

Figure 44: The interchangeable ring flip positions for the xylyl system.

Supporting evidence for this has been shown by studying complexes such as [(P-P)$PdCl_2$] where a fluxional process involving exchange of the CH_2 protons has been observed.[108] It is postulated that CH_2 proton exchange would be required for ring flipping

to occur. Thus by adding bulk to the benzene ring it is suggested that it is possible to influence the rate of this ring flipping process and consequently retard the rate of catalyst decay.

On moving to the ferrocenyl template with *tert*-butyl substituents on phosphorus the average productivity after 3 hours outperforms the xylyl standard to 300.9g or an average TON of 53,731. It has also been noted that from variable temperture NMR anlysis of 1,2-di-*tert*-butylphosphinomethyl ferrocene palladium complexes shows that the CH_2 protons are static at room temperature.[108] This indicates that in these complexes the ferrocenyl ring is not flipping at room temperature. This may be one reason for the ferrocenyl system's improved catalytic activity over the xylyl system and brings in the idea obtaining better control of the catalyst system.

3.4 Preliminary catalyst testing data for ruthenocenyl derived bis-phosphines.

3.4.1 General experimental.

Reaction solutions were prepared using standard Schlenk line techniques. In a nitrogen purge glove box, 9.9mg of [Pd_2dba_3] (1.45×10^{-5} moles) and 6 equivalents of phosphine ligand (8.7×10^{-5} moles), were weighed into a 500 ml round bottom flask. The flask was then transferred to a Schlenk line. The ligand and palladium was then dissolved in 125 ml of degassed methyl propanoate. In order to aid complexation, the palladium and ligand were dissolved initially in methyl propanoate and stirred for a period of 45 minutes, before addition of further solvents to the solution. This allows for the in situ formation of a neutral, trigonal planar Pd (0) complex [Pd(ligand)(dba)].

After complexation, 175 ml of methyl propanoate/methanol mixture (50% by weight methanol, 50% by weight methyl propanoate) was degassed and added to the flask. Addition of methanesulfonic acid (420µl) completes the preparation of the catalyst solution.

The catalytic solution was added to the pre evacuated 1 litre Hastelloy autoclave and heated to 100°C. The autoclave was then pressured with 8 bars of ethene above vapour pressure giving a total pressure of 10.2 bars at 100°C. The autoclave was then pressured to 12.2 bars with addition of CO:ethene (1:1 gas) charged from a 10 litre reservoir. A regulatory valve ensures that the pressure of the autoclave is maintained throughout the reaction at 12.2 bars through constant injection of gas from the reservoir. The number of moles of product produced at any point in the reaction can be calculated from the drop in reservoir pressure by assuming ideal gas behaviour and 100% selectivity for methyl propanoate. The depressurized unit was emptied and the final weight of the MeP solution produced was taken.

3.4.2 Results.

(1). 1,2-Bis-di-*tert*-butylphosphinomethyl benzene (7) (standard).

Figure 45 details the individual and average weight gains obtained for the standard benzyl ligand under these conditions. Again there was no evidence of catalyst decomposition in any of these runs with all solutions coming out of the autoclave being pale green/yellow solutions. Under these conditions the TON was increased in comparison with the previously reported conditions; section 3.3.2.

Ligand	Run	Wt Gain (g)	Avg. Wt Gain (g)	TON	Avg. TON
7	1	48.33	47.06	59,933	58,360
7	2	48.72		60,416	
7	3	43.15		53,509	
7	4	45.47		56,386	
7	5	48.95		60,701	
7	6	46.21		57,304	
7	7	50.19		62,239	
7	8	43.53		53,980	
7	9	49.01		60,776	

Figure 45: Catalytic results of the standard.

(2). 1,2-Bis-di-*tert*-butylphosphinomethyl ruthenocene (58).

Figure 46 details the individual and average weight gains obtained for the ligand 1,2-di-*tert*-butylphosphinomethyl ruthenocene **58** under the same conditions.

Ligand	Run	Wt Gain (g)	Avg. Wt Gain (g)	TON	Avg. TON
58	1	54.44	52.41	67,509	64,992
58	2	50.38		62,475	

Figure 46: Catalytic results of the ruthenocenyl analogue of the standard **58**.

The graph shown in figure 47 indicating these results show that the average catalyst activity of the ruthenocene analogue of the catalyst again outperforms the xylyl standard.

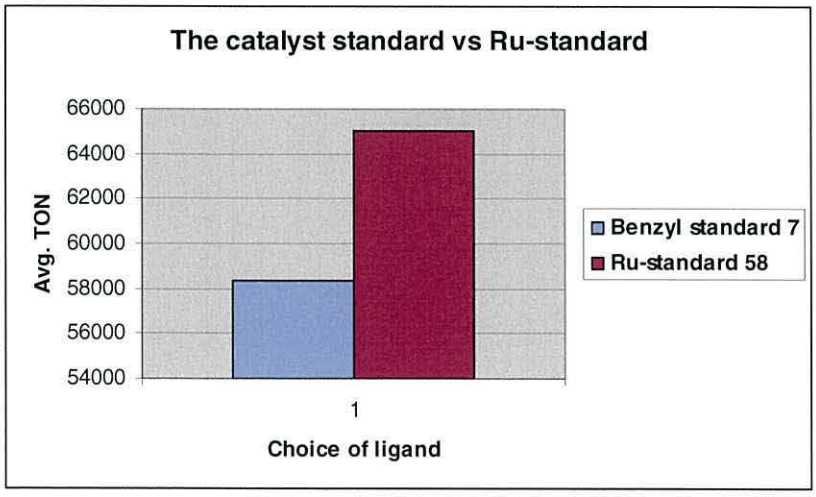

Figure 47: Catalytic activity of the standard ligands **7** and **58**.

Only two runs were made for the ruthenocene sample as a consequence of the small scale preparation of the sample due to the expense of the starting materials as explained in section 2.3.1 of chapter 2. It is noted that the xylyl standard is vastly improved in this experiment in comparison with the experiment described in section 3.3.2. This is due to the use of different Pd compounds: $Pd(OAc)_2$ was used in first experiment while Pd_2dba_3 was used for these reactions. This indicates that activity is not only dependent on the phosphine ligand (in which the ruthenocene system outperforms the xylyl) but also the performance is affected by the choice of Pd species. The overall conclusion though is that metallocene backbones show greater activity in the palladium catalysed methoxycarbonylation of ethene than the currently used xylyl systems.

3.5 Preliminary catalyst testing data for the functionalised bis phosphines.

3.5.1 General experimental.

These experiments were carried out as explained in section 3.4.1. In order to increase steric bulk within the catalyst system a novel phosphine ligand was prepared from the bis-amine precursors **64** and **67** (as discussed in chapter 2). These novel phosphine complexes **68** and **69** (figure 48) were prepared on site in the general methodology described in section 2.2.5 in chapter 2 but using an alternative phosphine quench.

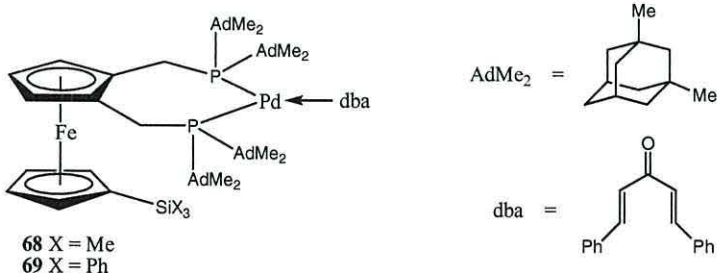

Figure 48: Two phosphine ligand complexes **68** and **69** used in catalysis.

3.5.2 Results.

(1) 1,2-Bis-di-*tert*-butylphosphinomethyl benezene (7) (standard).

Figure 49 details the individual and average weight gains obtained for the standard benzyl ligand under these conditions. There was no evidence of catalyst decomposition in any of these runs with all solutions coming out of the autoclave being pale green/yellow solutions.

Ligand	Run	Wt Gain (g)	Avg. Wt Gain (g)	TON	Avg. TON
7	1	64.0	60.25	79,365	74,714
7	2	56.5		70,064	

Figure 49: Catalytic results of the standard 7.

These were exceptional results for the standard system but the reason is unclear.

(2)1,2-Bis-di-(3,5-dimethyl)-1-adamantylphosphinomethyl-1'-trimethylsilylferrocene complex (68).

Figure 50 details the individual and average weight gains obtained for the 1,2-bis-di-(3,5-dimethyl)-1-adamantylphosphinomethyl-1'-trimethylsilyl ferrocene complex **68** under the same conditions.

Ligand	Run	Wt Gain (g)	Avg. Wt Gain (g)	TON	Avg. TON
68	1	59.6	59.6	73,908	73,908

Figure 50: Catalytic results of the trimethylsilyl functionalised analogue of the standard **68**.

The results disappointingly do not show any significant improvement from the standard however only one run was undertaken for this sample.

(3)1,2-Bis-di-(3,5-dimethyl)-1-adamantylphosphinomethyl-1'-triphenylsilylferrocene complex (69).

Figure 51 details the individual and average weight gains obtained for the 1,2-bis-di-(3,5-dimethyl)-1-adamantylphosphinomethyl-1'-triphenylsilyl ferrocene complex **69** under the same conditions.

Ligand	Run	Wt Gain (g)	Avg. Wt Gain (g)	TON	Avg. TON
69	1	74.28	74.28	93,192	93,192

Figure 51: Catalytic results of the triphenylsilyl functionalised analogue of the standard **69**.

The graph shown in figure 52 indicating these results shows the superior performance of the triphenylsilyl functionalised ferrocene **69** analogue of the catalyst. It is currently the most active catalyst to be tested in the methoxycarbonylation of ethene.

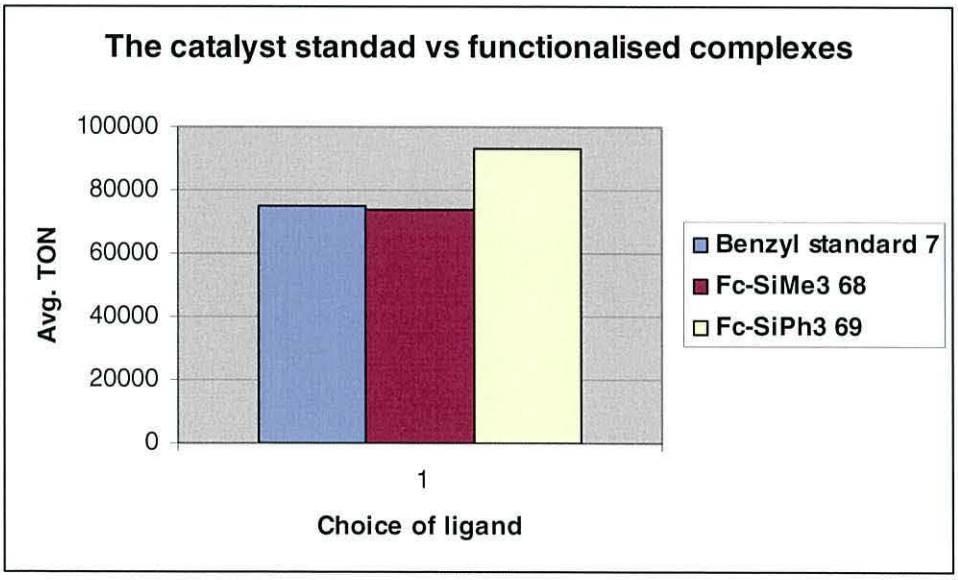

Figure 52: Catalytic activity of the functionalised complexes **68** and **69**.

Functionalising the ligands with bulky substituents therefore increases catalytic activity. The reason may be that the extra bulk present on the ferrocene forces the active site of the catalyst further away from the main body which possibly makes it less

hindering for free flowing substrates such as CO or ethylene to react (figure 53). It is already present that such systems also do not flip as in xylyl systems and so the combination of these effects is thought to optimise the catalytic activity.

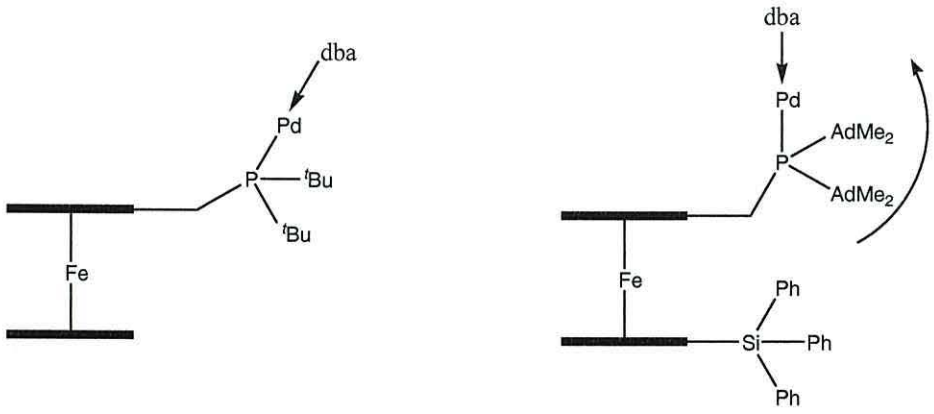

Figure 53: The addition of the bulky functionality forcing the placement of the active site.

It is clear that from each experiment that the metallocene backbone has a positive influence on catalytic activity in this process. This is mainly thought to be due to the steric bulk on these complexes restricting possible polymerization by selectively reacting with alternating CO and ethylene molecules. It also thought that the static characteristics of such complexes help control the system so that reaction conditions obtain maximum effect. It was therefore important to study the stability of such complexes through ligand recycling experiments.

3.6 The relative stability of metallocene catalysts.[109]

3.6.1 Introduction.

The synthesis of more stable catalysts for the methoxycarbonylation of ethene to produce methyl propanoate has been a target of recent research. Candidate ligands identified are those based on metallocene linkers bridging two phosphorus atoms of a

bidentate phosphine ligand. New ferrocene and ruthenocene based phosphine ligands have been synthesised and their successful activity in palladium phosphine catalysis has been studied. This section reports details on the results of recycling experiments designed to determine if the new ligands are likely to result in more stable catalyst systems. The ligands chosen were the adamantyl substituted ferrocene phosphines and compared against the xylyl standard **7** as they are thought to be the most active ferrocenyl based catalysts.

3.6.2 General experimental.

Using standard Schlenk line techniques, reaction solutions were prepared by dissolving $Pd(OAc)_2$ (22 mg, 0.1 mmol) and 0.5 mmoles of ligand in 300 ml of MeOH. The palladium and ligand were allowed to complex for 1 hour. Addition of 140 μl of methanesulfonic acid (150 eq) completed the preparation of the catalyst solution.

The autoclave was charged with the solution under vacuum and heated to 100°C with stirring (3.0 bar vapour pressure) at 1000 rpm. The reaction was induced by the introduction of CO/ethene (1:1) gaseous mixture to the autoclave to a total pressure of 13.0 bar. This resulted in a 1:1 ratio of ethene to CO with a total pressure of gasses of 10 bar above solvent vapour pressure and the temperature was maintained for 3 hours.

After the reaction period, the autoclave was cooled and vented. The reaction solution was collected from the base of the vessel and hastily placed in an inert atmosphere. The solution was then concentrated down to 50 ml which removed methanol (the most volatile component) and any traces of CO, both of which can reduce Pd (II) to Pd (0) causing the palladium to precipitate out of solution in metallic form.

This concentrated solution was left to stand overnight in an inert atmosphere and was then used to form the basis of the next reaction solution with addition of 300 ml of methanol and 140 µl of methansulfonic acid (150 eq). Excess acid was added to offset a possible loss in acid upon concentrating the solution. This recycled material was then added to the autoclave and reacted under the same set of conditions. The catalyst was recycled in this way until a significant drop in reaction TON was observed.

3.6.3 Results and discussion.[109]

Results are presented in table form with the reaction weight gain being used to calculate catalyst TON. This done by calculating the number of moles of MeP produced in each reaction based on the weight gain and dividing this by the number of moles of palladium (0.0001 moles in all cases).

(1) 1,2-Bis-di-*tert*-butylphosphinomethyl benzene (7) (standard).

Figure 54 details the individual and average weight gains obtained for the standard benzyl ligand under these conditions. There was no evidence of catalyst decomposition in any of these runs with all solutions coming out of the autoclave being pale green/yellow solutions.

Ligand	Recycle run	Wt Gain (g)	TON	Cumulative TON
7	1	246.13	43,952	
7	2	219.35	39,170	83,122
7	3	11.86	2,118	85,240

Table 54: Catalytic results of the standard.

(2) 1,2-Bis-di-adamantylphosphinomethyl ferrocene (99).

Figure 56 details the individual and average weight gains obtained for the ligand 1,2-bis-di-1-adamantylphosphinomethyl ferrocene **99** (figure 55) under the same conditions. The ligand is a direct result from the bis-amine precursor which was prepared as discussed in chapter 2.

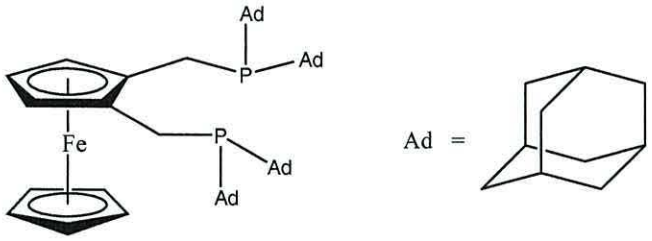

99

Figure 55: 1,2-bis-di-adamantylphosphinomethyl ferrocene **99** prepared on site as choice of ligand.

Ligand	Recycle run	Wt Gain (g)	TON	Cumulative TON
99	1	347.69	62,088	
99	2	282.00	50,357	112,445
99	3	179.80	32,107	144,552

Figure 56: Catalytic results of the ferrocenyl analogue of the standard **99**.

No further work was carried out on the sample as it was determined that leaving the sample over a weekend would lead to decay.

(3) 1,2-Bis-di-3,5-dimethyl-1-adamantylphosphinomethyl ferrocene (100).

Figure 58 details the individual and average weight gains obtained for the ligand 1,2-bis-di-3,5-dimethyl-1-adamantylphosphinomethyl ferrocene **100** (figure 57) under the same conditions. The ligand is a direct result from the bis-amine precursor which was prepared as discussed in chapter 2.

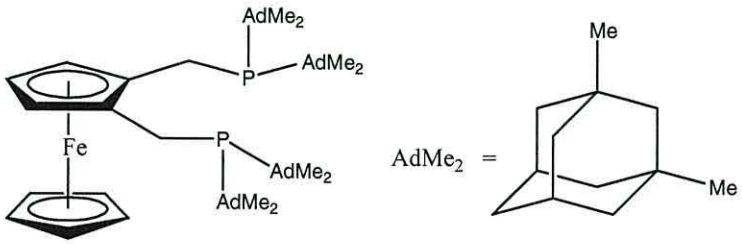

100

Figure 57: 1,2-bis-di-3,5-dimethyl-1-adamantylphosphinomethyl ferrocene **100** prepared on site as choice of ligand.

Ligand	Recycle run	Wt Gain (g)	TON	Cumulative TON
100	1	325.73	58,166	
100	2	295.12	52,700	110,866
100	3	271.50	48,482	159,348
100	4	264.01	47,145	206,493
100	5	191.10	34,125	240,618

Figure 58: Catalytic results of the ferrocenyl analogue of the standard **100**.

The data for all three phosphine evaluated in this series of experiments is illustrated in the two charts shown below. The first shows the activity for each ligand after their respective recycle runs (figure 59) and the second shows their cumulative amount i.e. the total activity for the same amount of sample for each ligand using the same experimental conditions (figure 60).

It is clear from these charts that the ligand 1,2-bis-di-3,5-dimethyl-1-adamantylphosphinomethyl ferrocene **100** gives rise to the most stable catalyst system. This catalyst system still retains approximately 58% of its original activity after five consecutive recycle runs. The equivalent standard xylyl system has lost approximately 95% of its activity after two recycles. The ligand 1,2-bis-di-adamantylphosphinomethyl ferrocene **99** still retains approximately 50% of its activity after two recycles however it needs further study. It was deemed non comparative to leave the sample to stand over a weekend period as this will lead to increased decay.

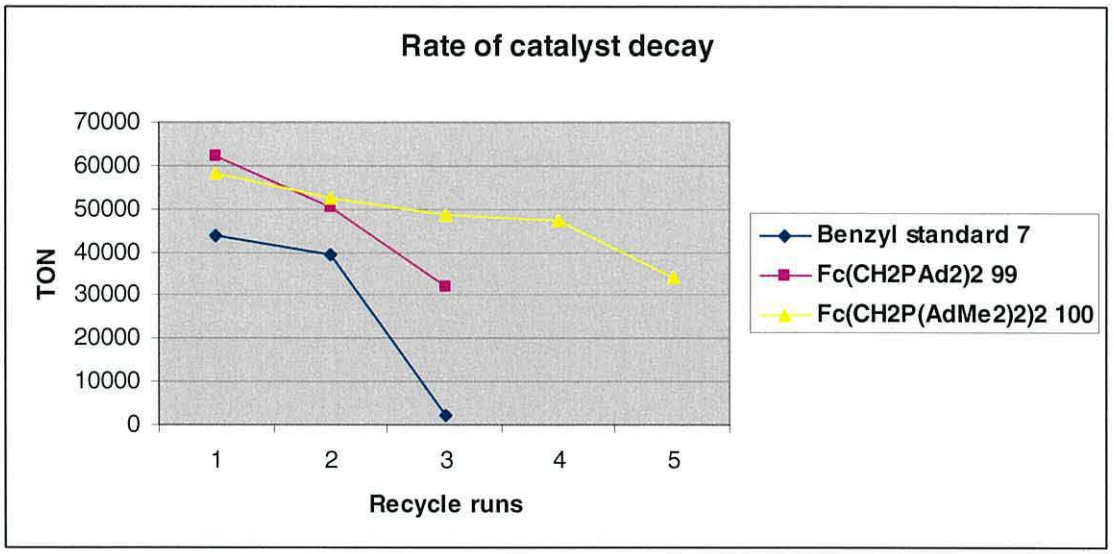

Figure 59: Rate of catalyst decay.

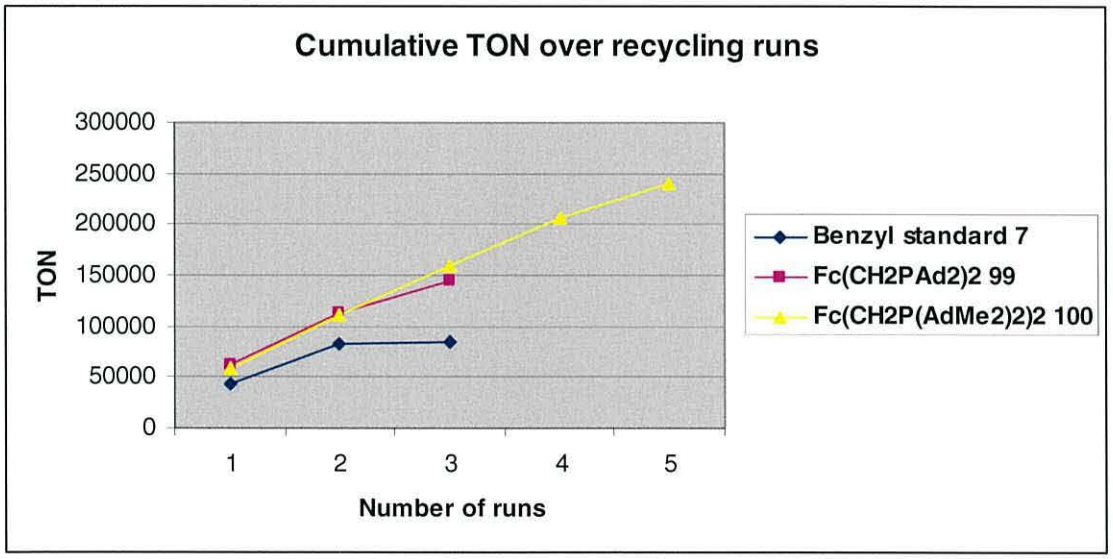

Figure 60: Cumulative activity produced over the recycling runs.

The productivity of adamantyl ferrocene systems had a higher TON value by 20,000 when compared to xylyl standards.

3.7 Summary of Chapter 3

Introducing a metallocene backbone into the catalytic system involved in the methoxycarbonylation of ethene has had a positive effect in both activity and sustainability of the process. It was shown that the ferrocene and ruthenocenyl analogues of the xylyl systems show improved activity under given experimental conditions. The most active catalyst was the substituted ligand 1,2-bis-di-(3,5-dimethyl)-1-adamantylphosphinomethyl-1'-triphenylsilyl ferrocene **69** complexed using Pd_2dba_3 however only a single run was attempted. The most stable i.e. the most active catalyst given a number of recycle runs, was 1,2-bis-di-3,5-dimethyl-1-adamantylphosphinomethyl ferrocene **100** complexed using $Pd(OAc)_2$. Though its initial rate was not as good as that for 1,2-bis-di-1-adamantylphosphinomethyl ferrocene **99**, it did show more uniform activity through its lifetime. Both catalysts greatly improved on the standard catalysts and are therefore regarded as viable alternatives. These encouraging initial catalytic tests in the carbonylation of ethene need further investigation due to the possibility of catalyst poisoning.

It is thought that the metallocene backbone gives improved activity and stability through its rigid system which adds control with further enhances in activity with the addition of a functionalised bulky group on both the ligand's phosphines and the un-substituted cyclopentadienyl ring. In short, a new and improved catalyst system in the methoxycarbonylation of ethene to selectively produce methyl propanoate from cheap materials has been tested and from initial experimentation seems to outperform the currently used xylyl system. This gives a rise to the potential of using these catalyst designs in the new industrial process for the manufacture of polymethylmethacrylate.

Chapter 4

Conclusions & Further Work

Conclusions

4.1 Chapter 4: Overview.

This research project was directed at the synthesis, characterisation and testing of a series of compounds containing phosphine-based ligands which as their palladium complexes may be used in an industrial catalytic process for the carbonylation of ethene to give a monomer unit as a precursor to methyl methacrylate **2**.

This methoxycarbonylation reaction has been shown to occur *via* a hydride rather than a methoxycarbonyl catalytic cycle in the presence of acid.[36] The process of producing polymethylmethacrylate **1** from methyl propanoate **4** has already been discussed in chapter 1. The important goal at the outset was to optimise the methoxycarbonylation cycle and methyl propanoate production on an industrial scale. This was implemented by producing stable substituted metallocene linkers bridging the two phosphorus atoms of a bidentate phosphine ligand. Ferrocene and ruthenocene based phosphine ligands were synthesised from the amine precursors (discussed in chapter 2) and their activity in the palladium phosphine catalysed methoxycarbonylation of ethene were studied (chapter 3).

A method of routinely preparing pure samples of bis-1,2-dimethylaminomethyl-ferrocene **41** has been developed by *ortho*-lithiation of dimethylaminomethyl ferrocene **32**, and quench with Eschenmoser'salt. The amine substituents can be cleanly substituted by phosphines following Togni's methodology of reflux in acetic acid containing together with at least two molar equivalents of the required phosphine.[71,39] This route gives the

precursor 1,2-di-*tert*-butylphosphino ferrocene **42** used (when coordinated as a Pd complex) as a catalyst in the carbonylation of ethene to prepare methyl propanoate **4**.

However due to the high cost of Eschenmoser's salt, an alternative, cost effective route towards 1,2-di-*tert*-butylphosphino ferrocene **42** was optimised. This was done by increasing the yield in the preparation of 1-(hydroxyl-methyl)-2-(dimethylaminomethyl) ferrocene **46,** a precursor of **42** by substantially increasing the quantity of calcined *p*-formaldehyde used.

The investigation to optimise the synthesis of the bidentate phosphine ligand **42** from 1-(hydroxyl-methyl)-2-(dimethylaminomethyl) ferrocene **46** was then carried out by NMR investigation to find the optimum reaction conditions. Two factors were considered to find the optimum conditions: the temperature needed for optimum conversion and the time taken for reaction completion. Both needed to be limited to acceptable industrial conditions for any viable potential for use in catalyst development. It was discovered that from initial results it seems that the optimum conditions for the reaction is a temperature around 80-100 °C and a reaction time of 30 min was enough for completion which were considered to be within acceptable limits.

The section ended with the development of two unreported palladium complexes of C_4 bridged diphosphine ligands [$PdCl_2$(P-P)] **52** and [Pd(dba)(P-P)] **53**: where (P-P) = bis-1,2-di-*tert*-butylphosphinomethyl ferrocene and (dba) = *trans,trans*-bis(dibenzylideneacetone). These complexes are examples of alternative and more efficient active catalyst tested in the methoxycarbonylation of ethene used in comparison with the current xylyl standard **7**.

The possibility of using ruthenocene analogues was examined and it is concluded that it may be problematic due to the cost of materials and poor yields despite outperforming the current standard.

The functionalisation of ferrocene-based ligands with bulky groups was carried out in an effort to increase the steric bulk resulted in improved catalytic activity in the carbonylation of ethene. This was done by increasing the bite angle of the ligands on the upper ring and stabilising the active conformation. These compounds were intended to be tested in comparison with the earlier ligands and therefore were sent to Lucite International for amine conversion into their corresponding tertiary phosphines and subsequent reaction with $Pd(dba)_2$ to form the active catalyst and tested in the carbonylation of ethene. It was important therefore to work on a large scale so that there was sufficient quantities of ligand can be isolated and tested for their catalytic activity.

Functionalising the ligands with bulky substituents increased catalytic activity. The reason may be that the extra bulk present on the ferrocene forces the active site of the catalyst further away from the main body which possibly makes it less hindering for free flowing substrates such as CO or ethylene to react. It is already present that such systems also do not flip as in xylyl systems and so the combination of these effects is thought to optimise the catalytic activity.

The most active catalyst was the substituted ligand 1,2-bis-di-(3,5-dimethyl)-1-adamantylphosphinomethyl-1'-triphenylsilyl ferrocene **96** complexed using Pd_2dba_3 however only a single run was attempted. The most stable i.e. the most active catalyst given a number of recycle runs was 1,2-bis-di-3,5-dimethyl-1-adamantylphosphinomethyl ferrocene **100** complexed using $Pd(OAc)_2$. Though its initial

rate was not as good as that for 1,2-bis-di-1-adamantylphosphinomethyl ferrocene **99**, it did show more uniform activity through its lifetime. Both greatly improved on the standard and are therefore regarded as viable alternatives. These encouraging initial catalytic tests in the carbonylation of ethene need further investigation due to the possibility of catalyst poisoning.

Additionally a novel route of preparing octamethylferrocenyl phosphine derivatives has been developed in a four step process starting from cheap and commercially available starting materials. Two examples were prepared, 1,1'-bis(diphenylphosphino)octamethyl ferrocene (dppomf) **86**, an existing example that generates a selective catalyst for methyl propanoate and an unpublished compound; 1,1'-bis(diisopropylphosphino)octamethyl ferrocene **88** in satisfactory yields. The attempt to synthesise another example however; namely 1,1'-bis(di-*tert*-butylphosphino)octamethylferrocene **90** only resulted in the formation of octamethylferrocene **91**. It would be interesting to see how the coordinated Pd-complexes of **86** and **88** would have compared to the existing ligands in catalytic reactions of ethene methoxycarbonylation and this is considered to be further work.

A series of investigations into the α-metallation of four carbon backbone benzyl derivatives with BuLi.*t*-BuOK was also carried out in order to produce different analogues of precursors to the known pre-catalyst 1,2-bis(di-*tert*-butylphosphinomethyl) benzene. This resulted in the preparation of (α-dimethylaminomethyl-dimethylaminomethyl) benzene **95** and a mixture of the 1,2-bis derivative **97** and derivative **98** formed by mono α-metallation. Further work would be to continue in converting these compounds to the corresponding phosphines, and after complexation

with Pd, to test their catalytic activity in the methoxycarbonylation of ethene in comparison with the existing ligand **7**.

Chapter 5

Experimental

5.1 General Experimental Details

5.1.1 Techniques

All reactions were carried out at ambient temperatures, under an atmosphere of nitrogen or argon using standard Schlenk techniques, unless otherwise indicated. Solvents were dried using standard procedures. Multi-element NMR spectra were recorded on a Bruker AC 250 spectrometer operating at 250 MHz for ^{1}H and 62.5 MHz for ^{13}C nuclei, and on a Bruker Avance 500 spectrometer operating at 500 MHz for ^{1}H, 125 MHz for ^{13}C and 202 MHz for ^{31}P nuclei. Chemical shifts (δ) are given in ppm and are relative to tetramethylsilane (for ^{1}H and ^{13}C) and phosphoric acid (for ^{31}P). Spin coupling values are given in Hz as J values, and refer to J_{HH} unless otherwise indicated. The solvent used for NMR analysis was $CDCl_3$ unless stated otherwise.

Mass spectra were recorded on a Waters (micromass) GCT time of flight mass spectrometer by direct insertion and samples were also sent to the EPSRC National Mass Spectrometry Service at the University of Wales, Swansea. Infrared spectra were recorded on a Perkin Elmer 197 infrared spectrophotometer as a thin film between NaCl plates and absorption bands are given in wavenumbers (cm^{-1}). Elemental analysis for carbon, hydrogen and nitrogen were conducted on a Carlo Erba elemental analyzer MOD (1106) using helium as a carrier gas. Melting points are uncorrected and were measured on a Gallerkamp melting point apparatus.

Crystal structures were determined by the EPSRC National Crystallography Service, University of Southampton.

5.1.2 Materials

Column chromatography was performed using a neutral or basic alumina (150 mesh, Brockmann Grade 1) or silica gel (Kieselgel 230-400 mesh) support, as specified. Thin-layer chromatography was conducted on precoated Kieselgel 60 F254 (Art. 5554; Merck) plates. Tetrahydrofuran (THF) and diethyl ether (or referred to as 'ether') were distilled from sodium benzophenone ketyl and dichloromethane was distilled from calcium carbonate prior to use. 'Petrol' refers to the fraction of light petroleum boiling between 40 and 60°C and was used without purification.

5.1.3 Chemicals

All commercial reagents were purchased and/or supplied from Lucite International UK Ltd, Aldrich Chemical Co. Ltd, Alfa Aesar Research Chemicals, Fluorochem Ltd. and Fisher Scientific UK and used as received or purified by standard methods.[110] *n*-Butyllithium was titrated with diphenylacetic acid solutions.

5.2 Experimental procedures

5.2.1 Preparation of N,N,N',N'-tetramethylmethylenediamine (51).

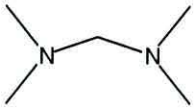

A solution of 37% aqueous formaldehyde solution (60.7g, 0.75mol) was placed in a round bottomed flask equipped with a stirrer and thermometer and cooled in an ice bath. A 40% aqueous solution of dimethylamine (190ml, 1.50mol) was added at such rate that the reaction temperature was maintained below 15°C. The solution was stirred for 30 minutes after the addition was complete, and potassium hydroxide flakes (≈150g) were added in portions until the reaction mixture became separated into two layers. The upper layer was separated, dried over potassium hydroxide overnight, and distilled to give the desired product as a clear colourless liquid: (58.81g, 77 % yield).

Formula: $C_5H_{14}N_2$

F.W. 102.18 g mol^{-1}

b.p. 84-86°C (lit. 83-84°C)[77]

^{1}H NMR (500 MHz, $CDCl_3$) δ = 2.16 (s, 6H, 4 x CH_3), 2.64 (s, 2H, NCH_2N).

^{13}C NMR (125 MHz, $CDCl_3$) δ = 43.12 (s, NCH_3) 80.16 (s, NCH_2N).

5.2.2 Preparation of dimethylaminomethyl ferrocene (32).

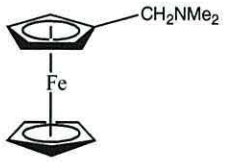

Ferrocene (46.4g, 0.25mol) was added to a well stirred solution of N,N,N',N'-tetramethyl-methylenediamine (43.2g, 57.7ml, 0.42mol) and phosphoric acid (43.2g) in acetic acid (400ml) in a three necked round bottomed flask equipped with a condenser, an N_2 inlet and an overhead mechanical stirrer. (N.B. As the mixing of the amine and acids was exothermic. It was necessary to add the amine dropwise to the solution of the acids with stirring and cooling in an ice bath).

The resulting suspension was heated on a steam bath under a slow stream of N_2 for 5 hours. The reaction mixture, a dark amber solution, was allowed to cool to room temperature and was diluted with water (550ml). The unreacted ferrocene was removed by extracting the solution with three 325ml portions of ether. The aqueous solution was then cooled in ice water and made alkaline by the addition of sodium hydroxide pellets (245g). The tertiary amine separated from the alkaline solution as an oil in the presence of some black tar. The mixture was extracted with ether (3 x 500ml). The organic solution was washed with water and dried over magnesium sulphate. Dimethylaminomethyl ferrocene was obtained as a dark red mobile liquid when the solvent is removed on a rotary evaporator: (30.77g, 51 % yield).

Formula: $C_{13}H_{17}NFe$

F.W. 243.13 g mol^{-1}

^{1}H NMR (250 MHz, $CDCl_3$) δ = 2.15 (s, 6H, 2 x CH_3), 3.26 (s, 2H, $CpCH_2N$), 4.09 (s, 5H, Cp), 4.12 (2H, Cp), 4.18 (2H, Cp).

^{13}C NMR (62.5 MHz, $CDCl_3$) δ = 44.76 (s; NCH_3), 59.15 ($CpCH_2N$), 67.97 (Cpα-C), 68.45 (Cp5), 70.05 (Cpβ-C), 83.32 (Cp *ipso*-C).

5.2.3 Preparation of bis-1,2-dimethylaminomethyl ferrocene (41).

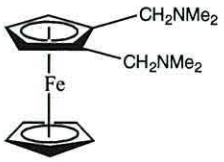

To dimethylaminomethyl ferrocene (10.82g, 44.50mmol) in dry diethyl ether (80ml) was added n-butyllithium (21.36ml, 53.40mol, 1.2eq) and the reaction was stirred under N_2 for four hours. The red reaction solution was cooled to -78°C (dry ice/acetone bath) and Eschenmoser's salt (9.06g, 48.97mmol) was added. The bright orange solution was then allowed to warm up to room temperature and further stirred for eighteen hours.

The reaction was then quenched with dilute sodium hydroxide, and stirred for a further fifteen minutes. The ethereal layer, containing product was separated and the aqueous layer was further extracted several times with diethyl ether. The combined ether fractions were dried over magnesium sulphate and filtered through celite. The ether solvent was removed by rotary evaporator (resulting in red/orange oil) and the crude product was placed in the freezer overnight. The product was recrystallised from petrol at -17°C, and the resulting orange crystals were washed with cold petrol and dried under vacuum: (4.85g, 36 % yield).

Formula: $C_{16}H_{24}N_2Fe$

F.W. 300.23 g mol^{-1}

m.p. 69-73°C (lit. 74°C)[13]

^{1}H NMR (250 MHz, $CDCl_3$) δ = 2.19 (s, 12H, 4 x CH_3), 3.19 (d, 2H, 13.12 Hz; NCH_2Cp), 3.31 (d, 2H, 12.82 Hz; NCH_2Cp), 4.11 (s, 5H, Cp5), 4.16 (t, 1H, Cpβ-H), 4.21 (d, 2H, 2.44 Hz; Cpα-H).

^{13}C NMR (62.5 MHz, $CDCl_3$) δ = 45.33 (s; NCH_3), 57.19 (s; NCH_2), 66.74 (Cpα-C), 69.04 (Cp5), 70.07 (Cpβ-C), 84.04 (Cp *ipso*-C).

Elemental analysis

Calculated: C %: 64.0, H %: 8.1, N %: 9.3.

Observed: C %: 63.3, H %: 7.9, N %: 9.4.

5.2.4 Preparation of 1-(hydroxyl-methyl)-2-(dimethylaminomethyl) ferrocene (46).

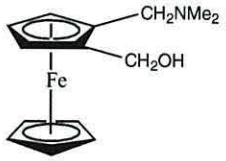

To dimethylaminomethyl ferrocene (30g, 24.42ml, 0.12mol) in dry diethyl ether (250ml) under nitrogen, was added n-butyllithium (98.71ml, 0.25mol) in 2:1 excess. The reaction was stirred for three hours, taking on a reddish colour. The solution was then cooled to -78°C (dry ice/acetone bath) and calcined *para*-formaldehyde (14.71 g, 0.49mol, 4 eq) was added in four times excess. Stirring was then continued overnight resulting in a bright yellow colouration and then the reaction was quenched with water, extracted with diethyl ether, dried over magnesium sulphate and filtered over celite. The solvent was removed *in vacuo* under rotary evaporator. The crude product was eluted through a neutral silica column. First dimethylaminomethyl ferrocene was brought off with petrol/diethyl ether (9:1), and the polarity was then increased substantially by using pure ethyl acetate to elute the hydroxyl product. Ethyl acetate was then removed *in vacuo*. The material was purged with vacuum for several hours to leave an analytically pure product as orange oil. The material partially crystallised on standing and was used in subsequent reaction as an oil and crystal mixture: (32.43g, 96 % yield).

Formula: $C_{14}H_{19}NOFe$

F.W. 273.16 g mol^{-1}

^{1}H NMR (250 MHz, $CDCl_3$) δ = 2.13 (s, 6H, 2 x CH_3), 2.78 (d, 1H, 12.36 Hz; NCH_2), 3.90 (d, 1H, 12.36 Hz; NCH_2), 4.00 (m, 1H, Cp-H), 4.05 (s, 5H, Cp5), 4.07 (d, 1H, CH_2O), 4.10 (m, 1H, Cp-H), 4.15 (m, 1H, Cp-H), 4.74 (d, 1H, 11.91 Hz; CH_2O).

^{13}C NMR (62.5 MHz, $CDCl_3$) δ = 44.56 (s; 2 x CH_3), 58.21 (s; CH_2N), 60.19 (s; CH_2O), 65.59 (s; Cp C_4), 68.65 (s; Cp5), 69.40 (s; Cp C_3), 70.53 (s; Cp C_5), 84.53 (s; Cp C_2), 87.68 (s; Cp C_1).

Infrared spectra ($CHCl_3$, thin film NaCl plates) 3350 cm^{-1} ν(OH), 3010 cm^{-1}, 2863 cm^{-1}, 2826 cm^{-1}, 2783 cm^{-1}, 1352 cm^{-1} ν(C-O), 1105 cm^{-1}, 1036 cm^{-1} (O-H bending).

Elemental analysis

Calculated: C %: 61.6, H %: 7.0, N %: 5.1.

Observed: C %: 61.5, H %: 7.4, N %: 4.6.

5.2.5 Preparation of 1,2-di-*tert*-butylphosphinomethyl ferrocene (42).

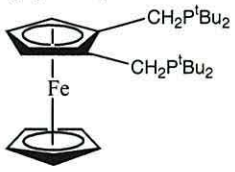

To 1-dimethylaminomethyl-2-hydroxymethyl ferrocene (0.68g, 2.5mmol) in acetic acid (51ml) stirred under argon, was added 4-equivalents of di-*tert*-butyl phosphine (1.46g, 1.85ml, 9.98mmol), followed by an excess of acetic anhydride (2ml).

The reaction solution turned from yellow to orange within 1 minute. The system was then heated to 80°C and stirred for 72 hours.

The solvent was removed *in vacuo* to leave orange oil. The crude product was recrystallised from refluxing ethanol (12ml) to yield the product as orange crystals: (0.67g, 53 % yield).

Formula: $C_{28}H_{48}P_2Fe$

F.W. 502.48 g mol^{-1}

m.p. 79-83°C

^{1}H NMR (500 MHz, $CDCl_3$) δ = 1.13 (d, 18H, $^3J_{HP}$ = 10.40 Hz), 1.16 (d, 18H, $^3J_{HP}$ = 10.72 Hz), 2.70 (d, 2H, $^2J_{HP}$ = 15.45 Hz), 2.87 (d, 2H, $^2J_{HP}$ = 14.50 Hz), 3.03 (d, 1H, Cpβ-H), 3.74 (t, 2H, Cpα-H), 4.04 (s, 5H, Cp).

^{13}C NMR (125 MHz, $CDCl_3$) δ = 21.08 (d, $^1J_{PC}$ = 24.47 Hz; CH_2P), 29.82 (d, $^2J_{PC}$ = 11.00 Hz; $CH_{3\ (inner)}$), 29.92 (d, $^2J_{PC}$ = 12.83 Hz; $CH_{3\ (outer)}$), 31.46 (d, $^1J_{PC}$ = 20.16 Hz; $PCMe_{3\ (inner)}$), 32.03 (d, $^1J_{PC}$ = 24.47 Hz; $PCMe_{3\ (outer)}$), 63.82 (s, Cpβ-C), 69.50 (s, Cp5), 70.08 (d, Cpα-C), 86.00 (d, Cp *ipso*-C).

^{31}P NMR (202 MHz, $CDCl_3$) δ = 22.97 (s).

MS (EI) m/z (rel. int): 502 M^+ (10%), 445 (20%), 389 (20%), 299 (30%), 242 (72%), 57 (100%).

Elemental analysis

Calculated: C %: 66.9, H %: 9.6, N %: 0.0.

Observed: C %: 66.4, H %: 11.9, N %: 0.0.

5.2.6 Preparation of the palladium complex $Fc(CH_2P^tBu_2)_2PdCl_2$ (52).

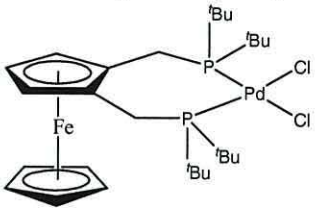

1,2-di-*tert*-butylphosphinomethyl ferrocene (0.17g, 0.34mmol) was placed in a dry Schlenk tube under N_2 with 1 equivalent of Pd[COD]Cl_2 (0.1g, 0.34mmol) and dissolved in dry dichloromethane (15ml). The orange solution was then left to stir at room temperature for 30 min. The solvent was evaporated until a red/orange residue was left. This residue was washed with petrol (3 x 10ml) and left to dry under vacuum overnight forming the red/orange crystalline complex: (0.19g, 83 % yield).

Formula: $C_{28}H_{48}P_2FePdCl_2$

F.W. 679.81 g mol^{-1}

m.p. 138-142°C decomposes.

^{1}H NMR (500 MHz, $CDCl_3$) δ = 1.45 (d, 18H, $^3J_{HP}$ = 7.57 Hz), 1.58 (d, 18H, $^3J_{HP}$ = 7.57 Hz), 3.09 (d, 2H), 3.37 (d, 2H), 3.68 (d, 1H, Cpβ-H), 4.03 (s, 5H, Cp), 4.41 (t, 2H, Cpα-H).

^{13}C NMR (125 MHz, $CDCl_3$) δ = 22.65 (s; CH_2P), 28.04 (s; $CH_{3\ (inner)}$), 28.92 (s; $CH_{3\ (outer)}$), 31.68 ($PCMe_{3\ (inner)}$), 32.37 ($PCMe_{3\ (outer)}$), 70.53 (Cp5), 71.15 (Cpβ-C), 78.60 (Cpα-C), 81.99 (Cp *ipso*-C).

^{31}P NMR (202 MHz, $CDCl_3$) δ = 42.67 (s).

MS (EI) m/z (rel. int): 610 (67%) 608 $[M\text{-}2Cl]^+$ (92%), 357 (26%), 286 (99%).

Elemental analysis

Calculated: C %: 49.5, H %: 7.1, N %: 0.0.

Observed: C %: 43.1, H %: 7.9, N %: 0.0.

5.2.7 Preparation of the palladium complex $Fc(CH_2P^tBu_2)_2Pd(dba)$ (53).

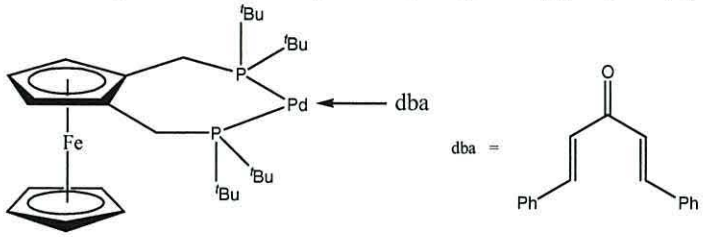

1,2-di-*tert*-butylphosphinomethyl ferrocene (0.17g, 0.34mmol) was placed in a dry Schlenk tube under N_2 with 1 equivalent of $Pd(dba)_2$ (0.2g, 0.34mmol) and dissolved in dry dichloromethane (15ml). The deep red solution was then left to stir at room temperature for 30 min. The solvent was evaporated until a deep red residue was left. This residue was washed with petrol (3 x 10ml) and left to dry under vacuum overnight forming the orange/yellow crystalline complex: (0.11g, 39 % yield).

Formula: $C_{45}H_{62}OP_2FePd$

F.W. 843.20 g mol^{-1}

m.p. 105-109°C decomposes.

^{1}H NMR (500 MHz, $CDCl_3$) δ = 1.43 (d, 18H, $^3J_{HP}$ = 14.19 Hz), 1.57 (d, 18H, $^3J_{HP}$ = 13.55 Hz), 3.11 (d, 2H, $^2J_{HP}$ = 14.50 Hz), 3.38 (d, 2H, $^2J_{HP}$ = 14.50 Hz), 3.88 (d, 1H, 2.52 Hz; Cpβ-H), 3.99 (s, 5H, Cp), 4.39 (t, 2H, 2.52 Hz; Cpα-H), 7.01 (s, 1H), 7.04 (s, 1H), 7.34 (t, 4H, 2.20 Hz), 7.36 (t, 2H, 1.58 Hz), 7.55 (t, 4H, 2.20 Hz), 7.66 (s, 1H), 7.69 (s, 1H).

^{13}C NMR (125 MHz, $CDCl_3$) δ = 19.44 (s; CH_2P), 27.14 (s; $CH_{3\ (inner)}$), 28.92 (s; $CH_{3\ (outer)}$), 30.94 ($PCMe_3$), 70.07 (Cpβ-C), 70.18 (Cp5), 73.18 (Cpα-C), 80.51 (Cp *ipso*-C), 125.44 (CHCO), 128.41 (*m*-CH), 128.98 (*o*-CH), 130.51 (*p*-CH), 134.82 (*ipso*-C), 143.34 (PhCH), 188.95 (C=O).

^{31}P NMR (202 MHz, $CDCl_3$) δ = 42.53 (s).

MS (EI) m/z (rel. int): 608 $[M\text{-dba}]^+$ (15%), 357 (100%), 503 (25%), 243 (25%), 235 (13%).

Infrared spectra ($CHCl_3$, thin film NaCl plates) 3063 cm^{-1}, 2964 cm^{-1}, 1670 cm^{-1} (C=O), 1621 cm^{-1} (C=C), 1339 cm^{-1}, 1188 cm^{-1}, 1103 cm^{-1}.

Elemental analysis

Calculated: C %: 64.1, H %: 7.4, N %: 0.0.

Observed: C %: 71.0, H %: 8.6, N %: 0.0.

5.2.8 Preparation of ruthenocene (54).

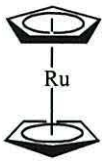

Hydrous ruthenium trichloride (10g, 0.038mol) was dissolved in absolute ethanol (150 ml) in a Schlenk tube under N_2. Freshly distilled cyclopentadiene (16.18ml, 0.237mol) was then added dropwise in excess. A small quantity of zinc dust (7.5g) was then added to the cooled solution until the reaction mixture turned from a black solution to grey-blue and left to stir at room temperature overnight. The resulting solution was then filtered, and the solid residue was washed through with benzene. The filtrate was then evaporated under reduced pressure and the solid/semi-liquid residue was extracted with petrol. Some product was obtained by extraction after evaporation while the rest of the product was isolated as yellow crystals by subliming the residue to 170°C under vacuum and subsequently dried on the high vacuum: (4.37g, 49 % yield).

Formula: $C_{10}H_{10}Ru$

F.W. 231.25 g mol^{-1}

m.p. 187-193°C (lit. 199-200°C)[83]

^{1}H NMR (250 MHz, $CDCl_3$) δ = 4.56 (s, 10H).

^{13}C NMR (62.5 MHz, $CDCl_3$) δ = 70.00 (s).

5.2.9 Preparation of dimethylaminomethylruthenocene (56).

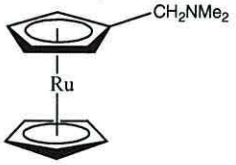

Ruthenocene (3.97g, 17mmol) and potassium *tert*-butoxide (250mg, 2.13mmol) was dissolved in dry THF (350ml) and cooled to -78°C. *t*-Butyllithum (14.7ml, 25.5mmol, 1.7M solution in pentane) was added over 10 min and stirred for a further 30 min maintaining a temperature below -70°C. Eschenmoser's salt (4.81g, 26mmol) was then added and the mixture was stirred for 12h allowing the mixture to warm to room temperature. The reaction was then quenched with HCl (20ml, 1M) and the reaction was treated with NaOH until the aqueous phase was pH 10. The organic layer was removed and aqueous phase washed with diethyl ether (2 x 75ml), the organic portions were combined, dried over anhydrous Na_2SO_4, filtered and the solvent removes *in vacuo*. The crude mixture was purified by column chromatography on deactivated alumina. Hexane was used to elute the un-reacted ruthenocene, (0.66g) and hexane/Et_2O (70:30) to elute the product. Recrystallisation from hexane at -15°C yielded the product as cream crystals and was dried under high vacuum: (1.71g, 35 % yield).

Formula: $C_{13}H_{17}NRu$

F.W. 288.35g mol^{-1}

m.p. 38-40°C (lit. 39-42°C)[90]

^{1}H NMR (250 MHz, $CDCl_3$) δ = 2.22 (s, 6H, 2 x CH_3), 3.10 (s, 2H, $CpCH_2N$), 4.52 (s, 5H, Cp), 4.53 (2H, Cp), 4.60 (2H, Cp).

^{13}C NMR (62.5 MHz, $CDCl_3$) δ = 44.76 (s; NCH_3), 58.97 ($CpCH_2N$), 70.23 (Cpα-C), 70.52 (Cp5), 72.37 (Cpβ-C), 86.96 (Cp *ipso*-C).

MS (EI) m/z (rel. int): 290 M^+ (100%), 245 (23%).

Elemental analysis

Calculated: C %: 54.2, H %: 5.9, N %: 4.8.

Observed: C %: 53.5, H %: 5.7, N %: 4.5.

5.2.10 Preparation of 1,2-bis-dimethylaminomethylruthenocene (58).

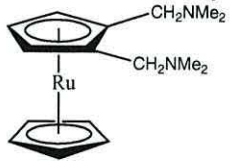

To dimethylaminomethyl ruthenocene (1.61g, 5.58mmol) in dry diethyl ether (80ml) was added *t*-butyllithium (4.60ml, 7.82mol, 1.4eq) and the reaction was stirred under N_2 for four hours. The yellow reaction solution was cooled to -78°C (dry ice/acetone bath) and Eschenmoser's salt (1.45g, 7.82mmol) was added. The cloudy white solution was then allowed to warm up to room temperature and further stirred for eighteen hours.

The reaction was then quenched with dilute sodium hydroxide, and stirred for a further fifteen minutes. The ethereal layer, containing product was separated and the aqueous layer was further extracted several times with diethyl ether. The combined ether fractions were dried over magnesium sulphate and filtered through celite. The ether solvent was removed by rotary evaporator (resulting in yellow oil) and the crude product was placed in the freezer overnight. The product was recrystallised from petrol at -17°C, and the resulting white crystals were washed with cold petrol and dried under vacuum: (1.78g, 92 % yield).

Formula: $C_{16}H_{24}N_2Ru$

F.W. 345.45 g mol^{-1}

m.p. 47-50°C

^{1}H NMR (500 MHz, $CDCl_3$) δ = 2.24 (s, 12H, 4 x CH_3), 3.05 (d, 2H, 13.13 Hz; NCH_2Cp), 3.26 (d, 2H, 13.13 Hz; NCH_2Cp), 4.45 (s, 5H, Cp5), 4.48 (t, 1H, 1.99 Hz; Cpβ-H), 4.64 (d, 2H, 1.99 Hz; Cpα-H).

^{13}C NMR (125 MHz, $CDCl_3$) δ = 45.50 (s, NCH_3), 57.28 (s, NCH_2), 70.53 (Cpα-C), 71.32 (Cp5), 72.57 (Cpβ-C), 88.21 (Cp *ipso*-C).

MS (EI) m/z (rel. int): 346 M^+ (10%), 343 (52%), 315 (60%), 300 (100%).

5.2.11 Preparation of bis-1,1'-dibromoferrocene (61).

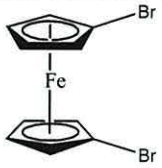

Ferrocene (30g, 0.161mol) was placed in a 1 litre two necked round-bottomed flask under N_2. Dry hexane (400ml) was added along with n-butyllithium (141.9ml, 0.354mol, 2.2eq) and TMEDA (24.34ml, 0.161mol, 1eq) and the reaction mixture was then left to stir overnight. Dry THF (200ml) was then added and the reaction mixture was cooled to -78°C (dry ice/acetone bath) followed by slow dropwise addition of 1,1,2,2-tetrabromoethane (41.33ml, 0.354mol, 2.2eq) which resulted in a dark solution. The mixture was then allowed to warm to room temperature and left to stir for five hours.

The mixture was then hydrolysed with water (300ml) and diethyl ether (100ml) was added. The mixture was extracted with ether and the combined organic phase was dried over magnesium sulphate, filtered and evaporated resulting in a dark amber oil. This was then flashed through a layer of silica with petrol and again reduced to an oil by rotary evaporator. Excess 1,1,2,2-tetrabromethane was removed by rotary evaporation at 90°C under high vacuum for 4h. The product was then allowed to crystallise out overnight. The dark orange/black crystal product were filtered, washed with cold petrol and dried under high vacuum: (34.40 g, 62 % yield).

Formula: $C_{10}H_8Br_2$

F.W. 343.83 g mol^{-1}

^{1}H NMR (250 MHz, $CDCl_3$) δ = 4.11 (s, 4H, Cp β-H), 4.44 (s, 4H, Cp α-H).

^{13}C NMR (62.5 MHz, $CDCl_3$) δ = 69.80 (s; Cp β-C), 72.54 (s; Cp α-C), 78.15 (s; Cp *ipso*-C).

5.2.12 Preparation of 1-bromo-1'-trimethylsilyl ferrocene (62).

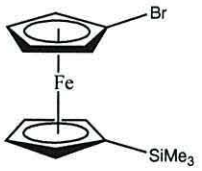

To 1,1'-dibromoferrocene (10g, 29.08mmol) in dry THF (200ml) cooled to -78°C (dry ice/acetone bath) was added n-butyllithium (11.05ml, 27.63mmol, 0.95eq) and the reaction was stirred under N_2 for 30 min. Chlorotrimethylsilane (3.7ml, 29.08mmol, 1eq) was then added dropwise and the solution was then allowed to warm up to room temperature and further stirred for twelve hours resulting in a red solution.

The reaction was then quenched with water, and stirred for a further fifteen minutes. The ethereal layer, containing product was separated and the aqueous layer was further extracted several times with diethyl ether. The combined ether fractions were dried over magnesium sulphate and filtered through celite. The ether solvent was removed by rotary evaporator (resulting in red oil). The product was eluted as the initial red band with petrol by column chromatography. The resulting red oil was finally dried under vacuum: (7.11g, 73 % yield).

Formula: $C_{13}H_{17}SiFeBr$

F.W. 337.11 g mol^{-1}

^{1}H NMR (500 MHz, $CDCl_3$) δ = 0.05 (s, 9H, 3 x CH_3), 3.85 (t, 1.89 Hz; 2 x CH), 3.96 (t, 1.89 Hz; 2 x CH), 4.16 (t, 1.89 Hz; 2 x CH), 4.19 (t, 1.89 Hz; 2 x CH).

^{13}C NMR (125 MHz, $CDCl_3$) δ = 0.00 (s; $SiCH_3$), 67.27 (s; $CpSiMe_3$ β-C), 70.12 (s; Cp CpBr β-C), 74.16 (s; $CpSiMe_3$ α-C), 76.95 (s; Cp CpBr α-C), 77.91 (s; $CpSiMe_3$ *ipso*-C), 78.45 (s; CpBr *ipso*-C).

5.2.13 Preparation of 1-dimethylaminomethyl-1'-trimethylsilyl ferrocene (63).

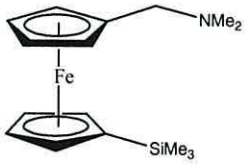

To 1-bromo-1'-trimethylsilyl ferrocene (5.52g, 16.37mmol) in dry diethyl ether (100ml) was added n-butyllithium (7.2ml, 18.01mmol, 1.1eq) and the reaction was stirred under N_2 for 1 hour at room temperature. Dry THF (100ml) was then added and solution was then cooled to -78°C (dry ice/acetone bath) and quenched with Eschenmoser's salt (3.33g, 18mmol, 1eq). The solution was then allowed to warm up to room temperature and further stirred for twelve hours resulting in a yellow solution.

The reaction was then quenched with water, and stirred for a further fifteen minutes. The ethereal layer, containing product was separated and the aqueous layer was further extracted several times with diethyl ether. The combined ether fractions were dried over magnesium sulphate and filtered through celite. The ether solvent was removed by rotary evaporator (resulting in red oil). The product was purified by column chromatography. Starting material was removed with 9:1 petrol/Et_2O and the product was then obtained with 1:1 petrol/Et_2O (5% triethylamine) as an orange band. The resulting red oil was finally dried under vacuum: (4.09g, 79 % yield).

Formula: $C_{16}H_{25}NSiFe$

F.W. 315.31 g mol^{-1}

^{1}H NMR (500 MHz, $CDCl_3$) δ = 0.00 (s, 9H, 3 x CH_3) 1.94 (s, 6H, 2 x CH_3), 3.04 (s, 2H, $CpCH_2N$), 3.79 (t, 2.00 Hz; 2 x CH), 3.84 (t, 1.89 Hz; 2 x CH), 3.91 (t, 1.90 Hz; 2 x CH), 4.04 (t, 1.89 Hz; 2 x CH).

^{13}C NMR (125 MHz, $CDCl_3$) δ = 0.00 (s; $SiCH_3$), 44.94 (s; NCH_3), 59.38 ($CpCH_2N$), 68.42 (s; $CpSiMe_3$ β-C), 70.39 (s; β-C), 71.59 (s; $CpSiMe_3$ α-C), 72.43 (s; α-C), 73.49 (s; $CpSiMe_3$ *ipso*-C), 83.43 (s; *ipso*-C).

MS (EI) m/z (rel. int): 316 $(M + H)^+$ (78%), 271 (100%).

5.2.14 Preparation of 1,2-bis-dimethylaminomethyl-1'-trimethylsilylferrocene (64).

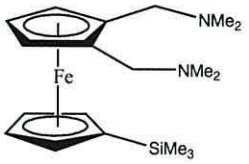

To 1-dimethylaminomethyl-1'-trimethylsilyl ferrocene (3.86g, 12.24mmol) in dry diethyl ether (100ml) was added n-butyllithium (5.88ml, 14.69mmol, 1.2eq) and the reaction was stirred under N_2 for 1 hour at room temperature. Dry THF (100ml) was then added and solution was then cooled to -78°C (dry ice/acetone bath) and quenched with Eschenmoser's salt (2.50g, 13.47mmol, 1.1eq). The solution was then allowed to warm up to room temperature and further stirred for twelve hours resulting in an orange solution.

The reaction was then quenched with water, and stirred for a further fifteen minutes. The ethereal layer, containing product was separated and the aqueous layer was further extracted several times with diethyl ether. The combined ether fractions were dried over magnesium sulphate and filtered through celite. The ether solvent was removed by rotary evaporator (resulting in red oil). The product was purified by column chromatography. Starting material was removed with 9:1 petrol/Et_2O and the product was then obtained with 1:1 petrol/Et_2O (5% triethylamine). The resulting red oil was finally dried under vacuum: (4.33g, 95 % yield).

Formula: $C_{19}H_{33}N_2SiFe$

F.W. 373.42 g mol^{-1}

^{1}H NMR (500 MHz, $CDCl_3$) δ = 0.00 (s, 9H, 3 x CH_3), 1.97 (s, 12H, 4 x CH_3), 2.99 (d, 2H, 12.92 Hz; NCH_2Cp), 3.13 (d, 2H, 12.93 Hz; NCH_2Cp), 3.76 (t, 2H, 2 x CH), 3.87 (t, 2H, 2 x CH), 3.81 (t, 1H, 2.84 Hz; 1 x CH), 3.97 (d, 2H, 2.21 Hz; 2 x CH).

^{13}C NMR (125 MHz, $CDCl_3$) δ = 0.00 (s; $SiCH_3$), 45.33 (s; NCH_3), 57.49 ($CpCH_2N$), 67.32 (s; $CpSiMe_3$ β-C), 68.37 (s; β-C), 70.78 (s; $CpSiMe_3$ α-C), 73.15 (s; α-C), 73.91 (s; $CpSiMe_3$ *ipso*-C), 83.92 (s; *ipso*-C).

MS (EI) m/z (rel. int): 373 M^+ (100%), 227 (25%).

Elemental analysis

Calculated: C %: 61.1, H %: 8.9, N %: 7.5.

Observed: C %: 59.8, H %: 8.7, N %: 7.4.

5.2.15 Preparation of 1-bromo-1'-triphenylsilyl ferrocene (65).

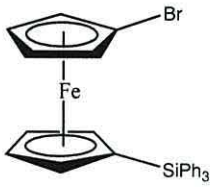

To 1,1'-dibromoferrocene (10.14g, 29.49mmol) in dry THF (200ml) cooled to -78°C (dry ice/acetone bath) was added n-butyllithium (12.56ml, 28.02mmol, 0.95eq) and the reaction was stirred under N_2 for 30 min. Chlorotriphenylsilane (8.26g, 28.02mmol, 0.95eq) dissolved in the minimum amount of dry THF was then added dropwise and the solution was then allowed to warm up to room temperature and further stirred for twelve hours resulting in a red solution.

The reaction was then quenched with water, and stirred for a further fifteen minutes. The ethereal layer, containing product was separated and the aqueous layer was further extracted several times with diethyl ether. The combined ether fractions were dried over magnesium sulphate and filtered through celite. The ether solvent was removed by rotary evaporator (resulting in red oil). The product was purified by column chromatography. Starting material was removed with petrol and the product was then obtained with 9:1 petrol/Et_2O as an orange band. The resulting oil was finally dried under vacuum leaving pure product as orange crystals: (11.09g, 72 % yield).

Formula: $C_{28}H_{23}SiFeBr$

F.W. 523.32 g mol^{-1}

^{1}H NMR (500 MHz, $CDCl_3$) δ = 3.79 (t, 2H, 1.57 Hz; 2 x CH), 4.23 (t, 2H, 1.58 Hz; 2 x CH), 4.28 (t, 2H, 2 x CH), 4.51(t, 2H, 2 x CH), 7.41 (t, 6H, 6.94 Hz), 7.45 (t, 3H, 6.94 Hz), 7.62 (t, 6H, 5.36 Hz).

^{13}C NMR (125 MHz, $CDCl_3$) δ = 68.15 (s; $CpSiPh_3$ β-C), 70.61 (s; Cp CpBr β-C), 73.03 (s; $CpSiPh_3$ α-C), 75.02 (s; Cp CpBr α-C), 77.36 (s; $CpSiPh_3$ *ipso*-C), 81.20 (s; CpBr *ipso*-C), 127.79 (Ar CH), 129.55 (Ar CH), 135.34 (Ar CH), 135.96 (Ar *ipso*-C).

MS (EI) m/z (rel. int): 524 (2%), 522 M^+ (2%) 444 (100%).

Elemental analysis

Calculated: C %: 64.3, H %: 4.4, N %: 0.0.

Observed: C %: 64.2, H %: 4.4, N %: 0.0.

5.2.16 Preparation of 1-dimethylaminomethyl-1'-triphenylsilylferrocene (66).

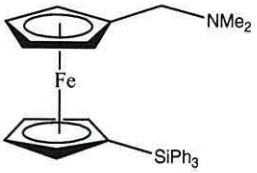

To 1-bromo-1'-triphenylsilyl ferrocene (8g, 15.29mmol) in dry diethyl ether (100ml) was added n-butyllithium (6.73ml, 16.82mmol, 1.1eq) and the reaction was stirred under N_2 for 1 hour at room temperature. Dry THF (100ml) was then added and solution was then cooled to -78°C (dry ice/acetone bath) and quenched with Eschenmoser's salt (3.11g, 16.82mmol, 1.1eq). The solution was then allowed to warm up to room temperature and further stirred for twelve hours resulting in a yellow solution.

The reaction was then quenched with water, and stirred for a further fifteen minutes. The ethereal layer, containing product was separated and the aqueous layer was further extracted several times with diethyl ether. The combined ether fractions were dried over magnesium sulphate and filtered through celite. The ether solvent was removed by rotary evaporator (resulting in red oil). The product was purified by column chromatography. Starting material was removed with 9:1 petrol/Et_2O and the product was then obtained with 1:1 petrol/Et_2O (5% triethylamine). The resulting red oil was finally dried under vacuum leaving pure product as red/orange crystals: (3g, 39 % yield).

Formula: $C_{31}H_{31}NSiFe$

F.W. 501.53 g mol^{-1}

m.p. 102-106°C

^{1}H NMR (500 MHz, $CDCl_3$) δ = 1.97 (s, 6H, 2 x CH_3), 2.84 (s, 2H, $CpCH_2N$), 3.83 (t, 2H, 1.26 Hz; 2 x CH), 3.93 (t, 2H, 1.27 Hz; 2 x CH), 4.05 (t, 2H, 1.26 Hz; 2 x CH), 4.31 (t, 2H, 1.26 Hz; 2 x CH), 7.33 (t, 6H, 1.26 Hz), 7.52 (t, 3H, 1.26 Hz), 7.54 (t, 6H, 1.26 Hz).

^{13}C NMR (125 MHz, $CDCl_3$) δ = 44.57 (s; NCH_3), 58.52 ($CpCH_2N$), 66.50 (s; $CpSiPh_3$ β-C), 69.31 (s; Cp CpBr β-C), 70.68 (s; $CpSiPh_3$ α-C), 72.02 (s; Cp CpBr α-C), 76.77 (s; $CpSiPh_3$ *ipso*-C), 83.47 (s; CpBr *ipso*-C), 127.75 (Ar CH), 129.46 (Ar CH), 135.63 (Ar CH), 136.00 (Ar *ipso*-C).

MS (EI) m/z (rel. int): 502 M^+ (100%), 457 (47%).

5.2.17 Preparation of 1,2-bis-dimethylaminomethyl-1'-triphenylsilylferrocene (67).

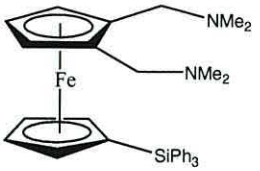

To 1-dimethylaminomethyl-1'-triphenylsilyl ferrocene (2.66g, 5.30mmol) in dry diethyl ether (100ml) was added n-butyllithium (2.55ml, 6.36mmol, 1.2eq) and the reaction was stirred under N_2 for 1 hour at room temperature. Dry THF (100ml) was then added and solution was then cooled to -78°C (dry ice/acetone bath) and quenched with Eschenmoser's salt (1.08g, 5.83mmol, 1.1eq). The solution was then allowed to warm up to room temperature and further stirred for twelve hours resulting in an orange solution. The reaction was then quenched with water, and stirred for a further fifteen minutes. The ethereal layer, containing product was separated and the aqueous layer was further extracted several times with diethyl ether. The combined ether fractions were dried over magnesium sulphate and filtered through celite. The ether solvent was removed by rotary evaporator (resulting in red oil). The product was purified by column chromatography. Starting material was removed with 9:1 petrol/Et_2O and the product was then obtained with 1:1 petrol/Et_2O (5% triethylamine). The resulting red oil was finally dried under vacuum: (2.94g, 99 % yield).

Formula: $C_{34}H_{38}N_2SiFe$

F.W. 558.62 g mol^{-1}

^{1}H NMR (500 MHz, $CDCl_3$) δ = 2.00 (s, 12H, 4 x CH_3), 2.87 (d, 2H, 12.46 Hz; NCH_2Cp), 3.13 (d, 2H, 12.46 Hz; NCH_2Cp), 3.88 (t, 2H, 1.57 Hz; 2 x CH), 3.93 (d, 2H, 2.05 Hz; 2 x CH), 4.01 (t, 2H, 1.57 Hz; 2 x CH), 4.25 (t, 1H, 2.05 Hz; 1 x CH), 7.29 (t, 6H, 1.26 Hz), 7.32 (t, 3H, 2.21 Hz), 7.47 (t, 6H, 1.26 Hz).

^{13}C NMR (125 MHz, $CDCl_3$) δ = 44.58 (s; NCH_3), 56.94 ($CpCH_2N$), 67.98 (s; $CpSiPh_3$ β-C), 69.04 (s; β-C), 70.67 (s; $CpSiPh_3$ α-C), 72.02 (s; α-C), 73.92 (s; $CpSiPh_3$ *ipso*-C), 75.55 (s; *ipso*-C), 127.74 (Ar CH), 129.46 (Ar CH), 135.57 (Ar CH), 136.00 (Ar *ipso*-C).

MS (EI) m/z (rel. int): 559 M^+ (100%), 502 (73%), 457 (38%).

Elemental analysis

Calculated: C %: 73.1, H %: 6.9, N %: 5.0.

Observed: C %: 72.8, H %: 6.9, N %: 4.8.

5.2.18 Preparation of 1-bromo-1'-dimethylaminomethylferrocene (70).

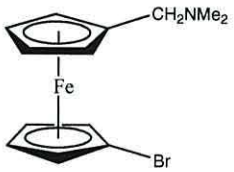

To dibromoferrocene (10.02g, 29.14mmol) in dry THF (250ml) under nitrogen cooled to -78°C (dry ice/acetone bath) was added n-butyllithium (11.10ml, 27.69mmol, 0.95eq). The reaction was kept cool and stirred for a further two hours, resulting in the formation of an orange precipitate. Eschenmoser's salt (6.47g, 34.97mmol, 1.2eq) was then added and the solution was then allowed to warm up to room temperature and further stirred for twelve hours. The reaction was quenched with water and extracted with diethyl ether. An acid/base extraction was performed to obtain the product. 10% Phosphoric acid was added to the ethereal layer and the aqueous layer was isolated and washed with diethyl ether. Any unreacted starting material or by-products was in the organic layer while the product was to be found in the aqueous layer due to the presence of the amine. The aqueous was then mixed with clean diethyl ether and sodium hydroxide (2M) was added until the aqueous layer was slightly alkaline. This organic layer was then extracted with diethyl ether, dried over magnesium sulphate and filtered over celite. The solvent was removed *in vacuo* under rotary evaporator and purified product was obtained as an orange oil (2.00g, 21 % yield).

Formula: $C_{13}H_{16}NFeBr$

F.W. 322.03 g mol^{-1}

^{1}H NMR (500 MHz, $CDCl_3$) δ = 2.11 (s, 6H, 2 x CH_3), 3.23 (s, 2H, $CpCH_2N$), 3.98 (t, 1.89 Hz; 2 x CH), 4.04 (t, 1.89 Hz; 2 x CH), 4.09 (t, 1.89 Hz; 2 x CH), 4.25 (t, 1.89 Hz; 2 x CH).

^{13}C NMR (62.5 MHz, $CDCl_3$) δ = 30.84 (s; NCH_3), 45.58 ($CpCH_2N$), 65.61 (s; Cp β-C), 67.35 (s; CpBr β-C), 67.73 (s; Cp α-C), 68.24 (s; CpBr α-C), 69.32 (s; Cp *ipso*-C), 70.52 (s; CpBr *ipso*-C).

Elemental analysis

Calculated: C %: 48.5, H %: 5.0, N %: 4.3.

Observed: C %: 47.2, H %: 4.8, N %: 4.1.

5.2.19 Preparation of 1-dimethylaminomethyl-5,1'-bis-trimethylsilyl ferrocene (71).

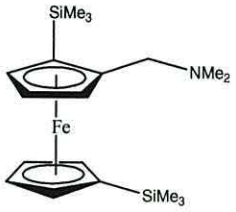

To dimethylaminomethylferrocene (30g, 123.39mmol) in dry diethyl ether (200ml) was added *n*-butyllithium (123.39ml, 308.48mmol, 2.5eq) and TMEDA (20.48ml, 135.73mmol, 1.1eq) and the reaction was stirred under N_2 for 12 hours at room temperature. The solution was then cooled to -78°C (dry ice/acetone bath) and quenched with chlorotrimethylsilane (34.45ml, 271.46mmol, 2.2eq). The solution was then allowed to warm up to room temperature and further stirred for twelve hours resulting in an orange solution. The reaction was then quenched with water, and stirred for a further fifteen minutes. The ethereal layer, containing product was separated and the aqueous layer was further extracted several times with diethyl ether. The combined ether fractions were dried over magnesium sulphate and filtered through celite. The ether solvent was removed by rotary evaporator (resulting in red oil). The product was purified by column chromatography. Small amounts of starting material were removed with petrol (5% triethylamine) and the product was then obtained with 1:1 petrol/Et_2O (5% triethylamine). The resulting red oil was finally dried under vacuum: (40g, 84 % yield).

Formula: $C_{19}H_{33}NSi_2Fe$

F.W. 387.49 g mol^{-1}

^{1}H NMR (500 MHz, $CDCl_3$) δ = 0.25 (s, 9H, 3 x CH_3), 0.30 (s, 9H, 3 x CH_3), 2.11 (s, 6H, 2 x CH_3), 3.00 (d, 1H, 12.45 Hz; NCH_2Cp), 3.45 (d, 1H, 12.45 Hz; NCH_2Cp), 3.98 (t, 2H, 1.26 Hz; 2 x CH), 4.06 (t, 2H, 1.26 Hz; 2 x CH), 4.19 (t, 1H, 1.74 Hz; 1 x CH), 4.27 (d, 1H, 1.74 Hz; 1 x CH), 4.29 (d, 1H, 1.74 Hz; 1 x CH).

^{13}C NMR (125 MHz, $CDCl_3$) δ = 0.00 (s; $SiCH_3$), 0.41 (s; $SiCH_3$), 45.03 (s; NCH_3), 59.72 ($CpCH_2N$), 70.03 (s; $CpSiMe_3$ β-C), 71.77 (s; β-C), 72.01 (s; $CpSiMe_3$ α-C), 72.68 (s; α-C), 72.88 (s; α-C), 74.00 (s; $CpSiMe_3$ *ipso*-C), 74.25 (s; *ipso*-C), 89.97 (s; *ipso*-C).

Elemental analysis

Calculated: C %: 58.9, H %: 8.6, N %: 3.6.

Observed: C %: 58.6, H %: 8.4, N %: 3.6.

5.2.20 Preparation of 1,2-bis-dimethylaminomethyl-5,1'-bis-trimethylsilyl ferrocene (72).

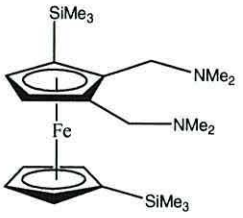

To 1-dimethylaminomethyl-5,1'-bis-trimethylsilyl ferrocene (30g, 77.42mmol) in dry diethyl ether (200ml) was added *n*-butyllithium (37.2ml, 92.91mmol, 1.2eq) and the reaction was stirred under N_2 for 20 hours at room temperature. Dry THF (250ml) was then added and solution was then cooled to -78°C (dry ice/acetone bath) and quenched with Eschenmoser's salt (17.18g, 92.91mmol, 1.2eq). The solution was then allowed to warm up to room temperature and further stirred for twelve hours resulting in a red solution.

The reaction was then quenched with water, and stirred for a further fifteen minutes. The ethereal layer, containing product was separated and the aqueous layer was further extracted several times with diethyl ether. The combined ether fractions were dried over magnesium sulphate and filtered through celite. The ether solvent was removed by rotary evaporator (resulting in red oil). The product was purified by column chromatography (large scale column). Small amounts of starting material were removed with petrol (5% triethylamine) and the product was then obtained with 1:1 petrol/Et_2O (5% triethylamine). The resulting red oil was finally dried under vacuum: (32.11g, 93 % yield).

Formula: $C_{22}H_{40}N_2Si_2Fe$

F.W. 444.59 g mol^{-1}

^{1}H NMR (500 MHz, $CDCl_3$) δ = 0.00 (s, 9H, 3 x CH_3), 0.03 (s, 9H, 3 x CH_3), 1.86 (s, 6H, 2 x CH_3), 1.93 (s, 6H, 2 x CH_3), 2.97 (d, 2H, 12.77 Hz; NCH_2Cp), 3.24 (d, 2H, 12.77 Hz; NCH_2Cp), 3.74 (t, 2H, 1.26 Hz; 2 x CH), 3.81 (t, 2H, 1.26 Hz; 2 x CH), 3.95 (d, 1H, 2.37 Hz; 1 x CH), 4.08 (d, 1H, 2.37 Hz; 1 x CH).

^{13}C NMR (125 MHz, $CDCl_3$) δ = 0.00 (s; $SiCH_3$), 0.09 (s; $SiCH_3$), 44.43 (s; NCH_3), 57.31 ($CpCH_2N$), 69.73 (s; $CpSiMe_3$ β-C), 71.43 (s; $CpSiMe_3$ α-C), 72.62 (s; α-C), 72.83 (s; α-C), 73.68 (s; $CpSiMe_3$ *ipso*-C), 74.94 (s; *ipso*-C), 87.25 (s; *ipso*-C), 89.68 (s; *ipso*-C).

Elemental analysis

Calculated: C %: 59.4, H %: 9.1, N %: 6.3.

Observed: C %: 57.2, H %: 8.6, N %: 6.0.

5.2.21 Preparation of 1-dimethylaminomethyl-5,1'-bis-triphenylsilyl ferrocene (73).

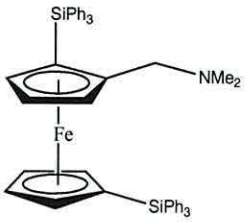

To dimethylaminomethylferrocene (20g, 82.26mmol) in dry diethyl ether (300ml) was added *n*-butyllithium (82.26ml, 205.65mmol, 2.5eq) and TMEDA (13.66ml, 90.49mmol, 1.1eq) and the reaction was stirred under N_2 for 12 hours at room temperature. The solution was then cooled to -78°C (dry ice/acetone bath) and quenched with chlorotriphenylsilane (50.94g, 172.75mmol, 2.1eq) dissolved in dry THF (200ml). The solution was then allowed to warm up to room temperature and further stirred for twelve hours resulting in a red solution.

The reaction was then quenched with water, and stirred for a further fifteen minutes. The ethereal layer, containing product was separated and the aqueous layer was further extracted several times with diethyl ether. The combined ether fractions were dried over magnesium sulphate and filtered through celite. The ether solvent was removed by rotary evaporator (resulting in red oil). The product was purified by layering the oil with petrol and diethyl ether and leaving to crystallize overnight. The liquid residue was decanted and the orange/red crystals were dried under vacuum. A second crop of orange/red crystals were obtained with the layering of the decanted liquid and repeating the process: (42.75g, 68 % yield).

Formula: $C_{49}H_{45}NSi_2Fe$

F.W. 759.98 g mol $^{-1}$

m.p. 154-157°C

^{1}H NMR (500 MHz, $CDCl_3$) δ = 1.71 (s, 6H, 2 x CH_3), 2.59 (d, 1H, 12.46 Hz; NCH_2Cp), 2.93 (d, 1H, 12.46 Hz; NCH_2Cp), 3.99 (t, 1H, 1.74 Hz; 1 x CH), 4.01 (t, 2H, 1.10 Hz; 2 x CH), 4.05 (t, 2H, 1.10 Hz; 2 x CH), 4.21 (d, 1H, 1 x CH), 4.28 (d, 1H, 1.74 Hz; 1 x CH) 7.38 (t, 6H, 1.58 Hz), 7.39 (t, 3H, 1.26 Hz), 7.42 (t, 6H, 1.57 Hz), 7.47 (t, 3H, 1.26 Hz), 7.60 (t, 6H, 1.57 Hz), 7.68 (t, 6H, 1.26 Hz).

^{13}C NMR (125 MHz, $CDCl_3$) δ = 44.61 (s; NCH_3), 58.43 ($CpCH_2N$), 66.86 (s; $CpSiPh_3$ β-C), 72.36 (s; β-C), 73.34 (s; $CpSiPh_3$ α-C), 74.67 (s; α-C), 74.77 (s; α-C), 75.66 (s; $CpSiPh_3$ *ipso*-C), 75.75 (s; *ipso*-C), 91.09 (s; *ipso*-C) 127.52 (Ar CH), 127.79 (Ar CH), 129.24 (Ar CH), 129.51 (Ar CH), 135.52 (Ar CH), 135.69 (Ar CH), 135.98 (Ar *ipso*-C), 136.46 (Ar *ipso*-C).

MS (EI) m/z (rel. int): 759 M^+ (8%), 715 (100%).

Elemental analysis

Calculated: C %: 77.5, H %: 6.0, N %: 1.8.

Observed: C %: 77.6, H %: 6.0, N %: 1.8.

5.2.22 Preparation of 1,2-bis-dimethylaminomethyl-5,1'-bis-triphenylsilyl ferrocene (74).

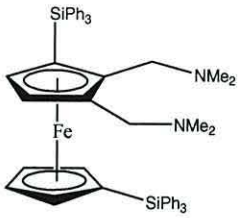

To 1-dimethylaminomethyl-5,1'-bis-triphenylsilyl ferrocene (40g, 52.63mmol) in dry diethyl ether (400ml) was added *n*-butyllithium (25.26ml, 63.16mmol, 1.2eq) and the reaction was stirred under N_2 for 20 hours at room temperature. Dry THF (250ml) was then added and solution was then cooled to -78°C (dry ice/acetone bath) and quenched with Eschenmoser's salt (12.65g, 68.42mmol, 1.3eq). The solution was then allowed to warm up to room temperature and further stirred for twelve hours resulting in an orange solution.

The reaction was then quenched with water, and stirred for a further fifteen minutes. The ethereal layer, containing product was separated and the aqueous layer was further extracted several times with diethyl ether. The combined ether fractions were dried over magnesium sulphate and filtered through celite. The ether solvent was removed by rotary evaporator (resulting in red oil). The product was purified by layering the oil with the minimum diethyl ether and a layer of petrol and leaving to crystallize overnight. The liquid residue was decanted and the red crystals were dried under vacuum. A second crop of red crystals were obtained with the layering of the decanted liquid and repeating the process: (21.50g, 50 % yield).

Formula: $C_{52}H_{52}N_2Si_2Fe$

F.W. 817.09 g mol^{-1}

m.p. 150-154°C

^{1}H NMR (500 MHz, $CDCl_3$) δ = 1.69 (s, 6H, 2 x CH_3), 2.08 (s, 6H, 2 x CH_3), 2.81 (d, 2H, 12.30 Hz; NCH_2Cp), 3.40 (d, 2H, 12.30 Hz; NCH_2Cp), 4.05 (t, 2H, 1.42 Hz; 2 x CH), 4.08 (t, 2H, 1.42 Hz; 2 x CH), 4.27 (d, 1H, 2.40 Hz; 1 x CH), 4.38 (d, 1H, 2.40 Hz; 1 x CH), 7.45 (t, 6H, 1.26 Hz), 7.47 (t, 3H, 1.57 Hz), 7.70 (t, 6H, 1.26 Hz), 7.71 (t, 3H, 1.57 Hz), 7.81 (t, 6H, 1.26 Hz), 7.83 (t, 6H, 1.57 Hz).

^{13}C NMR (125 MHz, $CDCl_3$) δ = 45.22 (s; NCH_3), 56.67 ($CpCH_2N$), 67.43 (s; $CpSiPh_3$ β-C), 68.63 (s; $CpSiPh_3$ α-C), 74.02 (s; α-C), 75.07 (s; α-C), 76.21 (s; $CpSiPh_3$ *ipso*-C), 77.95 (s; *ipso*-C), 88.31 (s; *ipso*-C), 90.73 (s; *ipso*-C), 127.45 (Ar CH), 127.94 (Ar CH), 129.07 (Ar CH), 129.61 (Ar CH), 135.53 (Ar CH), 136.07 (Ar CH), 136.17 (Ar *ipso*-C), 136.55 (Ar *ipso*-C).

MS (EI) m/z (rel. int): 817 M^+ (34%), 772 (100%).

Elemental analysis

Calculated: C %: 76.5, H %: 6.4, N %: 3.4.

Observed: C %: 74.6, H %: 6.2, N %: 3.1.

5.2.23 Preparation of bis-1-bromo-1'-dimethylsilyl bridged ferrocene (76).

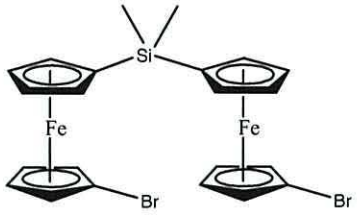

To 1,1'-dibromoferrocene (15.00g, 43.63mmol) in dry THF (350ml) cooled to -78°C (dry ice/acetone bath) was added *n*-butyllithium (16.58ml, 41.45mmol, 0.95eq) and the reaction was stirred under N_2 for 30 min. Dichlorodimethylsilane (2.55ml, 20.94mmol, 0.48eq) was then added dropwise and the solution was then allowed to warm up to room temperature and further stirred for twelve hours resulting in a red solution.

The reaction was then quenched with water, and stirred for a further fifteen minutes. The ethereal layer, containing product was separated and the aqueous layer was further extracted several times with diethyl ether. The combined ether fractions were dried over magnesium sulphate and filtered through celite. The ether solvent was removed by rotary evaporator (resulting in a brown residue). The product was purified by column chromatography. Starting material was removed with petrol and the product was then obtained with 9:1 petrol/Et_2O as an orange band. The resulting oil was finally dried under vacuum leaving pure product as an orange solid: (7.76g, 61 % yield).

Formula: $C_{22}H_{22}SiFe_2Br_2$

F.W. 585.999 g mol^{-1}

m.p. 37-39°C

^{1}H NMR (500 MHz, $CDCl_3$) δ = 0.33 (s, 6H, 2 x CH_3), 3.79 (d, 1.57 Hz; 4 x CH), 3.92 (d, 1.58 Hz; 4 x CH), 4.13 (d, 1.58 Hz; 4 x CH), 4.20 (d, 1.57 Hz; 4 x CH).

^{13}C NMR (62.5 MHz, $CDCl_3$) δ = 0.67 (s; $SiCH_3$), 67.41 (s; $CpSiMe_2$ β-C), 70.51 (s; β-C), 72.32 (s; $CpSiMe_2$ α-C), 74.05 (s; α-C), 75.64 (s; $CpSiMe_2$ *ipso*-C), 77.71 (s; *ipso*-C).

Elemental analysis

Calculated: C %: 45.1, H %: 3.8, N %: 0.0.

Observed: C %: 44.8, H %: 3.6, N %: 0.0.

5.2.24 Preparation of bis-1-dimethylaminomethyl-1'-dimethylsilyl bridged ferrocene (77).

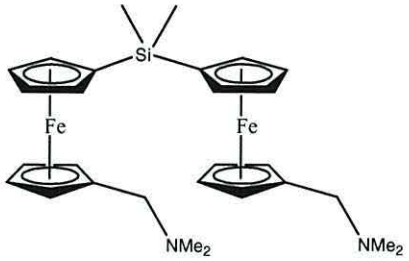

To bis-1-bromo-1'-dimethylsilyl bridged ferrocene (7.00g, 11.95mmol) in dry diethyl ether (100ml) was added n-butyllithium (10.03ml, 25.08mmol, 2.1eq) and the reaction was stirred under N_2 for 1 hour at room temperature. Dry THF (100ml) was then added and solution was then cooled to -78°C (dry ice/acetone bath) and quenched with Eschenmoser's salt (4.86g, 26.28mmol, 2.2eq). The solution was then allowed to warm up to room temperature and further stirred for twelve hours resulting in a yellow solution. The reaction was then quenched with water, and stirred for a further fifteen minutes. The ethereal layer, containing product was separated and the aqueous layer was further extracted several times with diethyl ether. The combined ether fractions were dried over magnesium sulphate and filtered through celite. The ether solvent was removed by rotary evaporator (resulting in red oil). The product was purified by column chromatography. Starting material was removed with petrol and the product was then obtained with 1:1 petrol/Et_2O (5% triethylamine) as an orange band. The resulting red oil was finally dried under vacuum: (4.93g, 76 % yield).

Formula: $C_{28}H_{38}SiFe_2N_2$

F.W. 542.39 g mol^{-1}

^{1}H NMR (500 MHz, $CDCl_3$) δ = 0.28 (s, 6H, 2 x CH_3) 0.69 (s, 6H, 2 x CH_3), 1.32 (s, 6H, 2 x CH_3), 2.05 (t, 4H, 7.91 Hz; $CpCH_2N$), 3.74 (t, 1.57 Hz; 4 x CH), 3.78 (t, 1.89 Hz; 4 x CH), 3.81 (t, 1.27 Hz; 4 x CH), 4.03 (t, 1.26 Hz; 4 x CH).

^{13}C NMR (125 MHz, $CDCl_3$) δ = 0.00 (s; $SiCH_3$), 29.97 (s; NCH_3), 34.14 (s; NCH_3), 42.11 ($CpCH_2N$), 68.10 (s; $CpSiMe_2$ β-C), 68.93 (s; β-C), 69.06 (s; $CpSiMe_2$ α-C), 72.29 (s; α-C), 74.33 (s; $CpSiMe_2$ *ipso*-C), 90.16 (s; *ipso*-C).

5.2.25 Preparation of 2,3,5,6-tetrahydro-2,3,5,6-tetramethyl-γ-pyrone (81).

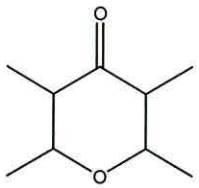

To a solution of potassium hydroxide (112.2g, 2mol) in methanol (750ml) (at 0°C) in a 5 litre flange flask equipped with an overhead stirrer and an N_2 inlet, diethyl ketone (516g, 635.47ml, 6mol) was added. After addition of lithium chloride (17g, 0.4mol) and gentle warming to 30°C (take reaction mixture out of the ice bath) acetaldehyde (1 litre, 17.8mol) was added very slowly over 5-7 hours from a pressure equalising dropping funnel. After 12 hours the deep red oily mixture (from an original white suspension) was neutralized with dilute hydrochloric acid.

The light red organic layer was separated and washed twice with water. Simple distillation under reduced pressure gave the crude product (clear, yellow liquid: 50-60°C at 9mb). Re-distillation under reduced pressure through a 20cm Vigreux-column yielded the product (clear, colourless liquid: 73-89°C at 9 mb): (388.37g, 42 % yield).

Formula: $C_9H_{16}O_2$

F.W. 156.22 g mol^{-1}

^{1}H NMR (250 MHz, $CDCl_3$) δ = 0.93 (d, 3H, 6.40 Hz; 2 x CH_3), 1.29 (d, 3H, 6.11 Hz; 2 x CH_3), 2.24 (m, 1H, 3.36 Hz), 3.28 (m, 1H, 3.36 Hz).

^{13}C NMR (62.5 MHz, $CDCl_3$) δ = 9.46 (s; 2 x CH_3), 20.41 (s; 2 x CH_3), 51.25 (s), 78.98 (s), 209.61 (s).

Infrared spectra (thin film NaCl plates) 2974 cm^{-1} (C-H str), 1714 cm^{-1} (C=O), 1379 cm^{-1} (C-O), 1160 cm^{-1} (C-C).

5.2.26 Preparation of 2,3,4,5-tetramethylcyclopent-2-enone (82).

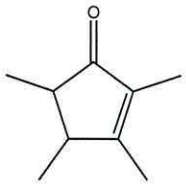

p-Toluenesulfonic acid (47.32g, 0.25mol) was added to 2,3,5,6-tetrahydro-2,3,5,6-tetramethyl-γ-pyrone (388.77g, 2.49mol) in benzene (188ml). The mixture was refluxed under Dean-Stark conditions. After about 20 hours; the elimination of water was complete. The mixture was neutralized with Na_2CO_3 solution and the organic layer was washed twice with water. Distillation under reduced pressure through a Vigreux-column yields the product (clear colourless liquid: 105-110°C at 8.6 mb) and an additional amount of α,β-unsaturated ketone by-product: (224.17g, 65 % yield).

Formula: $C_9H_{14}O$

F. W. 138.21 g mol^{-1}

^{1}H NMR (250 MHz, $CDCl_3$) δ = 1.07 (d, 3H, 7.62 Hz; CH_3), 1.13 (d, 3H, 7.02 Hz; CH_3), 1.61 (s, 3H, CH_3), 1.92 (s, 3H, CH_3), 2.20 (m, 1H, 7.02 Hz), 2.62 (m, 1H, 7.32 Hz).

^{13}C NMR (62.5 MHz, $CDCl_3$) δ = 8.05 (s, CH_3), 14.52 (s, CH_3), 14.98 (s, CH_3), 17.63 (s, CH_3), 46.27 (s, CH), 48.34 (s, CH), 134.43 (s, C=C), 136.58 (s, C=C), 210.93 (s, C=O).

Infrared spectra (thin film NaCl plates) 2962 cm^{-1} (C-H str), 1699 cm^{-1} (C=O), 1648 cm^{-1} (C=C), 1234 cm^{-1} (C-C).

MS (EI) m/z (rel. int.): 138 (100%) [M^+], 123 [M^+ - CH_3].

5.2.27 Preparation of 1,2,3,4-tetramethylcyclopentadiene (83).

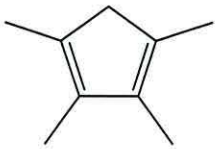

A 2 litre flange flask fitted with a reflux condenser and a 250ml pressure equalising dropping funnel was charged with $LiAlH_4$ (16.8g, 0.44mol). Dry diethyl ether (900ml), was then added to the flask and the mixture was cooled to 0°C (ice bath). Freshly distilled 2,3,4,5-tetramethylcyclopent-2-enone (210ml, 1.40mol) was added dropwise to the mixture with stirring over 1 hour. The mixture was allowed to warm to room temperature and stirred for 8 hours. Water (70ml) was then added dropwise to hydrolyse the remaining $LiAlH_4$. Solids were coagulated by the dropwise addition of 33% H_2SO_4 (70ml), and the ether layer was decanted into a 2 litre separating funnel. Water and 33% H_2SO_4 were added alternatively to the remaining solids in the flask until all solids dissolved. The solution was then back-extracted with Et_2O (3 x 50ml), and the extracts combined with the ethereal layer. The dehydration of the alcohol was monitored via GC by monitoring the disappearance of the alcohol. An aliquot, 33% H_2SO_4 (20ml) was added to the ethereal layer in the separating funnel and shaken for 2 minutes. The aqueous layer was removed and a GC of the ethereal layer was recorded. This procedure was repeated with 20ml aliquots of 33% H_2SO_4 until no alcohol could be detected by GC. The ether layer was then washed free of the majority of the acid with water. A saturated aqueous solution of potassium carbonate was then added until the aqueous layer was strongly alkaline. The aqueous layer was then removed, the combined water wash and aqueous layer were back-extracted with ether (2 x 250ml), and the ether layers were combined. Anhydrous potassium carbonate was added to the ether layer in a 2 litre flask. After subsequent filtration, the ether was removed by rotary evaporation leaving a yellow/orange liquid. A small amount of sodium metal (ca. 0.3g) was added to the flask and the product, a clear colourless liquid was purified by trap-to-trap distillation (b.p. 135-142°C): (64.15g, 37.49 % yield).

Formula: C_9H_{14}

F.W. 122.21 g mol^{-1}

^{1}H NMR (250 MHz, $CDCl_3$) δ = 1.84 (s, 6H, 2 x CH_3), 1.93 (s, 6H, 2 x CH_3), 2.74 (s, 2H, CH_2).

Infrared spectra (thin film NaCl plates) 2962 cm^{-1} (C-H str), 1652 cm^{-1} (C=C) 1444 cm^{-1} (C-H bend).

MS (EI) m/z (rel. int.): 122 (100%) [M^+], 107 (60%) [M^+ - CH_3], 91 [M^+- $2CH_3$] (40%).

5.2.28 Preparation of 1,1'-bis(diphenylphosphino)octamethyl ferrocene (86).

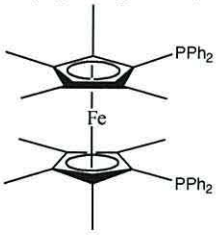

A solution of *n*-butyllithium (16.36ml, 41mmol) was added dropwise to a dry ethereal solution of 1,2,3,4-tetramethylcyclopentadiene (5g, 41mmol) at 0°C (ice bath). The reaction mixture was stirred under N_2 overnight at room temperature to give a white precipitate. This white precipitate was then filtered by means of a sinter under a N_2/vacuum line and washed with dry diethyl ether and dried under high vacuum to give a white solid. A solution of freshly distilled chlorodiphenylphosphine (33mmol, 5.9ml, 0.8eq) in THF (15ml) was added via pressure equalising dropping funnel to the stirred suspension of the white solid in THF (60ml) at -75°C (dry ice/acetone bath). The mixture was allowed to warm gradually to room temperature and stirred for another 30 minutes (solution clears). This suspension was then cooled again to -40°C (dry ice/acetone bath), relithiated with n-butyllithium (13.2ml, 33mmol, 0.8eq), warmed to room temperature and left to stir for an additional 30 minutes. Iron (II) chloride (2.1g, 16.5mmol, 0.5eq) was then added resulting in a black suspension which was left to stir overnight. The solvent was removed *in vacuo* and the product was then purified via column chromatography (isolated as the first major orange band using 9:1 CH_2Cl_2/MeOH). The orange product fraction was collected in a round bottomed flask under N_2 and the solvent was evaporated under vacuum leaving an orange product: (3.63g, 33 % yield).

Formula: $C_{42}H_{44}P_2Fe$

F.W. 666.60 g mol^{-1}

^{1}H NMR (500 MHz, $CDCl_3$) δ = 1.23 (s, 12H, 4 x β-CH_3), 1.69 (s, 12H, 4 x α-CH_3), 7.08 (t, 8H, 6.94 Hz; Ar-H), 7.16 (t, 8H, 1.58 Hz; Ar-H), 7.29 (t, 4H; Ar-H).

^{13}C NMR (125 MHz, $CDCl_3$) (weak resonances) δ = 9.94 (s, 4 x CH_3), 11.51 (s, 4 x CH_3), 127.86 (s, Ar-C), 128.18 (s, Ar-C), 132.80 (s, Ar-C), 134.97 (s, Ar-C).

^{31}P NMR (202 MHz, $CDCl_3$) δ = -22.27 (s).

MS (EI) m/z (rel. int): 666 (100%) [M^+], 667 (60%), 668 (15%).

5.2.29 Preparation of 1,1'-bis(diisopropylphosphino)octamethyl ferrocene (88).

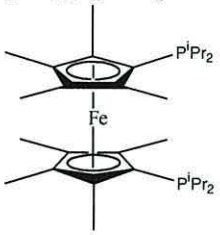

A solution of n-butyllithium (16.36ml, 41mmol) was added dropwise to the dry ethereal solution of 1,2,3,4-tetramethylcyclopentadiene (5g, 41mmol) at 0°C (ice bath). The reaction mixture was stirred under N_2 overnight at room temperature to give a white precipitate. This white precipitate was then filtered by means of a sinter under a N_2/vacuum line and washed with dry diethyl ether and dried under high vacuum to give a white solid. A solution of freshly distilled chlorodiisopropylphosphine (33mmol, 5.25ml, 0.8eq) in THF (15ml) was added via pressure equalising dropping funnel to the stirred suspension of the white solid in THF (60ml) at -75°C (dry ice/acetone bath). The mixture was allowed to warm gradually to room temperature and stirred for another 30 minutes (solution clears). This suspension was then cooled again to -40°C (dry ice/acetone bath), relithiated with n-butyllithium (13.2ml, 33mmol, 0.8eq), warmed to room temperature and left to stir for an additional 30 minutes. Iron (II) chloride (2.1g, 16.5mmol, 0.5eq) was then added resulting in a black suspension which was left to stir overnight. The solvent was removed *in vacuo* and the product was then purified via column chromatography (isolated as the first major red band using petrol). The red product fraction was collected in a round bottomed flask under N_2 and the solvent was evaporated under vacuum leaving red oil. Red crystalline product was formed when the oil was left to dry under high vacuum: (5.46g, 50.24 % yield).

Formula: $C_{30}H_{52}P_2Fe$

F.W. 530.54 g mol^{-1}

^{1}H NMR (500 MHz, $CDCl_3$) δ = 1.04 (d, 6H, 6.94 Hz; 2 x CH_3), 1.07 (d, 6H, 6.94 Hz; 2 x CH_3), 1.16 (d, 6H, 6.94 Hz; 2 x CH_3), 1.18 (d, 6H, 6.94 Hz; 2 x CH_3), 1.75 (s, 12H, 4 x β-CH_3), 1.84 (s, 12H, 4 x α-CH_3), 2.23 (q, 4H, 2.93 Hz; $PCHMe_2$).

^{13}C NMR (125 MHz, $CDCl_3$) δ = 10.33 (s, CH_3), 12.86 (d, $^3J_{PC}$ = 8.25 Hz; CH_3), 20.88 (d, $^2J_{PC}$ =10.99 Hz), 22.48 (d, $^2J_{PC}$ = 11.92 Hz), 30.46 (d, $^1J_{PC}$ = 18.32 Hz), 75.44 (s, β-Cp), 82.57 (s, α-Cp), 83.47 (d, $^1J_{PC}$ =10.99 Hz; Cp *ipso*-C).

^{31}P NMR (202 MHz, $CDCl_3$) δ = 1.04 (s).

MS [M^+] m/z (rel. int): 530 (100%), 531 (40%), 532 (10%).

Elemental analysis

Calculated: C %: 67.9, H %: 9.9, N %: 0.0.

Observed: C %: 67.7, H %: 9.7, N %: 0.0.

5.2.30 Preparation of mono-(α-dimethylaminomethyl-dimethylaminomethyl) benzene (95).

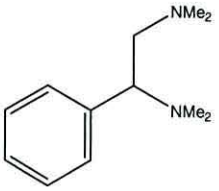

To a mixture of *N,N*-dimethyl benzylamine (6.76g, 7.5ml, 50mmol) and dry THF (20ml) was added a solution of n-butyllithium (20.4ml, 51mmol) in hexane (37ml) with cooling below -50°C (liq. N_2/acetone bath). A solution of *t*-BuOK (5.72g, 51mmol) in dry THF (30ml) was added over 15 minutes while keeping the temperature of the dark red solution between -70 and -80°C. After an additional 30 minutes, the cooling bath was removed and the temperature is allowed to rise to 0°C (ice/water bath) for 15 minutes. The solution was then cooled again to -78°C (liq. N_2/acetone bath) and eschenmoser's salt (9.25g, 50mmol) is added slowly over 10 minutes while maintaining the temperature between -70 and -80°C. At the last stages of addition the dark red solution became white. This white suspension was hydrolysed with water (100ml). The organic layer and three ethereal extracts were dried over potassium carbonate and then concentrated *in vacuo* resulting in yellow oil. This oil was then distilled under reduced pressure to yield two fractions; the starting material (a clear, colourless liquid: 65-67°C at 8.4mb) and the product (a clear, colourless liquid: 96-98°C at 8.4mb): (3.29g, 34.22 % yield).

Formula: $C_{12}H_{20}N_2$

F.W. 192.30 g mol^{-1}

^{1}H NMR (500 MHz, $CDCl_3$) δ = 2.14 (s, 6H, NCH_3), 2.20 (s, 6H, NCH_3), 3.35 (d, 2H, 5.35 Hz; CH_2N), 3.51 (t, 1H, 2.52 Hz, CHN), 7.16 (t, 1H, 1.58 Hz; Ar-H), 7.22 (t, 2H, 3.78 Hz; Ar-H), 7.29 (t; Ar-H).

^{13}C NMR (125 MHz, $CDCl_3$) δ = 41.99 (s, NCH_3), 46.08 (s, NCH_3), 62.21 (s, β-C), 67.31 (s, α-C), 127.14 (s, Ar-C), 127.89 (s, Ar-C), 128.69 (s, Ar-C), 138.08 (s, *ipso*-C).

MS (EI) m/z (rel. int.): [M^+] 191 (100), 192 (35), 193 (10).

Elemental analysis

Calculated: C %: 75.0, H %: 10.5, N %: 14.6.

Observed: C %: 74.9, H %: 10.2, N %: 14.4.

5.2.31 Preparation of bis-1,2-dimethylaminomethyl benzene (96).

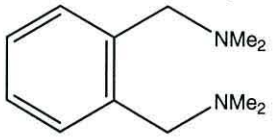

To a mixture of *N,N*-dimethyl benzylamine (7g, 52mmol) and dry ether (50ml), n-butyllithium (25ml, 62.4mmol) was added at room temperature in a Schlenk tube and the mixture was left to stir 24 hours. The solution was then cooled to -78°C (dry ice/acetone bath) and eschenmoser's salt (9.62g, 52mmol) was added slowly over 10 minutes with stirring, resulting in a white suspension. A small amount of THF was added to help dissolve the eschenmoser's salt. After overnight stirring the suspension was hydrolysed with water (100ml) and the organic layer and three ethereal extracts were dried over potassium carbonate and concentrated *in vacuo*. The product was purified by fractional distillation under reduced pressure yielding two fractions; the starting material (a clear, colourless liquid: 57-63°C at 8.8mb) and the product (a clear, yellow liquid: 105-110°C at 8.8mb): (7.59g, 75.90 % yield).

Formula: $C_{12}H_{20}N_2$

F.W. 192.30 g mol^{-1}

^{1}H NMR (500 MHz, $CDCl_3$) δ = 2.25 (s, 12H, NCH_3), 3.54 (s, 4H, CH_2N), 7.22 (t, 2H, 1.58 Hz; Ar-H), 7.30 (d, 2H, 1.57 Hz; Ar-H).

^{13}C NMR (125 MHz, $CDCl_3$) δ = 45.61 (s, NCH_3), 61.31 (s, α-C; CH_2N), 126.23 (s, Ar-C), 130.23 (s, Ar-C), 138.03 (s, *ipso*-C).

MS (GCMS) m/z (rel. int.): $[M^+ + H^+]$ 193 (100).

Elemental analysis

Calculated: C %: 75.0, H %: 10.5, N %: 14.6.

Observed: C %: 74.8, H %: 10.3, N %: 14.4.

5.2.32 Attempt at bis-1,2-(α-dimethylaminomethyl-dimethylaminomethyl) benzene (97).

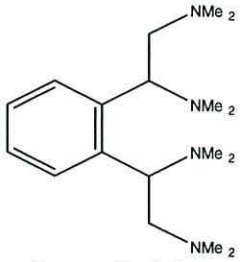

To a mixture of bis-1,2-dimethylaminomethyl benzene (3g, 15.6mmol) and dry THF (15ml) was added a solution of n-butyllithium (13.73ml, 34.32mmol, 2.2eq) in hexane (20ml) with cooling below -50°C (liq. N_2/acetone bath). A solution of *t*-BuOK (3.85g, 34.32mmol, 2.2eq) in dry THF (20ml) was added over 15 minutes while keeping the temperature of the dark red solution between -70 and -80°C. After an additional 30 minutes, the cooling bath was removed and the temperature allowed to rise to 0°C (ice/water bath) for 15 minutes. The solution was then cooled again to -78°C (liq. N_2/acetone bath) and eschenmoser's salt (6.35g, 34.32mmol, 2.2eq) was added slowly over 10 minutes while maintaining the temperature between -70 and -80°C. At the last stages of addition the dark red solution turned white. This white suspension was hydrolysed with water (50ml). The organic layer and three ethereal extracts were dried over potassium carbonate and then concentrated *in vacuo* resulting in yellow oil. This oil was then distilled under reduced pressure to yield a fraction; the starting material (a clear, colourless liquid: 65-67°C at 8.4mb) and a crude product was collected by Kugelrohr distillation (a clear, orange liquid: 240°C at r.t): (1.72g, potential 36 % yield).

Formula: $C_{18}H_{34}N_4$

F.W. 306.49 g mol^{-1}

^{1}H NMR (250 MHz, $CDCl_3$) = Mixture product/by-product resonances (impure sample).

MS: (ESI) m/z (rel. int.) $[M^+ + H^+]$ 307 (5), 250 (100).

Chapter 6

References

References

1. T. J. Kealy, P. J. Pauson. *Nature*, **1951**, 168, 1039.
2. S. A. Miller, J. A. Trebboth, J. F. Tremaine. *J. Chem. Soc.* **1952**, 632.
3. G. Wilkinson, M. Rosenblum, M. C. Whiting, R. B. Woodward. *J. Am. Chem. Soc.* **1952**, 74, 2125.
4. R. B. Woodward, M. Rosenblum, M. C. Whiting. *J. Am. Chem. Soc.* **1952**, 74, 3458.
5. D. E. Bublitz, K. L. Rinehart. *Org. React.* (N. Y.). **1969**, 17, 1.
6. R. S. Cahn, C. K. Ingold, V. Prelog. *Angew. Int. Ed. Engl.*, **1966**, 5, 385.
7. For a discussion of ferrocene chemistry from a stereochemical point of view, see the classical: K. Schlögl, *Top. Stereochem.* **1967**, 1, 39.
8. M. P. Stevens. *Polymer Chemistry, an introduction. 2nd ed.* **1990**, chapter 6, 189-233.
9. T. G. Fox, B. S. Garrett, W. E. Goode, S. Gratch, J. F. Kincaid, A. Spell, J. D. Stroupe. *J. Am. Chem. Soc.* **1958**, 80, 1768.
10. F. A. Bovey. *J. Polym. Sci.* **1960**, 46, 59.
11. D. J. Cram, K. R. Kopecky. *J. Am. Chem. Soc.* **1959**, 81, 2748-2755.
12. C. E. H. Bawn, W. H. Janes, A. M. North. *J. Polym. Sci. C.* **1963**, 4, 427.
13. K. M. Fortune. *'Nitrogen & sulphur donor complexes of molybdenum and tungsten and new routes to bis-1,2 & tris-1,2,3 substituted ferrocenes'*. Ph. D. thesis. University of Wales, Bangor. **2004**.
14. E. Drent, J. A. M. van Broekhoven, M. J. Doyle. *J. Organomet. Chem.* **1991**, 417, 235.
15. E. Drent, P. H. M. Budzelaar. *Chem. Rev.* **1996**, 96, 663.
16. A. Sen, T. Lai. *J. Am. Chem. Soc.* **1982**, 104, 3520.
17. A. Sen, T. Lai. *Organometallics.* **1984**, 3, 866.
18. A. Sen. *Adv. Polym. Sci.* **1986**, 73/74, 125.

19. A. Sen. *Acc. Chem. Res.* **1993**, 26, 303.
20. W. Keim, H. Maas. *J. Organomet. Chem.* **1996**, 514, 271.
21. M. M. Brubaker. *US Patent*, **1950**, 2,495,286.
22. P. Colombo, L. E. Kukacka, J. Fontana, R. N. Chapman, M. Steinberg. *J. Polym. Sci.* **1966**, A-1 4, 29.
23. Y. Iwashita, M. Sakuraba. *Tetrahedron Lett.* **1971**, 26, 2409.
24. R. A. M. Robertson, D. J. Cole-Hamilton. *Coord. Chem. Rev.* **2002**, 225, 67-90.
25. S. Doherty, G. R. Eastham, R. P. Tooze, T. H. Scanlan, D. Williams, M. R. J. Elsegood, W. Clegg. *Organometallics*. **1999**, 18, 3558-3560.
26. W. Clegg, G. R. Eastham, M. R. J. Elsegood, R. P. Tooze, X. L. Wang, K. Whiston. *Chem. Commun*. **1999**, 1877-1878.
27. G. R. Eastham, R. P. Tooze, X. L. Wang, K. Whiston (ICI), WO 96/19434, **1996**.
28. C. J. Moulton, B. L. Shaw. *J. Chem. Soc., Chem. Commun*. **1976**, 365.
29. L. E. Crascall, J. L. Spencer. *J. Chem. Soc., Dalton Trans*. **1992**, 3445.
30. F. Garbassi, A. Sommazzi, L. Meda, G. Mestroni, A. Sciutto. *Polymer*. **1998**, 39, 1503 and references therein.
31. S. Gibson, D. J. Cole-Hamilton, R. P. Tooze, G. R. Eastham, R. A. M. Robertson, J. A. Andersen. *Twelfth International Symposium on Homogeneous Catalysis*, Stockholm, Sweden, **2000**.
32. J.G. Knight, S. Doherty, A. Harriman, E.G. Robins, M. Betham, G. R. Eastham, R. P. Tooze, M. R. J. Elsegood, P. Champkin, W. Clegg. *Organometallics*. **2000**, 19, 4957-4967.
33. C. Bianchini, A. Meli. *Coord. Chem. Rev.* **2002**, 225, 35-66.
34. W. Keim, H. Maas. *J. Organomet. Chem*. **1993**, 514, 217.
35. D. Milstein. *Acc. Chem. Res.* **1988**, 21, 428.
36. G. R. Eastham, R. P. Tooze, B. T. Heaton, J. A. Iggo, R. Whyman, S. Zacchini. *Chem. Commun*. **2000**, 7, 609-610.
37. E. Drent, J. A. M. van Broekhoven, P. H. M. Budzelaar, in: W. A. Herrmann, B. Cornils (Eds.), *Applied Homogeneous Catalysis with Organometallic Compounds*, vol. 1, 1st ed., VCH, Weinheim, **1996**, p. 333.

38. G. R. Eastham, R. P. Tooze, M. L. Kilner, D. F. Foster, D. J. Cole-Hamilton. *J. Chem. Soc. Dalton Trans.* **2002**, 1613-1617.
39. A. Togni, T. Hayashi. *Ferrocenes*; VCH, **1995** and references therein.
40. Y. Yamamoto, T. Tanase, I. Mori, Y. Nakamura. *J. Chem. Soc., Dalton Trans.* **1994**, 3191-3192.
41. O. Riant, G. Argouarch, D. Guilaneux, O. Samuel, H. B. Kagan. *J. Org. Chem.* **1998**, 63, 3511-3514.
42. R. Broussier, E. Bentabet, M. Laly, P. Richard, L. G. Kuz'mina, P. Serp, N. Wheatley, P. Kalk, B. Gautheron. *J. Organomet. Chem.* **2000**, 613, 77-85.
43. R. Broussier, E. Bentabet, M. Laly, P. Mellet, O. Blacque, P. Boyer, M. M. Kubicki, B. Gautheron. *J. Organomet. Chem.* **2000**, 598, 365-373.
44. G. C. Fu, S. T. Nguyen, R. H. Grubbs. *J. Am. Chem. Soc.* **1993**, 115, 9856-9857.
45. M. Sawamura, H. Hamashima, M. Sugawara, R. Kuwanto, Y. Ito. *Organometallics.* **1995**, 14, 4549, and references therein.
46. A. Togni, U. Burckhardt, V. Gramlich, P. S. Pregosin, R. Salzmann. *J. Am. Chem. Soc.* **1996**, 118, 1031.
47. A. Togni, C. Breutel, A. Schnyder, F. Spindler, H. Landert, A. Tijani. *J. Am. Chem. Soc.* **1994**, 116, 4062.
48. A.Togni. *Angew. Chem. Int. Ed. Eng.* **1996**, 35, 1475.
49. J. McGarrity, F. Spindler, R. Fuchs, M. Eyer. (LONZA AG), EP-A 624 587 A2, **1995** [*Chem. Abstr.* **1995**, 122, P81369q].
50. For an account of the successful development of this process, see: F. Spindler, B. Pugin. H. P. Jalett, H. P. Buser, U. Pittelkow, H. U. Blaser. *Proceedings of the Conference on Catalysis of Organic Reactions,* Atlanta, **1996**; *Chem. Ind. (Dekker),* **1996**, 63, in press.
51. D. Marquarding, H. Klusacek, G. Gokel, P. Hoffmann, I. Ugi. *J. Am. Chem. Soc.* **1970**, 92, 5389-5393.
52. M. Hadlington, B. W. Rockett, A. Nelhans. *J. Chem. Soc.* **1967**, C, 1436-1440.
53. C. Gambs, S. Chaloupka, G. Consiglio, A. Togni. *Angew. Chem. Int. Ed.* **2000**, 39, 2486-2488.

54. O. V. Gusev, A. M. Kalsin, M. G. Peterleitner, P. V. Petrovskii, K. A. Lyssenko, N. G. Akhmedov, C. Bianchini, A. Meli, W. Oberhauser. *Organometallics.* **2002**, 21, 3637-3649.

55. R. Broussier, E. Bentabet, R. Amardeil, P. Richard, P. Meunier, P. Kalck, B. Gautheron. *J. Organomet. Chem.* **2001**, 126, 637-639.

56. J-C. Hierso, A. Fihiri, R. Amardeil, P. Meunier, H. Doucet, M. Santelli, V. V. Ivanov. *Org. Lett.* **2004**, 6, 3473-3476.

57. J-C. Hierso, V. V. Ivanov, R. Amardeil, P. Richard, P. Meunier. *Chem. Lett.* **2004**, 33, 1296-1297.

58. J-C. Hierso, A. Fihiri, V. V. Ivanov, B. Hanquet, N. Pirio, B. Donnadieu, B. Rebiere, R. Amardeil, P. Meunier. *J. Am. Chem. Soc.* **2004**, 126, 11077-11087.

59. E. Bentabet, R. Broussier, R. Amardeil, J-C. Hierso, P. Richard, D. Fasseur, B. Gautheron, P. Meunier. *J. Chem. Soc., Dalton Trans.* **2002**, 2322.

60. J-C. Hierso, A. Fihiri, R. Amardeil, P. Meunier, H. Doucet, M. Santelli, B. Donnadieu. *Organometallics.* **2003**, 22, 4490.

61. P. L. Pauson, W. E. Watts. *J. Chem. Soc.* **1963**, 2990-2996.

62. N. J. Goodwin, W. Henderson, B. Nicholson. *Chem. Commun.* **1997**, 31-32.

63. N. J. Goodwin, W. Henderson, B. Nicholson, J. K. Sarfo, J. Fawcett, D. R. Russell. *J. Chem. Soc., Dalton Trans.* **1997**, 4377-4384.

64. N. J. Goodwin, W. Henderson, B. Nicholson, J. Fawcett, D. R. Russell. *J. Chem. Soc., Dalton Trans.* **1999**, 1785-1793.

65. N. J. Goodwin, W. Henderson, J. K. Sarfo. *Chem. Commun.* **1996**, 1551-1552.

66. A. J. Downard, N. J. Goodwin, W. Henderson. *J. Organomet. Chem.* **2003**, 676, 52-72.

67. I. R. Butler, P. N. Horton, K. M. Fortune, K. Morris, C. H. Greenwell, G. R. Eastham, M. B. Hursthouse. *Inorg. Chem. Commun.* **2004**, 7, 923-928.

68. I. R. Butler, L. J. Hobson, S. M. E. Macan, D. J. Williams. *Polyhedron.* **1993**, 12, 1901-1905.

69. I. R. Butler, P. K. Baker, G. R. Eastham, K. M. Fortune, P. N. Horton, M. B. Hursthouse. *Inorg. Chem. Commun.* **2004**, 7, 1049-1052.

70. J. Schreiber, H. Maag, N. Hashimoto, A. Eschenmoser. *Angew. Chem., Int. Ed. Engl.,* **1971**, 10, 330.

71. H. C. L. Abbenhuis, U. Burckhardt, V. Gramlich, A. Togni, A. Albinati, B. Muller. *Organometallics*. **1994**, 13, 4481-4483.

72. P. E. Pfeffer, E. Kinsel, L. S. Silbert. *J. Org. Chem.* **1972**, 37, 1256-1258.

73. F. A. Cotton, G. Wilkinson. *Advanced Inorganic Chemistry;* Wiley-Intersience. **1988**, chapter 2, 64-67.

74. C. A. Tolman. *Chem. Rev.* **1977**, 77, 313.

75. T. A. Stephenson, S. M. Morehouse, A. R. Powell, J. P. Heffer, G. Wilkinson. *J. Chem. Soc.* **1965**, 3632.

76. N. Kataoka, Q. Shelby, J. P. Stambuli, J. F. Hartwig. *J. Org. Chem.* **2002**, 67, 5553.

77. D. Ledmicer, C. R. Hause. *Organic Synthesis*. 434.

78. Y. Nishibayashi, Y. Arikawa, K. Ohe, S. Uemura. *J. Org. Chem.* **1996**, 61, 1172-1174.

79. G. G. A. Balavoine, J-C. Daran, G. Iftime, E. Manoury, C. Moreau-Bossuet. *J. Organomet. Chem.* **1998**, 567, 191-198.

80. A. Patti, D. Lambusta, M. Piatelli, G. Nicolosi. *Tetrahedron: Asymmetry.* **1998**, 9, 3073-3080.

81. M. Lamac, I. Cisarova, P. Stepnicka. *J. Organomet. Chem.* **2005**, 690, 4285-4301.

82. G. Wilkinson, P. L. Pauson, F. A. Cotton. *J. Am. Chem. Soc.* **1954**, 76, 1970-1974.

83. D. E. Bublitz, W. E. McEwen, J. Kleinberg. *Organic Syntheses.* **1961**, 41, 96-98.

84. N. J. Long. *Metallocenes an Introduction to Sandwich Complexes.* Blackwell, Oxford. **1998**, chapter 4, 129-134.

85. R. Sanders, U. T. Mueller-Westerhoff. *J. Organomet. Chem.* **1997**, 512, 219.

86. M. D. Rausch, D. J. Ciappenelli. *J. Organomet. Chem.* **1967**, 10, 127.

87. I. R. Butler, W. R. Cullen, J. Ni, S. J. Rettig. *Organometallics.* **1985**, 4, 2196.

88. C. Glidewell, B. J. L. Royles, D. M. Smith. *J. Organomet. Chem.* **1967**, 527, 259.

89. For preparation of cyclopentadiene from the dimer see G. Wilkinson. *Organic Syntheses.* **1956**, 36, 31.

90. P. Beagley, M. A. L. Blackie, K. Chibale, C. Clarkson, J. R. Moss, P. J. Smith. *J. Chem. Soc., Dalton Trans.,* **2002**, 4426-4433.

91. G. W. Gokel, P. Hoffmann, I. K. Ugi. *J. Chem. Educ.* **1972**, 49, 294.
92. Y. Nishibayashi, K. Segawa, K. Ohe, S. Uemura. *Organometallics.* **1995**, 14, 5846, and references therein.
93. D. W. Slocum, R. L. Marchal, W. E. Jones. *Chem. Commun.* **1974**, 967.
94. I. R. Butler, M. G. B. Drew, C. H. Greenwell, E. Lewis, M. Plath, S. Mussig, J. Szewczyk. *Inorg. Chem. Commun.* **1999**, 2, 576.
95. M. Steurer, K. Tiedl, Y. Wang, W. Weissensteiner. *Chem. Commun.* **2005**, 4929-4931.
96. F. Rebiere, O. Riant, L. Ricard, H. B. Kagan. *Angew. Chem. Int. Engl.* **1993**, 32, 568.
97. F. Rebiere, O. Riant, L. Ricard, H. B. Kagan. *Angew. Chem. Int. Engl.* **1993**, 105, 644.
98. J. J. Bishop, A. Davidson. *J. Organomet. Chem.* **1971**, 27, 241.
99. A. W. Rudie, D. W. Lichtenberger, M. L. Katcher, A. Davison. *Inorg. Chem.* **1978**, 17, 2859.
100. I. R. Butler, W. R. Cullen, T. J. Kim, S. J. Rettig, J. Trotter. *Organometallics.* **1985**, 4, 972.
101. F. X. Kohl, P. Jutzi. *J. Organomet. Chem.* **1983**, 243, 119-121.
102. C. M. Fendrick, L. D. Schertz, V. W. Day, T. J. Marks. *Organometallics*. **1988**, 7, 1828-1838.
103. J. Szymoniak, J. Besancon, A. Dormond, C. Moise. *J. Org. Chem.* **1990**, 55, 1429-1432.
104. W. H. Puterbaugh, C. R. Hauser. *J. Am. Chem. Soc.* **1963**, 85, 2467.
105. J-E. Backvall. *Tetrahedron Lett.* **1977**, 163-166.
106. C. J. Michejda, D. H. Campbell. *J. Am. Chem. Soc.* **1979**, 101, 7687-7693.
107. K. Othmer. *Encyclopedia of Chemical Technology*, Wiley, New York, 4th edn, **1995**, vol. 16, p. 487.
108. G. Eastham, T. Scanlan, C. Barclay. *MeP Synthesis – Technical Report 138.* Lucite International – Project Alpha. **2005**.
109. G. Eastham, W. Wright, T. Scanlan, C. Barcley. *MeP Synthesis – Technical Report 139.* Lucite International – Project Alpha. **2005**.

110. Section 5.1.3 ref = D. D. Perrin, W. L. F. Armarego. *Purification of Laboratory Chemicals*. 3rd Ed., Pergamon. **1992**.

Chapter 7

Appendices

Appendices

Appendix 1: Crystal data of the palladium complex $Fc(CH_2P^tBu_2)_2PdCl_2$ (52).

Table 1. Crystal data and structure refinement.

Identification code	**04src0550**	
Empirical formula	$C_{29}H_{49}Cl_5FeP_2Pd$	
Formula weight	799.12	
Temperature	120(2) K	
Wavelength	0.71073 Å	
Crystal system	Monoclinic	
Space group	$P2_1/n$	
Unit cell dimensions	a = 11.5254(9) Å	α = 90°
	b = 14.3958(11) Å	β = 95.396(6)°
	c = 20.4783(12) Å	γ = 90°
Volume	3382.6(4) Å^3	
Z	4	
Density (calculated)	1.569 Mg / m^3	
Absorption coefficient	1.469 mm^{-1}	
F(000)	1640	
Crystal	Shard; Orange	
Crystal size	0.32 × 0.26 × 0.10 mm^3	
θ range for data collection	3.13 – 27.48°	
Index ranges	$-14 \le h \le 12$, $-17 \le k \le 18$, $-26 \le l \le 26$	
Reflections collected	33019	
Independent reflections	7725 [R_{int} = 0.0569]	
Completeness to θ = 27.48°	99.7 %	
Absorption correction	Semi–empirical from equivalents	
Max. and min. transmission	0.8670 and 0.6507	
Refinement method	Full-matrix least-squares on F^2	
Data / restraints / parameters	7725 / 6 / 392	
Goodness-of-fit on F^2	1.013	
Final R indices [$F^2 > 2\sigma(F^2)$]	$R1$ = 0.0366, $wR2$ = 0.0681	
R indices (all data)	$R1$ = 0.0651, $wR2$ = 0.0765	
Largest diff. peak and hole	0.593 and –0.870 e Å^{-3}	

Diffractometer: *Nonius KappaCCD* area detector (ϕ scans and ω scans to fill *asymmetric unit* sphere). **Cell determination:** DirAx (Duisenberg, A.J.M.(1992). J. Appl. Cryst. 25, 92-96.) **Data collection:** Collect (Collect: Data collection software, R. Hooft, Nonius B.V., 1998). **Data reduction and cell refinement**: *Denzo* (Z. Otwinowski & W. Minor, *Methods in Enzymology* (1997) Vol. **276**: *Macromolecular Crystallography*, part A, pp. 307–326; C. W. Carter, Jr. & R. M. Sweet, Eds., Academic Press). **Absorption correction**: *SORTAV* (R. H. Blessing, Acta Cryst. A**51** (1995) 33–37; R. H. Blessing, J. Appl. Cryst. **30** (1997) 421–426). **Structure solution**: *SHELXS97* (G. M. Sheldrick, Acta Cryst. (1990) A**46** 467–473). **Structure refinement**: *SHELXL97* (G. M. Sheldrick (1997), University of Göttingen, Germany). **Graphics:** Cameron - A Molecular Graphics Package. (D. M. Watkin, L. Pearce and C. K. Prout, Chemical Crystallography Laboratory, University of Oxford, 1993).

Special details:

All hydrogen atoms were fixed.
The solvent molecule of chloroform in the asymmetric unit is disordered over two sites.

Table 2. Atomic coordinates [$\times 10^4$], equivalent isotropic displacement parameters [$Å^2 \times 10^3$] and site occupancy factors. U_{eq} is defined as one third of the trace of the orthogonalized U^{ij} tensor.

Atom	*x*	*y*	*z*	U_{eq}	*S.o.f.*
C1	1988(2)	7019(2)	751(1)	16(1)	1
C2	3220(2)	7016(2)	745(1)	14(1)	1
C3	3485(3)	6936(2)	77(1)	18(1)	1
C4	2416(3)	6877(2)	−326(2)	19(1)	1
C5	1489(3)	6939(2)	86(1)	19(1)	1
C6	2417(3)	9316(2)	676(2)	30(1)	1
C7	3418(3)	9291(2)	345(2)	41(1)	1
C8	3042(4)	9189(2)	−331(2)	55(1)	1
C9	1822(4)	9156(2)	−385(2)	48(1)	1
C10	1461(3)	9235(2)	228(2)	36(1)	1
C11	1389(2)	7142(2)	1366(1)	15(1)	1
C12	4069(2)	7137(2)	1336(1)	15(1)	1
C13	119(2)	5364(2)	1368(1)	17(1)	1
C14	824(3)	4710(2)	961(2)	23(1)	1
C15	−685(3)	5955(2)	897(2)	23(1)	1
C16	−688(3)	4784(2)	1759(2)	22(1)	1
C17	581(2)	6636(2)	2611(1)	16(1)	1
C18	302(3)	5930(2)	3135(2)	26(1)	1
C19	1498(3)	7297(2)	2944(1)	21(1)	1
C20	−523(2)	7186(2)	2396(2)	21(1)	1
C21	5138(3)	5277(2)	1343(1)	18(1)	1
C22	5747(3)	4444(2)	1703(2)	24(1)	1
C23	6039(3)	5761(2)	954(2)	23(1)	1
C24	4151(3)	4858(2)	876(2)	24(1)	1
C25	5540(2)	6727(2)	2507(1)	18(1)	1
C26	4861(3)	7034(2)	3083(2)	22(1)	1
C27	6549(3)	6091(2)	2764(2)	24(1)	1
C28	6096(3)	7599(2)	2229(2)	23(1)	1
P1	1236(1)	6098(1)	1883(1)	14(1)	1
P2	4431(1)	6135(1)	1885(1)	14(1)	1
Cl1	1716(1)	4137(1)	2630(1)	22(1)	1
Cl2	4374(1)	4623(1)	3028(1)	22(1)	1
Fe1	2504(1)	8091(1)	183(1)	16(1)	1
Pd1	2928(1)	5334(1)	2310(1)	14(1)	1
C31	7640(8)	8432(10)	90(6)	25(4)	0.65(4)
Cl31	6138(4)	8247(3)	82(3)	40(2)	0.65(4)
Cl32	8351(5)	8475(6)	882(3)	37(1)	0.65(4)
Cl33	8226(8)	7590(5)	−397(4)	52(1)	0.65(4)
C36	7643(13)	8570(20)	50(9)	27(7)	0.35(4)
Cl36	6236(14)	8149(13)	137(8)	95(5)	0.35(4)
Cl37	8390(13)	8560(14)	840(7)	63(4)	0.35(4)
Cl38	8383(19)	7800(20)	−435(8)	80(4)	0.35(4)

Table 3. Bond lengths [Å] and angles [°].

C1–C2	1.422(4)	C17–C18	1.533(4)
C1–C5	1.432(4)	C17–C19	1.534(4)
C1–C11	1.502(4)	C17–P1	1.899(3)
C1–Fe1	2.055(3)	C18–H18A	0.9800
C2–C3	1.433(4)	C18–H18B	0.9800
C2–C12	1.494(4)	C18–H18C	0.9800
C2–Fe1	2.055(3)	C19–H19A	0.9800
C3–C4	1.419(4)	C19–H19B	0.9800
C3–Fe1	2.035(3)	C19–H19C	0.9800
C3–H3	0.9500	C20–H20A	0.9800
C4–C5	1.425(4)	C20–H20B	0.9800
C4–Fe1	2.032(3)	C20–H20C	0.9800
C4–H4	0.9500	C21–C23	1.535(4)
C5–Fe1	2.029(3)	C21–C24	1.538(4)
C5–H5	0.9500	C21–C22	1.541(4)
C6–C10	1.371(5)	C21–P2	1.896(3)
C6–C7	1.393(5)	C22–H22A	0.9800
C6–Fe1	2.039(3)	C22–H22B	0.9800
C6–H6	0.9500	C22–H22C	0.9800
C7–C8	1.418(6)	C23–H23A	0.9800
C7–Fe1	2.034(3)	C23–H23B	0.9800
C7–H7	0.9500	C23–H23C	0.9800
C8–C9	1.400(6)	C24–H24A	0.9800
C8–Fe1	2.027(3)	C24–H24B	0.9800
C8–H8	0.9500	C24–H24C	0.9800
C9–C10	1.363(5)	C25–C27	1.534(4)
C9–Fe1	2.036(3)	C25–C26	1.541(4)
C9–H9	0.9500	C25–C28	1.543(4)
C10–Fe1	2.045(3)	C25–P2	1.917(3)
C10–H10	0.9500	C26–H26A	0.9800
C11–P1	1.856(3)	C26–H26B	0.9800
C11–H11A	0.9900	C26–H26C	0.9800
C11–H11B	0.9900	C27–H27A	0.9800
C12–P2	1.853(3)	C27–H27B	0.9800
C12–H12A	0.9900	C27–H27C	0.9800
C12–H12B	0.9900	C28–H28A	0.9800
C13–C15	1.530(4)	C28–H28B	0.9800
C13–C16	1.532(4)	C28–H28C	0.9800
C13–C14	1.538(4)	P1–Pd1	2.3352(8)
C13–P1	1.905(3)	P2–Pd1	2.3176(7)
C14–H14A	0.9800	Cl1–Pd1	2.3502(7)
C14–H14B	0.9800	Cl2–Pd1	2.3520(8)
C14–H14C	0.9800	C31–Cl33	1.746(8)
C15–H15A	0.9800	C31–Cl32	1.747(8)
C15–H15B	0.9800	C31–Cl31	1.749(8)
C15–H15C	0.9800	C31–H31	1.0000
C16–H16A	0.9800	C36–Cl36	1.756(14)
C16–H16B	0.9800	C36–Cl37	1.758(14)
C16–H16C	0.9800	C36–Cl38	1.761(13)
C17–C20	1.528(4)	C36–H36	1.0000
C2–C1–C5	107.6(3)	C1–C2–C12	124.8(3)
C2–C1–C11	123.1(3)	C3–C2–C12	127.0(3)
C5–C1–C11	129.2(3)	C1–C2–Fe1	69.74(15)
C2–C1–Fe1	69.78(15)	C3–C2–Fe1	68.73(15)
C5–C1–Fe1	68.49(15)	C12–C2–Fe1	124.31(18)
C11–C1–Fe1	124.48(18)	C4–C3–C2	108.0(3)
C1–C2–C3	108.2(3)	C4–C3–Fe1	69.47(16)

C2–C3–Fe1	70.25(15)	C15–C13–P1	112.25(19)
C4–C3–H3	126.0	C16–C13–P1	115.1(2)
C2–C3–H3	126.0	C14–C13–P1	105.95(19)
Fe1–C3–H3	125.8	C13–C14–H14A	109.5
C3–C4–C5	108.1(3)	C13–C14–H14B	109.5
C3–C4–Fe1	69.68(16)	H14A–C14–H14B	109.5
C5–C4–Fe1	69.31(15)	C13–C14–H14C	109.5
C3–C4–H4	126.0	H14A–C14–H14C	109.5
C5–C4–H4	126.0	H14B–C14–H14C	109.5
Fe1–C4–H4	126.6	C13–C15–H15A	109.5
C4–C5–C1	108.2(3)	C13–C15–H15B	109.5
C4–C5–Fe1	69.59(15)	H15A–C15–H15B	109.5
C1–C5–Fe1	70.47(16)	C13–C15–H15C	109.5
C4–C5–H5	125.9	H15A–C15–H15C	109.5
C1–C5–H5	125.9	H15B–C15–H15C	109.5
Fe1–C5–H5	125.6	C13–C16–H16A	109.5
C10–C6–C7	108.8(3)	C13–C16–H16B	109.5
C10–C6–Fe1	70.64(19)	H16A–C16–H16B	109.5
C7–C6–Fe1	69.82(18)	C13–C16–H16C	109.5
C10–C6–H6	125.6	H16A–C16–H16C	109.5
C7–C6–H6	125.6	H16B–C16–H16C	109.5
Fe1–C6–H6	125.5	C20–C17–C18	108.8(2)
C6–C7–C8	106.7(3)	C20–C17–C19	109.0(2)
C6–C7–Fe1	70.19(18)	C18–C17–C19	106.3(2)
C8–C7–Fe1	69.32(19)	C20–C17–P1	111.5(2)
C6–C7–H7	126.7	C18–C17–P1	113.85(19)
C8–C7–H7	126.7	C19–C17–P1	107.13(19)
Fe1–C7–H7	125.4	C17–C18–H18A	109.5
C9–C8–C7	107.1(3)	C17–C18–H18B	109.5
C9–C8–Fe1	70.2(2)	H18A–C18–H18B	109.5
C7–C8–Fe1	69.81(19)	C17–C18–H18C	109.5
C9–C8–H8	126.5	H18A–C18–H18C	109.5
C7–C8–H8	126.5	H18B–C18–H18C	109.5
Fe1–C8–H8	125.1	C17–C19–H19A	109.5
C10–C9–C8	108.4(3)	C17–C19–H19B	109.5
C10–C9–Fe1	70.8(2)	H19A–C19–H19B	109.5
C8–C9–Fe1	69.5(2)	C17–C19–H19C	109.5
C10–C9–H9	125.8	H19A–C19–H19C	109.5
C8–C9–H9	125.8	H19B–C19–H19C	109.5
Fe1–C9–H9	125.4	C17–C20–H20A	109.5
C9–C10–C6	109.1(3)	C17–C20–H20B	109.5
C9–C10–Fe1	70.1(2)	H20A–C20–H20B	109.5
C6–C10–Fe1	70.12(19)	C17–C20–H20C	109.5
C9–C10–H10	125.4	H20A–C20–H20C	109.5
C6–C10–H10	125.4	H20B–C20–H20C	109.5
Fe1–C10–H10	125.9	C23–C21–C24	110.6(2)
C1–C11–P1	117.26(18)	C23–C21–C22	107.5(2)
C1–C11–H11A	108.0	C24–C21–C22	105.6(2)
P1–C11–H11A	108.0	C23–C21–P2	110.93(19)
C1–C11–H11B	108.0	C24–C21–P2	106.63(19)
P1–C11–H11B	108.0	C22–C21–P2	115.3(2)
H11A–C11–H11B	107.2	C21–C22–H22A	109.5
C2–C12–P2	119.58(18)	C21–C22–H22B	109.5
C2–C12–H12A	107.4	H22A–C22–H22B	109.5
P2–C12–H12A	107.4	C21–C22–H22C	109.5
C2–C12–H12B	107.4	H22A–C22–H22C	109.5
P2–C12–H12B	107.4	H22B–C22–H22C	109.5
H12A–C12–H12B	107.0	C21–C23–H23A	109.5
C15–C13–C16	105.8(2)	C21–C23–H23B	109.5
C15–C13–C14	108.5(2)	H23A–C23–H23B	109.5
C16–C13–C14	109.1(2)	C21–C23–H23C	109.5

H23A–C23–H23C	109.5
H23B–C23–H23C	109.5
C21–C24–H24A	109.5
C21–C24–H24B	109.5
H24A–C24–H24B	109.5
C21–C24–H24C	109.5
H24A–C24–H24C	109.5
H24B–C24–H24C	109.5
C27–C25–C26	109.4(2)
C27–C25–C28	106.5(2)
C26–C25–C28	108.0(2)
C27–C25–P2	113.50(19)
C26–C25–P2	106.35(19)
C28–C25–P2	113.0(2)
C25–C26–H26A	109.5
C25–C26–H26B	109.5
H26A–C26–H26B	109.5
C25–C26–H26C	109.5
H26A–C26–H26C	109.5
H26B–C26–H26C	109.5
C25–C27–H27A	109.5
C25–C27–H27B	109.5
H27A–C27–H27B	109.5
C25–C27–H27C	109.5
H27A–C27–H27C	109.5
H27B–C27–H27C	109.5
C25–C28–H28A	109.5
C25–C28–H28B	109.5
H28A–C28–H28B	109.5
C25–C28–H28C	109.5
H28A–C28–H28C	109.5
H28B–C28–H28C	109.5
C11–P1–C17	100.57(12)
C11–P1–C13	103.22(13)
C17–P1–C13	111.28(13)
C11–P1–Pd1	118.28(9)
C17–P1–Pd1	106.11(9)
C13–P1–Pd1	116.34(9)
C12–P2–C21	103.71(12)
C12–P2–C25	98.90(12)
C21–P2–C25	112.49(13)
C12–P2–Pd1	118.77(9)
C21–P2–Pd1	105.85(9)
C25–P2–Pd1	116.58(9)
C8–Fe1–C5	142.06(17)
C8–Fe1–C4	114.03(14)
C5–Fe1–C4	41.10(11)
C8–Fe1–C7	40.87(16)
C5–Fe1–C7	174.45(15)
C4–Fe1–C7	144.45(15)
C8–Fe1–C3	112.44(14)
C5–Fe1–C3	69.01(12)
C4–Fe1–C3	40.84(11)
C7–Fe1–C3	115.26(13)
C8–Fe1–C9	40.32(17)
C5–Fe1–C9	111.87(15)
C4–Fe1–C9	110.91(13)
C7–Fe1–C9	67.67(15)
C3–Fe1–C9	138.00(15)
C8–Fe1–C6	67.35(14)
C5–Fe1–C6	134.49(13)
C4–Fe1–C6	174.36(14)
C7–Fe1–C6	40.00(14)
C3–Fe1–C6	144.41(14)
C9–Fe1–C6	66.29(14)
C8–Fe1–C10	66.79(15)
C5–Fe1–C10	109.10(13)
C4–Fe1–C10	135.59(14)
C7–Fe1–C10	66.86(13)
C3–Fe1–C10	176.13(14)
C9–Fe1–C10	39.03(15)
C6–Fe1–C10	39.24(14)
C8–Fe1–C1	176.76(16)
C5–Fe1–C1	41.04(11)
C4–Fe1–C1	68.97(11)
C7–Fe1–C1	135.94(15)
C3–Fe1–C1	68.85(11)
C9–Fe1–C1	140.59(16)
C6–Fe1–C1	109.80(12)
C10–Fe1–C1	112.14(13)
C8–Fe1–C2	138.66(17)
C5–Fe1–C2	68.65(11)
C4–Fe1–C2	68.72(11)
C7–Fe1–C2	111.91(13)
C3–Fe1–C2	41.02(11)
C9–Fe1–C2	178.82(17)
C6–Fe1–C2	114.18(12)
C10–Fe1–C2	141.99(14)
C1–Fe1–C2	40.48(11)
P2–Pd1–P1	104.64(3)
P2–Pd1–Cl1	162.64(3)
P1–Pd1–Cl1	87.28(3)
P2–Pd1–Cl2	86.57(3)
P1–Pd1–Cl2	163.13(3)
Cl1–Pd1–Cl2	84.89(3)
Cl33–C31–Cl32	112.5(7)
Cl33–C31–Cl31	108.9(6)
Cl32–C31–Cl31	113.1(7)
Cl33–C31–H31	107.4
Cl32–C31–H31	107.4
Cl31–C31–H31	107.4
Cl36–C36–Cl37	106.3(13)
Cl36–C36–Cl38	109.9(12)
Cl37–C36–Cl38	107.0(13)
Cl36–C36–H36	111.2
Cl37–C36–H36	111.2
Cl38–C36–H36	111.2

Symmetry transformations used to generate equivalent atoms:

Table 4. Anisotropic displacement parameters [$Å^2 \times 10^3$]. The anisotropic displacement factor exponent takes the form: $-2\pi^2[h^2a^{*2}U^{11} + \cdots + 2\,h\,k\,a^*\,b^*\,U^{12}]$.

Atom	U^{11}	U^{22}	U^{33}	U^{23}	U^{13}	U^{12}
C1	18(2)	10(1)	18(2)	3(1)	0(1)	−1(1)
C2	17(2)	12(1)	13(2)	2(1)	1(1)	0(1)
C3	20(2)	16(1)	17(2)	0(1)	4(1)	−1(1)
C4	27(2)	17(1)	14(2)	−2(1)	1(1)	−4(1)
C5	18(2)	15(1)	22(2)	2(1)	−2(1)	−3(1)
C6	56(3)	16(2)	19(2)	4(1)	5(2)	4(2)
C7	19(2)	12(2)	90(3)	0(2)	−10(2)	−3(1)
C8	104(4)	14(2)	58(3)	5(2)	63(3)	1(2)
C9	88(4)	20(2)	31(2)	5(2)	−26(2)	0(2)
C10	26(2)	18(2)	64(3)	9(2)	4(2)	3(1)
C11	14(2)	12(1)	18(2)	3(1)	1(1)	−1(1)
C12	15(2)	14(1)	17(2)	−1(1)	5(1)	−1(1)
C13	14(2)	18(1)	19(2)	−2(1)	1(1)	−5(1)
C14	21(2)	23(2)	24(2)	−7(1)	1(1)	−4(1)
C15	16(2)	27(2)	24(2)	4(1)	−1(1)	−6(1)
C16	20(2)	22(2)	25(2)	−2(1)	1(1)	−6(1)
C17	17(2)	14(1)	17(2)	−1(1)	2(1)	0(1)
C18	33(2)	24(2)	22(2)	2(1)	10(2)	2(1)
C19	22(2)	26(2)	17(2)	−6(1)	1(1)	−2(1)
C20	15(2)	21(2)	26(2)	−6(1)	3(1)	1(1)
C21	17(2)	18(1)	19(2)	−2(1)	5(1)	6(1)
C22	26(2)	18(2)	29(2)	−2(1)	5(2)	6(1)
C23	21(2)	25(2)	23(2)	−1(1)	10(1)	3(1)
C24	28(2)	20(2)	25(2)	−5(1)	4(2)	2(1)
C25	16(2)	18(1)	18(2)	−1(1)	1(1)	−1(1)
C26	20(2)	25(2)	19(2)	−4(1)	−2(1)	0(1)
C27	17(2)	26(2)	28(2)	−1(1)	−3(1)	1(1)
C28	20(2)	22(2)	25(2)	−3(1)	1(1)	−5(1)
P1	14(1)	13(1)	15(1)	1(1)	2(1)	0(1)
P2	13(1)	14(1)	15(1)	0(1)	2(1)	1(1)
Cl1	21(1)	16(1)	29(1)	6(1)	4(1)	−2(1)
Cl2	20(1)	22(1)	24(1)	7(1)	−1(1)	2(1)
Fe1	20(1)	15(1)	14(1)	2(1)	2(1)	−1(1)
Pd1	14(1)	12(1)	15(1)	1(1)	2(1)	0(1)
C31	27(7)	12(4)	36(7)	16(4)	0(5)	2(3)
Cl31	20(2)	31(2)	68(2)	9(1)	8(1)	−1(1)
Cl32	45(3)	38(2)	28(2)	3(2)	−3(2)	12(2)
Cl33	56(3)	61(3)	37(2)	−5(1)	−10(2)	28(2)
C36	15(11)	38(12)	27(11)	3(8)	2(8)	−12(7)
Cl36	53(6)	114(9)	117(7)	48(7)	11(5)	−31(5)
Cl37	98(8)	32(3)	54(6)	10(3)	−26(5)	17(4)
Cl38	52(5)	154(11)	36(3)	−3(6)	13(3)	58(7)

Table 5. Hydrogen coordinates [$\times 10^4$] and isotropic displacement parameters [$Å^2 \times 10^3$].

Atom	*x*	*y*	*z*	U_{eq}	*S.o.f.*
H3	4242	6923	−70	21	1
H4	2333	6809	−789	23	1
H5	681	6928	−55	22	1
H6	2400	9378	1137	36	1
H7	4201	9334	535	50	1
H8	3526	9150	−680	66	1
H9	1330	9090	−781	58	1
H10	673	9234	328	43	1
H11A	600	7392	1240	18	1
H11B	1822	7618	1639	18	1
H12A	3767	7638	1606	18	1
H12B	4807	7366	1184	18	1
H14A	1300	4296	1256	34	1
H14B	1331	5078	703	34	1
H14C	288	4340	666	34	1
H15A	−1251	5552	647	34	1
H15B	−219	6284	593	34	1
H15C	−1098	6407	1148	34	1
H16A	−1196	5198	1984	34	1
H16B	−218	4408	2084	34	1
H16C	−1165	4376	1461	34	1
H18A	1012	5591	3290	39	1
H18B	−288	5492	2945	39	1
H18C	3	6257	3504	39	1
H19A	1645	7803	2642	32	1
H19B	2223	6956	3062	32	1
H19C	1211	7556	3341	32	1
H20A	−845	7447	2782	31	1
H20B	−1099	6774	2163	31	1
H20C	−333	7692	2103	31	1
H22A	6009	4006	1381	36	1
H22B	5199	4132	1968	36	1
H22C	6420	4664	1989	36	1
H23A	6649	6037	1259	34	1
H23B	5656	6249	679	34	1
H23C	6389	5305	676	34	1
H24A	3718	5359	638	36	1
H24B	3623	4504	1130	36	1
H24C	4484	4445	562	36	1
H26A	4559	6485	3294	32	1
H26B	4211	7435	2919	32	1
H26C	5383	7377	3404	32	1
H27A	7013	5929	2403	36	1
H27B	6236	5523	2945	36	1
H27C	7043	6414	3108	36	1
H28A	6699	7842	2553	34	1
H28B	5496	8073	2130	34	1
H28C	6447	7435	1826	34	1
H31	7752	9049	−119	30	0.65(4)
H36	7614	9213	−139	32	0.35(4)

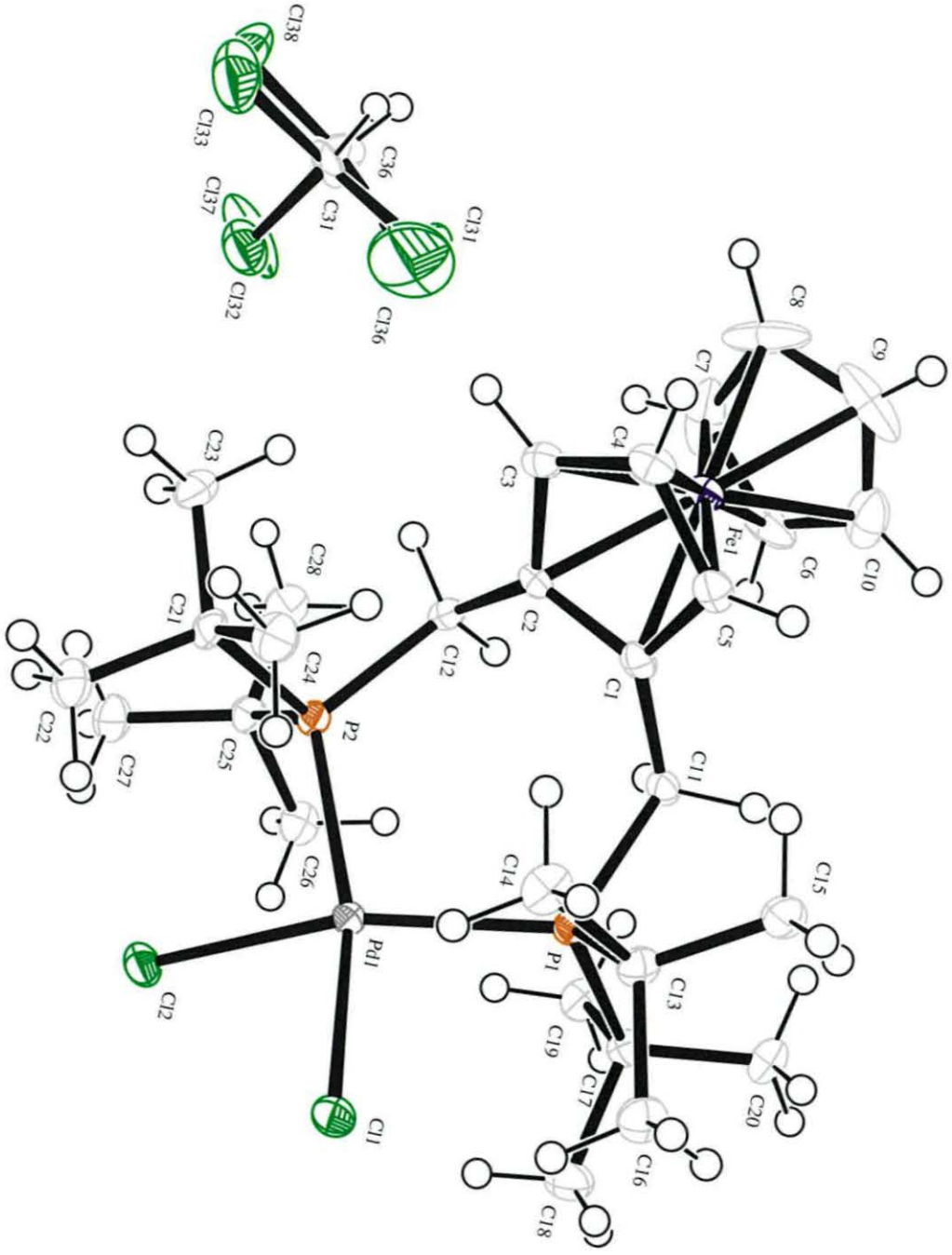

Appendix 2: Crystal data of 1,2-dimethylaminomethyl ruthenocene (58).

Table 1. Crystal data and structure refinement.

Identification code	**2005src0328**	
Empirical formula	$C_{16}H_{24}N_2Ru$	
Formula weight	345.44	
Temperature	120(2) K	
Wavelength	0.71073 Å	
Crystal system	Orthorhombic	
Space group	*Pbca*	
Unit cell dimensions	$a = 7.747(9)$ Å	$\alpha = 90°$
	$b = 15.519(18)$ Å	$\beta = 90°$
	$c = 25.745(8)$ Å	$\gamma = 90°$
Volume	3095(5) Å^3	
Z	8	
Density (calculated)	1.483 Mg / m^3	
Absorption coefficient	1.002 mm^{-1}	
F(000)	1424	
Crystal	Needle; colourless	
Crystal size	0.18 × 0.03 × 0.02 mm^3	
θ range for data collection	3.04 – 27.48°	
Index ranges	$-7 \le h \le 9, -19 \le k \le 19, -33 \le l \le 21$	
Reflections collected	13333	
Independent reflections	3397 [$R_{int} = 0.1721$]	
Completeness to $\theta = 27.48°$	95.9 %	
Absorption correction	Semi–empirical from equivalents	
Max. and min. transmission	0.9802 and 0.8402	
Refinement method	Full-matrix least-squares on F^2	
Data / restraints / parameters	3397 / 423 / 352	
Goodness-of-fit on F^2	1.114	
Final R indices [$F^2 > 2\sigma(F^2)$]	$R1 = 0.1089$, $wR2 = 0.1905$	
R indices (all data)	$R1 = 0.2192$, $wR2 = 0.2333$	
Largest diff. peak and hole	1.116 and –1.582 e Å^{-3}	

Diffractometer: *Nonius KappaCCD* area detector (ϕ scans and ω scans to fill *asymmetric unit* sphere). **Cell determination:** DirAx (Duisenberg, A.J.M.(1992). J. Appl. Cryst. 25, 92-96.) **Data collection:** Collect (Collect: Data collection software, R. Hooft, Nonius B.V., 1998). **Data reduction and cell refinement**: *Denzo* (Z. Otwinowski & W. Minor, *Methods in Enzymology* (1997) Vol. **276**: *Macromolecular Crystallography*, part A, pp. 307–326; C. W. Carter, Jr. & R. M. Sweet, Eds., Academic Press). **Absorption correction**: *SADABS Version 2.10.* (G. M. Sheldrick (2003)) Bruker AXS Inc., Madison, Wisconsin, USA. **Structure solution**: *SHELXS97* (G. M. Sheldrick, Acta Cryst. (1990) A**46** 467–473). **Structure refinement**: *SHELXL97* (G. M. Sheldrick (1997), University of Göttingen, Germany). **Graphics:** *ORTEP3 for Windows* (L. J. Farrugia, J. Appl. Crystallogr. 1997, 30, 565).

Special details:

All hydrogen atoms were fixed.
The molecule was completely disordered over two sites.

Table 2. Atomic coordinates [$\times 10^4$], equivalent isotropic displacement parameters [$Å^2 \times 10^3$] and site occupancy factors. U_{eq} is defined as one third of the trace of the orthogonalized U^{ij} tensor.

Atom	*x*	*y*	*z*	U_{eq}	*S.o.f.*
C1	886(15)	7469(8)	4102(4)	19(2)	0.852(2)
C2	−349(15)	7477(8)	3694(4)	20(2)	0.852(2)
C3	−1138(15)	8323(8)	3679(4)	20(2)	0.852(2)
C4	−367(15)	8816(8)	4065(4)	20(2)	0.852(2)
C5	884(15)	8331(8)	4341(4)	19(2)	0.852(2)
C6	4102(16)	8138(8)	3163(5)	24(2)	0.852(2)
C7	2819(15)	8173(8)	2772(4)	24(2)	0.852(2)
C8	2103(15)	9033(8)	2768(4)	22(2)	0.852(2)
C9	2956(14)	9500(8)	3148(4)	21(2)	0.852(2)
C10	4239(15)	8990(8)	3395(5)	22(2)	0.852(2)
C11	1985(15)	6737(8)	4262(5)	18(2)	0.852(2)
C12	2239(19)	5391(9)	4733(6)	23(3)	0.852(2)
C13	744(18)	6562(10)	5120(5)	24(3)	0.852(2)
C14	−871(17)	6691(10)	3342(6)	25(2)	0.852(2)
C15	−3010(20)	6238(9)	3949(5)	34(3)	0.852(2)
C16	−3170(20)	5820(10)	3078(6)	40(3)	0.852(2)
N1	1135(13)	6129(7)	4632(4)	17(2)	0.852(2)
N2	−2717(16)	6506(9)	3436(5)	30(2)	0.852(2)
Ru1	1631(1)	8424(1)	3521(1)	18(1)	0.852(2)
C21	4130(40)	7437(17)	4091(10)	20(4)	0.148(2)
C22	5380(30)	7451(17)	3688(12)	21(4)	0.148(2)
C23	6180(20)	8290(20)	3686(14)	21(4)	0.148(2)
C24	5400(40)	8780(20)	4073(12)	20(4)	0.148(2)
C25	4150(50)	8290(20)	4341(8)	20(4)	0.148(2)
C26	940(30)	8140(20)	3160(15)	20(2)	0.148(2)
C27	2230(50)	8180(20)	2770(9)	22(2)	0.148(2)
C28	2980(50)	9030(20)	2769(10)	22(2)	0.148(2)
C29	2140(40)	9503(18)	3150(14)	21(2)	0.148(2)
C30	830(30)	9000(20)	3393(14)	20(2)	0.148(2)
C31	3040(50)	6700(20)	4249(17)	19(3)	0.148(2)
C32	4310(90)	6530(40)	5101(18)	21(6)	0.148(2)
C33	2910(90)	5340(30)	4700(30)	22(5)	0.148(2)
C34	5850(50)	6720(30)	3287(19)	21(5)	0.148(2)
C35	8890(70)	7120(40)	3350(30)	22(7)	0.148(2)
C36	8000(70)	5840(40)	2950(30)	22(7)	0.148(2)
N21	3960(60)	6100(20)	4608(16)	20(4)	0.148(2)
N22	7660(50)	6470(30)	3360(20)	21(5)	0.148(2)
Ru21	3415(8)	8411(4)	3522(3)	21(1)	0.148(2)

Table 3. Bond lengths [Å] and angles [°].

C1–C2	1.422(14)	C21–C22	1.418(19)
C1–C5	1.471(15)	C21–C25	1.47(2)
C1–C11	1.479(15)	C21–C31	1.48(2)
C1–Ru1	2.183(11)	C21–Ru21	2.178(17)
C2–C3	1.449(15)	C22–C23	1.449(19)
C2–C14	1.572(17)	C22–C34	1.57(2)
C2–Ru1	2.171(12)	C22–Ru21	2.173(18)
C3–C4	1.390(14)	C23–C24	1.387(19)
C3–Ru1	2.189(11)	C23–Ru21	2.191(18)
C3–H3	0.9500	C23–H23	0.9500
C4–C5	1.418(14)	C24–C25	1.417(19)
C4–Ru1	2.175(12)	C24–Ru21	2.170(18)
C4–H4	0.9500	C24–H24	0.9500
C5–Ru1	2.193(11)	C25–Ru21	2.192(17)
C5–H5	0.9500	C25–H25	0.9500
C6–C7	1.417(15)	C26–C27	1.42(2)
C6–C10	1.455(15)	C26–C30	1.47(2)
C6–Ru1	2.170(12)	C26–Ru21	2.174(18)
C6–H6	0.9500	C26–H26	0.9500
C7–C8	1.445(15)	C27–C28	1.447(19)
C7–Ru1	2.171(11)	C27–Ru21	2.176(17)
C7–H7	0.9500	C27–H27	0.9500
C8–C9	1.386(14)	C28–C29	1.387(19)
C8–Ru1	2.188(11)	C28–Ru21	2.188(17)
C8–H8	0.9500	C28–H28	0.9500
C9–C10	1.421(14)	C29–C30	1.422(19)
C9–Ru1	2.183(11)	C29–Ru21	2.184(17)
C9–H9	0.9500	C29–H29	0.9500
C10–Ru1	2.226(12)	C30–Ru21	2.224(18)
C10–H10	0.9500	C30–H30	0.9500
C11–N1	1.494(14)	C31–N21	1.50(2)
C11–H11A	0.9900	C31–H31A	0.9900
C11–H11B	0.9900	C31–H31B	0.9900
C12–N1	1.453(16)	C32–N21	1.46(2)
C12–H12A	0.9800	C32–H32A	0.9800
C12–H12B	0.9800	C32–H32B	0.9800
C12–H12C	0.9800	C32–H32C	0.9800
C13–N1	1.456(15)	C33–N21	1.45(2)
C13–H13A	0.9800	C33–H33A	0.9800
C13–H13B	0.9800	C33–H33B	0.9800
C13–H13C	0.9800	C33–H33C	0.9800
C14–N2	1.479(18)	C34–N22	1.47(3)
C14–H14A	0.9900	C34–H34A	0.9900
C14–H14B	0.9900	C34–H34B	0.9900
C15–N2	1.404(19)	C35–N22	1.39(3)
C15–H15A	0.9800	C35–H35A	0.9800
C15–H15B	0.9800	C35–H35B	0.9800
C15–H15C	0.9800	C35–H35C	0.9800
C16–N2	1.451(16)	C36–N22	1.45(2)
C16–H16A	0.9800	C36–H36A	0.9800
C16–H16B	0.9800	C36–H36B	0.9800
C16–H16C	0.9800	C36–H36C	0.9800
C2–C1–C5	107.5(10)	C11–C1–Ru1	124.1(8)
C2–C1–C11	126.9(11)	C1–C2–C3	108.1(10)
C5–C1–C11	125.6(10)	C1–C2–C14	126.3(11)
C2–C1–Ru1	70.5(6)	C3–C2–C14	125.4(11)
C5–C1–Ru1	70.7(6)	C1–C2–Ru1	71.4(6)

C3–C2–Ru1	71.3(6)	H14A–C14–H14B	108.5
C14–C2–Ru1	126.1(8)	C12–N1–C13	109.3(10)
C4–C3–C2	107.4(10)	C12–N1–C11	110.7(9)
C4–C3–Ru1	70.9(7)	C13–N1–C11	110.4(10)
C2–C3–Ru1	69.9(6)	C15–N2–C16	109.9(13)
C4–C3–H3	126.3	C15–N2–C14	111.6(13)
C2–C3–H3	126.3	C16–N2–C14	106.0(12)
Ru1–C3–H3	124.5	C6–Ru1–C2	124.8(4)
C3–C4–C5	111.0(10)	C6–Ru1–C7	38.1(4)
C3–C4–Ru1	72.0(6)	C2–Ru1–C7	111.1(5)
C5–C4–Ru1	71.8(7)	C6–Ru1–C4	163.4(5)
C3–C4–H4	124.5	C2–Ru1–C4	63.6(4)
C5–C4–H4	124.5	C7–Ru1–C4	157.5(4)
Ru1–C4–H4	123.3	C6–Ru1–C9	63.6(4)
C4–C5–C1	106.0(10)	C2–Ru1–C9	160.1(4)
C4–C5–Ru1	70.4(6)	C7–Ru1–C9	63.1(4)
C1–C5–Ru1	70.0(6)	C4–Ru1–C9	113.8(5)
C4–C5–H5	127.0	C6–Ru1–C1	112.6(5)
C1–C5–H5	127.0	C2–Ru1–C1	38.1(4)
Ru1–C5–H5	124.3	C7–Ru1–C1	126.8(4)
C7–C6–C10	107.9(10)	C4–Ru1–C1	63.9(4)
C7–C6–Ru1	71.0(6)	C9–Ru1–C1	160.9(4)
C10–C6–Ru1	72.8(7)	C6–Ru1–C8	64.2(4)
C7–C6–H6	126.0	C2–Ru1–C8	126.3(4)
C10–C6–H6	126.0	C7–Ru1–C8	38.7(4)
Ru1–C6–H6	121.9	C4–Ru1–C8	124.7(4)
C6–C7–C8	108.1(10)	C9–Ru1–C8	37.0(4)
C6–C7–Ru1	70.9(6)	C1–Ru1–C8	160.8(4)
C8–C7–Ru1	71.3(6)	C6–Ru1–C3	158.2(4)
C6–C7–H7	125.9	C2–Ru1–C3	38.8(4)
C8–C7–H7	125.9	C7–Ru1–C3	124.5(4)
Ru1–C7–H7	123.5	C4–Ru1–C3	37.2(4)
C9–C8–C7	107.1(10)	C9–Ru1–C3	126.7(4)
C9–C8–Ru1	71.3(6)	C1–Ru1–C3	64.2(4)
C7–C8–Ru1	70.0(6)	C8–Ru1–C3	111.0(4)
C9–C8–H8	126.4	C6–Ru1–C5	128.9(4)
C7–C8–H8	126.4	C2–Ru1–C5	64.6(4)
Ru1–C8–H8	123.9	C7–Ru1–C5	162.6(4)
C8–C9–C10	111.0(10)	C4–Ru1–C5	37.9(4)
C8–C9–Ru1	71.7(6)	C9–Ru1–C5	126.8(4)
C10–C9–Ru1	72.9(7)	C1–Ru1–C5	39.3(4)
C8–C9–H9	124.5	C8–Ru1–C5	157.8(4)
C10–C9–H9	124.5	C3–Ru1–C5	63.8(4)
Ru1–C9–H9	122.5	C6–Ru1–C10	38.6(4)
C9–C10–C6	105.8(10)	C2–Ru1–C10	159.7(4)
C9–C10–Ru1	69.5(6)	C7–Ru1–C10	63.7(4)
C6–C10–Ru1	68.6(7)	C4–Ru1–C10	129.0(5)
C9–C10–H10	127.1	C9–Ru1–C10	37.6(4)
C6–C10–H10	127.1	C1–Ru1–C10	127.4(4)
Ru1–C10–H10	126.3	C8–Ru1–C10	63.2(4)
C1–C11–N1	114.1(9)	C3–Ru1–C10	160.8(4)
C1–C11–H11A	108.7	C5–Ru1–C10	113.9(5)
N1–C11–H11A	108.7	C22–C21–C25	107.6(15)
C1–C11–H11B	108.7	C22–C21–C31	127(2)
N1–C11–H11B	108.7	C25–C21–C31	125(2)
H11A–C11–H11B	107.6	C22–C21–Ru21	70.8(9)
N2–C14–C2	107.8(11)	C25–C21–Ru21	70.9(9)
N2–C14–H14A	110.1	C31–C21–Ru21	125.0(19)
C2–C14–H14A	110.1	C21–C22–C23	107.9(15)
N2–C14–H14B	110.1	C21–C22–C34	129(2)
C2–C14–H14B	110.1	C23–C22–C34	123(2)

C21–C22–Ru21	71.2(9)	H32A–C32–H32C	109.5
C23–C22–Ru21	71.3(9)	H32B–C32–H32C	109.5
C34–C22–Ru21	122(2)	N21–C33–H33A	109.5
C24–C23–C22	107.6(16)	N21–C33–H33B	109.5
C24–C23–Ru21	70.7(10)	H33A–C33–H33B	109.5
C22–C23–Ru21	69.9(9)	N21–C33–H33C	109.5
C24–C23–H23	126.2	H33A–C33–H33C	109.5
C22–C23–H23	126.2	H33B–C33–H33C	109.5
Ru21–C23–H23	124.8	N22–C34–C22	110(2)
C23–C24–C25	110.8(17)	N22–C34–H34A	109.8
C23–C24–Ru21	72.3(10)	C22–C34–H34A	109.8
C25–C24–Ru21	71.9(10)	N22–C34–H34B	109.8
C23–C24–H24	124.6	C22–C34–H34B	109.8
C25–C24–H24	124.6	H34A–C34–H34B	108.2
Ru21–C24–H24	122.8	N22–C35–H35A	109.5
C24–C25–C21	106.0(16)	N22–C35–H35B	109.5
C24–C25–Ru21	70.2(10)	H35A–C35–H35B	109.5
C21–C25–Ru21	69.9(9)	N22–C35–H35C	109.5
C24–C25–H25	127.0	H35A–C35–H35C	109.5
C21–C25–H25	127.0	H35B–C35–H35C	109.5
Ru21–C25–H25	124.6	N22–C36–H36A	109.5
C27–C26–C30	107.0(16)	N22–C36–H36B	109.5
C27–C26–Ru21	71.1(10)	H36A–C36–H36B	109.5
C30–C26–Ru21	72.4(10)	N22–C36–H36C	109.5
C27–C26–H26	126.5	H36A–C36–H36C	109.5
C30–C26–H26	126.5	H36B–C36–H36C	109.5
Ru21–C26–H26	121.8	C33–N21–C32	109(3)
C26–C27–C28	108.7(16)	C33–N21–C31	110(3)
C26–C27–Ru21	70.9(9)	C32–N21–C31	110(3)
C28–C27–Ru21	71.1(9)	C35–N22–C36	111(3)
C26–C27–H27	125.7	C35–N22–C34	117(3)
C28–C27–H27	125.7	C36–N22–C34	105(3)
Ru21–C27–H27	123.9	C24–Ru21–C22	63.6(8)
C29–C28–C27	107.2(16)	C24–Ru21–C26	163.2(12)
C29–C28–Ru21	71.3(9)	C22–Ru21–C26	124.7(11)
C27–C28–Ru21	70.2(9)	C24–Ru21–C27	157.9(12)
C29–C28–H28	126.4	C22–Ru21–C27	110.8(10)
C27–C28–H28	126.4	C26–Ru21–C27	38.0(6)
Ru21–C28–H28	123.8	C24–Ru21–C21	64.0(8)
C28–C29–C30	110.7(17)	C22–Ru21–C21	38.0(5)
C28–C29–Ru21	71.7(10)	C26–Ru21–C21	112.3(11)
C30–C29–Ru21	72.7(10)	C27–Ru21–C21	126.2(11)
C28–C29–H29	124.6	C24–Ru21–C29	113.8(11)
C30–C29–H29	124.6	C22–Ru21–C29	159.3(12)
Ru21–C29–H29	122.6	C26–Ru21–C29	64.1(8)
C29–C30–C26	106.2(16)	C27–Ru21–C29	63.1(8)
C29–C30–Ru21	69.7(9)	C21–Ru21–C29	161.8(12)
C26–C30–Ru21	68.7(9)	C24–Ru21–C28	124.9(11)
C29–C30–H30	126.9	C22–Ru21–C28	125.6(11)
C26–C30–H30	126.9	C26–Ru21–C28	64.5(8)
Ru21–C30–H30	126.3	C27–Ru21–C28	38.7(6)
C21–C31–N21	112(2)	C21–Ru21–C28	159.9(12)
C21–C31–H31A	109.1	C29–Ru21–C28	37.0(5)
N21–C31–H31A	109.1	C24–Ru21–C23	37.1(5)
C21–C31–H31B	109.1	C22–Ru21–C23	38.8(6)
N21–C31–H31B	109.1	C26–Ru21–C23	158.3(12)
H31A–C31–H31B	107.9	C27–Ru21–C23	124.8(11)
N21–C32–H32A	109.5	C21–Ru21–C23	64.1(8)
N21–C32–H32B	109.5	C29–Ru21–C23	126.2(11)
H32A–C32–H32B	109.5	C28–Ru21–C23	110.9(11)
N21–C32–H32C	109.5	C24–Ru21–C25	37.9(6)

C22–Ru21–C25	64.5(7)
C26–Ru21–C25	128.6(11)
C27–Ru21–C25	162.0(12)
C21–Ru21–C25	39.2(6)
C29–Ru21–C25	127.4(11)
C28–Ru21–C25	158.5(12)
C23–Ru21–C25	63.5(8)
C24–Ru21–C30	128.8(11)
C22–Ru21–C30	160.3(12)
C26–Ru21–C30	39.0(6)
C27–Ru21–C30	63.6(8)
C21–Ru21–C30	128.1(11)
C29–Ru21–C30	37.6(6)
C28–Ru21–C30	63.2(8)
C23–Ru21–C30	160.4(12)
C25–Ru21–C30	114.4(11)

Symmetry transformations used to generate equivalent atoms:

Table 4. Anisotropic displacement parameters [$Å^2 \times 10^3$]. The anisotropic displacement factor exponent takes the form: $-2\pi^2[h^2a^{*2}U^{11} + \cdots + 2\,h\,k\,a^*\,b^*\,U^{12}]$.

Atom	U^{11}	U^{22}	U^{33}	U^{23}	U^{13}	U^{12}
C1	21(3)	23(4)	13(3)	1(3)	1(3)	−1(3)
C2	21(4)	23(4)	17(3)	−2(3)	2(3)	−1(3)
C3	19(4)	24(4)	16(4)	1(4)	7(3)	5(4)
C4	22(4)	25(4)	13(4)	3(4)	4(4)	3(4)
C5	23(4)	24(4)	9(4)	1(4)	4(3)	2(4)
C6	20(3)	26(3)	25(3)	9(3)	7(3)	−3(3)
C7	22(4)	26(3)	23(3)	5(3)	6(3)	−3(3)
C8	19(4)	24(3)	20(3)	7(3)	7(3)	−5(3)
C9	19(3)	23(3)	21(3)	7(3)	6(3)	−7(3)
C10	16(3)	24(3)	27(3)	8(3)	6(3)	−6(3)
C11	17(4)	21(4)	14(3)	3(3)	3(3)	−1(3)
C12	28(7)	24(6)	17(5)	−2(5)	5(6)	3(5)
C13	27(6)	31(6)	16(6)	−2(6)	7(5)	8(6)
C14	27(4)	25(4)	24(4)	−6(4)	−2(4)	0(4)
C15	40(8)	23(6)	40(7)	−11(6)	5(6)	−15(6)
C16	40(7)	37(7)	42(7)	−4(6)	−2(7)	−10(7)
N1	16(4)	23(4)	11(4)	0(3)	7(3)	5(4)
N2	31(4)	26(4)	31(5)	−9(4)	−1(4)	−4(4)
Ru1	20(1)	23(1)	12(1)	2(1)	1(1)	0(1)
C21	22(7)	19(7)	19(7)	4(6)	1(7)	−3(7)
C22	23(8)	18(8)	21(7)	5(7)	−1(7)	−5(7)
C23	24(8)	18(8)	20(8)	5(8)	−2(8)	−6(8)
C24	23(8)	18(8)	20(8)	5(8)	0(8)	−5(8)
C25	23(8)	19(8)	19(8)	4(7)	0(8)	−4(8)
C26	20(3)	24(3)	17(3)	3(3)	4(3)	−2(3)
C27	20(4)	25(4)	20(3)	5(3)	6(3)	−4(4)
C28	20(4)	25(3)	21(3)	6(3)	6(3)	−5(3)
C29	19(4)	24(4)	20(3)	6(3)	6(4)	−4(4)
C30	19(3)	23(3)	17(3)	4(3)	4(3)	−2(3)
C31	20(6)	21(5)	18(5)	3(5)	2(5)	0(5)
C32	21(12)	21(12)	20(11)	2(11)	1(11)	3(12)
C33	24(9)	22(8)	18(8)	1(8)	3(9)	3(8)
C34	23(9)	17(9)	22(9)	5(8)	−1(8)	−7(8)
C35	24(14)	14(13)	29(13)	2(13)	−4(13)	−12(13)
C36	23(14)	18(13)	26(13)	5(13)	0(13)	−11(13)
N21	21(7)	21(7)	18(6)	2(6)	2(7)	1(7)
N22	23(10)	16(10)	24(10)	5(9)	−1(9)	−8(9)
Ru21	15(2)	19(2)	30(2)	2(3)	3(2)	−1(2)

Table 5. Hydrogen coordinates [$\times 10^4$] and isotropic displacement parameters [$Å^2 \times 10^3$].

Atom	*x*	*y*	*z*	U_{eq}	*S.o.f.*
H3	–2019	8507	3448	24	0.852(2)
H4	–641	9401	4136	24	0.852(2)
H5	1579	8522	4622	22	0.852(2)
H6	4758	7645	3258	28	0.852(2)
H7	2486	7711	2551	28	0.852(2)
H8	1214	9239	2546	26	0.852(2)
H9	2715	10084	3232	25	0.852(2)
H10	5024	9168	3658	27	0.852(2)
H11A	3046	6966	4426	21	0.852(2)
H11B	2337	6413	3948	21	0.852(2)
H12A	2568	5121	4404	34	0.852(2)
H12B	1616	4972	4948	34	0.852(2)
H12C	3280	5581	4917	34	0.852(2)
H13A	214	6151	5361	37	0.852(2)
H13B	–57	7039	5055	37	0.852(2)
H13C	1813	6787	5272	37	0.852(2)
H14A	–680	6832	2972	30	0.852(2)
H14B	–161	6181	3431	30	0.852(2)
H15A	–2148	5806	4047	51	0.852(2)
H15B	–4168	5986	3976	51	0.852(2)
H15C	–2925	6735	4183	51	0.852(2)
H16A	–2897	5998	2722	59	0.852(2)
H16B	–4412	5700	3105	59	0.852(2)
H16C	–2520	5300	3165	59	0.852(2)
H23	7076	8482	3460	25	0.148(2)
H24	5674	9364	4148	25	0.148(2)
H25	3455	8469	4625	24	0.148(2)
H26	271	7650	3253	24	0.148(2)
H27	2544	7716	2545	26	0.148(2)
H28	3882	9228	2550	26	0.148(2)
H29	2399	10084	3236	25	0.148(2)
H30	51	9186	3654	24	0.148(2)
H31A	2671	6384	3935	23	0.148(2)
H31B	1993	6925	4423	23	0.148(2)
H32A	3212	6676	5268	31	0.148(2)
H32B	4979	7050	5038	31	0.148(2)
H32C	4962	6137	5327	31	0.148(2)
H33A	3536	4935	4922	32	0.148(2)
H33B	2640	5062	4367	32	0.148(2)
H33C	1829	5510	4871	32	0.148(2)
H34A	5091	6217	3341	25	0.148(2)
H34B	5671	6935	2928	25	0.148(2)
H35A	9350	7190	2999	33	0.148(2)
H35B	9830	6979	3590	33	0.148(2)
H35C	8350	7666	3461	33	0.148(2)
H36A	7118	5891	2680	33	0.148(2)
H36B	7974	5260	3098	33	0.148(2)
H36C	9141	5952	2799	33	0.148(2)

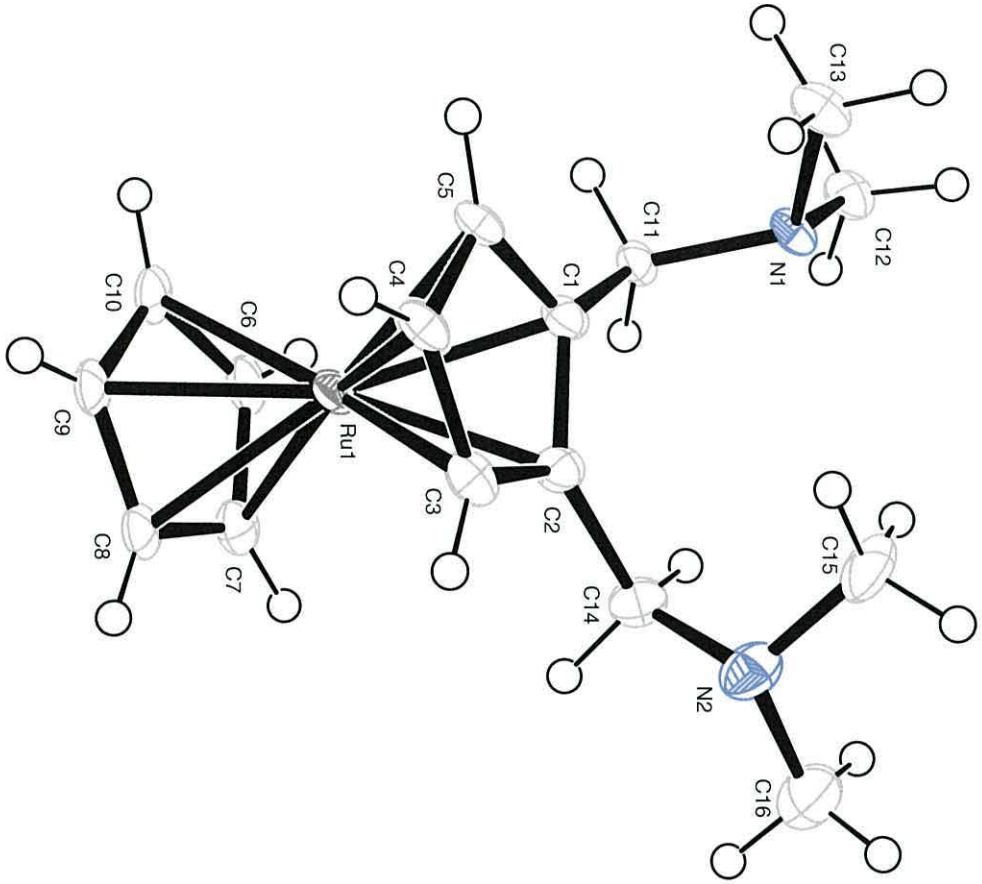

Appendix 3: Crystal data of 1-dimethylaminomethyl-5,1'-bis-triphenylsilyl ferrocene (73).

Table 1. Crystal data and structure refinement.

Identification code	**2006src1007 (KM138)**	
Empirical formula	$C_{49}H_{45}FeNSi_2$	
Formula weight	759.89	
Temperature	120(2) K	
Wavelength	0.71073 Å	
Crystal system	Monoclinic	
Space group	$P2_1/c$	
Unit cell dimensions	$a = 10.9639(2)$ Å	$\alpha = 90°$
	$b = 26.5737(5)$ Å	$\beta = 109.7280(10)°$
	$c = 14.4021(2)$ Å	$\gamma = 90°$
Volume	3949.79(12) Å^3	
Z	4	
Density (calculated)	1.278 Mg / m^3	
Absorption coefficient	0.478 mm^{-1}	
F(000)	1600	
Crystal	Block; orange	
Crystal size	0.12 × 0.05 × 0.02 mm^3	
θ range for data collection	2.96 – 27.49°	
Index ranges	$-14 \le h \le 13$, $-32 \le k \le 34$, $-18 \le l \le 18$	
Reflections collected	44731	
Independent reflections	9033 [$R_{int} = 0.0558$]	
Completeness to $\theta = 27.49°$	99.5 %	
Absorption correction	Semi–empirical from equivalents	
Max. and min. transmission	0.9905 and 0.9449	
Refinement method	Full-matrix least-squares on F^2	
Data / restraints / parameters	9033 / 0 / 480	
Goodness-of-fit on F^2	1.031	
Final R indices [$F^2 > 2\sigma(F^2)$]	$R1 = 0.0470$, $wR2 = 0.1013$	
R indices (all data)	$R1 = 0.0642$, $wR2 = 0.1090$	
Largest diff. peak and hole	0.536 and –0.480 e Å^{-3}	

Diffractometer: *Nonius KappaCCD* area detector (ϕ scans and ω scans to fill *asymmetric unit* sphere). **Cell determination:** DirAx (Duisenberg, A.J.M.(1992). J. Appl. Cryst. 25, 92-96.) **Data collection:** Collect (Collect: Data collection software, R. Hooft, Nonius B.V., 1998). **Data reduction and cell refinement**: *Denzo* (Z. Otwinowski & W. Minor, *Methods in Enzymology* (1997) Vol. **276**: *Macromolecular Crystallography*, part A, pp. 307–326; C. W. Carter, Jr. & R. M. Sweet, Eds., Academic Press). **Absorption correction**: *SORTAV* (R. H. Blessing, Acta Cryst. A**51** (1995) 33–37; R. H. Blessing, J. Appl. Cryst. **30** (1997) 421–426). **Structure solution**: *SHELXS97* (G. M. Sheldrick, Acta Cryst. (1990) A**46** 467–473). **Structure refinement**: *SHELXL97* (G. M. Sheldrick (1997), University of Göttingen, Germany). **Graphics:** Cameron - A Molecular Graphics Package. (D. M. Watkin, L. Pearce and C. K. Prout, Chemical Crystallography Laboratory, University of Oxford, 1993).

Special details:

Table 2. Atomic coordinates [$\times 10^4$], equivalent isotropic displacement parameters [$Å^2 \times 10^3$] and site occupancy factors. U_{eq} is defined as one third of the trace of the orthogonalized U^{ij} tensor.

Atom	*x*	*y*	*z*	U_{eq}	*S.o.f.*
C1	9057(2)	2716(1)	1909(2)	20(1)	1
C2	9624(2)	2404(1)	2772(2)	22(1)	1
C3	9452(2)	1890(1)	2474(2)	26(1)	1
C4	8805(2)	1869(1)	1443(2)	26(1)	1
C5	8564(2)	2372(1)	1094(2)	23(1)	1
C6	10319(2)	2577(1)	3809(2)	28(1)	1
C7	12179(3)	2987(1)	4921(2)	45(1)	1
C8	12444(3)	2443(1)	3681(2)	43(1)	1
C9	7446(2)	3674(1)	970(2)	21(1)	1
C10	6448(2)	3392(1)	321(2)	24(1)	1
C11	5318(2)	3618(1)	−283(2)	29(1)	1
C12	5156(2)	4132(1)	−251(2)	31(1)	1
C13	6127(2)	4422(1)	388(2)	33(1)	1
C14	7257(2)	4193(1)	988(2)	28(1)	1
C15	9412(2)	3756(1)	2988(2)	22(1)	1
C16	8409(2)	3835(1)	3363(2)	28(1)	1
C17	8606(3)	4092(1)	4240(2)	34(1)	1
C18	9823(3)	4275(1)	4765(2)	36(1)	1
C19	10829(3)	4204(1)	4411(2)	35(1)	1
C20	10632(2)	3948(1)	3528(2)	28(1)	1
C21	10267(2)	3563(1)	1157(2)	22(1)	1
C22	9931(2)	3849(1)	294(2)	27(1)	1
C23	10818(3)	3945(1)	−184(2)	34(1)	1
C24	12052(3)	3752(1)	191(2)	38(1)	1
C25	12407(3)	3465(1)	1037(2)	37(1)	1
C26	11531(2)	3371(1)	1522(2)	30(1)	1
C27	6114(2)	1803(1)	2069(2)	20(1)	1
C28	5710(2)	2271(1)	1547(2)	21(1)	1
C29	6189(2)	2680(1)	2204(2)	21(1)	1
C30	6890(2)	2476(1)	3145(2)	24(1)	1
C31	6848(2)	1944(1)	3064(2)	23(1)	1
C32	5246(2)	1091(1)	267(2)	20(1)	1
C33	4542(2)	673(1)	−209(2)	27(1)	1
C34	4178(2)	608(1)	−1219(2)	29(1)	1
C35	4498(2)	966(1)	−1785(2)	30(1)	1
C36	5179(3)	1388(1)	−1338(2)	33(1)	1
C37	5566(2)	1448(1)	−321(2)	27(1)	1
C38	4239(2)	960(1)	1977(2)	22(1)	1
C39	3913(2)	455(1)	2045(2)	30(1)	1
C40	2820(3)	321(1)	2265(2)	37(1)	1
C41	2035(3)	692(1)	2432(2)	42(1)	1
C42	2330(2)	1190(1)	2367(2)	39(1)	1
C43	3421(2)	1325(1)	2144(2)	27(1)	1
C44	7038(2)	701(1)	2254(2)	21(1)	1
C45	7886(2)	531(1)	1782(2)	24(1)	1
C46	8834(2)	176(1)	2214(2)	30(1)	1
C47	8953(3)	−19(1)	3124(2)	34(1)	1
C48	8142(3)	142(1)	3616(2)	36(1)	1
C49	7197(2)	499(1)	3182(2)	28(1)	1
N1	11584(2)	2798(1)	3915(2)	32(1)	1
Si1	9056(1)	3414(1)	1781(1)	19(1)	1
Si2	5689(1)	1149(1)	1639(1)	19(1)	1
Fe1	7702(1)	2242(1)	2137(1)	18(1)	1

Table 3. Bond lengths [Å] and angles [°].

C1–C5	1.442(3)	C24–C25	1.379(4)
C1–C2	1.447(3)	C25–C26	1.388(4)
C1–Si1	1.865(2)	C27–C31	1.436(3)
C1–Fe1	2.057(2)	C27–C28	1.443(3)
C2–C3	1.426(3)	C27–Si2	1.851(2)
C2–C6	1.502(3)	C27–Fe1	2.070(2)
C2–Fe1	2.040(2)	C28–C29	1.420(3)
C3–C4	1.415(3)	C28–Fe1	2.061(2)
C3–Fe1	2.041(2)	C29–C30	1.421(3)
C4–C5	1.421(3)	C29–Fe1	2.055(2)
C4–Fe1	2.064(2)	C30–C31	1.419(3)
C5–Fe1	2.056(2)	C30–Fe1	2.038(2)
C6–N1	1.466(3)	C31–Fe1	2.032(2)
C7–N1	1.462(3)	C32–C37	1.393(3)
C8–N1	1.451(3)	C32–C33	1.394(3)
C9–C10	1.394(3)	C32–Si2	1.876(2)
C9–C14	1.394(3)	C33–C34	1.383(3)
C9–Si1	1.888(2)	C34–C35	1.375(3)
C10–C11	1.387(3)	C35–C36	1.379(4)
C11–C12	1.380(4)	C36–C37	1.390(3)
C12–C13	1.383(4)	C38–C43	1.396(3)
C13–C14	1.389(3)	C38–C39	1.400(3)
C15–C16	1.395(3)	C38–Si2	1.882(2)
C15–C20	1.398(3)	C39–C40	1.386(3)
C15–Si1	1.881(2)	C40–C41	1.382(4)
C16–C17	1.387(3)	C41–C42	1.372(4)
C17–C18	1.382(4)	C42–C43	1.387(3)
C18–C19	1.374(4)	C44–C49	1.396(3)
C19–C20	1.394(3)	C44–C45	1.399(3)
C21–C22	1.396(3)	C44–Si2	1.873(2)
C21–C26	1.402(3)	C45–C46	1.386(3)
C21–Si1	1.879(2)	C46–C47	1.374(4)
C22–C23	1.392(3)	C47–C48	1.379(4)
C23–C24	1.376(4)	C48–C49	1.388(3)
C5–C1–C2	105.69(19)	C10–C9–Si1	125.20(18)
C5–C1–Si1	124.27(17)	C14–C9–Si1	117.64(17)
C2–C1–Si1	129.80(16)	C11–C10–C9	121.4(2)
C5–C1–Fe1	69.46(12)	C12–C11–C10	120.3(2)
C2–C1–Fe1	68.71(12)	C11–C12–C13	119.6(2)
Si1–C1–Fe1	130.46(12)	C12–C13–C14	119.7(2)
C3–C2–C1	108.42(19)	C13–C14–C9	121.9(2)
C3–C2–C6	124.3(2)	C16–C15–C20	117.5(2)
C1–C2–C6	127.3(2)	C16–C15–Si1	119.10(17)
C3–C2–Fe1	69.56(13)	C20–C15–Si1	123.42(18)
C1–C2–Fe1	69.93(12)	C17–C16–C15	121.8(2)
C6–C2–Fe1	127.64(17)	C18–C17–C16	119.7(2)
C4–C3–C2	108.7(2)	C19–C18–C17	119.7(2)
C4–C3–Fe1	70.74(13)	C18–C19–C20	120.7(2)
C2–C3–Fe1	69.52(13)	C19–C20–C15	120.6(2)
C3–C4–C5	107.6(2)	C22–C21–C26	117.5(2)
C3–C4–Fe1	68.94(13)	C22–C21–Si1	121.60(18)
C5–C4–Fe1	69.53(13)	C26–C21–Si1	120.83(18)
C4–C5–C1	109.5(2)	C23–C22–C21	121.5(2)
C4–C5–Fe1	70.13(13)	C24–C23–C22	119.8(2)
C1–C5–Fe1	69.48(12)	C23–C24–C25	120.0(2)
N1–C6–C2	111.8(2)	C24–C25–C26	120.5(3)
C10–C9–C14	117.1(2)	C25–C26–C21	120.7(2)

C31–C27–C28	105.46(19)	C30–Fe1–C3	124.87(10)
C31–C27–Si2	124.74(17)	C2–Fe1–C3	40.91(9)
C28–C27–Si2	129.55(17)	C31–Fe1–C29	68.44(9)
C31–C27–Fe1	68.11(12)	C30–Fe1–C29	40.61(9)
C28–C27–Fe1	69.21(12)	C2–Fe1–C29	125.98(9)
Si2–C27–Fe1	131.11(12)	C3–Fe1–C29	163.27(9)
C29–C28–C27	109.45(19)	C31–Fe1–C5	166.52(9)
C29–C28–Fe1	69.61(12)	C30–Fe1–C5	152.60(9)
C27–C28–Fe1	69.91(12)	C2–Fe1–C5	68.40(9)
C28–C29–C30	107.6(2)	C3–Fe1–C5	67.90(10)
C28–C29–Fe1	70.02(12)	C29–Fe1–C5	121.09(9)
C30–C29–Fe1	69.05(13)	C31–Fe1–C1	149.49(9)
C31–C30–C29	108.1(2)	C30–Fe1–C1	116.07(9)
C31–C30–Fe1	69.37(13)	C2–Fe1–C1	41.37(9)
C29–C30–Fe1	70.33(12)	C3–Fe1–C1	69.34(9)
C30–C31–C27	109.4(2)	C29–Fe1–C1	107.37(9)
C30–C31–Fe1	69.82(13)	C5–Fe1–C1	41.05(8)
C27–C31–Fe1	70.92(12)	C31–Fe1–C28	68.07(9)
C37–C32–C33	117.1(2)	C30–Fe1–C28	68.01(9)
C37–C32–Si2	123.71(17)	C2–Fe1–C28	165.41(9)
C33–C32–Si2	119.18(17)	C3–Fe1–C28	153.61(9)
C34–C33–C32	122.1(2)	C29–Fe1–C28	40.37(9)
C35–C34–C33	119.8(2)	C5–Fe1–C28	112.13(9)
C34–C35–C36	119.5(2)	C1–Fe1–C28	129.30(9)
C35–C36–C37	120.7(2)	C31–Fe1–C4	127.26(10)
C36–C37–C32	120.8(2)	C30–Fe1–C4	163.55(10)
C43–C38–C39	117.4(2)	C2–Fe1–C4	68.48(9)
C43–C38–Si2	120.44(18)	C3–Fe1–C4	40.32(9)
C39–C38–Si2	122.16(18)	C29–Fe1–C4	155.32(9)
C40–C39–C38	121.5(3)	C5–Fe1–C4	40.34(9)
C41–C40–C39	119.6(3)	C1–Fe1–C4	69.15(9)
C42–C41–C40	120.1(2)	C28–Fe1–C4	122.05(9)
C41–C42–C43	120.4(3)	C31–Fe1–C27	40.97(9)
C42–C43–C38	121.0(2)	C30–Fe1–C27	69.10(9)
C49–C44–C45	117.0(2)	C2–Fe1–C27	149.94(9)
C49–C44–Si2	121.35(18)	C3–Fe1–C27	117.46(9)
C45–C44–Si2	121.59(17)	C29–Fe1–C27	69.02(9)
C46–C45–C44	121.5(2)	C5–Fe1–C27	130.25(9)
C47–C46–C45	120.0(2)	C1–Fe1–C27	168.11(9)
C46–C47–C48	120.2(2)	C28–Fe1–C27	40.88(9)
C47–C48–C49	119.6(2)	C4–Fe1–C27	109.09(9)
C48–C49–C44	121.7(2)		
C8–N1–C7	110.2(2)		
C8–N1–C6	112.4(2)		
C7–N1–C6	109.3(2)		
C1–Si1–C21	106.26(10)		
C1–Si1–C15	113.27(10)		
C21–Si1–C15	112.41(10)		
C1–Si1–C9	113.23(10)		
C21–Si1–C9	106.91(10)		
C15–Si1–C9	104.71(10)		
C27–Si2–C44	111.76(10)		
C27–Si2–C32	112.12(10)		
C44–Si2–C32	109.11(10)		
C27–Si2–C38	107.70(10)		
C44–Si2–C38	107.98(10)		
C32–Si2–C38	108.02(10)		
C31–Fe1–C30	40.80(9)		
C31–Fe1–C2	115.06(9)		
C30–Fe1–C2	104.48(9)		
C31–Fe1–C3	105.60(10)		

Symmetry transformations used to generate equivalent atoms:

Table 4. Anisotropic displacement parameters [$Å^2 \times 10^3$]. The anisotropic displacement factor exponent takes the form: $-2\pi^2[h^2a^{*2}U^{11} + \cdots + 2\,h\,k\,a^*\,b^*\,U^{12}]$.

Atom	U^{11}	U^{22}	U^{33}	U^{23}	U^{13}	U^{12}
C1	18(1)	18(1)	23(1)	−2(1)	8(1)	−2(1)
C2	17(1)	20(1)	28(1)	2(1)	6(1)	−1(1)
C3	19(1)	21(1)	37(1)	3(1)	10(1)	2(1)
C4	23(1)	22(1)	37(1)	−7(1)	16(1)	−1(1)
C5	24(1)	24(1)	25(1)	−4(1)	12(1)	−4(1)
C6	25(1)	24(1)	27(1)	3(1)	2(1)	−2(1)
C7	41(2)	38(2)	40(2)	1(1)	−8(1)	−7(1)
C8	25(1)	37(2)	62(2)	7(1)	9(1)	5(1)
C9	22(1)	24(1)	20(1)	1(1)	11(1)	2(1)
C10	25(1)	23(1)	22(1)	2(1)	8(1)	−2(1)
C11	23(1)	38(2)	24(1)	3(1)	5(1)	−2(1)
C12	22(1)	39(2)	30(1)	11(1)	7(1)	6(1)
C13	32(1)	27(1)	38(1)	3(1)	11(1)	8(1)
C14	27(1)	28(1)	28(1)	−2(1)	7(1)	1(1)
C15	29(1)	15(1)	20(1)	1(1)	7(1)	−1(1)
C16	30(1)	30(1)	23(1)	−4(1)	9(1)	−3(1)
C17	44(2)	35(2)	25(1)	−3(1)	16(1)	1(1)
C18	55(2)	29(1)	22(1)	−6(1)	10(1)	−3(1)
C19	38(2)	31(2)	28(1)	−4(1)	2(1)	−7(1)
C20	31(1)	23(1)	28(1)	−1(1)	8(1)	−4(1)
C21	24(1)	19(1)	25(1)	−6(1)	10(1)	−5(1)
C22	31(1)	25(1)	26(1)	−2(1)	12(1)	−4(1)
C23	47(2)	29(1)	32(1)	−2(1)	23(1)	−8(1)
C24	40(2)	40(2)	45(2)	−13(1)	28(1)	−14(1)
C25	24(1)	43(2)	46(2)	−11(1)	16(1)	−4(1)
C26	25(1)	34(2)	32(1)	−4(1)	12(1)	−2(1)
C27	17(1)	19(1)	26(1)	1(1)	11(1)	−1(1)
C28	18(1)	22(1)	24(1)	1(1)	7(1)	−1(1)
C29	22(1)	16(1)	29(1)	−1(1)	13(1)	1(1)
C30	28(1)	25(1)	22(1)	−4(1)	13(1)	−1(1)
C31	25(1)	24(1)	24(1)	3(1)	13(1)	−1(1)
C32	18(1)	20(1)	24(1)	1(1)	9(1)	1(1)
C33	29(1)	23(1)	30(1)	3(1)	13(1)	−3(1)
C34	29(1)	25(1)	31(1)	−6(1)	8(1)	−5(1)
C35	34(1)	32(1)	22(1)	0(1)	7(1)	−1(1)
C36	44(2)	31(1)	27(1)	5(1)	16(1)	−8(1)
C37	29(1)	24(1)	30(1)	−2(1)	12(1)	−8(1)
C38	21(1)	26(1)	20(1)	−1(1)	7(1)	−5(1)
C39	34(1)	29(1)	30(1)	−2(1)	14(1)	−9(1)
C40	40(2)	42(2)	31(1)	−3(1)	15(1)	−23(1)
C41	29(1)	68(2)	34(1)	−13(1)	17(1)	−23(1)
C42	21(1)	58(2)	39(1)	−13(1)	12(1)	−2(1)
C43	22(1)	33(1)	26(1)	−2(1)	8(1)	−1(1)
C44	22(1)	16(1)	25(1)	−1(1)	8(1)	−2(1)
C45	24(1)	19(1)	32(1)	0(1)	12(1)	−3(1)
C46	24(1)	21(1)	45(2)	−6(1)	13(1)	−3(1)
C47	29(1)	23(1)	43(2)	0(1)	3(1)	6(1)
C48	44(2)	31(2)	27(1)	6(1)	6(1)	5(1)
C49	32(1)	28(1)	25(1)	1(1)	10(1)	5(1)
N1	23(1)	26(1)	38(1)	2(1)	−1(1)	−1(1)
Si1	20(1)	17(1)	20(1)	−1(1)	7(1)	−2(1)
Si2	20(1)	16(1)	22(1)	1(1)	9(1)	−1(1)

Fe1	18(1)	16(1)	19(1)	−1(1)	6(1)	−1(1)

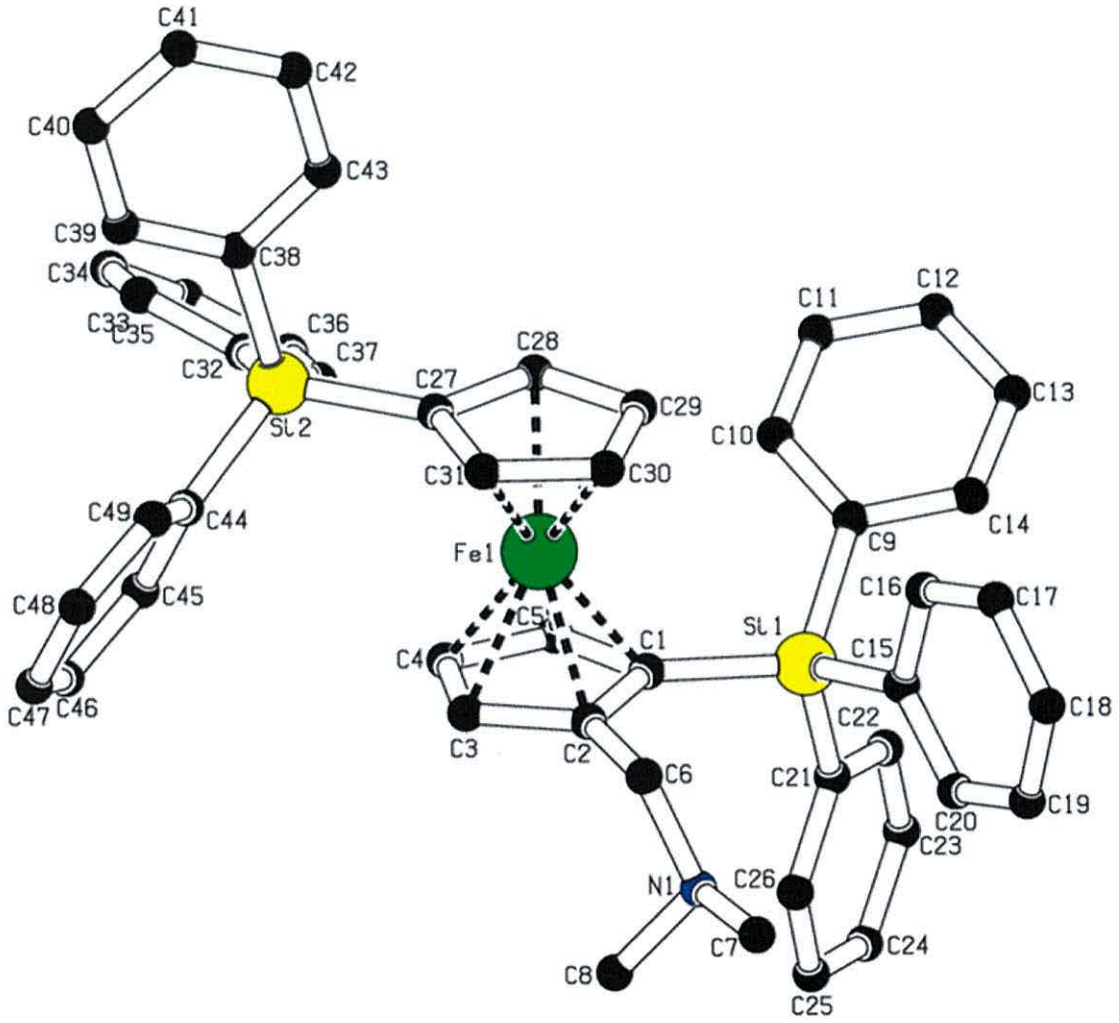

Appendix 4: Crystal data of 1,2-bis-dimethylaminomethyl-5,1'-bis-triphenylsilyl ferrocene (74).

Table 1. Crystal data and structure refinement.

Identification code	**2006src1008 (KM140)**	
Empirical formula	$C_{52}H_{52}FeN_2Si_2$	
Formula weight	816.99	
Temperature	120(2) K	
Wavelength	0.71073 Å	
Crystal system	Monoclinic	
Space group	$P2_1/c$	
Unit cell dimensions	$a = 36.5522(7)$ Å	$\alpha = 90°$
	$b = 11.9918(3)$ Å	$\beta = 130.9130(10)°$
	$c = 26.1980(5)$ Å	$\gamma = 90°$
Volume	8678.0(3) Å^3	
Z	8	
Density (calculated)	1.251 Mg / m^3	
Absorption coefficient	0.441 mm^{-1}	
F(000)	3456	
Crystal	Block; orange	
Crystal size	$0.14 \times 0.10 \times 0.08$ mm^3	
θ range for data collection	3.11 – 27.50°	
Index ranges	$-47 \le h \le 47, -15 \le k \le 15, -34 \le l \le 31$	
Reflections collected	68207	
Independent reflections	9919 [$R_{int} = 0.0706$]	
Completeness to $\theta = 27.50°$	99.6 %	
Absorption correction	Semi–empirical from equivalents	
Max. and min. transmission	0.9656 and 0.9409	
Refinement method	Full-matrix least-squares on F^2	
Data / restraints / parameters	9919 / 0 / 518	
Goodness-of-fit on F^2	1.023	
Final R indices [$F^2 > 2\sigma(F^2)$]	$R1 = 0.0441$, $wR2 = 0.0918$	
R indices (all data)	$R1 = 0.0645$, $wR2 = 0.1008$	
Largest diff. peak and hole	0.341 and –0.296 e Å^{-3}	

Diffractometer: *Nonius KappaCCD* area detector (ϕ scans and ω scans to fill *asymmetric unit* sphere). **Cell determination:** DirAx (Duisenberg, A.J.M.(1992). J. Appl. Cryst. 25, 92-96.) **Data collection:** Collect (Collect: Data collection software, R. Hooft, Nonius B.V., 1998). **Data reduction and cell refinement**: *Denzo* (Z. Otwinowski & W. Minor, *Methods in Enzymology* (1997) Vol. **276**: *Macromolecular Crystallography*, part A, pp. 307–326; C. W. Carter, Jr. & R. M. Sweet, Eds., Academic Press). **Absorption correction**: *SORTAV* (R. H. Blessing, Acta Cryst. A**51** (1995) 33–37; R. H. Blessing, J. Appl. Cryst. **30** (1997) 421–426). **Structure solution**: *SHELXS97* (G. M. Sheldrick, Acta Cryst. (1990) A**46** 467–473). **Structure refinement**: *SHELXL97* (G. M. Sheldrick (1997), University of Göttingen, Germany). **Graphics:** Cameron - A Molecular Graphics Package. (D. M. Watkin, L. Pearce and C. K. Prout, Chemical Crystallography Laboratory, University of Oxford, 1993).

Special details:

Table 2. Atomic coordinates [$\times 10^4$], equivalent isotropic displacement parameters [$Å^2 \times 10^3$] and site occupancy factors. U_{eq} is defined as one third of the trace of the orthogonalized U^{ij} tensor.

Atom	*x*	*y*	*z*	U_{eq}	*S.o.f.*
C1	1566(1)	5862(2)	4640(1)	22(1)	1
C2	1687(1)	5267(2)	5216(1)	23(1)	1
C3	1638(1)	6031(2)	5591(1)	24(1)	1
C4	1481(1)	7069(2)	5251(1)	24(1)	1
C5	1440(1)	6971(2)	4679(1)	23(1)	1
C6	1817(1)	4059(2)	5385(1)	27(1)	1
C7	2368(1)	2580(2)	5738(1)	42(1)	1
C8	2678(1)	4358(2)	6247(1)	40(1)	1
C9	1749(1)	5828(2)	6244(1)	29(1)	1
C10	2416(1)	7133(3)	6878(1)	56(1)	1
C11	2378(1)	5643(3)	7444(1)	52(1)	1
C12	343(1)	6244(2)	4368(1)	25(1)	1
C13	534(1)	5220(2)	4745(1)	27(1)	1
C14	585(1)	4439(2)	4390(1)	30(1)	1
C15	431(1)	4954(2)	3791(1)	29(1)	1
C16	283(1)	6053(2)	3775(1)	27(1)	1
C17	2220(1)	5394(2)	4311(1)	24(1)	1
C18	2615(1)	5602(2)	4987(1)	28(1)	1
C19	3086(1)	5516(2)	5240(1)	32(1)	1
C20	3170(1)	5251(2)	4811(1)	34(1)	1
C21	2786(1)	5076(2)	4135(1)	34(1)	1
C22	2314(1)	5126(2)	3887(1)	30(1)	1
C23	1256(1)	4174(2)	3511(1)	24(1)	1
C24	1467(1)	3167(2)	3857(1)	30(1)	1
C25	1234(1)	2159(2)	3577(1)	34(1)	1
C26	783(1)	2123(2)	2936(1)	34(1)	1
C27	569(1)	3101(2)	2577(1)	32(1)	1
C28	804(1)	4113(2)	2861(1)	28(1)	1
C29	1299(1)	6737(2)	3366(1)	26(1)	1
C30	1575(1)	7428(2)	3302(1)	32(1)	1
C31	1383(1)	8397(2)	2915(1)	41(1)	1
C32	913(1)	8703(2)	2589(1)	43(1)	1
C33	631(1)	8033(2)	2640(1)	38(1)	1
C34	820(1)	7064(2)	3019(1)	32(1)	1
C35	214(1)	8811(2)	4221(1)	26(1)	1
C36	484(1)	8878(2)	4019(1)	29(1)	1
C37	506(1)	9851(2)	3753(1)	32(1)	1
C38	258(1)	10787(2)	3685(1)	33(1)	1
C39	−20(1)	10742(2)	3870(1)	35(1)	1
C40	−39(1)	9771(2)	4136(1)	32(1)	1
C41	−465(1)	7338(2)	4220(1)	28(1)	1
C42	−792(1)	6710(2)	3641(1)	36(1)	1
C43	−1275(1)	6628(2)	3343(1)	44(1)	1
C44	−1435(1)	7176(2)	3627(1)	42(1)	1
C45	−1120(1)	7799(2)	4201(1)	44(1)	1
C46	−639(1)	7876(2)	4495(1)	39(1)	1
C47	584(1)	7638(2)	5529(1)	29(1)	1
C48	911(1)	8510(2)	5887(1)	36(1)	1
C49	1226(1)	8554(3)	6592(1)	48(1)	1
C50	1217(1)	7709(3)	6942(1)	53(1)	1
C51	898(1)	6834(3)	6602(1)	46(1)	1
C52	581(1)	6804(2)	5901(1)	36(1)	1
N1	2296(1)	3776(2)	5623(1)	30(1)	1
N2	2267(1)	5984(2)	6824(1)	37(1)	1
Si1	1580(1)	5509(1)	3957(1)	23(1)	1
Si2	178(1)	7509(1)	4586(1)	24(1)	1
Fe1	994(1)	5837(1)	4626(1)	21(1)	1

Table 3. Bond lengths [Å] and angles [°].

C1–C5	1.432(3)	C21–C22	1.390(3)
C1–C2	1.452(3)	C23–C28	1.397(3)
C1–Si1	1.872(2)	C23–C24	1.399(3)
C1–Fe1	2.0682(19)	C23–Si1	1.876(2)
C2–C3	1.437(3)	C24–C25	1.381(3)
C2–C6	1.498(3)	C25–C26	1.383(3)
C2–Fe1	2.0362(19)	C26–C27	1.382(3)
C3–C4	1.415(3)	C27–C28	1.387(3)
C3–C9	1.498(3)	C29–C30	1.399(3)
C3–Fe1	2.047(2)	C29–C34	1.399(3)
C4–C5	1.412(3)	C29–Si1	1.882(2)
C4–Fe1	2.054(2)	C30–C31	1.392(3)
C5–Fe1	2.059(2)	C31–C32	1.375(4)
C6–N1	1.463(3)	C32–C33	1.382(4)
C7–N1	1.453(3)	C33–C34	1.384(3)
C8–N1	1.456(3)	C35–C36	1.396(3)
C9–N2	1.469(3)	C35–C40	1.400(3)
C10–N2	1.454(4)	C35–Si2	1.880(2)
C11–N2	1.452(3)	C36–C37	1.388(3)
C12–C16	1.436(3)	C37–C38	1.380(3)
C12–C13	1.439(3)	C38–C39	1.382(3)
C12–Si2	1.856(2)	C39–C40	1.381(3)
C12–Fe1	2.060(2)	C41–C42	1.387(3)
C13–C14	1.416(3)	C41–C46	1.394(3)
C13–Fe1	2.039(2)	C41–Si2	1.877(2)
C14–C15	1.416(3)	C42–C43	1.389(3)
C14–Fe1	2.054(2)	C43–C44	1.376(4)
C15–C16	1.415(3)	C44–C45	1.370(4)
C15–Fe1	2.062(2)	C45–C46	1.387(3)
C16–Fe1	2.051(2)	C47–C48	1.391(3)
C17–C18	1.391(3)	C47–C52	1.402(3)
C17–C22	1.397(3)	C47–Si2	1.877(2)
C17–Si1	1.873(2)	C48–C49	1.399(3)
C18–C19	1.386(3)	C49–C50	1.381(4)
C19–C20	1.381(3)	C50–C51	1.376(4)
C20–C21	1.377(3)	C51–C52	1.389(3)
C5–C1–C2	106.07(17)	C4–C5–C1	109.64(18)
C5–C1–Si1	119.22(15)	C4–C5–Fe1	69.72(11)
C2–C1–Si1	134.58(16)	C1–C5–Fe1	70.04(11)
C5–C1–Fe1	69.35(11)	N1–C6–C2	114.23(17)
C2–C1–Fe1	68.10(11)	N2–C9–C3	111.21(17)
Si1–C1–Fe1	129.86(10)	C16–C12–C13	105.57(18)
C3–C2–C1	107.88(18)	C16–C12–Si2	127.80(16)
C3–C2–C6	124.91(18)	C13–C12–Si2	126.54(15)
C1–C2–C6	127.15(18)	C16–C12–Fe1	69.21(11)
C3–C2–Fe1	69.79(11)	C13–C12–Fe1	68.69(11)
C1–C2–Fe1	70.46(11)	Si2–C12–Fe1	129.14(11)
C6–C2–Fe1	123.09(14)	C14–C13–C12	109.05(19)
C4–C3–C2	108.16(17)	C14–C13–Fe1	70.33(12)
C4–C3–C9	123.85(19)	C12–C13–Fe1	70.22(11)
C2–C3–C9	127.94(19)	C15–C14–C13	108.2(2)
C4–C3–Fe1	70.07(11)	C15–C14–Fe1	70.17(12)
C2–C3–Fe1	68.99(11)	C13–C14–Fe1	69.19(12)
C9–C3–Fe1	128.61(14)	C16–C15–C14	107.78(19)
C5–C4–C3	108.23(18)	C16–C15–Fe1	69.46(12)
C5–C4–Fe1	70.13(11)	C14–C15–Fe1	69.59(12)
C3–C4–Fe1	69.56(12)	C15–C16–C12	109.43(19)

C15–C16–Fe1	70.30(12)	C23–Si1–C29	111.92(9)
C12–C16–Fe1	69.89(11)	C12–Si2–C41	107.70(10)
C18–C17–C22	117.58(19)	C12–Si2–C47	109.57(9)
C18–C17–Si1	122.30(15)	C41–Si2–C47	109.22(9)
C22–C17–Si1	120.09(16)	C12–Si2–C35	112.10(9)
C19–C18–C17	121.5(2)	C41–Si2–C35	108.16(9)
C20–C19–C18	119.8(2)	C47–Si2–C35	110.02(10)
C21–C20–C19	120.0(2)	C2–Fe1–C13	120.17(8)
C20–C21–C22	120.1(2)	C2–Fe1–C3	41.21(8)
C21–C22–C17	121.0(2)	C13–Fe1–C3	104.47(8)
C28–C23–C24	117.1(2)	C2–Fe1–C16	158.24(8)
C28–C23–Si1	124.35(17)	C13–Fe1–C16	68.08(8)
C24–C23–Si1	118.50(15)	C3–Fe1–C16	160.45(8)
C25–C24–C23	121.6(2)	C2–Fe1–C4	68.77(8)
C24–C25–C26	120.1(2)	C13–Fe1–C4	120.78(8)
C27–C26–C25	119.6(2)	C3–Fe1–C4	40.37(8)
C26–C27–C28	120.2(2)	C16–Fe1–C4	126.64(9)
C27–C28–C23	121.4(2)	C2–Fe1–C14	104.63(9)
C30–C29–C34	116.7(2)	C13–Fe1–C14	40.48(8)
C30–C29–Si1	120.99(16)	C3–Fe1–C14	119.12(9)
C34–C29–Si1	122.05(16)	C16–Fe1–C14	67.71(9)
C31–C30–C29	121.6(2)	C4–Fe1–C14	155.26(9)
C32–C31–C30	120.2(2)	C2–Fe1–C5	68.50(8)
C31–C32–C33	119.5(2)	C13–Fe1–C5	157.95(8)
C32–C33–C34	120.3(2)	C3–Fe1–C5	67.80(8)
C33–C34–C29	121.7(2)	C16–Fe1–C5	111.98(8)
C36–C35–C40	116.7(2)	C4–Fe1–C5	40.15(8)
C36–C35–Si2	122.95(16)	C14–Fe1–C5	161.44(8)
C40–C35–Si2	120.32(16)	C2–Fe1–C12	157.49(8)
C37–C36–C35	121.8(2)	C13–Fe1–C12	41.09(8)
C38–C37–C36	119.9(2)	C3–Fe1–C12	121.73(8)
C37–C38–C39	119.7(2)	C16–Fe1–C12	40.90(8)
C40–C39–C38	120.1(2)	C4–Fe1–C12	107.70(8)
C39–C40–C35	121.8(2)	C14–Fe1–C12	68.83(9)
C42–C41–C46	117.2(2)	C5–Fe1–C12	124.03(8)
C42–C41–Si2	120.89(16)	C2–Fe1–C15	120.93(9)
C46–C41–Si2	121.82(17)	C13–Fe1–C15	68.01(9)
C41–C42–C43	121.5(2)	C3–Fe1–C15	155.59(9)
C44–C43–C42	119.7(2)	C16–Fe1–C15	40.25(9)
C45–C44–C43	120.3(2)	C4–Fe1–C15	163.32(9)
C44–C45–C46	119.6(2)	C14–Fe1–C15	40.24(9)
C45–C46–C41	121.7(2)	C5–Fe1–C15	127.34(8)
C48–C47–C52	117.5(2)	C12–Fe1–C15	68.76(8)
C48–C47–Si2	122.68(18)	C2–Fe1–C1	41.44(8)
C52–C47–Si2	119.74(18)	C13–Fe1–C1	158.13(8)
C47–C48–C49	121.3(2)	C3–Fe1–C1	69.17(8)
C50–C49–C48	119.5(3)	C16–Fe1–C1	124.36(8)
C51–C50–C49	120.5(2)	C4–Fe1–C1	68.66(8)
C50–C51–C52	119.8(3)	C14–Fe1–C1	123.01(8)
C51–C52–C47	121.4(3)	C5–Fe1–C1	40.61(8)
C7–N1–C8	109.30(19)	C12–Fe1–C1	159.87(8)
C7–N1–C6	108.66(18)	C15–Fe1–C1	108.71(8)
C8–N1–C6	111.54(18)		
C11–N2–C10	110.2(2)		
C11–N2–C9	110.38(19)		
C10–N2–C9	111.7(2)		
C1–Si1–C17	110.57(9)		
C1–Si1–C23	112.74(9)		
C17–Si1–C23	108.68(9)		
C1–Si1–C29	105.54(9)		
C17–Si1–C29	107.24(9)		

Table 4. Anisotropic displacement parameters [$Å^2 \times 10^3$]. The anisotropic displacement factor exponent takes the form: $-2\pi^2[h^2a^{*2}U^{11} + \cdots + 2\,h\,k\,a^*\,b^*\,U^{12}]$.

Atom	U^{11}	U^{22}	U^{33}	U^{23}	U^{13}	U^{12}
C1	20(1)	22(1)	23(1)	1(1)	13(1)	−1(1)
C2	20(1)	24(1)	22(1)	1(1)	13(1)	0(1)
C3	20(1)	27(1)	22(1)	−2(1)	12(1)	−2(1)
C4	22(1)	23(1)	23(1)	−4(1)	13(1)	−1(1)
C5	21(1)	21(1)	22(1)	0(1)	12(1)	−2(1)
C6	28(1)	26(1)	30(1)	4(1)	21(1)	4(1)
C7	46(1)	33(1)	50(2)	12(1)	34(1)	14(1)
C8	30(1)	44(2)	38(1)	6(1)	18(1)	8(1)
C9	29(1)	34(1)	25(1)	1(1)	18(1)	0(1)
C10	45(2)	76(2)	31(1)	−10(1)	18(1)	−28(2)
C11	50(2)	70(2)	26(1)	4(1)	20(1)	1(1)
C12	21(1)	28(1)	25(1)	−1(1)	15(1)	−1(1)
C13	23(1)	28(1)	29(1)	0(1)	17(1)	−2(1)
C14	27(1)	24(1)	38(1)	−4(1)	21(1)	−5(1)
C15	24(1)	33(1)	28(1)	−11(1)	16(1)	−6(1)
C16	21(1)	31(1)	23(1)	−2(1)	12(1)	−1(1)
C17	27(1)	21(1)	26(1)	2(1)	18(1)	0(1)
C18	28(1)	29(1)	26(1)	0(1)	17(1)	−3(1)
C19	27(1)	31(1)	28(1)	1(1)	14(1)	−4(1)
C20	28(1)	29(1)	44(1)	3(1)	23(1)	−1(1)
C21	35(1)	34(1)	42(1)	−1(1)	29(1)	0(1)
C22	29(1)	30(1)	27(1)	−1(1)	17(1)	−1(1)
C23	24(1)	26(1)	25(1)	−2(1)	18(1)	−1(1)
C24	28(1)	32(1)	29(1)	−2(1)	18(1)	−1(1)
C25	40(1)	26(1)	39(1)	1(1)	26(1)	3(1)
C26	41(1)	28(1)	38(1)	−8(1)	28(1)	−8(1)
C27	30(1)	36(1)	25(1)	−8(1)	16(1)	−5(1)
C28	31(1)	29(1)	26(1)	−1(1)	20(1)	1(1)
C29	30(1)	26(1)	19(1)	−1(1)	14(1)	1(1)
C30	35(1)	29(1)	26(1)	2(1)	18(1)	−1(1)
C31	51(2)	33(1)	33(1)	2(1)	25(1)	−6(1)
C32	55(2)	28(1)	24(1)	3(1)	16(1)	5(1)
C33	38(1)	37(1)	24(1)	2(1)	14(1)	9(1)
C34	32(1)	33(1)	24(1)	0(1)	16(1)	3(1)
C35	23(1)	26(1)	21(1)	−3(1)	11(1)	0(1)
C36	24(1)	27(1)	29(1)	2(1)	15(1)	5(1)
C37	26(1)	34(1)	32(1)	3(1)	18(1)	2(1)
C38	34(1)	26(1)	29(1)	3(1)	16(1)	2(1)
C39	40(1)	27(1)	35(1)	1(1)	23(1)	9(1)
C40	33(1)	33(1)	30(1)	−1(1)	20(1)	5(1)
C41	25(1)	30(1)	28(1)	5(1)	18(1)	4(1)
C42	32(1)	46(2)	34(1)	−3(1)	23(1)	−5(1)
C43	32(1)	60(2)	35(1)	−3(1)	20(1)	−11(1)
C44	28(1)	58(2)	40(1)	17(1)	22(1)	4(1)
C45	38(1)	55(2)	50(2)	7(1)	34(1)	10(1)
C46	33(1)	46(2)	39(1)	−4(1)	24(1)	2(1)
C47	26(1)	34(1)	26(1)	−2(1)	18(1)	6(1)
C48	32(1)	41(1)	32(1)	−6(1)	21(1)	1(1)
C49	37(1)	63(2)	35(1)	−16(1)	21(1)	−1(1)
C50	45(2)	81(2)	28(1)	−2(1)	22(1)	17(2)
C51	52(2)	59(2)	36(1)	12(1)	33(1)	22(1)
C52	39(1)	41(1)	35(1)	3(1)	28(1)	9(1)
N1	28(1)	27(1)	36(1)	7(1)	21(1)	9(1)
N2	31(1)	52(1)	22(1)	0(1)	15(1)	0(1)
Si1	22(1)	23(1)	21(1)	1(1)	14(1)	1(1)

Si2	22(1)	26(1)	24(1)	−1(1)	14(1)	2(1)
Fe1	20(1)	21(1)	20(1)	−1(1)	12(1)	0(1)

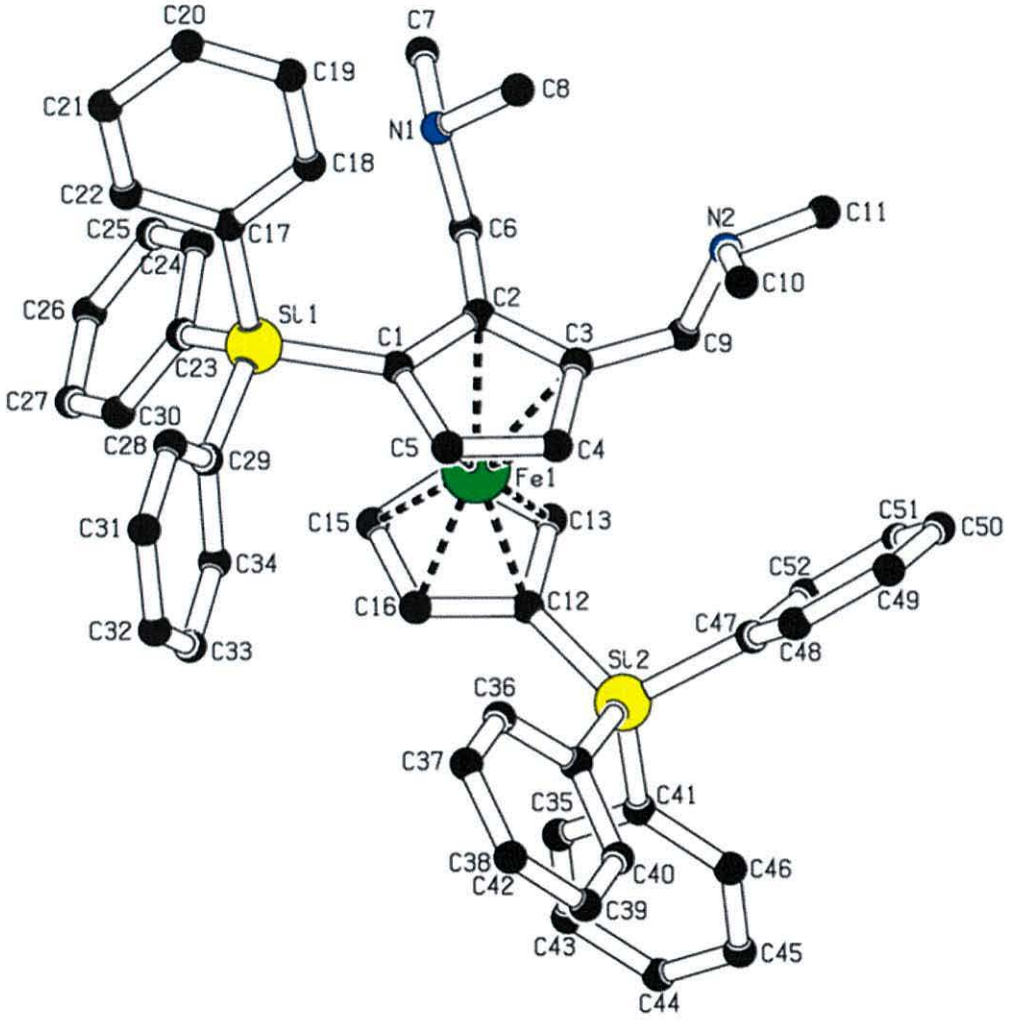

Chapter 8

Publications

Available online at www.sciencedirect.com
SCIENCE DIRECT®
Inorganic Chemistry Communications 7 (2004) 923–928
INORGANIC CHEMISTRY COMMUNICATIONS
www.elsevier.com/locate/inoche

The first 1,2,3-tris(phosphinomethyl)ferrocene

Ian R. Butler [a,*], Peter N. Horton [b], Kevin M. Fortune [a], Kevin Morris [a], Christopher H. Greenwell [a], Graham R. Eastham [c], Michael B. Hursthouse [b]

[a] *Department of Chemistry, University of Wales, Bangor, Gwynedd LL57 2UW, UK*
[b] *Department of Chemistry, University of Southampton, Highfield, Southampton SO17 1BJ, UK*
[c] *Lucite International, P.O. Box 90, Wilton, Middlesborough, Cleveland TS90 8JE, UK*

Received 31 March 2004; accepted 10 April 2004
Available online 17 June 2004

Abstract

The synthesis of the first 1,2,3-tris(phosphinomethyl)ferrocene is reported using an efficient lithiation and quench technique in which dimethylaminomethylferrocenes are useful intermediates.

Keywords: Ferrocene; Phosphines; Ligand

Ferrocenylphosphines continue to be useful ligands in both academic and industrial synthetic methodologies [1,2]. In a recent paper the general synthesis of a 1,2-bis(phosphinomethyl)ferrocene **2**, from the bis-methylamine **1**, was described. The ligand **1** was subsequently found to be effective in the palladium-catalysed synthesis of methylpropionate exhibiting extremely high selectivity towards the product (rather than towards polymer formation) and high turnover numbers [3].

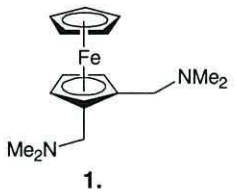

1.

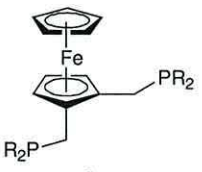

2.

Although two synthetic routes to this ligand **2** were described it was clear that it may be possible to further extend the one of these routes to obtain 1,2,3-trisubstituted ferrocenes and perhaps beyond this to obtain ultimately penta- or even deca-substituted ferrocenes by extension of the methodology, Scheme 1.

This paper describes the first extension of the work to obtain 1,2,3-trisubstituted derivatives. Such derivatives, in addition to being unusual in their own right, should exhibit enhanced stability when used in metal-catalysed processes.

Previous attempts to find a synthesis of tris-1,2,3-substituted ferrocenes had proven fruitless, although tridentate ferrocenylphosphines were known. For example, the preparation of two such species, tris-1,2, 1,-diphenylphosphino ferrocene (tdppf) and tris-1,3,1′-diphenylphosphino ferrocene (tdppf) [4], have been reported and these are illustrated in Fig. 1. In addition Broussier et al. [5] have reported the elegant synthesese of poly-phosphinoferrocenes using appropriately substituted cyclopentadienes as ferrocene precursors.

As previously noted, there are two possible synthetic routes to the tri-substituted compounds the first using 1,2,3-tris (dimethylaminomethyl)ferrocene **3** as precursor to compound tris-phosphine **8** by following the methodology adopted, [3] for the bis-methylamine compound, although initial results were unpromising. It was originally thought that Eschenmoser's salt was insufficiently electrophilic to substitute the 3-position of the largely deactivated disubstituted ferrocene. The alternative approach was to use formaldehyde as the

* Corresponding author. Tel.: +441248382390; fax: +441248370528.
E-mail addresses: i.r.butler@bangor.ac.uk, i.r.butler@ferrocene.com, chs026@bangor.ac.uk (I.R. Butler).

1387-7003/$ - see front matter © 2004 Elsevier B.V. All rights reserved.
doi:10.1016/j.inoche.2004.04.006

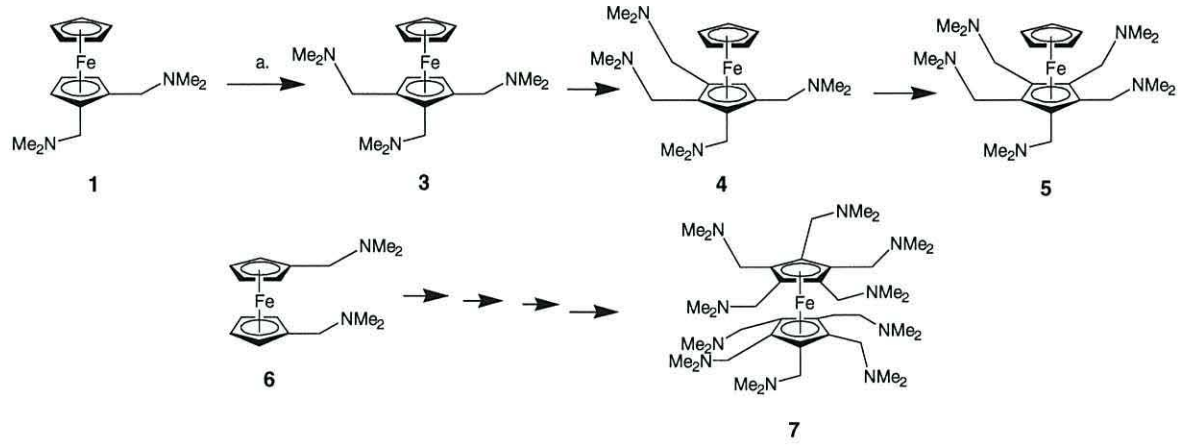

Scheme 1. Potential route to multisubstituted ferrocenes.

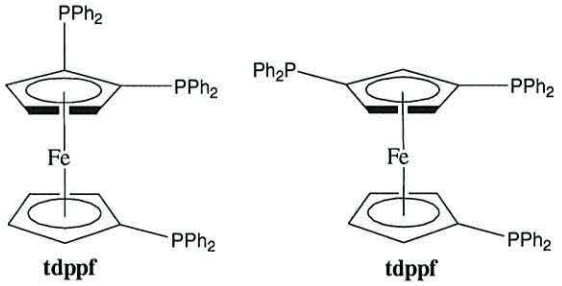

Fig. 1. Tridentate diphenylphosphinoferrocenes.

electrophile, thereby incorporting an hydroxymethyl group to give the NNO tris-substituted ferrocene, **8**. Initial reactions of the lithium salt derived from compound **1** with commercial *para*-formaldehyde were unsuccessful, giving only small quantities of product. Again it was postulated the formaldehyde in its polymeric form may have been insufficiently electrophilic due to the energy cost of breaking the bonds of the polymer precursor to formaldehyde, thus it was decided to attempt the thermal depolymerisation of *para*-formaldehyde and subsequent reaction of molecular formaldehyde with the lithiated bis-substituted ferrocene. Pfeffer et al. [6] reported the thermal decomposition of formaldehyde and its subsequent reaction with substrates in solution, by heating to 180 °C and carrying the molecular formaldehyde into a reaction vessel by a stream of inert gas. Employing this methodology, an attempt was again made to prepare 1-hydroxymethyl-bis-2,3-dimethylaminomethyl ferrocene. The depolymerised formaldehyde was carried over the solution of *ortho*-lithiated-bis-1,2-(dimethylaminomethyl)ferrocene by a stream of nitrogen. As a safety measure, the effluent gas was bubbled through a KOH bath, to re-polymerize the formaldehyde. This last step was necessary due to the highly toxic nature of molecular formaldehyde. Initial ^{1}H NMR analysis showed the target compound to be present in the reaction mixture in good yield, but there were other unidentified products present, presumably resulting from reaction between the amine and the highly reactive formaldehyde. Thus it was decided that molecular formaldehyde was too reactive for a process intended for industrial application. However, after several hours heating the *para*-formaldehyde, it was recognized that the residual formaldehyde in the heating vessel had become quite thoroughly calcined. This realisation came after one run in which vapours from the decomposition vessel were carried over to the lithiated ferrocene using argon too early and the reaction immediately quenched with water vapour; thus the thermal decomposition process was initially driving off water from the formaldehyde polymer (see Schemes 2 and 3).

After workup only starting material was obtained and it was realised that the presence of water had been the reason for poor yields and high percentage recovery of ferrocenyl starting materials all along. This was despite attempted vacuum drying of the formaldehyde prior to use. Thus, calcined formaldehyde was used for the first time. In order to check this theory, for simplicity, the mono-substituted ferrocene *N*,*N*-dimethylaminomethylferrocene was used as a precursor, to give the known N–O disubstituted product **10** [7]. Once prepared, the aim was to react it with di-*tert*-butyl

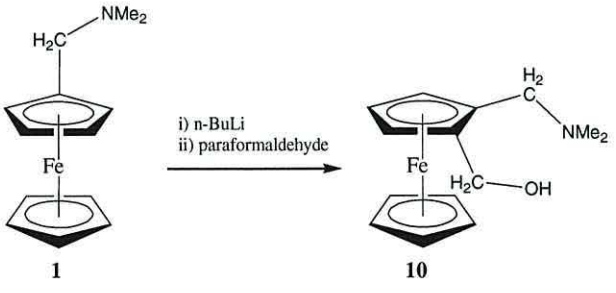

Scheme 2. Formation of ferrocenylmethlalcohols by lithiation/quench.

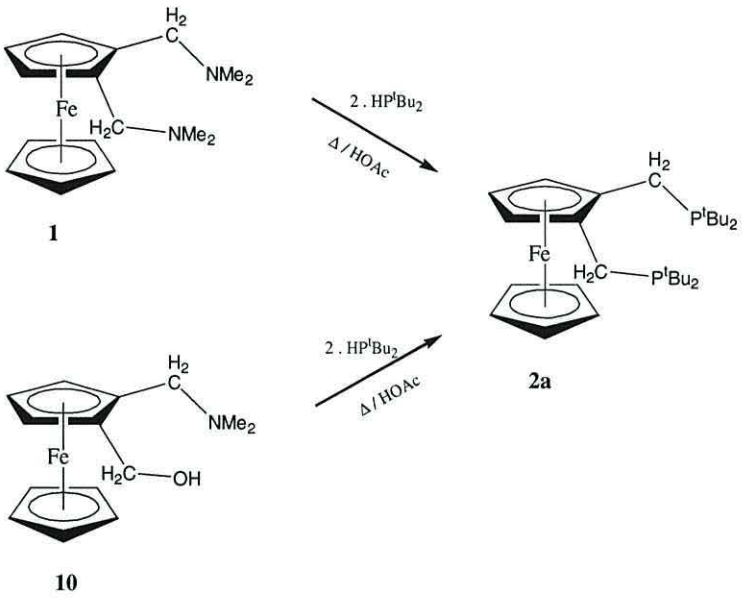

Scheme 3. Routes to bis-1,2-di-*tert*-butyl phosphino ferrocene.

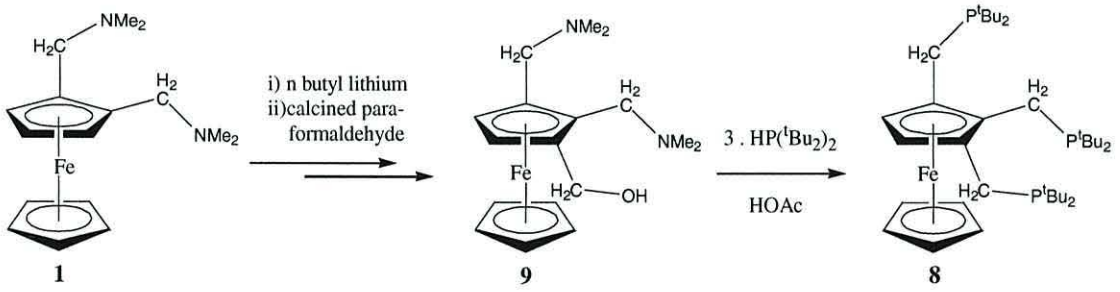

Scheme 4. Route to tris-1,2,3-di-*tert*-butylphosphino ferrocene.

phosphine, and check that phosphine would substitute *both* the amine and the hydroxyl group. The preparation of **10** was successful, and the subsequent reaction with the di-*tert*-butylphosphine was successfully carried out to furnish compound **2a** [3].

This success meant there we now had two, high yielding, synthetic approaches to the bis-1,2-phosphinomethyl ferrocene. Once the problem of poor yields of the hydroxymethyl ferrocene had been overcome, the method could be extended to preparing first the tris-substituted ferrocene 1-hydroxymethyl-bis-2,3-dimethylaminomethyl ferrocene **9**, then to proceed with substituting the two amines and the hydroxyl group with three equivalents phosphine to furnish tris-1,2,3-di-*tert*-butylphosphino ferrocene (tris-P) **8** (Scheme 4). Thus *ortho*-lithiation of 1,2-bis-dimethylaminomethyl ferrocene **1** and subsequent treatment with calcined *para*-formaldehyde in a twofold excess, and subsequent aqueous workup, ether extraction, filtration and evaporation furnished **9** as an orange oil in 91% yield, Scheme 4. The product crystallises on cooling to −17 °C, but the solid again melts, reforming the oil on warming to room temperature (≈20 °C). Compound **9** was characterised by elemental analysis (C, H and N), infrared spectroscopy, ^{1}H NMR spectroscopy and ^{13}C{^{1}H} NMR spectroscopy. [1]

The *N*-methyl group resonances in compound **9** are observed at 2.13 and 2.17 ppm, respectively, with the sterically shielded 'inner' dimethylamino-group *ortho* to

[1] Compound **9**: F.W. 330.08 g mol^{-1}; Formula: $C_{17}H_{26}N_2FeO$. Yield: 0.70 g (91%); ^{1}H (250 MHz, $CDCl_3$): δ 2.13 (s, 6 H; NCH_3), δ 2.171 (s, 6H; NCH_3), δ 2.91 (d, 1H, 12.817 Hz; NCH_2 inner), δ 3.00 (d, 1H, 12.512 Hz; NCH_2 outer), δ 3.43 (d, 1H, 12.817 Hz; NCH_2 inner), δ 3.81 (d, 1H, 12.512 Hz; NCH_2 outer), δ 3.96 (s, 5 H; cp-5), δ 3.99 (d, 1H, 12.207 Hz; OCH_2) (partly obscured by large cp-ring peak at δ 3.962), δ 4.07 (d, 1H, δ 2.136 Hz; cp H_4), δ 4.13 (d, 1H, δ 2.136 Hz; cp H_5), δ 4.747 (d, 1H, 12.207 Hz; OCH_2). ^{13}C (62 MHz, $CDCl_3$): δ 44.53 (s; NCH_3 outer), δ 45.28 (s; NCH_3 inner), δ 55.80 (s; NCH_2 outer), δ 57.90 (s; NCH_2 inner), δ 60.27 (s; OCH_2), δ 67.94 (s; cp C_4), 68.28 (s; cp C_5), δ 69.60 (s; cp 5), δ 84.77 (s; cp C_3), δ 84.84 (s; cp C_2), δ 88.32 (s; cp C_1). Infrared spectra ($CHCl_3$/thin film NaCl plates): ν(OH)(hydrogen bonded): 3381 cm^{-1} (br), 2956 cm^{-1} (m), 2863 cm^{-1}, 2826 cm^{-1} (m), 2774 cm^{-1} (m), ν(C–O):1354 cm^{-1} (m), 1105 cm^{-1} (m), O–H bending 1039 cm^{-1} (m), 1008 cm^{-1} (s). Elemental Anal. $C_{17}H_{26}N_2FeO$ Calcd (found): C, 61.8 (62.3); H, 7.9 (7.8); N, 8.5(8.8)%.

Table 1
assignment of CH_2 protons to substituents on compound **9**

Species (compound)	Chemical shift (ppm)	Δ Chemical shift (ppm)	Coupling constant ($^2J_{HH}$)
NCH_2, **1**	3.20 (d)		12.8
	3.32 (d)	0.12	12.8
NCH_2 inner, **8**	3.00 (d)		12.5
	3.81 (d)	0.81	12.5
NCH_2 outer, **8**	2.91 (d)		12.8
	3.43 (d)	0.52	12.8
OCH_2 **8**	3.99 (d)		12.2
	4.75 (d)	0.76	12.2

the hydroxymethyl group observed at 2.13 ppm. A similar effect occurs with the NCH_2 AB quartet signals. In compound **9** three AB spin systems are observed. Identification of their origin was made on the basis of their coupling constants (Table 1).

The assignment of the NCH_2 groups is made by comparison to the ^1H NMR spectra for the AB spin system in bis-1,2-dimethylaminomethyl ferrocene **1**, in which the AB quartet signals are centred on 3.20 and 3.32 ppm. The outer NCH_2 group (cp ring position 3) is most similar to the amine arms in compound **1**. As in the precursor, NCH_2 outer has as neighbour, another NCH_2 group. However, the inner NCH_2 group has a very different environment, as it has both a NCH_2 group and an OCH_2 group as its neighbours. The data in Table 1 shows that the most similar NCH_2 group to those in the bis-1,2 disubstituted ferrocene occurs as a pair of doublets at 2.91 and 3.43 ppm. These resonances have the same $^2J_{HH}$ coupling constant, although this may be coincidence, and have the most similar magnitude of difference in chemical shift between the AB pair of protons. Other spectral data are relatively easily interpreted and the data are listed in the footnotes (see Fig. 2).

Refluxing 1-hydroxymethyl-2,3-bis-dimethylaminomethyl ferrocene **9** in acetic acid together with di-*tert*-butyl phosphine in greater than three molar equivalents – (a twofold excess was used), in the presence of acetic anhydride, for 7 days, gave after removal of solvent and recrystallisation from refluxing ethanol,

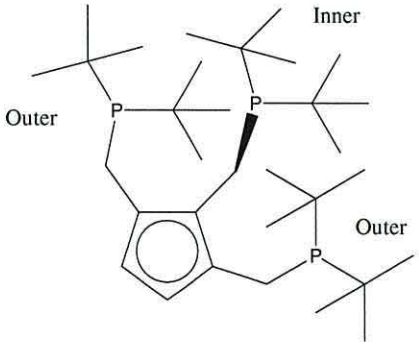

Fig. 2. Schematic diagram of tris-1,2,3-substitution on a cp ring.

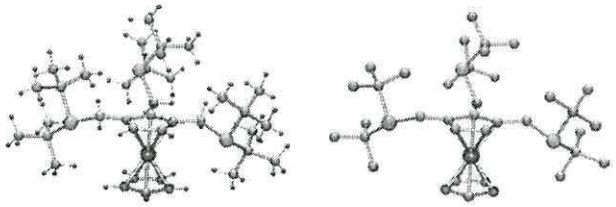

Fig. 3. ORTEP drawings of tris-1,2,3-ditertbutylphosphinomethyl ferrocene **8** shown with and without H atoms.

filtration and washing with ethanol, then drying in vacuo, 1,2,3-tris-di-*tert*-butyl-phosphanyl-methyl ferrocene **8** as analytically pure yellow/orange powder. Several days were allowed for the reaction to complete due to increased steric hindrance provided by three adjacent di-tert-butyl substituted phosphorus atoms. Acetic anhydride was included in the reaction solution to scavenge any water formed during the dehydration reaction in the functional group interconversion of the alcohol into the phosphane. The product was quite air stable for short periods, though the phosphane would oxidise if left exposed for 20 min or more. Compound **8** was soluble in chlorinated solvents (chloroform and dichloromethane), diethyl ether, and sparingly soluble in ethanol. Again the compound was fully characterised. [2]

It was interesting to note that the phosphorus–carbon coupling constants also reflect a substituents location as inner or outer. It is conjectured that the cause of this sensitivity is that the outer groups 'turn away' from the inner group in order to minimise steric interactions. In doing so, the phosphorus lone pairs are pointed toward the inner set of *tert*-butyl groups, and it is this interaction that reduces the $^2J_{PC}$ spin–spin coupling. A ^2J coupling constant of 13.7 Hz seems rather low, and suggests that the sign of the coupling constant becomes negative, so whilst the couplings *magnitude* is normal, the observed coupling magnitude is reduced. The unsubstituted cp ring carbon atoms are observed

[2] Compound **8**: F.W. 660.336 g mol^{-1}; Formula: $C_{37}H_{67}FeP_3$. Yield: 0.43 g (31%); ^1H (250 MHz, $CDCl_3$): δ 1.12 (dd – pseudo triplet, 36H, 12.1 Hz; CH_3 outer), δ 1.26 (d, 18H, $^3J_{PH}$ = 10.7 Hz; CH_3 inner), δ 2.68 (d, 2H, 17.7 Hz; CH_2 outer), δ 2.95 (s, 2H; CH_2 outer), δ 3.07, (m, 2H; CH_2 inner), δ 4.01 (s, 5H; cp 5) δ 4.33 (s, 2H; cpγ-H). ^{13}C {^1H} ($CDCl_3$, 125.77 MHz) δ 21.38 (d, $^1J_{CP}$ = 20.16 Hz; CH_2; inner), δ 21.43 (d, 25.66 Hz; CH_2; outer), δ 29.73 (d, $^2J_{cp}$ = 13.7 Hz; 2 × CH_3; inner), δ 29.95 (d, $^2J_{cp}$ = 25.6 Hz; outer down), δ 30.05 (d, $^2J_{cp}$ = 25.6 Hz; outer up), δ 31.54 (d, $^1J_{CP}$ = 19.25 Hz; *tert*-C inner), δ 31.64 (d, $^1J_{CP}$ = 24.74 Hz; *tert*-C outer down), δ 32.18 (d, $^1J_{CP}$ = 22.00 Hz; *tert*-C outer up), δ 67.97 (s; CH), δ 70.32 (s; Cp 5), δ 86.21 (d, $^2J_{cp}$ = 17.41 Hz; Cp-subst). $^{13}C\{^1H\}$ DEPT ($CDCl_3$, 125.77 MHz),δ 21.3 (CH_2), δ 21.4 (CH_2), δ 29.73 (d) (CH_3), δ 29.95 (d) (CH_3), δ 30.05 (d) (CH_3), δ 67.97 (s) (CH), δ 70.32 (s) (cp5). {^1H} ^{31}P NMR (202.4 MHz,$CDCl_3$):δ 20.58 (s, 2 P), δ 21.35 (s, 1 P).Infrared spectra ($CHCl_3$/thin film NaCl plates): ν(C–H): 2939, 2897, 2863, 2357 cm^{-1}; ν(C–P): 1470 cm^{-1}, ν(C–P): 1366 cm^{-1}. M.p. 115–118 °C. Elemental Anal. Calcd (found): C, 67.2(67.4); H, 10.2(10.2)%.

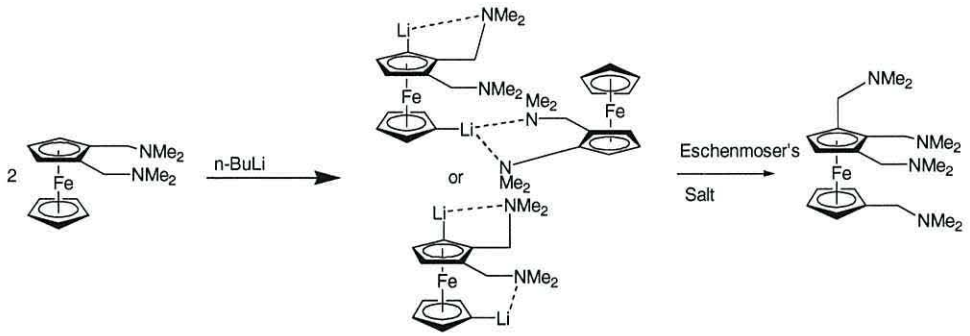

Scheme 5. Example of formation of byproducts by multiple lithiation.

as a doublet at 67.97 ppm coupling constant 18.3 Hz for the two non-substituted positions, and one resonance for substituted ring positions at ca. 86.21 ppm coupling constant also 18.3 Hz (remaining substituted ring carbon was not observed). In the ^{31}P NMR spectrum of compound **8**, two resonances were observed in ≈2:1 ratio. The two outer methylphosphinyl arms are observed at 20.58 ppm. and the unique inner arm at 21.35 ppm. Further evidence is provided by the X-ray crystal structure of a crystal obtained by recrystallisation from ethanol and the structure is shown in Fig. 3. Examination of the crystal structure reveals how the very high degree of steric influence the six tert-butyl groups impose on this structure. The conformation of the substituents in the crystal structure shows each outer phosphine group oriented with one *t*-butyl group above the cp ring plane and the other below it. The inner arm's *t*-butyl groups are positioned both above the ring plane, with a much more uniform environment. The inner arm is twisted slightly so as to pack most efficiently, and it can be envisaged that the conformer will also exist with this arm twisted toward the opposite outer substituents.

The pertinent crystallographic data has been deposited with the Cambridge Crystallographic Database, CCDC 233766. The work was subsequently continued with the second synthetic method and it was found it was possible to obtain pure samples of the tris-dimethylaminomethyl-substituted ferrocene compound **3** as an orange oil, in approximately 60% yield under the standard conditions and again this compound was fully characterized. [3] This compound is also a precursor to compound **8** under the same reaction conditions. Clearly this result opens the possibility to extend the synthetic method to tetra- and possibly penta-substituted derivatives although the relatively low yield obtained does not bode well. The reason for the low yield is that ferrocenyl amines of the type shown may be considered to be independent as a ferrocene and a diamine (cf. TMEDA and congeners) which are well known to activate butyl lithiums. Thus the conditions are also ideal for lithiation of the unsubstituted ferrocenyl-cyclopentadienyl ring in addition to the normal amine-nitrogen directing influences which may be expected. It is therefore not surprising that the byproducts observed by NMR derive from lithium salts where the unsubstituted ring has also been lithiated, (see Scheme 5).

It is therefore clear that the more pendant arms on the ferrocene the more likely it is that large quantities of byproducts will be formed from the lithiation reactions. Clearly a study of the relative rates of lithiation of substituted and unsubstituted cyclopentadienyl rings in these compounds would be important and this will be the subject of future work in this area. The coordination chemistry of the new ferrocenylphosphine will be reported in a future communication.

[3] Standard synthesis involved the lithiation of the1,2-bis(methylamino)ferrocene with *n*-butlyllithium at ambient temperature followed by a quench with Eschenmosers salt [7]. Compound **3**: (yellow/orange oil): ^1H NMR: 2.12 (s, 6H, NMe_2's, inner), 2.17 (s, 12H, NMe_2's, outer), 3.21 (ad, 2H, $J = 13$ Hz), 3.25 (s, 2H) 3.31(ad, 2H, $J = 13$ Hz) 3.90 (s, 5H), 4.21 (s, 2H). ^{13}C NMR: 45.27 (inner CH3's of NMe_2), 45.44 (outer CH_3's of NMe_2), 55.44 (methylene CH_2 inner) 57.43 (methylene CH_2's outer), 68.44, (fc C-2,3), 69.77(unsubstituted cp), 85.42 (fc *ipso* C outer), 83.54 (fcC-*ipso* inner). Mass spec.: parent ion observed at m/z 357.

Acknowledgements

This work was funded by the University of Wales and some chemicals were supplied by Lucite International to whom we are grateful. Mass spectral data were obtained by the EPSRC National Service at the University of Wales, Swansea whom we gratefully thank.

References

[1] (a) See for example: N.J. Long, Metallocenes: An Introduction to Sandwich Complexes, Blackwell Science, Oxford, 1998;
(b) A. Togni, T. Hayashi (Eds.), Ferrocenes, VCH Press, Weinheim, 1995;
(c) A. Togni, R.L. Halterman (Eds.), Metallocenes, Wiley, Weinheim, 1998.
[2] H.-U. Blaiser, W. Brieden, B. Pugin, F. Spindler, M. Studer, A. Togni, Top. Catal. 19 (2002) 3.

[3] I.R. Butler, P.K. Baker, G.R. Eastham, K. Fortune, P.N. Horton, M.B. Hursthouse, Chem. Commun. (submitted).
[4] I.R. Butler, L.J. Hobson, S.M.E. Macan, D.J. Williams, Polyhedron 12 (1993) 1901.
[5] (a) R. Broussier, E. Bentabet, R. Amardeil, P. Meunier, P. Kalck, B. Gautheron, J. Organomet. Chem. 637 (2001) 126;
(b) J.C. Hierso, R. Amardeil, E. Bentabet, R. Broussier, B. Gautheron, P. Meunier, P. Kalck, Coord. Chem. Rev. 236 (2003) 143.
[6] P.E. Pfeffer, E. Kinsel, L.S. Silbert, J. Org. Chem. 37 (1972) 1256.
[7] C. Glidewell, B.J.L. Royles, D.M. Smith, J. Organomet. Chem. 527 (1997) 259.